

LONDON  
SCHOOL of  
HYGIENE  
& TROPICAL  
MEDICINE



**Exploring the Potential of Vaccination to Combat  
*Trypanosoma cruzi* Infection using Bioluminescent  
Imaging**

**Gurdip Singh Mann**

**Thesis submitted in accordance with the requirements for the  
degree of Doctor of Philosophy of the University of London**

**January 2020**

**Department of Infection Biology  
Faculty of Infectious and Tropical Diseases  
LONDON SCHOOL OF HYGIENE & TROPICAL MEDICINE**

**Research group affiliation(s): Professor John M Kelly (Supervisor)  
Dr Martin C Taylor (Co-Supervisor)**

**Funded by Medical Research Council, UK**

## **Declaration**

I, Gurdip Singh Mann, confirm that the work presented in this thesis is my own. Where information has been derived from other sources, I confirm that this has been indicated in the thesis.

Gurdip Singh Mann

January 2020

## Preface

This thesis is written in part as a research paper style thesis and in part as a book style thesis, in accordance with the research degree regulations of LSHTM 2018/2019.

The first chapter is a broad overview of *Trypanosoma cruzi* and the burden of the disease it causes, the immunology of the infection, the rationale of vaccination as an intervention and the history of vaccine development. I also introduce the novel technologies that I have applied in my research. I highlight the specific aims of this work. The second chapter is written in a research paper style and is a submitted manuscript. The remaining chapters are written in the standard book style format. Chapter three includes relevant but unpublished work related to the submitted manuscript. The fourth and fifth chapters are each self-contained works which address the aims set out in chapter one, each with their own introductions, methods, results and discussions.

Finally, I bring together the collective findings of this thesis and how they address the initial aims of the project and narrow the gaps in our understanding of *T. cruzi* infection biology.

## Abstract

*Trypanosoma cruzi* is the causative agent of Chagas disease. It is responsible for the highest disease burden of any parasitic infection in Latin America. There is no prophylaxis and the only available therapeutic treatments frequently report toxic side-effects. A prophylactic vaccine would provide a valuable tool for reducing the disease burden. Despite this, no vaccine has progressed into clinical testing. A major obstacle has been the lack of available tools to monitor the parasite burden *in vivo*, particularly during the chronic stage.

Here, we have applied highly sensitive bioluminescent imaging technology to develop our understanding of vaccination strategies aimed at combating *T. cruzi* infection in mice. First, we applied the system to test a viral vectored vaccine, designed to express two leading *T. cruzi* vaccine targets (ASP2 and TS). Although this reduced the parasite burden during the acute stage (~70%), it had no long term impact on the course of the infection. We then assessed how this outcome compared to protection conferred by drug cured natural infections. We found that the level of protection was considerably greater than that achieved with viral vaccines (>99%, with several instances of sterile protection) and that the degree of protection was associated with the *T. cruzi*-specific IFN- $\gamma$ <sup>+</sup> T cell response. We also utilised the *in vivo* bioluminescence model to investigate if induction of gut inflammation could cure chronically infected mice. By administering a chemical inducer of colitis, we assessed the feasibility of eliminating *T. cruzi* from the colon, a major parasitological niche in the chronic stage. Finally, we sought to develop attenuated parasites to use as tools for studying live attenuated vaccination by generating null mutant strains of *T. cruzi* using Cas9 genome engineering.

This thesis therefore highlights some of the applications of highly sensitive bioluminescent imaging in furthering our understanding of *T. cruzi* infection and in accelerating the development of vaccines in the pre-clinical stage.

## **Acknowledgements**

I would like to express my gratitude to John Kelly and the research group, whose support have allowed this PhD to be a truly fulfilling experience. Their guidance throughout these four years have allowed me to present at international conferences and together we have truly pushed the boundaries of *T. cruzi* research.

I would like to thank my mother and father. Their unwavering belief in my abilities and the many sacrifices they have made for me at every stage of my life are no doubt the reason I find myself in this position today. Without them none of this would have been possible.

Finally I would like to thank my wife, Dr Ravneek Kaur Thind whom I have relied upon during the most difficult times of this process. Her love and encouragement have kept me on the path to completion when I would otherwise have abandoned my goals.

# Table of Contents

<b>Declaration</b>	<b>2</b>
<b>Preface</b>	<b>3</b>
<b>Abstract</b>	<b>4</b>
<b>Acknowledgements</b>	<b>5</b>
<b>List of Abbreviations</b>	<b>8</b>
<b>Chapter 1: Introduction</b>	<b>10</b>
1.1 Trypanosoma cruzi: The causative agent of Chagas disease	
1.1.1 Chagas disease	11
1.1.2 Epidemiology	12
1.1.3 Molecular epidemiology	14
1.1.4 Life cycle of <i>T. cruzi</i>	16
1.1.5 <i>T. cruzi</i> cell biology of infection	19
1.2 Clinical disease	22
1.3 Pathogenesis	25
1.4 Immunity	
1.4.1 Innate immunity	27
1.4.2 Adaptive immunity: T cell response	33
1.4.3 Adaptive immunity: B cell response	36
1.5 Vaccination	38
1.6 The animal model: Bioluminescent imaging	42
1.7 Research questions and aims	44
1.8 References	46
<b>Chapter 2: Submitted Manuscript</b>	
<b>Title: Immunity conferred by drug-cured experimental <i>Trypanosoma Cruzi</i> infections is long-lasting and cross-strain protective</b>	<b>61</b>
Abstract	65
Introduction	66
Materials and Methods	70
Results	73
Discussion	92
Supplementary Materials	97
References	101
<b>Chapter 3: Correlates of protection in viral vectored vaccination and in a live vaccine</b>	<b>107</b>
3.1 Introduction	
3.1.1 Vaccine induced immunity	108
3.1.2 Correlates of protection in re-infection	110
3.2 Methods	111
3.3 Results	
3.3.1 Exploring mechanisms of vaccine induced protection	115
3.3.2 Studying antibodies as a correlate of immune protection in infection experienced mice	122
3.4 Discussion	125
3.5 Supplementary	131
3.6 References	132

<b>Chapter 4: The effects of chemical induced colonic inflammation on chronic <i>T. cruzi</i> infection</b>	<b>135</b>
4.1 Introduction	
4.1.1 Parasitological niche of <i>T. cruzi</i> in the mammal	136
4.1.2 Murine Models of Colitis	138
4.2 Methods	141
4.3 Results	
4.3.1 TNBS tolerability in a chronic dosing schedule	145
4.3.2 Impact of TNBS colitis on a chronic infection	149
4.4 Discussion	157
4.5 Supplementary	162
4.6 References	167
<b>Chapter 5: Generating attenuated <i>T. cruzi</i> parasites using Cas9 genome engineering</b>	<b>170</b>
5.1 Introduction	
5.1.1 Live vaccines	171
5.1.2 Cas9 Technology for the development of Genetically Modified Parasites	173
5.1.3 The <i>T. cruzi</i> genes AP-1 and TcPOT	174
5.2 Methods	176
5.3 Results	
5.3.1 Targeted deletion of the diamine transporter TcPOT and of the AP1 gamma subunit TcAP1- $\gamma$	178
5.3.2 Targeted gene deletion in parasites not constitutively expressing the Cas9 endonuclease	182
5.4 Discussion	185
5.5 Supplementary	188
5.6 References	192
<b>Chapter 6: Discussion</b>	<b>195</b>
6.1 General Discussion	196
6.2 Conclusions and further work	200
6.3 References	203
<b>Appendix</b>	<b>206</b>

## Abbreviations

ACK :	Ammonium-Chloride-Potassium
APC :	Antigen presenting cell
APC-eFluor :	Allophycocyanin -eFluor
ASM :	Acid sphingomyelinase
ASP2 :	Amastigote surface protein 2
BCG :	Bacillus Calmette-Guérin
CCC :	Chronic chagasic cardiomyopathy
CD :	Chagas disease
CK-MB :	Creatine kinase myocardial band
CNS :	Central nervous system
CpG :	5'—C—phosphate—G—3'
DAF :	Decay accelerating factor
DMSO :	Dimethyl sulfoxide
DNA :	Deoxyribonucleic acid
DSS :	Dextran sulfate sodium
ECG :	Electrocardiogram
ELISA :	Enzyme-linked immunosorbent assay
ELISPOT :	Enzyme-linked immunospot
FACS :	Fluorescence-activated cell sorting
FCS :	Foetal calf serum
FITC :	Fluorescein isothiocyanate
FMO :	Fluorescence minus one
GIPL :	Glycoinositolphospholipid
GIT :	Gastrointestinal tract
GPI :	Glycosylphosphatidylinositol
H&E :	Haematoxylin and eosin
HRP :	Horseradish peroxidase
IFN- $\gamma$ :	Interferon gamma
Ig :	Immunoglobulin
IL :	Interleukin
IRF :	Interferon regulatory transcription factor
KO :	Knockout
LCMV :	Lymphocytic choriomeningitis
MASP :	Mannan-binding lectin-associated serine protease

MBL :	Mannose-binding lectin
MHC :	Major histocompatibility complex
MIF :	Macrophage migration inhibitory factor
NF- $\kappa$ B :	Nuclear factor kappa-light-chain-enhancer of activated B cells
NO :	Nitric Oxide
PAM :	Protospacer adjacent motif
PAMP :	Pathogen-associated molecular pattern
PBMC :	Peripheral blood mononuclear cell
PBS :	Phosphate-buffered saline
PCR :	Polymerase chain reaction
PE-Cy7 :	Phycoerythrin-Cy7
PerCP-Cy5.5 :	Peridinin-chlorophyll-protein -Cy5.5
PFA :	Paraformaldehyde
RBC :	Red blood cell
RNA :	Ribonucleic acid
ROS :	Reactive oxygen species
T-DAF :	Trypanosoma-decay accelerating factor
TCR :	T-cell receptor
TLR :	Toll-like receptor
TNBS :	Trinitrobenzene sulfonic acid
TNF- $\alpha$ :	Tumor necrosis factor alpha
TS :	Trans-sialidase
UC :	Ulcerative colitis
WT :	Wild-type

# Chapter 1 :

## Introduction

## **1.1 *Trypanosoma cruzi*: The causative agent of Chagas disease**

### **1.1.1 Chagas disease**

Chagas Disease is a neglected tropical disease and results from an infection with the protozoan parasite *Trypanosoma cruzi*. Discovered over 100 years ago by the Brazilian physician Carlos Chagas, the causative agent, the clinical disease and the insect vector have long been known<sup>1</sup>. However Chagas disease remains the single greatest burden of any parasitic infection in Latin America<sup>2</sup>. Untreated infections are life-long and can give rise to debilitating cardiac, digestive and neurological complications which are progressive and in some cases ultimately fatal<sup>3</sup>.

A joint continental wide effort in implementing vector control programmes, coupled with the rolling out of blood screening and improving access to diagnosis and treatment have all led to significant reductions in transmission in several countries<sup>4,5</sup>. However a number of factors such as a large wild reservoir of infection, severe drug toxicity and no licensed vaccine mean that elimination of the infection in the human population is a complicated and difficult task<sup>6</sup>. In addition, there are modes of transmission that bypass the traditional vector route. Infections can be passed on congenitally from mother to child, orally in contaminated foods and through contaminated blood or solid tissues<sup>7</sup>.

A long-standing problem has been the toxicity of the only available front line treatments<sup>8,9</sup>. The nitroheterocyclic drugs benznidazole and nifurtimox both have long recommended treatment periods, but also display a range of side effects which impacts on compliance. Treatment failures are often reported<sup>10</sup>.

An effective vaccine that is able to either reduce disease severity or prevent the onset of disease as a stand-alone or in combination with currently available drug treatments would therefore be a useful tool. Vaccination has been predicted to be economically cost-effective, with the savings made in treating the chronic disease outweighing the

costs of developing and producing a vaccine across a range of scenarios<sup>11</sup>. Several research groups are working toward this goal<sup>12-14</sup>, however to date, there are no licensed vaccines and no vaccines in clinical trials.

### **1.1.2 Epidemiology**

Chagas Disease is endemic to 21 countries in South America, ranging from the north of Argentina / Chile to the Southern United States. The highest incidence of infection is in Bolivia, where around 6 in every 100 people are infected. Other highly infected regions are Argentina (3-4 per 100) and Paraguay (2-3 per 100). However smaller hyperendemic regions exist, such as the Gran Chaco, a lowland region divided between eastern Bolivia, western Paraguay and northern Argentina, where the incidence of infection amongst adults is almost 100%<sup>15</sup>.

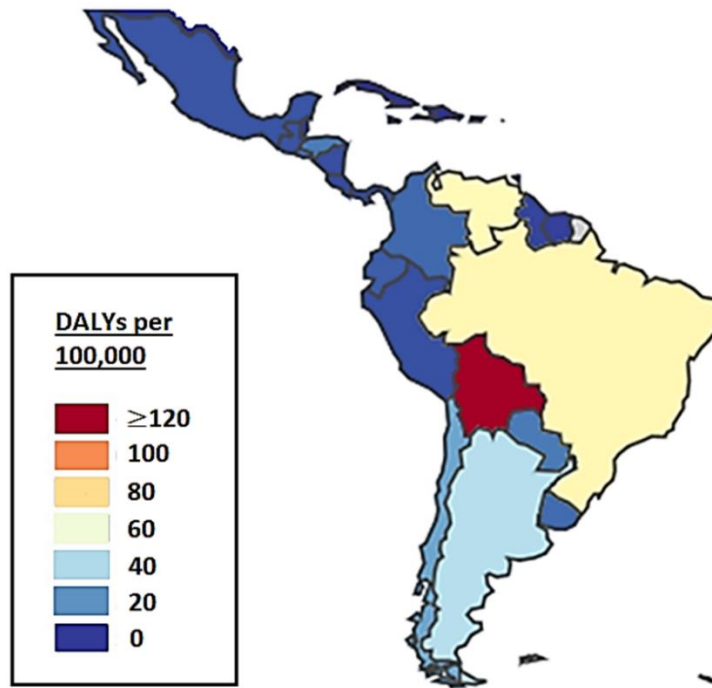


**Figure 1.1** – Map of South America showing the number of Disability adjusted life years lost to Chagas Disease per 100,000. The worst affected countries include Bolivia (red) at 132 DALYs per 100,000, Brazil at 69.6 DALYs per 100,000 and Venezuela at 68 DALYs per 100,000. Data from IHME website<sup>16</sup>

Changing migration patterns both domestically and globally have greatly altered the disease epidemiology. The migration of people from rural areas of high disease incidence into the cities as well as the migration of people out of South America has brought Chagas disease to areas that were previously not affected (Figure 1.2)<sup>17,18</sup>. Today, the number of people infected is estimated to be between 6 and 7 million<sup>19</sup>. The vast majority of these are in Central and South America, with a few hundred thousand cases collectively in North America, Europe and the Western Pacific region<sup>20</sup>.

Overall, with only a few exceptions<sup>21</sup>, the global incidence of disease is declining due to large scale control programmes. However, with the number of cases outside of South America steadily increasing, or rather with increased screening and realisation of the true burden of the infection<sup>22</sup> there are fears surrounding the emergence of new epidemics<sup>23</sup>.

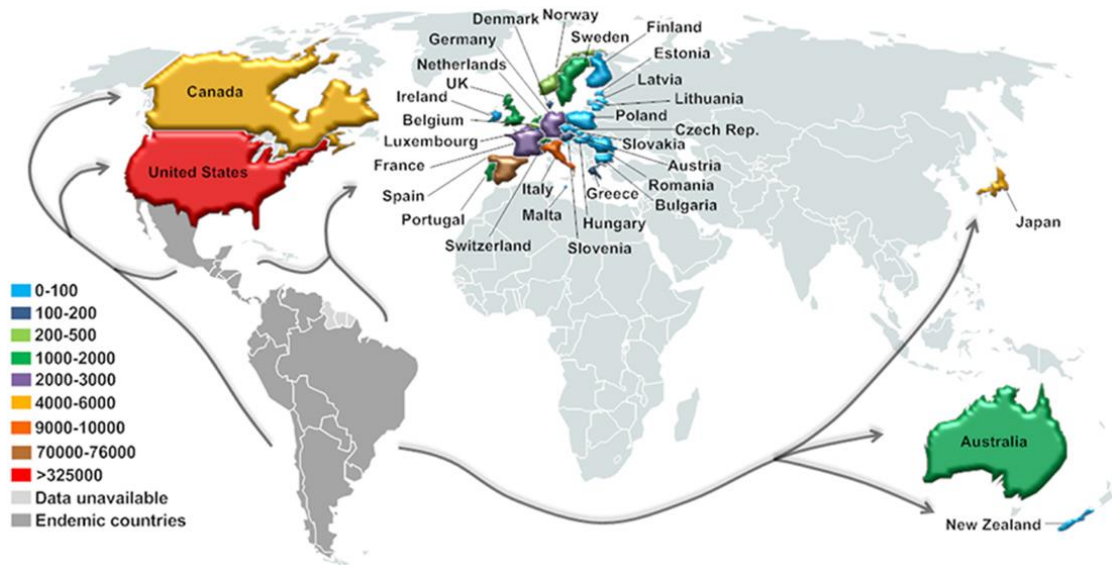


**Figure 1.2** – World map estimating number of migrants with *T. cruzi* in non-endemic countries, resulting from emigration out of South and Central America. The United States has a higher burden of disease than any other non-endemic country, this is likely due to migration in addition to recently identified autochthonous transmission in the southern states<sup>17</sup>

### 1.1.3 Molecular epidemiology

*T. cruzi* is a member of a group of organisms commonly referred to as kinetoplastids, flagellated protozoans that are identifiable by the presence of an organelle known as the kinetoplast, a network of circular DNA which lies within a mitochondrion<sup>24</sup>. Kinetoplastids are eukaryotic organisms that are widespread and that can be found as free living in the environment, or as parasites of plants, vertebrates and invertebrates<sup>25</sup>. Amongst the kinetoplastids are other important insect transmitted parasites, which can also cause devastating human diseases. The parasite *Trypanosoma brucei* is the causative agent of sleeping sickness and *Leishmania spp* can cause various forms of the disease known as leishmaniasis<sup>26,27</sup>.

*T. cruzi* comprises a single species, however there are great differences between strains. Differences in morphology, infectivity, drug sensitivity and many other features vary greatly<sup>28-30</sup>. This is exemplified by the fact that in a study of 54 isolates of *T. cruzi*, differences of up to 47.5% were observed in DNA content, with the estimated range in DNA content amongst isolates between 80 and 150 Mb<sup>31</sup>. For decades, there have been different classification systems used to group parasites. In 2009 at a satellite meeting held amongst notable experts in the field it was decided that strains of *T. cruzi* were to be classified into one of six groups, termed discrete typing units (DTUs)<sup>32</sup>. These are clusters of *T. cruzi* strains that are genetically more similar to one another than they are to parasites belonging to any other DTU. Although *T. cruzi* is recognised as a single species, the distinction between different parasites as members of different DTUs is important considering that *T. cruzi* displays such intraspecific diversity (Figure 1.3)<sup>33</sup>.

These differences in parasite genetics are reflected in the geographical distribution and in host specificity of strains. Some DTUs are commonly sampled from the sylvatic cycle of transmission, with human infection being uncommon. This is generally the case for Tc III and Tc IV. Whereas other DTUs are more commonly sampled from human infections, with infection in wild animals being less common, this is the case for Tc II, V and VI. Tc I is the most widely dispersed of all the DTUs and is sampled from wild and domestic cycles<sup>34</sup>.

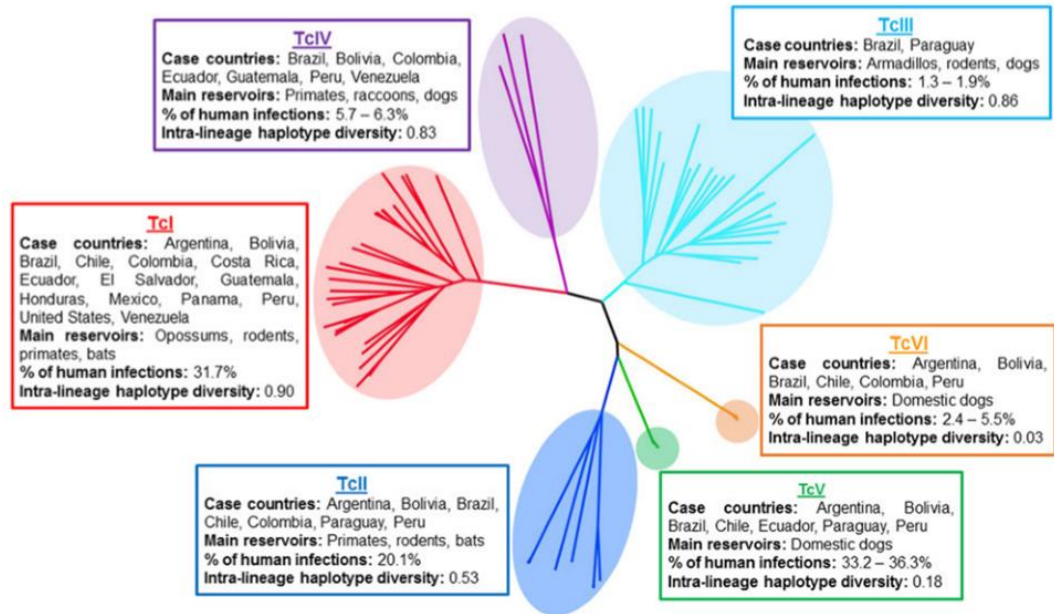


**Figure 1.3** – key characteristics of *T. cruzi* which demonstrate its inter-lineage and intra-lineage diversity. Tree is representative of parasites collected from diverse geographical locations<sup>35</sup>. Intra-lineage haplotype diversity represents the likelihood that two randomly selected haplotypes from the same lineage will be different<sup>33</sup>.

#### 1.1.4 Life cycle of *T. cruzi*

*T. cruzi* is heteroxenous, infecting insect species of the *Triatominae* subfamily of bugs as well as over 70 genera of mammals, both wild and domestic<sup>36</sup>. As a result of having to infect vertebrate and invertebrate hosts and having both intracellular and extracellular forms, *T. cruzi* has a complex life cycle, undergoing several morphological changes throughout.

Transmission occurs when the mammalian host comes into contact with the contaminated faeces of the insect vector. There are over 140 species of insect from the *Triatominae* subfamily which can act as vectors of the parasite. Of these, the species *Triatoma infestans*, *Triatoma dimidiata* and *Rhodnius prolixus* are amongst the most important in transmission of *T. cruzi* to humans, owing to their adaptability to living in human dwellings<sup>34,37,38</sup>. Triatomine bugs are hematophagous and it is upon feeding that

the infected bug will defecate and deposit the infective metacyclic form of the parasite onto the skin of its prey. Should the contaminated faeces break the skin barrier through the bite site or via the mucous membranes such as the mouth, nose or eyes, the host becomes infected<sup>39</sup>.

Metacyclic trypomastigotes are slender, flagellated and highly motile, capable of infecting a wide range of nucleated cells. The parasite will either actively invade a host cell by a process involving contact with the cell membrane and the recruitment of lysosomes to the invasion site, or through a pathway that involves actin rearrangement in the host cell and uptake into an endosome. In either scenario, parasites enter via a parasitophorous vacuole. They then rapidly escape and enter the cytosol<sup>40</sup>.

Once inside the cytosol the metacyclic trypomastigote will begin to transform into an amastigote. Amastigogenesis occurs via cell division, during which the flagellum is released and two small spherical daughter cells are produced<sup>41</sup>. After several cycles of binary division over the course of several days, the amastigotes transform back to long, slender, flagellated forms known as bloodstream trypomastigotes<sup>42</sup>. These forms of the parasite are morphologically similar to the metacyclic form when observed down a light microscope, however the blood stream form shows distinct surface molecule expression compared to the metacyclic form<sup>43</sup>.

Bloodstream trypomastigotes are not replicative, however like metacyclic trypomastigotes they are able to invade and productively infect host cells. In addition, bloodstream trypomastigotes can be picked up by the triatomine bug upon taking a blood meal and continue down an alternative pathway of development inside the vector<sup>44</sup>.

In the vector, between one and four weeks after a bloodmeal, epimastigote forms of the parasite can be found in the small intestine. These are the largest forms of the parasite, long and slender with a flagellum. Epimastigotes are replicative and also divide by binary fission. Therefore in the weeks following a bloodmeal, the number of epimastigotes in

the small intestine of the bug will gradually increase. In the rectum, epimastigotes will undergo another transformation, turning into the non-replicative metacyclic forms, ready to exit the bug and infect a new host<sup>44,45</sup>.

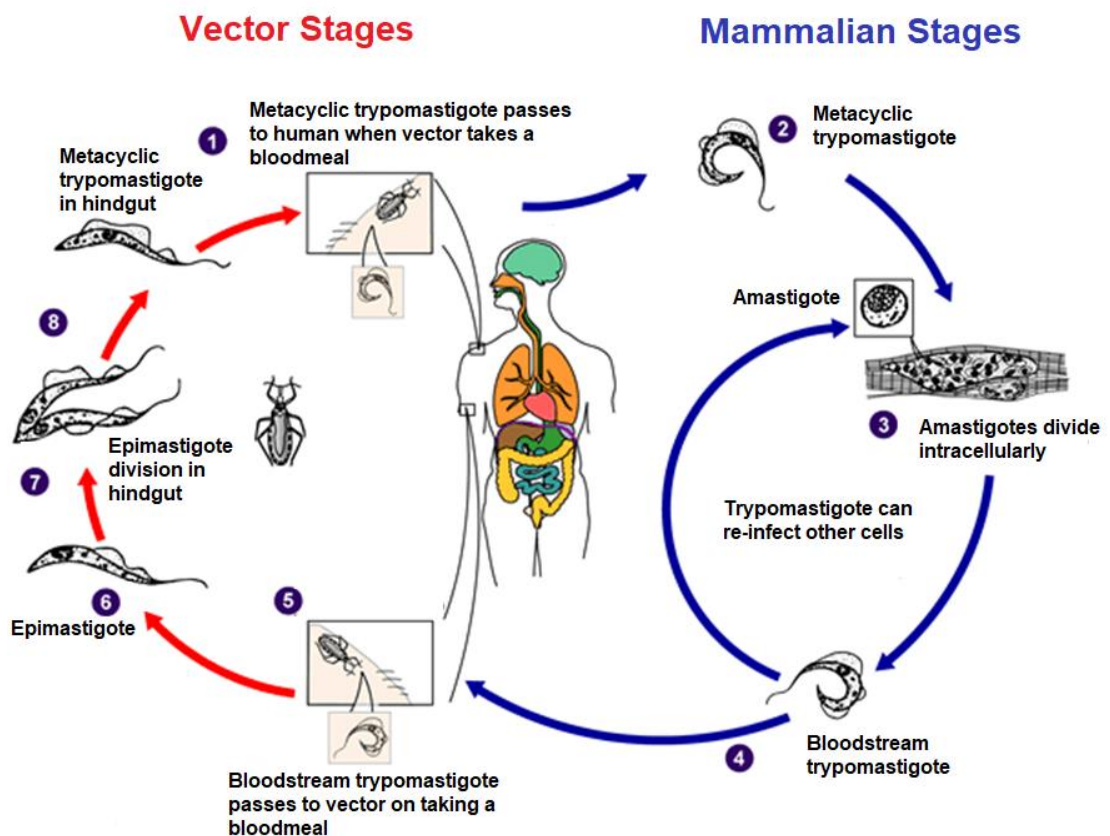


**Figure 1.4** – Life cycle of *T. cruzi* in the vertebrate and invertebrate host, depicting the classical route of transmission. Adapted from CDC.

### 1.1.5 *T. cruzi* cell biology of infection

As an obligate intracellular parasite, adhesion and invasion are key processes for *T. cruzi*, allowing it to replicate and develop in the vertebrate host. The study of these processes is complicated by the fact that multiple parasite ligands and host receptors are involved. These cell surface ligands can often be developmentally regulated and can even display antagonistic roles, with some promoting parasite invasion and others acting to inhibit invasion<sup>46</sup>. Members of the TS group II family of glycoproteins play an important role in these processes as they encode a number of molecules important to parasite adhesion and invasion<sup>47</sup>. The binding of these glycoproteins to receptors on the host cell induces calcium mobilisation in both the parasite and host and is necessary for efficient parasite invasion<sup>48</sup>.

Two glycoproteins that have been characterised on the metacyclic trypomastigote are gp90 and gp82. The parasite surface glycoprotein gp90 is antiphagocytic, its binding to host cells prevents parasite invasion. On the other hand, the surface glycoprotein gp82 is involved in promoting parasite invasion into the host cell. The differential activities of these surface ligands is associated with the ability of gp82 to induce intracellular  $\text{Ca}^{2+}$  signalling, whereas the binding of gp90 induces no such signalling. Therefore, parasite strains which display higher gp90 expression are less invasive<sup>48</sup>.

Metacyclic trypomastigotes are not the only form capable of invasion. Both the vertebrate bloodstream stage and the amastigote stage of *T. cruzi* have been documented to invade host cells. The Tc-85 group of surface proteins are present on bloodstream trypomastigotes. Like other members of the TS group II family, Tc-85 glycoproteins lack trans-sialidase enzymatic activity, but perform a role in cell adhesion and invasion. These parasite ligands are multi-adhesive and have been shown to be able to bind the extracellular matrix components laminin and fibronectin<sup>49,50</sup>. A 21kDa

secreted protein from amastigotes has also been identified as being involved in invasion by extracellular amastigotes<sup>51</sup>.

Invasion is not solely dependent upon parasite surface proteins, but it is also dependent on host cell surface molecules. Lectins are a class of receptors which have been implicated in parasite entry. Specifically, Galectin-3 expression has been demonstrated to be upregulated on the surface of splenocytes in a murine infection model. This receptor has been suggested to be involved in infection of dendritic cells<sup>52</sup>. Furthermore, this same receptor has been demonstrated to bind *T. cruzi* trypomastigotes on human smooth muscle cells<sup>53</sup>. Other work using electron microscopy identified a number of carbohydrate residues on heart muscle cells that were internalised together with parasites, identifying galactosyl, mannosyl, and sialyl residues as additional host receptors for attachment and invasion<sup>54</sup>.

A variety of additional host receptors include the TGF- $\beta$  receptor, the bradykinin receptor, the nerve growth factor receptor TrkA and TLR2/CD14<sup>55-57</sup>. The sheer variety of host cell surface receptors identified as taking part in *T. cruzi* adhesion and invasion explain the pan-tropic nature of the acute infection<sup>58</sup>.

Following ligand binding, the parasite begins the process of invasion. There are multiple mechanisms that have been described in invasion, however there are some common features that are shared amongst these 'invasion styles'. Invasion involves the endocytic pathway, allowing the parasite to cross the plasma membrane within an endosome. Another common feature is the involvement of lysosomes, these acidic organelles perform a role in acidifying the endosome. Each of the modes of entry culminate in the formation of a parasitophorous vacuole.

One of the mechanisms by which parasites enter host cells is by phagocytosis. This process begins following *T. cruzi* attachment to host cells, resulting in actin dependent extensions of the host cell membrane, engulfing the parasite<sup>59,60</sup>. This process of *T. cruzi*

entry has been observed amongst both professional and well as non-professional phagocytic cells<sup>61</sup>. Following the entry of the parasite in the endocytic pathway, the endosome matures into a late endosome, this process is characterised by the movement of the vesicle toward the perinuclear area and the acquisition of endosomal markers<sup>62</sup>. The fusion of lysosomes with this late endosome gives rise to the parasitophorous vacuole, an organelle with a pH of 4-4.5 and which expresses the surface molecules LAMP1 and LAMP2<sup>63</sup>.

Another mechanism of entry used by *T. cruzi* is one that takes advantage of a known membrane repair pathway in host cells<sup>64</sup>. *T. cruzi* trypomastigote binding to host cells can cause membrane damage, this results in a  $\text{Ca}^{2+}$  dependent translocation of lysosomes to the damaged membrane<sup>65</sup>. Lysosome secreted acid sphingomyelinase (ASM) then cleaves a sphingolipid in the plasma membrane, generating ceramide. This conversion to ceramide allows the plasma membrane to bud off inwardly, internalising the parasite within a vesicle as it does so. Fluorescent imaging reveals that the parasitophorous vacuole is closely associated with lysosomes and quickly becomes enriched in LAMP1, suggesting lysosomal fusion<sup>65</sup>.

The acidic parasitophorous vacuole is only a temporary environment, from which the parasite quickly escapes. The parasite proteins, trans-sialidase and Tc-TOX promote the degradation of the vacuole membrane, allowing the parasite to be released into the cytosol. Trans-sialidase is a parasite surface bound protein (which can also be shed) that catalyses the removal of sialic acid residues that coat the inner surface of the membrane of the parasitophorous vacuole<sup>66</sup>. This makes the membrane susceptible to the action of another parasite protein, the secreted enzyme Tc-Tox<sup>67</sup>. At an acidic pH, this enzyme has haemolytic activity and forms a pore in the vacuole, thereby contributing to its breakdown. Upon release of the parasite into the cytosol, the parasite, which has already begun transforming into an amastigote, completes its transformation and commences replication. Infection by a single trypomastigote can result in around 500

parasites within a single cell. Within 5-7 days following an initial infection, flagellated trypomastigotes escape the cell and are immediately able to infect another<sup>42</sup>.

## **1.2 Clinical disease**

Chagas disease is often categorised into three distinct stages. The symptomatic acute stage of the infection, an asymptomatic stage named the indeterminate stage and a symptomatic stage termed the chronic stage<sup>17</sup>. The acute stage occurs upon infection and may last for several weeks. It is characterised by the uncontrolled proliferation of parasites, during which parasites are readily detectable in the blood by microscopic examination<sup>17</sup>. This stage of the disease can be accompanied by a range of non-specific symptoms such as fever, lethargy, diarrhoea and drowsiness amongst others<sup>68</sup>. Most individuals are unaware that they are infected with *T. cruzi*. In the case of the classical route of transmission, by the insect vector, the only tell-tale sign may be swelling near the site of parasite inoculation<sup>69</sup>. The acute stage is not usually life-threatening and is self-resolving due to the generation of a robust immune response. However in a small percentage of cases the acute infection can lead to fatality due to meningoencephalitis or an acute heart failure<sup>70,71</sup>.

Infected hosts will then transition to the indeterminate stage of the infection, during which parasite numbers are brought under tight control due the generation of robust immunity (see below). Parasite numbers during this stage are reduced to levels not readily detectable in the blood, even by methods such as PCR<sup>72</sup>. For the majority of infected immune competent individuals, they will live out the remainder of their lives without any further clinical presentations. However in 30 – 40% of cases, clinical signs will emerge decades later. This is often in the form of heart disease, the most common clinical manifestation of Chagas disease<sup>73</sup> (referred to as chronic chagasic cardiomyopathy) Less commonly, the infection will present in the form of a digestive megasyndrome<sup>73</sup>.

Chronic chagasic cardiomyopathy occurs as a result of cardiac inflammation and infection of the cardiac tissue. This results in damage to, and loss of, cardiomyocytes; the cardiac conduction system; and/or the development of tissue fibrosis during the reparative process. This can lead to a number of different clinical presentations. The damage is progressive and ultimately leads to heart failure, which is the leading cause of death due to Chagas disease<sup>74</sup>. In around a third of symptomatic disease cases, patients will present with a digestive disorder. Referred to as megasyndromes, those that present with the digestive form of the disease suffer from a dilated digestive tract, usually in the colon and/or the oesophagus. This process is irreversible and in severe cases also leads to death<sup>75</sup>.

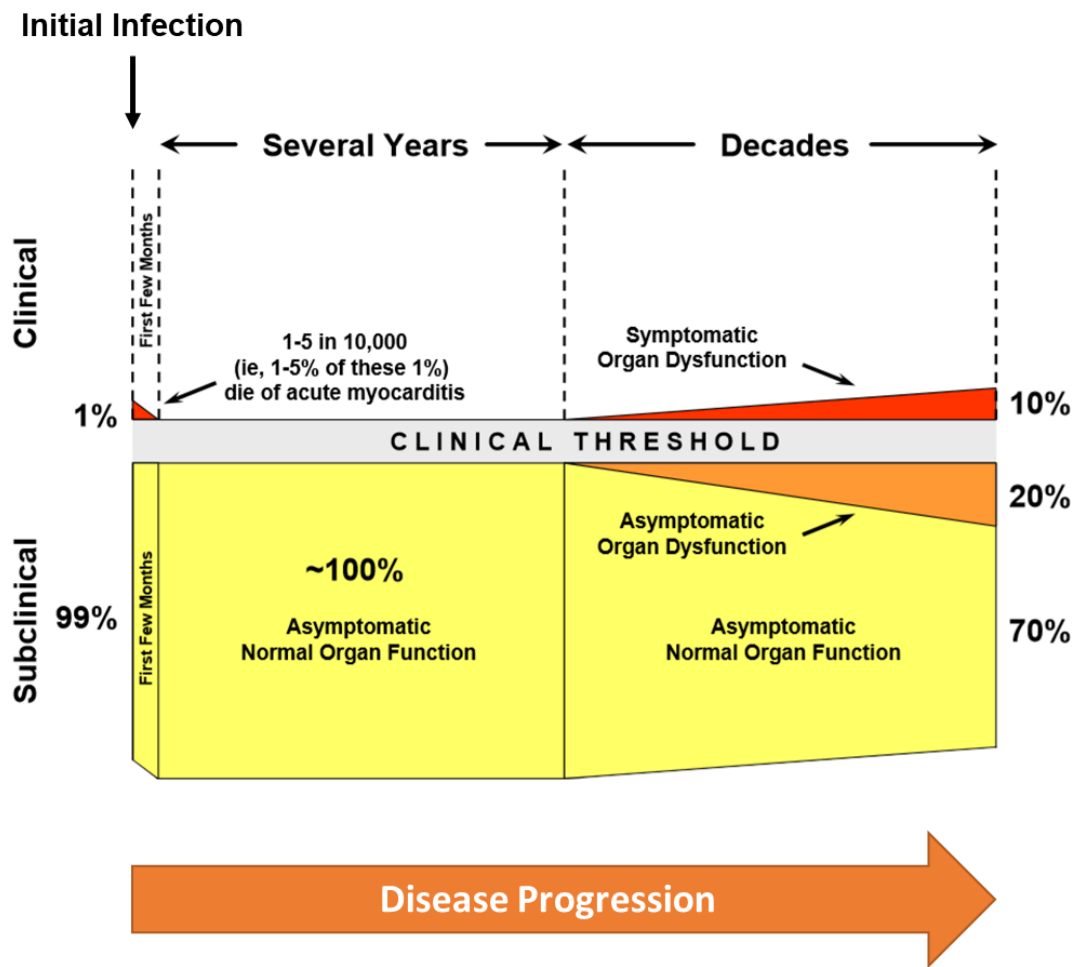


**Figure 1.5** – Clinical progression of Chagas heart disease. After the initial infection, in the acute stage, most individuals are unaware of the infection. Symptoms are often non-specific and only around 1% of cases present clinically with myocarditis, which usually resolves. Following resolution of the acute stage, the majority of cases remain asymptomatic for a variable number of years. The disease progresses with time, around 30% of patients will develop heart dysfunction which can be detected clinically, around 10% in total will be symptomatic<sup>73</sup>

A less common occurrence in *T. cruzi* infection is the involvement of the central nervous system (CNS). CNS involvement usually stems from immunosuppression of an infected person. It is characterised by amastigote nests in the brain tissue and/or trypomastigotes in the cerebrospinal fluid<sup>76-78</sup>. Symptoms are varied and can be mild, including malaise and headaches or more severe and result in cognitive impairment and seizures<sup>79,80</sup>.

### **1.3 Pathogenesis**

Chagas disease pathogenesis has been proposed to occur via multiple mechanisms. The two most widely explored of these are the autoimmune hypothesis and the hypothesis of parasite persistence. The autoimmune hypothesis argues that Chagas disease pathogenesis results from a self-reactive immune response, resulting from a breakdown in tolerance<sup>73</sup>. The parasite persistence hypothesis proposes that Chagas disease is a consequence of chronic inflammation, resulting from the persistence of *T. cruzi* at specific sites<sup>81</sup>.

A number of interesting observations lent credibility to the autoimmune hypothesis. Amongst these were reports of chronic disease patients in which parasites were not identified in the cardiac tissue<sup>82</sup>. Other studies reported on the presence of auto-reactive lymphocytes and molecular mimicry between parasite antigens and human cardiac myosin<sup>83,84</sup>.

The view that autoimmunity was the main mechanism of disease progression began to change in light of evidence which supported the requirement for the presence of parasites for disease progression. For example, heart tissue from chagasic patients were shown to be PCR positive and were also positive for parasite antigens<sup>85,86</sup>. This finding, coupled with previous reports of a lack of live parasites in the hearts of chagasic patients makes sense when we consider that the induction of robust immunity is the norm in a *T. cruzi* infection. Other supporting evidence comes from positive patient outcomes as a result of antiparasitic drug treatment. Chronic human patients receiving benznidazole show improved clinical outcomes, such as fewer ECG changes, in the years following the cessation of antiparasitic treatment compared to infected and non-treated patients<sup>87</sup>.

A new model, which used bioluminescence to describe the infection dynamics in the chronic stage throws further support behind the theory of parasite persistence. Lewis et

al<sup>88</sup> reported on the infection dynamics of a number of *T. cruzi* strains in the mouse model. It was found that throughout the infection, parasites trafficked from a niche in the gut to other organs such as the heart before being eliminated by an effective immune response. The rate at which these transient infections trafficked to the heart correlated with the accumulation of heart damage.

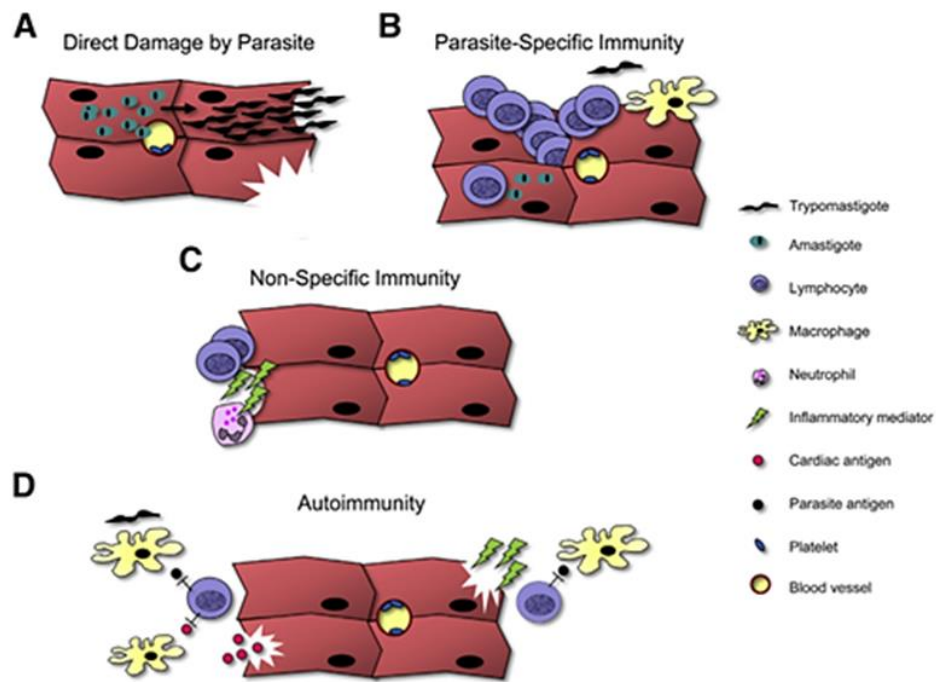


**Figure 1.6** – A number of mechanisms have been proposed in disease pathogenesis. A, the ability of *T. cruzi* to infect and replicated in cardiomyocytes can lead to direct parasite mediated damage. B, damage can occur because of an immune response targeted toward intracellular parasites. C, bystander injury may occur as a result of the activation of innate immune responses such as the activation of polymorphonuclear cells, which release their granules into the environment. D, autoimmunity as a result of molecular mimicry or activation of self-reactive T cells caused by cell lysis in an already inflammatory environment<sup>73</sup>

## **1.4 Immunity to infection**

The immunological response to *T. cruzi* is a significant determinant in the outcome for the patient. Understanding the immunological response that controls both the acute parasite burden and the mechanisms that allow the parasite to persist are necessary to inform the development of interventions. Both the innate immune system and the adaptive immune system are important in controlling the infection. Defects in either can lead to lethal outcomes.

### **1.4.1 Innate immunity**

Innate immunity is important in the days following a *T. cruzi* infection, it is necessary for controlling parasite replication and spread before the generation of an adaptive immune response. However, as will be discussed, the parasite has evolved mechanisms to avert the immune response at each step.

#### **Complement**

Upon infection, the first host defence that the parasite will encounter is the complement system. This is constituted by blood circulating proteins which recognise and bind to the surface of the pathogen in a sequential manner, targeting the pathogen for destruction by other immune effector cells, thereby 'complementing' our immune system. Alternatively, the complement system can proceed through additional steps of protein binding to form pores in the parasite membrane, effectively lysing the parasite. There are three pathways of complement activation, the classical pathway, the lectin pathway and the alternative pathway. Although all three of these pathways are initiated by different molecules, they all converge and eventually all follow the same pathway<sup>89</sup>.

The classical pathway is initiated by IgG or IgM binding to the pathogen surface. These antibodies are bound by a complement protein complex known as the C1 complex. The

C1 complex cleaves two other proteins, C2 and C4, to form the C3 convertase. The lectin pathway describes when mannan-binding lectins (MBL) or proteins known as ficolins bind the pathogen surface. This pathway is favoured over the classical pathway in non-immune serum<sup>90</sup>. The pathogen bound MBL or ficolins associate with an MBL-associated serine protease (MASP), and then, like the classical pathway, cleave C2 and C4 to form the C3 convertase. The alternative pathway results from the spontaneous hydrolysis of C3 in the blood and results in C3b binding to the pathogen surface. This C3b associates with another blood protein, known as Bb, forming the C3 convertase<sup>91</sup>. Regardless of the initiating steps, all 3 of the pathways converge on the C3 convertase and the following steps are the same in all of the pathways. After formation of the C3 convertase, C3 is cleaved to give C3a and C3b, the binding of C3b to the C3 convertase forms the C5 convertase. This then cleaves C5 to give C5a and C5b. C5b then combines with C6, C7, C8 and C9 to give the membrane attack complex. This is a protein complex which inserts into the membrane of a pathogen and to which epimastigotes, and to some extent, also trypomastigotes are susceptible<sup>92,93</sup>.

Depletion of the complement system in mice prior to infection leads to higher parasitaemia<sup>94</sup>. However, metacyclic trypomastigotes have evolved resistance to complement and exposure to mammalian serum is not 100% effective at mediating their lysis<sup>90</sup>. This is because trypomastigotes express regulatory proteins on their surface which are functionally analogous to human complement regulatory proteins. One such example is the trypomastigote decay accelerating factor (T-DAF), which is similar to the human complement inhibitor DAF, a protein which prevents the assembly of the C3 convertase, thereby preventing further binding of other complement proteins<sup>95</sup>.

### Innate recognition

Recognition of *T. cruzi* by cells of the innate immune system is mediated by germline encoded receptors – the Toll Like Receptors (TLRs). These are highly conserved

receptors in the animal kingdom, with 10 TLRs described in humans and 11 in mice<sup>96</sup>. TLRs differ in their cellular localisation and in the specificity of their recognition, with different TLRs adapted to recognise different pathogen associated molecular patterns (PAMPs). Triggering of TLRs by *T. cruzi* results in a cascade of downstream signals via the adaptor molecules, myd88 or TRIF, leading to signalling which targets the transcription factors NF- $\kappa$ B and interferon regulatory factor (IRF)<sup>97</sup>. These in turn induce the expression of pro-inflammatory cytokines TNF- $\alpha$ , IL-12 and the Type I interferons. These receptors, although not implicated in the internalisation of parasites, are essential in parasite sensing and the subsequent functioning of cells of innate immunity.

TLR2 and 4 are cell surface receptors, both of which have been demonstrated to participate in recognising *T. cruzi*. TLR2 recognises glycosylphosphatidylinositol (GPI) anchored mucin-like glycoproteins on the parasites cell surface, whereas TLR4 recognises *T. cruzi* glycoinositolphospholipids (GIPLs)<sup>98</sup>. While exposure of TLR2<sup>-/-</sup> macrophages to live parasites leads to a robust pro-inflammatory response, TLR4<sup>-/-</sup> macrophages show a defective phenotype. Upon exposure to live parasites, TLR4<sup>-/-</sup> macrophages have an increased susceptibility to parasite replication, associated with lower NO production<sup>99</sup>.

TLR9 and TLR7 are essential for nucleic acid sensing and are located on cell membranes in the endosome. TLR9 is able to recognise CpG sequences in *T. cruzi* DNA, whereas TLR7 recognises *T. cruzi* RNA. TLR9, like TLR2, signals via myd88 and TLR9<sup>-/-</sup> mice are more susceptible to infection than wild type (WT). Interestingly, both TLR 9<sup>-/-</sup> and TLR 2/9 double KO mice show a susceptibility to infection which TLR2<sup>-/-</sup> do not. This susceptibility is associated with a decrease in IL-12/IFN- $\gamma$  and suggests that TLR9 is the main TLR involved in myd88 signalling<sup>100</sup>.

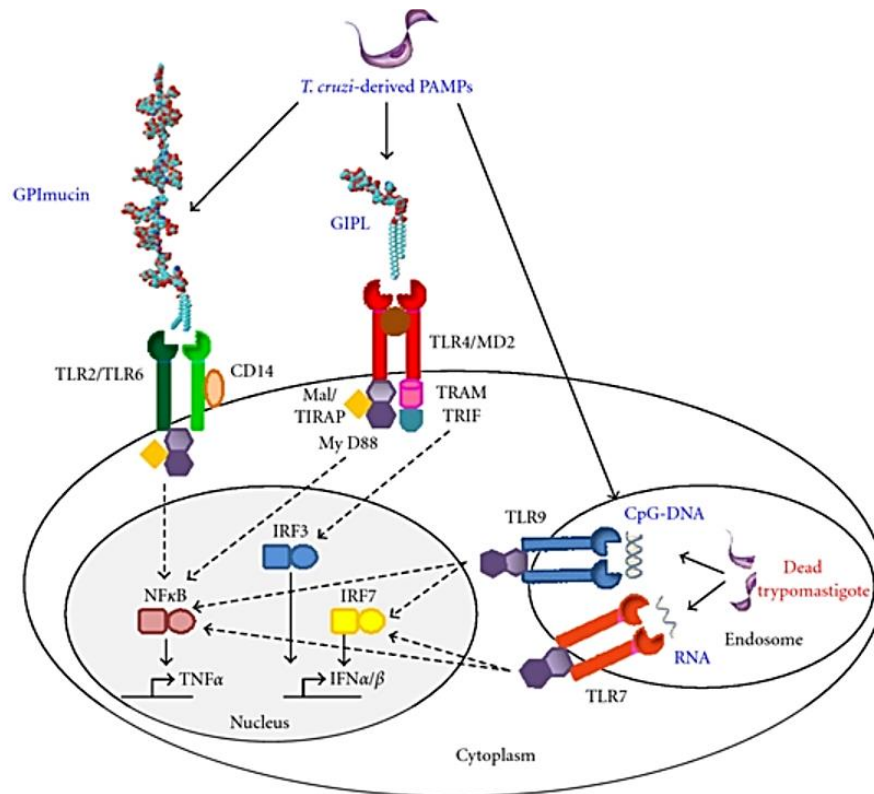


**Figure 1.7** – The TLR2/6 heterodimer and the TLR4 homodimer are cell membrane bound receptors which recognise the *T. cruzi* PAMPs present on GPI mucins or GPIs in the extracellular environment. The endosome bound TLR7 and TLR9 homodimers recognise nucleic acids that are released by internalised parasites. Upon recognition of the PAMPs, these receptors initiate signalling which results in activation of the transcription factors NF-κB, or one of a number of IRFs. These transcription factors initiate the transcription of pro-inflammatory genes<sup>101</sup>

## Macrophages

Paramount to parasite control in the initial stages of an infection is the microbicidal activity of macrophages<sup>102</sup>. However early on in the infection, in naïve individuals, macrophages are a permissive environment for parasites. This is because unstimulated macrophages produce little nitric oxide (NO) or reactive oxygen species (ROS), upon which a great deal of microbicidal activity is dependent. However, macrophages do not remain permissive and following the initial infection they secrete pro-inflammatory

cytokines, such as macrophage migration inhibitory factor (MIF) and TNF- $\alpha$ , which can act in an autocrine or paracrine manner to activate other macrophages to produce NO and peroxynitrite, an oxidant which arises from the simultaneous production of NO and ROS<sup>103,104</sup>. Furthermore, other macrophage secreted cytokines, such as IL-12, signal to NK cells and to T helper cells to secrete IFN- $\gamma$  and IL-17, two potent activators of macrophage microbicidal activity<sup>105</sup>. These activated macrophages are markedly better than non-activated macrophages at limiting parasite replication<sup>106</sup>.

### Dendritic cells

Dendritic cells (DCs), like macrophages, are phagocytic cells of the innate immune system and recognise pathogens via TLRs. After phagocytosing a pathogen, the primary role of the DC is in antigen presentation to cells of the adaptive immune system, thereby bridging innate and adaptive immunity<sup>107</sup>.

Once DCs come into contact with a pathogen, they undergo a process of maturation. This involves migration to lymphoid organs and the expression of the surface receptors CD80 and CD86, in preparation for interaction with a resting T cell. The DC then provides 3 signals to the resting T cell in order to activate it<sup>108</sup>. The first signal is the MHC receptor on the DC engaging the T cell receptor (TCR) on the T cell. The second signal is the molecules CD80 and CD86, known as co-receptors, binding to CD28 on the T cell. The third signal is the DC released cytokines, which will influence the developmental pathway in that T cell. *T. cruzi* resistant mouse strains control the parasite through the expression of IL-12 and the skewing of the T cell response to a Th1 profile, associated with IFN- $\gamma$  secretion and cellular immunity<sup>109</sup>.

### Antigen Processing

There are two major pathways of antigen presentation which differ in respect to the source of the peptide, the type of receptor used for presentation and in the subcellular

compartments utilised for peptide processing. Proteins acquired from outside the cell go through the exogenous pathway of protein presentation whereas proteins from inside the cell go through the endogenous pathway<sup>110</sup>.

All nucleated cells are capable of presenting proteins via the endogenous pathway. These proteins may be presented as a result of a cell's turnover of its intracellular material, a normal housekeeping process. However, pathogens that have invaded a host cell are also degraded and presented via this same pathway<sup>111</sup>. Peptides entering the endogenous pathway are processed within the cytosol of the cell. The resulting peptide product is presented on the cell surface in a peptide-receptor complex with an MHC I molecule, where it is recognised by CD8<sup>+</sup> T cells.

Cytosolic proteins are degraded by the host cell proteasome, a specialised protein complex present in the cytosol of cells and which functions to break down proteins into smaller subunits. After degradation by the proteasome, these subunits are transported into the host cell endoplasmic reticulum, where they are loaded onto MHC I receptors. This MHC-peptide complex is transported to the cell surface where it is recognised by CD8 T cells<sup>112</sup>. Because *T. cruzi* escapes the phagolysosome and is free within the cytoplasm of the host cell during the normal course of infection, it is perhaps not surprising that many of the *T. cruzi* peptides identified as being presented via this pathway are parasite secreted or parasite surface anchored proteins<sup>113,114</sup>.

Unlike with the endogenous pathway, the exogenous pathway of peptide presentation is restricted to professional antigen presenting cells. These cells are macrophages, dendritic cells and B cells. Peptides generated via this pathway are loaded onto MHC II cell surface receptors where they are recognised by CD4<sup>+</sup> T cells<sup>112</sup>. The exogenous pathway describes the presentation process for pathogens that are taken up from the extracellular environment within an endocytic vesicle, this can be by endocytosis, phagocytosis or macropinocytosis<sup>115</sup>. As described in section 1.1.5, the endocytic

vesicle that encompasses *T. cruzi* fuses with lysosomes as it transforms into a late endosome, becoming acidic and obtaining proteases such as cathepsins, which aid in the degradation of pathogens<sup>116</sup>. In phagocytic cells, MHC II, which is transported from the endoplasmic reticulum, localises with the late endosome and peptide is loaded into the MHC II molecule, after which the complex migrates to the cell surface<sup>111</sup>. Although *T. cruzi* has evolved mechanisms that allow it to escape the phagolysosome, this escape is not 100% effective in an infection and some parasites succumb to lysosomal degradation<sup>117</sup>. This is important in the development of host immunity as the presentation of *T. cruzi* peptides on MHC II is required for the development of an effective CD8<sup>+</sup> T cell response<sup>118</sup>.

Another, more recently discovered and less well understood pathway of antigen presentation is called cross-presentation. This is where protein from the exogenous pathway crosses into the endogenous pathway and is presented on MHC I. This is an important way for the host to be able to generate both CD4<sup>+</sup> and CD8<sup>+</sup> T cell immunity toward pathogens that have been phagocytosed by host innate immune cells<sup>115</sup>. There are two different mechanisms, or routes by which this has been shown to occur. The cytosolic route is when exogenous protein is taken up via an endosome, the protein is released into the cytosol where it is degraded by the proteasome before being loaded onto MHC I in the endoplasmic reticulum<sup>119</sup>. The other route that has been described is the vacuolar route. This does not involve proteasomes, but instead, MHC I molecules from the endoplasmic reticulum are diverted toward the early endosomes which contain the exogenous material, or pathogen<sup>120</sup>.

#### **1.4.2 Adaptive immunity : T cell response**

Adaptive immunity is notoriously slow to develop in a *T. cruzi* infection. However, once a mature immune response develops, it is effective at reducing parasite numbers and

keeping them under tight control for the remainder of the host's lifetime. There are several 'arms' of adaptive immunity, which collectively, alongside the innate immune cells, provide an integrated and effective immune response.

### CD4 T cells

Being an intracellular pathogen, *T. cruzi* induces strong cellular immunity. Part of this response is the induction of Th1 CD4<sup>+</sup> T cells. The Th1 cell is defined by the induction of the transcription factor T-bet and its ability to secrete IFN- $\gamma$  and TNF- $\alpha$  in an antigen specific manner<sup>121</sup>. The role of the CD4<sup>+</sup> T cell in *T. cruzi* infections is to help other immune cells. The primary functions of CD4<sup>+</sup> T cells are the activation of macrophages, helping to generate maximal CD8 T cell immunity and also in the development of parasite specific humoral immunity<sup>122</sup>.

CD4<sup>+</sup> T cells are antigen specific, therefore they are able to recognise and activate infected cells in a discriminate manner through recognition of *T. cruzi* antigen in association with MHC I. CD4<sup>+</sup> T cells recognise infected macrophages, and upon binding to them, secrete IFN- $\gamma$ . As discussed above, this promotes parasite killing. In addition to this essential role, Th1 CD4<sup>+</sup> T cells are also necessary for maximal CD8<sup>+</sup> T cell expansion in a natural infection. MHC II KO mice that lack CD4<sup>+</sup> T cells have lower frequencies of CD8<sup>+</sup> T cells<sup>118</sup>.

Though less well studied, another CD4<sup>+</sup> T cell subset, Th17 cells, also have a protective role in *T. cruzi* infection. These cells become committed to differentiation by activation of the transcription factor ROR $\gamma$ T in the naïve CD4<sup>+</sup> T cell<sup>123</sup>. These cells are capable of IL-17A secretion and IL-17A deficient mice have a lower survival rate and higher parasitaemia compared to WT<sup>105</sup>. Adoptive transfer experiments have revealed that the mechanisms of protection for Th17 cells are similar to Th1 cells. Th17 cells increase parasite killing in phagocytic cells through retention of the parasite in the phagolysosome and also promote CD8<sup>+</sup> T cell proliferation<sup>124,125</sup>.

## CD8 T cells

Because for the majority of its life cycle, *T. cruzi* is an intracellular pathogen, the recognition of infected cells and their targeted destruction is essential to preventing the propagation of an infection. This role is performed primarily by CD8<sup>+</sup> T cells<sup>126</sup>. CD8<sup>+</sup> T cells are cytotoxic cells which are generated in great numbers in a *T. cruzi* infection. They are able to recognise and lyse infected cells through the delivery of lytic granules directly into the infected cell or through a receptor mediated self-destruct message delivered via the Fas ligand<sup>127</sup>. KO mice that are devoid of CD8<sup>+</sup> T cells succumb to the acute infection, even in a usually non-lethal challenge<sup>128</sup>.

Aside from cytolysis, which is an important function of these cells, part of the protective function of CD8<sup>+</sup> T cells is their ability to secrete IFN- $\gamma$ . This has been demonstrated experimentally in some elegant adoptive transfer experiments, which used T cell lines that had cytolytic activity, but did not secrete IFN- $\gamma$ . These T cells were unable to protect mice in an experimental infection. In contrast, T cell lines that did express IFN- $\gamma$  were able to protect mice from a lethal infection. Therefore, the protection that is provided in adoptive transfer of CD8<sup>+</sup> T cells is dependent on IFN- $\gamma$  and not on the cytolytic activity of the CD8<sup>+</sup> T cell<sup>129</sup>. Evidence for this also exists in natural human infections whereby patients with higher circulating numbers of IFN- $\gamma$ <sup>+</sup> CD8<sup>+</sup> T cells have less severe clinical disease<sup>130</sup>.

Given the effectiveness with which CD8<sup>+</sup> T cells are able to combat *T. cruzi*, they are widely considered the most important cell type in the immune response. Vaccine regimens therefore often aim to induce swift and strong CD8<sup>+</sup> T cell mediated immunity<sup>131</sup>. Despite this, *T. cruzi* infections are life-long. Recent work confirmed that life-long infection does not result from exhaustion of the T cell response, which remains competent throughout<sup>132</sup>. The more likely explanation for this is that the parasite has evolved mechanisms of evasion which supersede the capabilities of adaptive immunity.

The CD8<sup>+</sup> T cell response in *T. cruzi* infections, curiously so, is heavily biased toward a small number of epitopes contained within the trans-sialidase (TS) family of proteins. Up to 30% of the CD8<sup>+</sup> T cells in a mouse can be specific for a small number of peptides<sup>114</sup>. The TS family of proteins is encoded by thousands of genes. It is important for the parasite life-cycle and performs functions such as cell invasion and evasion of the complement system<sup>114,133</sup>. These proteins are also expressed late in the infection cycle on the surface of infected cells, only becoming visible between 24 and 48 hours into an infection<sup>41</sup>. Therefore, a large proportion of the host CD8<sup>+</sup> T cells are specific for an ever changing target that is expressed late in the infection.

In addition, *T. cruzi* has been shown to invade host cells in a silent process by which it does not activate host defence mechanisms for 24-48 hours. This means that the resulting T cell response is also delayed. With the Y strain parasite, CD8<sup>+</sup> T cells are first detectable in the mouse around day 9 and quickly rise between days 9 and 15. This is much slower than with other intracellular infections such as *Plasmodium*, *Listeria* and lymphocytic choriomeningitis virus (LCMV)<sup>128</sup>.

#### **1.4.3 Adaptive immunity : B cell response**

B cells are also mononuclear lymphocytic cells. There are several types, with follicular B cells being the most numerous subset in the spleen and lymph nodes. Unlike T cells, B cells and the antibodies they secrete recognise antigen in their native conformation and not as a peptide-MHC complex.

Following infection, follicular B cells undergo proliferation and differentiation in the spleen and secondary lymphoid tissues in a T cell dependent manner<sup>134</sup>. This process occurs in microenvironments within the spleen and lymphoid tissue referred to as the B cell follicle, inside which B cells develop into terminally differentiated plasma cells or long-lived memory B cells. In the initial stages of the infection, B cells differentiate into

IgM secreting plasma cells. Through a process of continued B cell maturation following the initial infection, a germinal centre develops in the B cell follicle and gives rise to plasma cells, which secrete antibodies of a different class and with a much higher affinity for their target<sup>135</sup>. These are IgG antibodies.

Following a *T. cruzi* infection, IgM is the first detectable antibody in the serum, appearing around two weeks following infection<sup>136</sup>. They are initially present at very high titres, but then decreases after the acute stage and are undetectable in chronic patients<sup>137,138</sup>. Experimentally, the early production of high titres of IgM are associated with resistance to infection in the acute stage, with resistant mouse strains producing higher IgM titres than susceptible mice<sup>122,139</sup>. In humans, antibody production in the acute phase is associated with lytic activity and complement mediated killing of blood trypomastigotes<sup>140</sup>.

IgG antibodies begin to appear between a few days and week after IgM, however unlike the IgM response, they remain detectable for many years after the resolution of the acute stage<sup>137</sup>. IgG antibodies from chronically infected mice have been shown to be effective at protecting naïve mice from infection by clearing blood trypomastigotes. This occurs independently of complement mediated lysis and instead relies on Fc mediated phagocytosis, with antibodies binding the blood trypomastigotes and being taken up by phagocytic mononuclear cells and polymorphonuclear cells such as neutrophils<sup>141,142</sup>.

As with the T cell response, the humoral response to *T. cruzi* is delayed, with the parasite inducing a polyclonal B cell activation prior to the development of parasite specific humoral immunity<sup>122</sup>. It is not clear whether this is a mechanism of immune subversion and exactly how this benefits the parasite. However, the activation of non-specific B cell clones may act to delay the activation of B cells with specificity for the parasite<sup>143</sup>. Mouse strains which are more resistant to the infection experience a lower

hypergammaglobulinemia and instead they generate a much quicker parasite specific IgG response, correlating with a Th1 cytokine profile<sup>122</sup>.

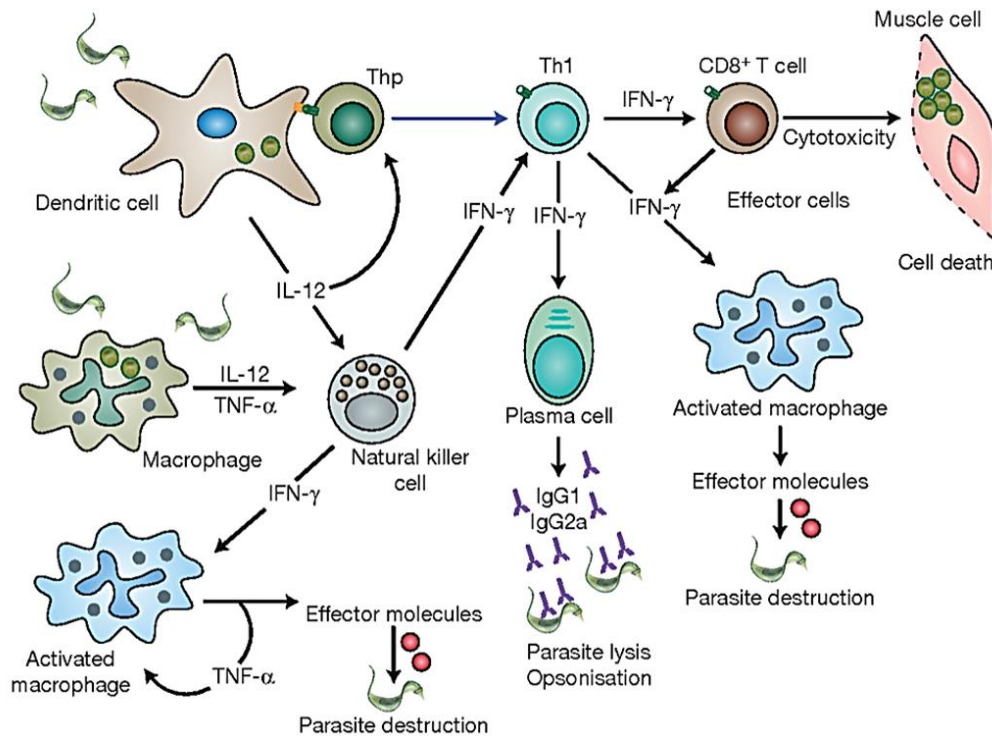


**Figure 1.8** – Generation of protective immunity in a *T. cruzi* infection. DC interaction with a naïve T cell (Thp) results in the development of Th1 cells, which secrete IFN-γ. These T helper cells promote the generation of mature CD8 T cells, with cytotoxic and cytokine secreting capability. T helper cells also secrete cytokines which activate macrophages and are associated with the generation of a parasite specific antibody response<sup>144</sup>

## 1.5 Vaccination

The rationale for vaccinating against Chagas disease comes from the fact that disease severity is linked to parasite persistence and previous experimental vaccinations have demonstrated positive outcomes in pre-clinical models<sup>13,145</sup>. Therefore, evidence suggests that vaccination with a view to reducing the parasite burden would be conducive to an improved clinical outcome. Alternatively, transmission blocking vaccines

or a vaccine that complements current drug treatments by reducing the length of the treatment or improving the chances of successful treatment would also help to reduce the overall disease burden<sup>146</sup>.

The first vaccines for Chagas disease were based on the observations that animals surviving an acute infection developed resistance to re-infection. Therefore, early attempts at vaccination used killed parasites, culture-attenuated parasites or crude methods of parasite attenuation such as a pressure chamber. Some of these methods showed partial success and were later the subject of further confirmatory experiments<sup>147</sup>.

These first vaccines were limited by the available technology of the time, but provided support for the idea that vaccinating against the parasite could improve the hosts control over the infection. In later years, with technological advancements, came more detailed vaccine studies. For example, cell fractionation by centrifugation revealed that specific subcellular fractions of the parasite had different protective capacities<sup>148</sup>. Later on, advances in our scientific knowledge of protozoology led to the testing of non-virulent *T. cruzi*-related organisms as live vaccines, owing to the fact that these related organisms shared antigens with *T. cruzi*<sup>149</sup>. Because these related organisms, *Phytomonas serpens* and *Trypanosoma rangeli*, are non-disease causing in humans, they were seen as risk-free alternatives for vaccination against *T. cruzi*. Unfortunately, despite their relatedness, these organisms provided incomplete protection in the face of a *T. cruzi* challenge<sup>149,150</sup>.

The biggest leap in our technological capability arrived with the advent of modern biotechnology. The vaccines that have been produced with these new tools are today the best studied and furthest in development. One of these vaccines is based on the parasite protein Tc24<sup>11</sup>. This is a calcium binding protein which localises to the trypanosome flagellum. It was first identified in 1989 and has since been widely studied for its potential as a vaccine candidate. Tc24 administered as a recombinant protein, adjuvanted, either alone or alongside other candidate proteins has proven to be

immunogenic in mice and recall responses to the protein have been detected in chronic human patients <sup>12,151</sup>. Much work has gone into the modification, streamlining and upscaling the production of the protein for manufacture <sup>152,153</sup>.

Advances in vaccination technologies have in part been driven by our constantly developing understanding of immunology, in particular, the types of immunological responses that are protective. This is indeed true for the most recent technological leap, the development of viral vectored vaccination. The use of viral vectors to deliver *T. cruzi* genes is a particularly promising approach given that this vaccination strategy induces strong cellular immunity<sup>154</sup>. Due to the intracellular nature of the infection, T cells are widely considered the most important mediator of parasite killing (section 1.4.2 Adaptive immunity). Specifically, CD8<sup>+</sup> T cells are considered crucial in determining the outcome of infection due to their ability to directly lyse infected host cells <sup>155</sup>. One viral vectored vaccine study was shown not only to preserve heart function, but to reverse chagasic cardiomyopathy in chronically infected mice when administered as a therapeutic <sup>13</sup>. The immunogenic potential of viral vectors, coupled with their proven safety profile in humans has led to their advancement through clinical trials for a number of infections and cancers. They remain a bright prospect for the development of a *T. cruzi* vaccine <sup>156,157</sup>.

Despite the advances in vaccine technology, it is still the case that not a single *T. cruzi* vaccine has advanced from pre-clinical trials<sup>158</sup>. Much of this is due to the nature of the disease, it only presents decades after the initial infection, making vaccine testing difficult. However, the other feature of the infection, the fact that parasites are rare in the chronic stage of the disease means that it is difficult to monitor the parasite burden beyond the acute stage. Therefore testing vaccine efficacy has long been a near impossible task and is subject to sampling biases when using techniques such as PCR. Methods that would allow for accurate monitoring of the parasite burden in a non-time consuming fashion, and without bias, would be a significant step in advancing pre-clinical testing of vaccines.

## **1.6 The animal model: Bioluminescent imaging**

Research in *T. cruzi* benefits greatly from the fact that the parasite is capable of infecting all mammalian species. This means that the study of *T. cruzi in vivo* requires no specific or specialised animal models and has been studied in several mammalian model species, including but not limited to the mouse, guinea pig, rabbit, rat, dog and primates<sup>159</sup>.

The most commonly used animal model is the mouse, which has long been used for the study of the immunology and pathophysiology of the infection, as well as the biology of the host-parasite interaction<sup>160</sup>. The ability to use a wide range of parasite strains, a growing number of which are having their genomes published<sup>161,162</sup>, and the ability to use mice with well-defined genotypes and phenotypes mean that the mouse model is a tractable system.

Different parasite and mouse combinations give rise to different infection dynamics and can give different clinical outcomes ranging from a mild infection, where the host suffers almost no ill effect, to lethal infections where 100% of mice succumb in less than a month<sup>163,164</sup>. This complicates the task of comparing different studies by different research groups. However, it can be advantageous to individual groups, as different strain-host combinations can reliably give rise to a desired clinical outcome, allowing for the study of specific aspects of the disease.

Clinically, the pathological outcome of the chronic infection in mice resembles that in humans, particularly in terms of heart disease<sup>165</sup>. Histological analysis reveals inflammation and fibrosis which parallels human histological observations. In addition, ECG alternations can also be observed in chronically infected mice, with the specific alteration showing a mouse and parasite strain dependent pattern<sup>166</sup>. The GI abnormalities seen in a small percentage of patients in the chronic disease can also be replicated in the mouse. Some infected mouse strains undergo intestinal dilation and

damage of the myenteric plexus, as a result they suffer from reduced gastric motility and gut transit times<sup>167,168</sup>. Clinically speaking, the infection in the mouse is a useful proxy for human infection.

A relatively new tool in the arsenal for studying *T. cruzi* is *in vivo* bioluminescent imaging<sup>58</sup>. The approach is based on exploiting transgenic parasites which express a modified firefly luciferase enzyme. This enzyme reduces its natural substrate luciferin in an ATP-dependent reaction, resulting in the emission of light. This gives live parasites bioluminescent properties, allowing murine infections to be monitored in real time, without the need for invasive procedures. The system developed in our lab makes use of a codon-optimised modified firefly luciferase that emits light at the red end of the spectrum (617 nm)<sup>88,169</sup>. Red light has greater tissue penetrating properties than the normal green/yellow light emitted by wild type luciferase, because longer wavelength light is subject to reduced scatter and is not absorbed by haemoglobin. The system is sensitive enough to detect as few as 100 transgenic parasites when injected i.p. into a mouse, and allows the routine detection of parasites during the chronic stage of an infection. This had not previously been possible<sup>58</sup>. Bioluminescent imaging has been revolutionary in *T. cruzi* research, quickly being utilised as a tool for drug testing<sup>170</sup>. Additionally, it has provided new insights into *T. cruzi* infection biology that would not have been possible without these tools<sup>171,172</sup>.

It has been observed that chronic *T. cruzi* infection is truly dynamic, with parasites appearing and disappearing from tissues within a matter of hours<sup>172</sup>. In addition, the study of different bioluminescent parasite and mouse strain combinations has revealed that infections in clinically relevant tissues, such as the GI tract and the heart, show very different infection dynamics<sup>58,88</sup>. The GI tract seems to be a reservoir, from which the infection regularly seeds and migrates to other peripheral sites, including the heart. Novel findings such as these would not have been possible without the bioluminescence

system. These observations could hold the key to developing new therapeutic strategies.

It is abundantly clear that the bioluminescent system has scope to be utilised for studying *T. cruzi* immunology, infection biology and importantly for advancing the field of vaccine research. Despite the progress made in the development of vaccines for intracellular infections over recent years<sup>173</sup>, detailed analysis of vaccine efficacy for *T. cruzi* has long been restricted by an inability to accurately monitor the parasite burden during the chronic stage.

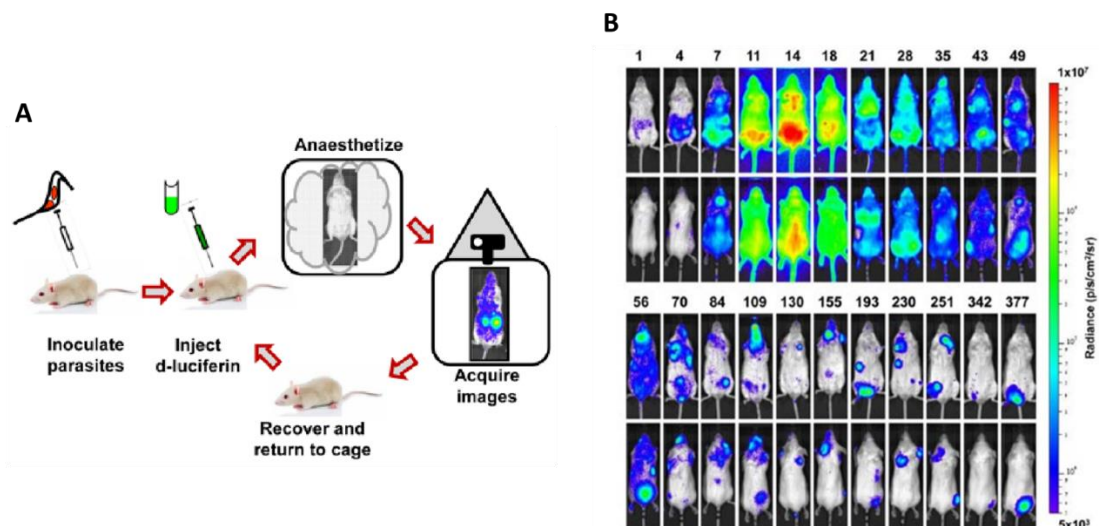


**Figure 1.9** – *In vivo* bioluminescent imaging. A, the procedure for bioluminescent imaging follows a standardised set of procedures. Infected mice are injected i.p. with the luciferin substrate prior to anaesthesia. Anaesthetised mice are imaged before recovery and return to their cage. This process is repeated each time an image is acquired. B, Example images of an infected BALB/c mouse taken over a year long period, the day post infection is above each image. Bioluminescence is overlaid on the image of the mouse and the intensity is demonstrated using a heatmap, the red colour indicates the most intense bioluminescence and the violet represents the least intense<sup>58</sup>

## **1.7 Research questions and aims**

To our knowledge, this is the first time that a bioluminescent system, capable of imaging the chronic stage parasite burden has been available to study aspects of *T. cruzi* immunology and vaccinology. We have therefore set out to exploit the benefits of bioluminescent imaging, combined with other more established techniques such as histopathology, cell biology and molecular biology to better understand the potential for vaccinating against *T. cruzi*. To this end, we set out the following aims.

1. To use highly sensitive bioluminescent imaging as a method of assessing the efficacy of a prophylactic *T. cruzi* vaccine in the acute and the chronic stage, with a view to establish the value of this technology for future pre-clinical applications.
2. To use the system to provide a more complete picture of natural immunity to *T. cruzi* infection, with a view to understanding the full potential of the immune response to establish correlates of natural protection.
3. Capitalise on our understanding of the gut as a niche site for parasite persistence to test whether locally administered immune modulating agents could be used to combat the infection, with a view to informing the development of novel therapeutic strategies.
4. Depending on the outcomes of the above, to begin a study of the potential of live attenuated vaccines to protect against Chagas disease.

In order to achieve these aims we have set out the following objectives.

1. Develop a *T. cruzi* vaccine for testing with the bioluminescent system, using a proven immunogenic vaccine platform and based on known effective *T. cruzi* antigens.
2. Develop an effective protocol and an appropriate timeline for an infection-re-infection study in order to observe (a) the maximum immune mediated protection

and (b) to correlate immunological parameters with protection in an infection-experienced host.

3. Optimise a dosing regimen for the administration of an immune modulating agent to the colon of chronically infected mice.
4. Identify appropriate genes for targeted replacement with drug-resistance cassettes and generate stably transfected cell lines for testing as live vaccines.

## 1.8 References

- 1 Steverding, D. The history of Chagas disease. *Parasit Vectors* **7**, 317, doi:10.1186/1756-3305-7-317 (2014).
- 2 Chagas disease in Latin America: an epidemiological update based on 2010 estimates. *Wkly Epidemiol Rec* **90**, 33-43 (2015).
- 3 Clayton, J. Chagas disease 101. *Nature* **465**, S4-5, doi:10.1038/nature09220 (2010).
- 4 Dias, J. C. Southern Cone Initiative for the elimination of domestic populations of *Triatoma infestans* and the interruption of transfusional Chagas disease. Historical aspects, present situation, and perspectives. *Mem Inst Oswaldo Cruz* **102 Suppl 1**, 11-18, doi:10.1590/s0074-02762007005000092 (2007).
- 5 Pereira Gde, A., Louzada-Neto, F., Barbosa Vde, F., Ferreira-Silva, M. M. & de Moraes-Souza, H. Performance of six diagnostic tests to screen for Chagas disease in blood banks and prevalence of *Trypanosoma cruzi* infection among donors with inconclusive serology screening based on the analysis of epidemiological variables. *Rev Bras Hematol Hemoter* **34**, 292-297, doi:10.5581/1516-8484.20120074 (2012).
- 6 Jansen, A. M., Xavier, S. & Roque, A. L. R. *Trypanosoma cruzi* transmission in the wild and its most important reservoir hosts in Brazil. *Parasit Vectors* **11**, 502, doi:10.1186/s13071-018-3067-2 (2018).
- 7 Gascon, J., Bern, C. & Pinazo, M. J. Chagas disease in Spain, the United States and other non-endemic countries. *Acta Trop* **115**, 22-27, doi:10.1016/j.actatropica.2009.07.019 (2010).
- 8 Aldasoro, E. *et al.* What to expect and when: benznidazole toxicity in chronic Chagas' disease treatment. *J Antimicrob Chemother* **73**, 1060-1067, doi:10.1093/jac/dkx516 (2018).
- 9 Crespillo-Andujar, C. *et al.* Toxicity of nifurtimox as second-line treatment after benznidazole intolerance in patients with chronic Chagas disease: when available options fail. *Clin Microbiol Infect* **24**, 1344 e1341-1344 e1344, doi:10.1016/j.cmi.2018.06.006 (2018).
- 10 Sales Junior, P. A. *et al.* Experimental and Clinical Treatment of Chagas Disease: A Review. *Am J Trop Med Hyg* **97**, 1289-1303, doi:10.4269/ajtmh.16-0761 (2017).
- 11 Dumonteil, E. *et al.* Accelerating the development of a therapeutic vaccine for human Chagas disease: rationale and prospects. *Expert Rev Vaccines* **11**, 1043-1055, doi:10.1586/erv.12.85 (2012).

- 12 Villanueva-Lizama, L. E. *et al.* Trypanosoma cruzi vaccine candidate antigens Tc24 and TSA-1 recall memory immune response associated with HLA-A and -B supertypes in Chagasic chronic patients from Mexico. *PLoS Negl Trop Dis* **12**, e0006240, doi:10.1371/journal.pntd.0006240 (2018).
- 13 Pereira, I. R. *et al.* A human type 5 adenovirus-based Trypanosoma cruzi therapeutic vaccine re-programs immune response and reverses chronic cardiomyopathy. *PLoS Pathog* **11**, e1004594, doi:10.1371/journal.ppat.1004594 (2015).
- 14 Portillo, S. *et al.* A prophylactic alpha-Gal-based glycovaccine effectively protects against murine acute Chagas disease. *NPJ Vaccines* **4**, 13, doi:10.1038/s41541-019-0107-7 (2019).
- 15 Samuels, A. M. *et al.* Epidemiology of and impact of insecticide spraying on Chagas disease in communities in the Bolivian Chaco. *PLoS Negl Trop Dis* **7**, e2358, doi:10.1371/journal.pntd.0002358 (2013).
- 16 <https://vizhub.healthdata.org/gbd-compare>.
- 17 Lidani, K. C. F. *et al.* Chagas Disease: From Discovery to a Worldwide Health Problem. *Front Public Health* **7**, 166, doi:10.3389/fpubh.2019.00166 (2019).
- 18 Pinto Dias, J. C. Human chagas disease and migration in the context of globalization: some particular aspects. *J Trop Med* **2013**, 789758, doi:10.1155/2013/789758 (2013).
- 19 WHO. Chagas disease (American trypanosomiasis). (2019).
- 20 Klein, N., Hurwitz, I. & Durvasula, R. Globalization of Chagas Disease: A Growing Concern in Nonendemic Countries. *Epidemiology Research International* **2012**, 13, doi:10.1155/2012/136793 (2012).
- 21 Gurevitz, J. M. *et al.* Intensified surveillance and insecticide-based control of the Chagas disease vector Triatoma infestans in the Argentinean Chaco. *PLoS Negl Trop Dis* **7**, e2158, doi:10.1371/journal.pntd.0002158 (2013).
- 22 Hernandez, S. *et al.* Autochthonous Transmission of Trypanosoma Cruzi in Southern California. *Open Forum Infect Dis* **3**, ofw227, doi:10.1093/ofid/ofw227 (2016).
- 23 Schmunis, G. A. & Yadon, Z. E. Chagas disease: a Latin American health problem becoming a world health problem. *Acta Trop* **115**, 14-21, doi:10.1016/j.actatropica.2009.11.003 (2010).
- 24 Lukes, J. *et al.* Kinetoplast DNA network: evolution of an improbable structure. *Eukaryot Cell* **1**, 495-502, doi:10.1128/ec.1.4.495-502.2002 (2002).

- 25 d'Avila-Levy, C. M. *et al.* Exploring the environmental diversity of kinetoplastid flagellates in the high-throughput DNA sequencing era. *Mem Inst Oswaldo Cruz* **110**, 956-965, doi:10.1590/0074-02760150253 (2015).
- 26 Stuart, K. *et al.* Kinetoplastids: related protozoan pathogens, different diseases. *J Clin Invest* **118**, 1301-1310, doi:10.1172/JCI33945 (2008).
- 27 Filardy, A. A. *et al.* Human Kinetoplastid Protozoan Infections: Where Are We Going Next? *Front Immunol* **9**, 1493, doi:10.3389/fimmu.2018.01493 (2018).
- 28 Bice, D. E. & Zeledon, R. Comparison of infectivity of strains of *Trypanosoma cruzi* (Chagas, 1909). *J Parasitol* **56**, 663-670 (1970).
- 29 Martinez-Diaz, R. A., Escario, J. A., Nogal-Ruiz, J. J. & Gomez-Barrio, A. Biological characterization of *Trypanosoma cruzi* strains. *Mem Inst Oswaldo Cruz* **96**, 53-59, doi:10.1590/s0074-02762001000100006 (2001).
- 30 Brener, Z. & Chiari, E. [Morphological Variations Observed in Different Strains of *Trypanosoma Cruzi*]. *Rev Inst Med Trop Sao Paulo* **5**, 220-224 (1963).
- 31 Lewis, M. D. *et al.* Flow cytometric analysis and microsatellite genotyping reveal extensive DNA content variation in *Trypanosoma cruzi* populations and expose contrasts between natural and experimental hybrids. *Int J Parasitol* **39**, 1305-1317, doi:10.1016/j.ijpara.2009.04.001 (2009).
- 32 Zingales, B. *et al.* A new consensus for *Trypanosoma cruzi* intraspecific nomenclature: second revision meeting recommends TcI to TcVI. *Mem Inst Oswaldo Cruz* **104**, 1051-1054, doi:10.1590/s0074-02762009000700021 (2009).
- 33 Francisco, A. F., Jayawardhana, S., Lewis, M. D., Taylor, M. C. & Kelly, J. M. Biological factors that impinge on Chagas disease drug development. *Parasitology* **144**, 1871-1880, doi:10.1017/S0031182017001469 (2017).
- 34 Zingales, B. *et al.* The revised *Trypanosoma cruzi* subspecific nomenclature: rationale, epidemiological relevance and research applications. *Infect Genet Evol* **12**, 240-253, doi:10.1016/j.meegid.2011.12.009 (2012).
- 35 Lewis, M. D. *et al.* Recent, independent and anthropogenic origins of *Trypanosoma cruzi* hybrids. *PLoS Negl Trop Dis* **5**, e1363, doi:10.1371/journal.pntd.0001363 (2011).
- 36 Zingales, B. *Trypanosoma cruzi* genetic diversity: Something new for something known about Chagas disease manifestations, serodiagnosis and drug sensitivity. *Acta Trop* **184**, 38-52, doi:10.1016/j.actatropica.2017.09.017 (2018).

- 37 Gurtler, R. E. & Cardinal, M. V. Reservoir host competence and the role of domestic and commensal hosts in the transmission of *Trypanosoma cruzi*. *Acta Trop* **151**, 32-50, doi:10.1016/j.actatropica.2015.05.029 (2015).
- 38 Noireau, F., Diosque, P. & Jansen, A. M. *Trypanosoma cruzi*: adaptation to its vectors and its hosts. *Vet Res* **40**, 26, doi:10.1051/vetres/2009009 (2009).
- 39 Marsden, P. D. *Trypanosoma cruzi* infections in CFI mice. II. Infections induced by different routes. *Ann Trop Med Parasitol* **61**, 62-67 (1967).
- 40 Fernandes, M. C. & Andrews, N. W. Host cell invasion by *Trypanosoma cruzi*: a unique strategy that promotes persistence. *FEMS Microbiol Rev* **36**, 734-747, doi:10.1111/j.1574-6976.2012.00333.x (2012).
- 41 Kurup, S. P. & Tarleton, R. L. The *Trypanosoma cruzi* flagellum is discarded via asymmetric cell division following invasion and provides early targets for protective CD8(+) T cells. *Cell Host Microbe* **16**, 439-449, doi:10.1016/j.chom.2014.09.003 (2014).
- 42 Dvorak, J. A. & Hyde, T. P. *Trypanosoma cruzi*: interaction with vertebrate cells in vitro. 1. Individual interactions at the cellular and subcellular levels. *Exp Parasitol* **34**, 268-283 (1973).
- 43 Yoshida, N. & Cortez, M. *Trypanosoma cruzi*: parasite and host cell signaling during the invasion process. *Subcell Biochem* **47**, 82-91 (2008).
- 44 Nogueira, N. P. *et al.* Proliferation and differentiation of *Trypanosoma cruzi* inside its vector have a new trigger: redox status. *PLoS One* **10**, e0116712, doi:10.1371/journal.pone.0116712 (2015).
- 45 Kollien, A. H. & Schaub, G. A. The development of *Trypanosoma cruzi* in triatominae. *Parasitol Today* **16**, 381-387 (2000).
- 46 Cordero, E. M. *et al.* Expression of GP82 and GP90 surface glycoprotein genes of *Trypanosoma cruzi* during in vivo metacyclogenesis in the insect vector *Rhodnius prolixus*. *Acta Trop* **105**, 87-91, doi:10.1016/j.actatropica.2007.08.004 (2008).
- 47 Pech-Canul, A. C., Monteon, V. & Solis-Oviedo, R. L. A Brief View of the Surface Membrane Proteins from *Trypanosoma cruzi*. *J Parasitol Res* **2017**, 3751403, doi:10.1155/2017/3751403 (2017).
- 48 Ruiz, R. C. *et al.* Infectivity of *Trypanosoma cruzi* strains is associated with differential expression of surface glycoproteins with differential Ca<sup>2+</sup> signalling activity. *Biochem J* **330 ( Pt 1)**, 505-511, doi:10.1042/bj3300505 (1998).
- 49 Yoshida, N. Molecular basis of mammalian cell invasion by *Trypanosoma cruzi*. *An Acad Bras Cienc* **78**, 87-111, doi:10.1590/s0001-37652006000100010 (2006).

- 50 Magdesian, M. H. *et al.* Infection by *Trypanosoma cruzi*. Identification of a parasite ligand and its host cell receptor. *J Biol Chem* **276**, 19382-19389, doi:10.1074/jbc.M011474200 (2001).
- 51 da Silva, C. V. *et al.* Characterization of a 21kDa protein from *Trypanosoma cruzi* associated with mammalian cell invasion. *Microbes Infect* **11**, 563-570, doi:10.1016/j.micinf.2009.03.007 (2009).
- 52 Vray, B. *et al.* Up-regulation of galectin-3 and its ligands by *Trypanosoma cruzi* infection with modulation of adhesion and migration of murine dendritic cells. *Glycobiology* **14**, 647-657, doi:10.1093/glycob/cwh068 (2004).
- 53 Kleshchenko, Y. Y. *et al.* Human galectin-3 promotes *Trypanosoma cruzi* adhesion to human coronary artery smooth muscle cells. *Infect Immun* **72**, 6717-6721, doi:10.1128/IAI.72.11.6717-6721.2004 (2004).
- 54 Barbosa, H. S. & de Meirelles Mde, N. Ultrastructural detection in vitro of WGA-, RCA I-, and Con A-binding sites involved in the invasion of heart muscle cells by *Trypanosoma cruzi*. *Parasitol Res* **78**, 404-409, doi:10.1007/bf00931696 (1992).
- 55 Hall, B. S. & Pereira, M. A. Dual role for transforming growth factor beta-dependent signaling in *Trypanosoma cruzi* infection of mammalian cells. *Infect Immun* **68**, 2077-2081, doi:10.1128/iai.68.4.2077-2081.2000 (2000).
- 56 Scharfstein, J. *et al.* Host cell invasion by *Trypanosoma cruzi* is potentiated by activation of bradykinin B(2) receptors. *J Exp Med* **192**, 1289-1300, doi:10.1084/jem.192.9.1289 (2000).
- 57 Maganto-Garcia, E., Punzon, C., Terhorst, C. & Fresno, M. Rab5 activation by Toll-like receptor 2 is required for *Trypanosoma cruzi* internalization and replication in macrophages. *Traffic* **9**, 1299-1315, doi:10.1111/j.1600-0854.2008.00760.x (2008).
- 58 Lewis, M. D., Francisco, A. F., Taylor, M. C. & Kelly, J. M. A new experimental model for assessing drug efficacy against *Trypanosoma cruzi* infection based on highly sensitive in vivo imaging. *J Biomol Screen* **20**, 36-43, doi:10.1177/1087057114552623 (2015).
- 59 Nogueira, N. & Cohn, Z. *Trypanosoma cruzi*: mechanism of entry and intracellular fate in mammalian cells. *J Exp Med* **143**, 1402-1420, doi:10.1084/jem.143.6.1402 (1976).
- 60 Carvalho, T. M., De Souza, W. & Coimbra, E. S. Internalization of components of the host cell plasma membrane during infection by *Trypanosoma cruzi*. *Mem Inst Oswaldo Cruz* **94 Suppl 1**, 143-147, doi:10.1590/s0074-02761999000700016 (1999).

- 61 Barbosa, H. S. & Meirelles, M. N. Evidence of participation of cytoskeleton of heart muscle cells during the invasion of *Trypanosoma cruzi*. *Cell Struct Funct* **20**, 275-284, doi:10.1247/csf.20.275 (1995).
- 62 Huotari, J. & Helenius, A. Endosome maturation. *EMBO J* **30**, 3481-3500, doi:10.1038/emboj.2011.286 (2011).
- 63 Barrias, E. S., de Carvalho, T. M. & De Souza, W. *Trypanosoma cruzi*: Entry into Mammalian Host Cells and Parasitophorous Vacuole Formation. *Front Immunol* **4**, 186, doi:10.3389/fimmu.2013.00186 (2013).
- 64 Tam, C. *et al.* Exocytosis of acid sphingomyelinase by wounded cells promotes endocytosis and plasma membrane repair. *J Cell Biol* **189**, 1027-1038, doi:10.1083/jcb.201003053 (2010).
- 65 Fernandes, M. C. *et al.* *Trypanosoma cruzi* subverts the sphingomyelinase-mediated plasma membrane repair pathway for cell invasion. *J Exp Med* **208**, 909-921, doi:10.1084/jem.20102518 (2011).
- 66 Albertti, L. A., Macedo, A. M., Chiari, E., Andrews, N. W. & Andrade, L. O. Role of host lysosomal associated membrane protein (LAMP) in *Trypanosoma cruzi* invasion and intracellular development. *Microbes Infect* **12**, 784-789, doi:10.1016/j.micinf.2010.05.015 (2010).
- 67 Andrews, N. W. & Whitlow, M. B. Secretion by *Trypanosoma cruzi* of a hemolysin active at low pH. *Mol Biochem Parasitol* **33**, 249-256, doi:10.1016/0166-6851(89)90086-8 (1989).
- 68 Carter, Y. L., Juliano, J. J., Montgomery, S. P. & Qvarnstrom, Y. Acute Chagas disease in a returning traveler. *Am J Trop Med Hyg* **87**, 1038-1040, doi:10.4269/ajtmh.2012.12-0354 (2012).
- 69 Hemmige, V., Tanowitz, H. & Sethi, A. *Trypanosoma cruzi* infection: a review with emphasis on cutaneous manifestations. *Int J Dermatol* **51**, 501-508, doi:10.1111/j.1365-4632.2011.05380.x (2012).
- 70 Medeiros, M. B., Guerra, J. A. & Lacerda, M. V. Meningoencephalitis in a patient with acute Chagas disease in the Brazilian Amazon. *Rev Soc Bras Med Trop* **41**, 520-521 (2008).
- 71 Puigbo, J. J. *et al.* Diagnosis of Chagas' cardiomyopathy. Non-invasive techniques. *Postgrad Med J* **53**, 527-532, doi:10.1136/pgmj.53.623.527 (1977).

- 72 Galvao, L. M. *et al.* PCR assay for monitoring *Trypanosoma cruzi* parasitemia in childhood after specific chemotherapy. *J Clin Microbiol* **41**, 5066-5070, doi:10.1128/jcm.41.11.5066-5070.2003 (2003).
- 73 Bonney, K. M. & Engman, D. M. Autoimmune pathogenesis of Chagas heart disease: looking back, looking ahead. *Am J Pathol* **185**, 1537-1547, doi:10.1016/j.ajpath.2014.12.023 (2015).
- 74 Rassi, A., Jr., Marin, J. A. N. & Rassi, A. Chronic Chagas cardiomyopathy: a review of the main pathogenic mechanisms and the efficacy of aetiological treatment following the BENznidazole Evaluation for Interrupting Trypanosomiasis (BENEFIT) trial. *Mem Inst Oswaldo Cruz* **112**, 224-235, doi:10.1590/0074-02760160334 (2017).
- 75 Lopes, E. R. *et al.* [Prevalence of visceromegalies in necropsies carried out in Triangulo Mineiro from 1954 to 1988]. *Rev Soc Bras Med Trop* **22**, 211-215 (1989).
- 76 Camargos, S. *et al.* CNS chagoma: Reactivation in an immunosuppressed patient. *Neurology* **88**, 605-606, doi:10.1212/WNL.0000000000003600 (2017).
- 77 Yasukawa, K. *et al.* *Trypanosoma cruzi* meningoencephalitis in a patient with acquired immunodeficiency syndrome. *Am J Trop Med Hyg* **91**, 84-85, doi:10.4269/ajtmh.14-0058 (2014).
- 78 Almeida, E. A., Ramos Junior, A. N., Correia, D. & Shikanai-Yasuda, M. A. Co-infection *Trypanosoma cruzi*/HIV: systematic review (1980-2010). *Rev Soc Bras Med Trop* **44**, 762-770, doi:10.1590/s0037-86822011000600021 (2011).
- 79 Oliveira-Filho, J. *et al.* Chagas disease is independently associated with brain atrophy. *J Neurol* **256**, 1363-1365, doi:10.1007/s00415-009-5105-7 (2009).
- 80 Silva, A. e. A. d. *Trypanosoma cruzi*-Induced Central Nervous System Alterations: From the Entry of Inflammatory Cells to Potential Cognitive and Psychiatric Abnormalities. *Journal of Neuroparasitology* **1**, doi:10.4303/jnp/N100901 (2010).
- 81 Tarleton, R. L. Parasite persistence in the aetiology of Chagas disease. *Int J Parasitol* **31**, 550-554, doi:10.1016/s0020-7519(01)00158-8 (2001).
- 82 Dias, E., Laranja, F. S., Miranda, A. & Nobrega, G. Chagas' disease; a clinical, epidemiologic, and pathologic study. *Circulation* **14**, 1035-1060, doi:10.1161/01.cir.14.6.1035 (1956).
- 83 McCormick, T. S. & Rowland, E. C. *Trypanosoma cruzi*: cross-reactive anti-heart autoantibodies produced during infection in mice. *Exp Parasitol* **69**, 393-401, doi:10.1016/0014-4894(89)90088-x (1989).

- 84 Abel, L. C., Kalil, J. & Cunha Neto, E. Molecular mimicry between cardiac myosin and *Trypanosoma cruzi* antigen B13: identification of a B13-driven human T cell clone that recognizes cardiac myosin. *Braz J Med Biol Res* **30**, 1305-1308, doi:10.1590/s0100-879x1997001100007 (1997).
- 85 Jones, E. M. *et al.* Amplification of a *Trypanosoma cruzi* DNA sequence from inflammatory lesions in human chagasic cardiomyopathy. *Am J Trop Med Hyg* **48**, 348-357, doi:10.4269/ajtmh.1993.48.348 (1993).
- 86 Higuchi Mde, L. *et al.* Correlation between *Trypanosoma cruzi* parasitism and myocardial inflammatory infiltrate in human chronic chagasic myocarditis: Light microscopy and immunohistochemical findings. *Cardiovasc Pathol* **2**, 101-106, doi:10.1016/1054-8807(93)90021-S (1993).
- 87 Viotti, R., Vigliano, C., Armenti, H. & Segura, E. Treatment of chronic Chagas' disease with benznidazole: clinical and serologic evolution of patients with long-term follow-up. *Am Heart J* **127**, 151-162, doi:10.1016/0002-8703(94)90521-5 (1994).
- 88 Lewis, M. D. *et al.* Bioluminescence imaging of chronic *Trypanosoma cruzi* infections reveals tissue-specific parasite dynamics and heart disease in the absence of locally persistent infection. *Cell Microbiol* **16**, 1285-1300, doi:10.1111/cmi.12297 (2014).
- 89 Ricklin, D., Hajishengallis, G., Yang, K. & Lambris, J. D. Complement: a key system for immune surveillance and homeostasis. *Nat Immunol* **11**, 785-797, doi:10.1038/ni.1923 (2010).
- 90 Cestari, I. & Ramirez, M. I. Inefficient complement system clearance of *Trypanosoma cruzi* metacyclic trypomastigotes enables resistant strains to invade eukaryotic cells. *PLoS One* **5**, e9721, doi:10.1371/journal.pone.0009721 (2010).
- 91 Lambris, J. D., Ricklin, D. & Geisbrecht, B. V. Complement evasion by human pathogens. *Nat Rev Microbiol* **6**, 132-142, doi:10.1038/nrmicro1824 (2008).
- 92 Almeida, I. C., Milani, S. R., Gorin, P. A. & Travassos, L. R. Complement-mediated lysis of *Trypanosoma cruzi* trypomastigotes by human anti-alpha-galactosyl antibodies. *J Immunol* **146**, 2394-2400 (1991).
- 93 Krettli, A. U., Weisz-Carrington, P. & Nussenzweig, R. S. Membrane-bound antibodies to bloodstream *Trypanosoma cruzi* in mice: strain differences in susceptibility to complement-mediated lysis. *Clin Exp Immunol* **37**, 416-423 (1979).
- 94 Budzko, D. B., Pizzimenti, M. C. & Kierszenbaum, F. Effects of complement depletion in experimental chagas disease: immune lysis of virulent blood forms of *Trypanosoma cruzi*. *Infect Immun* **11**, 86-91 (1975).

- 95 Tambourgi, D. V. *et al.* A partial cDNA clone of trypomastigote decay-accelerating factor (T-DAF), a developmentally regulated complement inhibitor of *Trypanosoma cruzi*, has genetic and functional similarities to the human complement inhibitor DAF. *Infect Immun* **61**, 3656-3663 (1993).
- 96 Rehli, M. Of mice and men: species variations of Toll-like receptor expression. *Trends Immunol* **23**, 375-378 (2002).
- 97 Kawasaki, T. & Kawai, T. Toll-like receptor signaling pathways. *Front Immunol* **5**, 461, doi:10.3389/fimmu.2014.00461 (2014).
- 98 Oliveira, A. C. *et al.* Expression of functional TLR4 confers proinflammatory responsiveness to *Trypanosoma cruzi* glycoinositolphospholipids and higher resistance to infection with *T. cruzi*. *J Immunol* **173**, 5688-5696, doi:10.4049/jimmunol.173.9.5688 (2004).
- 99 Oliveira, A. C. *et al.* Impaired innate immunity in Tlr4(-/-) mice but preserved CD8+ T cell responses against *Trypanosoma cruzi* in Tlr4-, Tlr2-, Tlr9- or Myd88-deficient mice. *PLoS Pathog* **6**, e1000870, doi:10.1371/journal.ppat.1000870 (2010).
- 100 Bafica, A. *et al.* Cutting edge: TLR9 and TLR2 signaling together account for MyD88-dependent control of parasitemia in *Trypanosoma cruzi* infection. *J Immunol* **177**, 3515-3519, doi:10.4049/jimmunol.177.6.3515 (2006).
- 101 Rodrigues, M. M., Oliveira, A. C. & Bellio, M. The Immune Response to *Trypanosoma cruzi*: Role of Toll-Like Receptors and Perspectives for Vaccine Development. *J Parasitol Res* **2012**, 507874, doi:10.1155/2012/507874 (2012).
- 102 Melo, R. C. & Machado, C. R. *Trypanosoma cruzi*: peripheral blood monocytes and heart macrophages in the resistance to acute experimental infection in rats. *Exp Parasitol* **97**, 15-23, doi:10.1006/expr.2000.4576 (2001).
- 103 Alvarez, M. N., Peluffo, G., Piacenza, L. & Radi, R. Intraphagosomal peroxynitrite as a macrophage-derived cytotoxin against internalized *Trypanosoma cruzi*: consequences for oxidative killing and role of microbial peroxiredoxins in infectivity. *J Biol Chem* **286**, 6627-6640, doi:10.1074/jbc.M110.167247 (2011).
- 104 Cutrullis, R. A., Petray, P. B. & Corral, R. S. MIF-driven activation of macrophages induces killing of intracellular *Trypanosoma cruzi* dependent on endogenous production of tumor necrosis factor, nitric oxide and reactive oxygen species. *Immunobiology* **222**, 423-431, doi:10.1016/j.imbio.2016.08.007 (2017).

- 105 Miyazaki, Y. *et al.* IL-17 is necessary for host protection against acute-phase Trypanosoma cruzi infection. *J Immunol* **185**, 1150-1157, doi:10.4049/jimmunol.0900047 (2010).
- 106 Gazzinelli, R. T., Oswald, I. P., Hieny, S., James, S. L. & Sher, A. The microbicidal activity of interferon-gamma-treated macrophages against Trypanosoma cruzi involves an L-arginine-dependent, nitrogen oxide-mediated mechanism inhibitable by interleukin-10 and transforming growth factor-beta. *Eur J Immunol* **22**, 2501-2506, doi:10.1002/eji.1830221006 (1992).
- 107 Guermonprez, P., Valladeau, J., Zitvogel, L., Thery, C. & Amigorena, S. Antigen presentation and T cell stimulation by dendritic cells. *Annu Rev Immunol* **20**, 621-667, doi:10.1146/annurev.immunol.20.100301.064828 (2002).
- 108 Curtsinger, J. M. & Mescher, M. F. Inflammatory cytokines as a third signal for T cell activation. *Curr Opin Immunol* **22**, 333-340, doi:10.1016/j.coi.2010.02.013 (2010).
- 109 Planelles, L., Thomas, M. C., Maranon, C., Morell, M. & Lopez, M. C. Differential CD86 and CD40 co-stimulatory molecules and cytokine expression pattern induced by Trypanosoma cruzi in APCs from resistant or susceptible mice. *Clin Exp Immunol* **131**, 41-47, doi:10.1046/j.1365-2249.2003.02022.x (2003).
- 110 Blum, J. S., Wearsch, P. A. & Cresswell, P. Pathways of antigen processing. *Annu Rev Immunol* **31**, 443-473, doi:10.1146/annurev-immunol-032712-095910 (2013).
- 111 in *Primer to the Immune Response (Second Edition)* (eds Tak W. Mak, Mary E. Saunders, & Bradley D. Jett) 161-179 (Academic Cell, 2014).
- 112 Neefjes, J., Jongma, M. L., Paul, P. & Bakke, O. Towards a systems understanding of MHC class I and MHC class II antigen presentation. *Nat Rev Immunol* **11**, 823-836, doi:10.1038/nri3084 (2011).
- 113 Garg, N., Nunes, M. P. & Tarleton, R. L. Delivery by Trypanosoma cruzi of proteins into the MHC class I antigen processing and presentation pathway. *J Immunol* **158**, 3293-3302 (1997).
- 114 Martin, D. L. *et al.* CD8+ T-Cell responses to Trypanosoma cruzi are highly focused on strain-variant trans-sialidase epitopes. *PLoS Pathog* **2**, e77, doi:10.1371/journal.ppat.0020077 (2006).
- 115 Fehres, C. M., Unger, W. W., Garcia-Vallejo, J. J. & van Kooyk, Y. Understanding the biology of antigen cross-presentation for the design of vaccines against cancer. *Front Immunol* **5**, 149, doi:10.3389/fimmu.2014.00149 (2014).

- 116 Watts, C. The exogenous pathway for antigen presentation on major histocompatibility complex class II and CD1 molecules. *Nat Immunol* **5**, 685-692, doi:10.1038/ni1088 (2004).
- 117 Ley, V., Robbins, E. S., Nussenzweig, V. & Andrews, N. W. The exit of *Trypanosoma cruzi* from the phagosome is inhibited by raising the pH of acidic compartments. *J Exp Med* **171**, 401-413, doi:10.1084/jem.171.2.401 (1990).
- 118 Padilla, A., Xu, D., Martin, D. & Tarleton, R. Limited role for CD4+ T-cell help in the initial priming of *Trypanosoma cruzi*-specific CD8+ T cells. *Infect Immun* **75**, 231-235, doi:10.1128/IAI.01245-06 (2007).
- 119 Kovacsovics-Bankowski, M. & Rock, K. L. A phagosome-to-cytosol pathway for exogenous antigens presented on MHC class I molecules. *Science* **267**, 243-246, doi:10.1126/science.7809629 (1995).
- 120 Pfeifer, J. D. *et al.* Phagocytic processing of bacterial antigens for class I MHC presentation to T cells. *Nature* **361**, 359-362, doi:10.1038/361359a0 (1993).
- 121 Kumar, S. & Tarleton, R. L. Antigen-specific Th1 but not Th2 cells provide protection from lethal *Trypanosoma cruzi* infection in mice. *J Immunol* **166**, 4596-4603, doi:10.4049/jimmunol.166.7.4596 (2001).
- 122 Bryan, M. A., Guyach, S. E. & Norris, K. A. Specific humoral immunity versus polyclonal B cell activation in *Trypanosoma cruzi* infection of susceptible and resistant mice. *PLoS Negl Trop Dis* **4**, e733, doi:10.1371/journal.pntd.0000733 (2010).
- 123 Ivanov, I. *et al.* The orphan nuclear receptor ROR $\gamma$  directs the differentiation program of proinflammatory IL-17+ T helper cells. *Cell* **126**, 1121-1133, doi:10.1016/j.cell.2006.07.035 (2006).
- 124 Erdmann, H. *et al.* IL-17A promotes macrophage effector mechanisms against *Trypanosoma cruzi* by trapping parasites in the endolysosomal compartment. *Immunobiology* **218**, 910-923, doi:10.1016/j.imbio.2012.10.005 (2013).
- 125 Cai, C. W., Blase, J. R., Zhang, X., Eickhoff, C. S. & Hoft, D. F. Th17 Cells Are More Protective Than Th1 Cells Against the Intracellular Parasite *Trypanosoma cruzi*. *PLoS Pathog* **12**, e1005902, doi:10.1371/journal.ppat.1005902 (2016).
- 126 Tarleton, R. L. CD8+ T cells in *Trypanosoma cruzi* infection. *Semin Immunopathol* **37**, 233-238, doi:10.1007/s00281-015-0481-9 (2015).
- 127 Muller, U. *et al.* Concerted action of perforin and granzymes is critical for the elimination of *Trypanosoma cruzi* from mouse tissues, but prevention of early host

- death is in addition dependent on the FasL/Fas pathway. *Eur J Immunol* **33**, 70-78, doi:10.1002/immu.200390009 (2003).
- 128 Tzelepis, F. *et al.* Distinct kinetics of effector CD8+ cytotoxic T cells after infection with *Trypanosoma cruzi* in naive or vaccinated mice. *Infect Immun* **74**, 2477-2481, doi:10.1128/IAI.74.4.2477-2481.2006 (2006).
- 129 Martin, D. & Tarleton, R. Generation, specificity, and function of CD8+ T cells in *Trypanosoma cruzi* infection. *Immunol Rev* **201**, 304-317, doi:10.1111/j.0105-2896.2004.00183.x (2004).
- 130 Laucella, S. A. *et al.* Frequency of interferon- gamma -producing T cells specific for *Trypanosoma cruzi* inversely correlates with disease severity in chronic human Chagas disease. *J Infect Dis* **189**, 909-918, doi:10.1086/381682 (2004).
- 131 Dos Santos Virgilio, F. *et al.* CD8(+) T cell-mediated immunity during *Trypanosoma cruzi* infection: a path for vaccine development? *Mediators Inflamm* **2014**, 243786, doi:10.1155/2014/243786 (2014).
- 132 Pack, A. D., Collins, M. H., Rosenberg, C. S. & Tarleton, R. L. Highly competent, non-exhausted CD8+ T cells continue to tightly control pathogen load throughout chronic *Trypanosoma cruzi* infection. *PLoS Pathog* **14**, e1007410, doi:10.1371/journal.ppat.1007410 (2018).
- 133 Minning, T. A., Weatherly, D. B., Flibotte, S. & Tarleton, R. L. Widespread, focal copy number variations (CNV) and whole chromosome aneuploidies in *Trypanosoma cruzi* strains revealed by array comparative genomic hybridization. *BMC Genomics* **12**, 139, doi:10.1186/1471-2164-12-139 (2011).
- 134 Bermejo, D. A. *et al.* *Trypanosoma cruzi* infection induces a massive extrafollicular and follicular splenic B-cell response which is a high source of non-parasite-specific antibodies. *Immunology* **132**, 123-133, doi:10.1111/j.1365-2567.2010.03347.x (2011).
- 135 Wabl, M. & Steinberg, C. Affinity maturation and class switching. *Curr Opin Immunol* **8**, 89-92, doi:10.1016/s0952-7915(96)80110-5 (1996).
- 136 Antas, P. R. *et al.* Early, intermediate, and late acute stages in Chagas' disease: a study combining anti-galactose IgG, specific serodiagnosis, and polymerase chain reaction analysis. *Am J Trop Med Hyg* **61**, 308-314, doi:10.4269/ajtmh.1999.61.308 (1999).
- 137 Lidani, K. C. F., Bavia, L., Ambrosio, A. R. & de Messias-Reason, I. J. The Complement System: A Prey of *Trypanosoma cruzi*. *Front Microbiol* **8**, 607, doi:10.3389/fmicb.2017.00607 (2017).

- 138 Umezawa, E. S., Shikanai-Yasuda, M. A. & Stolf, A. M. Changes in isotype composition and antigen recognition of anti-*Trypanosoma cruzi* antibodies from acute to chronic Chagas disease. *J Clin Lab Anal* **10**, 407-413, doi:10.1002/(SICI)1098-2825(1996)10:6<407::AID-JCLA16>3.0.CO;2-0 (1996).
- 139 Powell, M. R. & Wassom, D. L. Host genetics and resistance to acute *Trypanosoma cruzi* infection in mice. I. Antibody isotype profiles. *Parasite Immunol* **15**, 215-221 (1993).
- 140 Umekita, L. F. & Mota, I. How are antibodies involved in the protective mechanism of susceptible mice infected with *T. cruzi*? *Braz J Med Biol Res* **33**, 253-258, doi:10.1590/s0100-879x2000000300001 (2000).
- 141 Umekita, L. F., Carneiro, S. M., Sesso, A. & Mota, I. One fate of bloodstream trypomastigote forms of *Trypanosoma cruzi* after immune clearance: an ultrastructural study. *J Parasitol* **85**, 867-872 (1999).
- 142 Umekita, L. F., Takehara, H. A. & Mota, I. Role of the antibody Fc in the immune clearance of *Trypanosoma cruzi*. *Immunol Lett* **17**, 85-89 (1988).
- 143 Montes, C. L., Acosta-Rodriguez, E. V., Merino, M. C., Bermejo, D. A. & Gruppi, A. Polyclonal B cell activation in infections: infectious agents' devilry or defense mechanism of the host? *J Leukoc Biol* **82**, 1027-1032, doi:10.1189/jlb.0407214 (2007).
- 144 Junqueira, C. *et al.* The endless race between *Trypanosoma cruzi* and host immunity: lessons for and beyond Chagas disease. *Expert Rev Mol Med* **12**, e29, doi:10.1017/S1462399410001560 (2010).
- 145 Gupta, S. & Garg, N. J. TcVac3 induced control of *Trypanosoma cruzi* infection and chronic myocarditis in mice. *PLoS One* **8**, e59434, doi:10.1371/journal.pone.0059434 (2013).
- 146 Jones, K. *et al.* Vaccine-Linked Chemotherapy Improves Benznidazole Efficacy for Acute Chagas Disease. *Infect Immun* **86**, doi:10.1128/IAI.00876-17 (2018).
- 147 Gonzalez Cappa, S. M., Schmunis, G. A., Traversa, O. C., Yanovsky, J. F. & Parodi, A. S. Complement-fixation tests, skin tests, and experimental immunization with antigens of *Trypanosoma cruzi* prepared under pressure. *Am J Trop Med Hyg* **17**, 709-715, doi:10.4269/ajtmh.1968.17.709 (1968).
- 148 Ruiz, A. M., Esteva, M., Cabeza Meckert, P., Laguens, R. P. & Segura, E. L. Protective immunity and pathology induced by inoculation of mice with different subcellular fractions of *Trypanosoma cruzi*. *Acta Trop* **42**, 299-309 (1985).

- 149 Breganó, J. W. *et al.* Phytomonas serpens, a tomato parasite, shares antigens with Trypanosoma cruzi that are recognized by human sera and induce protective immunity in mice. *Pathogens and Disease* **39**, 257-264, doi:10.1016/s0928-8244(03)00256-6 (2003).
- 150 Basso, B., Moretti, E. & Fretes, R. Vaccination with epimastigotes of different strains of Trypanosoma rangeli protects mice against Trypanosoma cruzi infection. *Mem Inst Oswaldo Cruz* **103**, 370-374, doi:10.1590/s0074-02762008000400010 (2008).
- 151 Martinez-Campos, V. *et al.* Expression, purification, immunogenicity, and protective efficacy of a recombinant Tc24 antigen as a vaccine against Trypanosoma cruzi infection in mice. *Vaccine* **33**, 4505-4512, doi:10.1016/j.vaccine.2015.07.017 (2015).
- 152 Seid, C. A. *et al.* Cysteine mutagenesis improves the production without abrogating antigenicity of a recombinant protein vaccine candidate for human chagas disease. *Hum Vaccin Immunother* **13**, 621-633, doi:10.1080/21645515.2016.1242540 (2017).
- 153 Biter, A. B. *et al.* Characterization and Stability of Trypanosoma cruzi 24-C4 (Tc24-C4), a Candidate Antigen for a Therapeutic Vaccine Against Chagas Disease. *J Pharm Sci* **107**, 1468-1473, doi:10.1016/j.xphs.2017.12.014 (2018).
- 154 Seder, R. A. & Hill, A. V. Vaccines against intracellular infections requiring cellular immunity. *Nature* **406**, 793-798, doi:10.1038/35021239 (2000).
- 155 Nickell, S. P., Stryker, G. A. & Arevalo, C. Isolation from Trypanosoma cruzi-infected mice of CD8+, MHC-restricted cytotoxic T cells that lyse parasite-infected target cells. *J Immunol* **150**, 1446-1457 (1993).
- 156 Folegatti, P. M. *et al.* Safety and Immunogenicity of the Heterosubtypic Influenza A Vaccine MVA-NP+M1 Manufactured on the AGE1.CR.pIX Avian Cell Line. *Vaccines (Basel)* **7**, doi:10.3390/vaccines7010033 (2019).
- 157 Cappuccini, F., Stribbling, S., Pollock, E., Hill, A. V. & Redchenko, I. Immunogenicity and efficacy of the novel cancer vaccine based on simian adenovirus and MVA vectors alone and in combination with PD-1 mAb in a mouse model of prostate cancer. *Cancer Immunol Immunother* **65**, 701-713, doi:10.1007/s00262-016-1831-8 (2016).
- 158 Beaumier, C. M. *et al.* Status of vaccine research and development of vaccines for Chagas disease. *Vaccine* **34**, 2996-3000, doi:10.1016/j.vaccine.2016.03.074 (2016).
- 159 Chatelain, E. & Konar, N. Translational challenges of animal models in Chagas disease drug development: a review. *Drug Des Devel Ther* **9**, 4807-4823, doi:10.2147/DDDT.S90208 (2015).
- 160 Guarner, J. *et al.* Mouse model for Chagas disease: immunohistochemical distribution of different stages of Trypanosoma cruzi in tissues throughout infection. *Am J Trop Med Hyg* **65**, 152-158, doi:10.4269/ajtmh.2001.65.152 (2001).
- 161 Callejas-Hernandez, F., Girones, N. & Fresno, M. Genome Sequence of Trypanosoma cruzi Strain Bug2148. *Genome Announc* **6**, doi:10.1128/genomeA.01497-17 (2018).

- 162 Berna, L. *et al.* Expanding an expanded genome: long-read sequencing of  
Trypanosoma cruzi. *Microb Genom* **4**, doi:10.1099/mgen.0.000177 (2018).
- 163 Marinho, C. R. *et al.* Infection by the Sylvio X10/4 clone of Trypanosoma cruzi:  
relevance of a low-virulence model of Chagas' disease. *Microbes Infect* **11**, 1037-1045,  
doi:10.1016/j.micinf.2009.07.011 (2009).
- 164 Dumonteil, E., Escobedo-Ortegon, J., Reyes-Rodriguez, N., Arjona-Torres, A. &  
Ramirez-Sierra, M. J. Immunotherapy of Trypanosoma cruzi infection with DNA  
vaccines in mice. *Infect Immun* **72**, 46-53, doi:10.1128/iai.72.1.46-53.2004 (2004).
- 165 Blyszczuk, P. Myocarditis in Humans and in Experimental Animal Models. *Front*  
*Cardiovasc Med* **6**, 64, doi:10.3389/fcvm.2019.00064 (2019).
- 166 Eickhoff, C. S. *et al.* ECG detection of murine chagasic cardiomyopathy. *J Parasitol* **96**,  
758-764, doi:10.1645/GE-2396.1 (2010).
- 167 Mori, T. *et al.* Intestinal transit and opaque enema study in chagasic mice. *Rev Hosp*  
*Clin Fac Med Sao Paulo* **50**, 63-66 (1995).
- 168 Guillen-Pernia, B., Lugo-Yarbuh, A. & Moreno, E. [Digestive tract dilation in mice  
infected with Trypanosoma cruzi]. *Invest Clin* **42**, 195-209 (2001).
- 169 Branchini, B. R. *et al.* Red-emitting luciferases for bioluminescence reporter and  
imaging applications. *Anal Biochem* **396**, 290-297, doi:10.1016/j.ab.2009.09.009  
(2010).
- 170 Francisco, A. F. *et al.* Limited Ability of Posaconazole To Cure both Acute and Chronic  
Trypanosoma cruzi Infections Revealed by Highly Sensitive In Vivo Imaging. *Antimicrob*  
*Agents Chemother* **59**, 4653-4661, doi:10.1128/AAC.00520-15 (2015).
- 171 Lewis, M. D. *et al.* Imaging the development of chronic Chagas disease after oral  
transmission. *Sci Rep* **8**, 11292, doi:10.1038/s41598-018-29564-7 (2018).
- 172 Lewis, M. D., Francisco, A. F., Taylor, M. C., Jayawardhana, S. & Kelly, J. M. Host and  
parasite genetics shape a link between Trypanosoma cruzi infection dynamics and  
chronic cardiomyopathy. *Cell Microbiol* **18**, 1429-1443, doi:10.1111/cmi.12584 (2016).
- 173 Dhama, K. *et al.* Advances in Designing and Developing Vaccines, Drugs, and Therapies  
to Counter Ebola Virus. *Front Immunol* **9**, 1803, doi:10.3389/fimmu.2018.01803  
(2018).

Chapter 2 :

Submitted Manuscript

**Immunity conferred by drug-cured experimental *Trypanosoma cruzi* infections is long-lasting and cross-strain protective**

Gurdip Singh Mann, Amanda F. Francisco, Shiromani Jayawardhana, Martin C. Taylor, Michael D. Lewis, Francisco Olmo, Elisangela Oliveira de Freitas<sup>1</sup>, Cesar López-Camacho<sup>1</sup>, Arturo Reyes-Sandoval<sup>1</sup> and John M. Kelly\*

Department of Infection Biology,

London School of Hygiene and Tropical Medicine,

Keppel Street,

London WC1E 7HT, UK.

<sup>1</sup>The Jenner Institute,

Old Road Campus Research Building,

Roosevelt Drive,

Oxford OX3 7DQ, UK

\*corresponding author ([john.kelly@lshtm.ac.uk](mailto:john.kelly@lshtm.ac.uk))

Short title: Monitoring immunity against *T. cruzi* infections by *in vivo* imaging

## RESEARCH PAPER COVER SHEET

Please note that a cover sheet must be completed for each research paper included within a thesis.

### SECTION A – Student Details

Student ID Number	415943	Title	Mr
First Name(s)	Gurdip Singh		
Surname/Family Name	Mann		
Thesis Title	Exploring the Potential of Vaccination to Combat Trypanosoma cruzi Infection using Bioluminescent Imaging		
Primary Supervisor	Professor John M Kelly		

If the Research Paper has previously been published please complete Section B, if not please move to Section C.

### SECTION B – Paper already published

Where was the work published?			
When was the work published?			
If the work was published prior to registration for your research degree, give a brief rationale for its inclusion			
Have you retained the copyright for the work?*	Choose an item.	Was the work subject to academic peer review?	Choose an item.

\*If yes, please attach evidence of retention. If no, or if the work is being included in its published format, please attach evidence of permission from the copyright holder (publisher or other author) to include this work.

### SECTION C – Prepared for publication, but not yet published

Where is the work intended to be published?	PLOS Neglected Tropical Diseases
Please list the paper's authors in the intended authorship order:	Gurdip Singh Mann, Amanda F. Francisco, Shiromani Jayawardhana, Martin C. Taylor, Michael D. Lewis, Francisco Olmo, Elisangela Oliveira de Freitas, Fabiana M. S. Leoratti, Cesar López-Camacho, Arturo Reyes-Sandoval, John M. Kelly

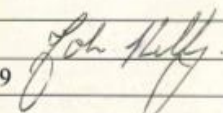
Stage of publication	Submitted
----------------------	-----------

**SECTION D – Multi-authored work**

<p>For multi-authored work, give full details of your role in the research included in the paper and in the preparation of the paper. (Attach a further sheet if necessary)</p>	<p>My role in this work was in the formulation of ideas, the generation of data through the various experiments outlined in the paper and in the preparation of the figures and text of the manuscript.</p> <p>The generation of ideas was a collective effort to which the two PIs (John Kelly and Arturo Reyes Sandoval) and myself contributed significantly. The other authors also offered their critical appraisal on ideas and how they might be tested experimentally.</p> <p>All of the experiments outlined in the paper were performed by myself both at LSHTM and at the Jenner Institute, occasionally with the aid of the other authors. The analysis of the data generated was also performed by myself.</p> <p>I contributed significantly to the written manuscript, generating all of the figures. I also wrote the infrastructure of the body of text which made up the introduction, results and discussion.</p>
---	--

**SECTION E**

Student Signature	
Date	28/08/2019

Supervisor Signature	
Date	28/08/2019

## ABSTRACT

**Background** The long term and complex nature of Chagas disease in humans has restricted studies on vaccine feasibility. Animal models also have limitations due to technical difficulties in monitoring the extremely low parasite burden that is characteristic of chronic stage infections. Advances in imaging technology offer alternative approaches that circumvent these problems. Here, we describe the use of highly sensitive whole body *in vivo* imaging to assess the efficacy of recombinant viral vector vaccines and benznidazole-cured infections to protect mice from challenge with *Trypanosoma cruzi*.

**Methodology/Principal Findings** Mice were infected with *T. cruzi* strains modified to express a red-shifted luciferase reporter. Using bioluminescence imaging, we assessed the degree of immunity to re-infection conferred after benznidazole-cure. Mice infected for 14 days or more, prior to the initiation of treatment, were highly protected from challenge with both homologous and heterologous strains (>99% reduction in parasite burden). Sterile protection against homologous challenge was frequently observed. This level of protection was considerably greater than that achieved with recombinant vaccines. It was also independent of the route of infection or size of the challenge inoculum, and was long-lasting, with no significant diminution in immunity after almost a year. When the primary infection was benznidazole-treated after 4 days (before completion of the first cycle of intracellular infection), the degree of protection was much reduced, an outcome associated with a minimal *T. cruzi*-specific IFN- $\gamma$ <sup>+</sup> T cell response.

**Conclusions/Significance** Our findings suggest that a protective Chagas disease vaccine must have the ability to eliminate parasites before they reach organs/tissues, such as the GI tract, where once established, they become largely refractory to the induced immune response.

## INTRODUCTION

Chagas disease is caused by the insect-transmitted protozoan *Trypanosoma cruzi* and is the most serious parasitic infection in the Americas. More than 5 million people are infected with this obligate intracellular parasite<sup>1,2</sup>, resulting in a financial burden estimated at \$7 billion annually<sup>3</sup>. In humans, the disease is characterised by an acute stage that occurs 2-8 weeks post-infection, during which bloodstream parasites are often detectable. Symptoms during this period are normally mild, although lethal outcomes can occur in 5% of diagnosed cases. The parasite numbers are then controlled by a vigorous adaptive immune response. However, sterile immunity is not achieved and infected individuals transition to a chronic stage, which in most cases, appears to be life-long<sup>4</sup>. Around 30-40% of those infected eventually develop chronic disease pathology, a process that can take decades to become symptomatic. Cardiomyopathy is the most common clinical manifestation<sup>5,6</sup>, although 10-15% of people can develop digestive tract megasyndromes, sometimes in addition to cardiac disease.

Attempts to control Chagas disease have been challenging. For example, although public health measures have been successful in reducing disease transmission in several regions of South America, there is a vast zoonotic reservoir that complicates disease eradication by this route<sup>7-9</sup>. The only drugs currently available to treat the infection, the nitroheterocycles benznidazole and nifurtimox, have limited efficacy and cause toxic side effects that can impact on patient compliance<sup>10,11</sup>. There have been no new treatments for almost 50 years, but progress in discovering new chemotherapeutic agents is now being accelerated by a range of drug development consortia encompassing both the academic and commercial sectors<sup>12</sup>. For many years, vaccine development against Chagas disease has been inhibited by concerns that autoimmunity could play a role in disease pathogenesis<sup>13,14</sup>. Although not excluded as a contributory

factor, the current consensus is that the risk has been overstated, and that the continued presence of the parasite is required to drive disease pathology<sup>15-17</sup>.

The host response to *T. cruzi* infection involves a complex combination of both innate and adaptive immune mechanisms<sup>18,19</sup>. The innate system is key to controlling parasite proliferation and dissemination during the initial stages of infection<sup>20</sup>, with important roles for both Toll-like receptor (TLR)-mediated inflammatory responses and TLR-independent processes<sup>21</sup>. As the acute phase progresses, the development of an antigen-specific immune response, in which CD8<sup>+</sup> IFN- $\gamma$ <sup>+</sup> T cells are the key effectors<sup>18,22</sup>, is the critical step in controlling the infection. In both humans and mice, the major targets of this cellular response are a small set of immunodominant epitopes within specific members of the trans-sialidase super-family of surface antigens<sup>23</sup>. The observation that the pattern of this recognition displays strain variation has been interpreted as indicative that immune evasion could be operating at a population level. The adaptive response reduces the parasite burden by >99%, with the infection becoming highly focal, and in BALB/c mice at least, confined predominantly to the large intestine, stomach, and to a lesser extent, the gut mesentery tissue and sites in the skin<sup>24,25</sup>. The reason why the immune system is not able to eradicate the infection is unresolved. It does not appear to involve exhaustion of the CD8<sup>+</sup> IFN- $\gamma$ <sup>+</sup> T cell response, which continues to suppress, but not eliminate, the parasite burden throughout the long chronic stage<sup>26</sup>. These findings have questioned the feasibility of developing an effective anti-*T. cruzi* vaccine.

Experimental vaccination of animal models against *T. cruzi* infection has a long history<sup>27</sup>, although there have been few instances in which unequivocal sterile protection has been reported. Approaches have included the use of attenuated parasites<sup>28,29</sup>, immunisation with cell fractions<sup>30</sup>, purified or recombinant proteins<sup>31,32</sup> and the use of DNA vaccines.

In the latter case, viral backbones based on vaccinia<sup>33</sup>, yellow fever<sup>34</sup> and adenovirus<sup>35</sup> have been used to facilitate expression of a range of parasite antigens such as trans-sialidase, Tc24, and the amastigote surface protein-2 (ASP-2) (also a member of the trans-sialidase super-family). Reported outcomes include protection from lethal infection, reduction in the acute stage parasite burden, induction of a favourable cytokine profile, and reduction in disease pathology. However, detailed analysis of vaccine efficacy has been limited by an inability to accurately monitor parasite levels during the chronic stage and technical difficulties in assessing the effect of the immune response on tissue distribution following challenge infections.

Recently, in vivo imaging approaches have been exploited to provide new insights into infection dynamics during experimental chronic Chagas disease<sup>24,25,36</sup>. These studies have revealed the pantropic nature of acute stage infections, and shown that during the chronic stage, the adaptive immune response restricts parasites to small infection foci, predominantly within the GI tract. Other tissues and organs, including the heart and skeletal muscle, are infected sporadically, the extent of which is influenced by host:parasite genetics and immune status. Additional factors such as nutrition, environmental stimuli, age and co-infections could also play a role in this complex chronic infection profile<sup>37</sup>. The survival of the small parasite foci within apparently tolerant sites is crucial for long-term infection, although the immunological context of these reservoirs is unknown. Another contributor to the long-term nature of *T. cruzi* infections could be the phenomenon of parasite dormancy; individual intracellular amastigotes can enter an apparently quiescent state in which they cease to replicate and exhibit reduced drug sensitivity<sup>38</sup>. Neither the mechanisms involved, nor the potential implications for immune evasion have yet been established.

Highly sensitive bioluminescence imaging involves the use of *T. cruzi* strains that have been modified to express a red-shifted luciferase reporter<sup>39</sup>. The system allows the real-time monitoring of parasite burden in experimental mice during chronic stage infections. There is a robust correlation between parasite numbers and whole animal bioluminescence, with a limit of detection close to 100 parasites<sup>24</sup>. Here, we describe the use of this imaging technology to assess the extent of protection in benznidazole-cured mice following re-challenge with homologous and heterologous strains. Our findings have important implications for vaccine strategies.

## **MATERIALS AND METHODS**

### Generation of recombinant ASP-2/TS vaccines

The fusion gene encoding the ASP-2 and TS peptides (Figure 1A) was generated by linking sequences corresponding to the mouse Ig kappa chain signal peptide, ASP-2 amino acids 1-694 (GenBank accession no. U77951) and TS amino acids 1-624 (GenBank accession no. L38457). The furin 2A splice site linker was inserted between the trypanosome sequences to ensure the subsequent generation of two separate peptides from a single open reading frame<sup>40</sup>. The ASP-2/TS fusion gene was cloned into the ChAdOx1<sup>41</sup> and MVA<sup>42,43</sup> viral-vectored vaccine platforms, and confirmed by sequencing prior to use in protection studies.

### Assessment of recombinant vaccine immunogenicity

Vaccines were prepared in PBS and administered intramuscularly into the left and right quadriceps muscles of mice. The ChAdOx1 vaccine was administered at  $1 \times 10^8$  infectious units per dose. With MVA:ASP-2/TS, each dose was equivalent to  $1 \times 10^6$  plaque forming units. ELISpots were carried out using either peripheral blood mononuclear cells (PBMCs) or splenocytes. Briefly, MAIP ELISpot plates (Millipore) were coated at 4°C overnight with anti-mouse IFN- $\gamma$  mAb AN-18 (Mabtech), at 250 ng per well, and then blocked for 1 h with complete DMEM medium (10% foetal calf serum). Whole blood was sampled by venesection of the tail vein and PBMCs were isolated using histopaque 1083 (Sigma), and plated at  $5 \times 10^5$  cells per well with 20-mer specific peptides overlapping by 10 amino acids ( $10 \mu\text{g ml}^{-1}$ ) (Pepscan Presto). Splenocytes from naïve mice were plated  $2.5 \times 10^5$  per well. After 16 h incubation, cells were discarded and plates washed with PBS. 50  $\mu\text{l}$  of biotinylated anti-mouse IFN- $\gamma$  mAb RA-6A2 (1:1000 in PBS) was then added to each well and incubated for 2 h. After another washing step, streptavidin peroxidase (Sigma) was added and incubated at 37°C for 1

h. The plates were washed and developed with TMB substrate solution (Mabtech). When spots were visible, the reaction was stopped by washing the plate with water. Spots were analysed using an ELISpot reader, and the number of spot-forming cells/ $10^6$  PBMCs producing IFN- $\gamma$  was calculated.

#### Murine infections and bioluminescence imaging

Animal work was performed under UK Home Office project licence (PPL 70/8207) and approved by the LSHTM Animal Welfare and Ethical Review Board. Procedures were in accordance with the UK Animals (Scientific Procedures) Act 1986 (ASPA). BALB/c mice were purchased from Charles River (UK), and CB17 SCID mice were bred in-house. Animals were maintained under specific pathogen-free conditions in individually ventilated cages. They experienced a 12 h light/dark cycle, with access to food and water ad libitum. SCID mice were infected with  $1 \times 10^4$  bioluminescent bloodstream trypomastigotes (BTs) in 0.2 ml PBS via intraperitoneal (i.p.) injection (24, 25, 36). BALB/c female mice, aged 8-10 weeks, were infected i.p with  $1 \times 10^3$  BTs derived from SCID mouse blood. At experimental end-points, mice were sacrificed by exsanguination under terminal anaesthesia.

For in vivo imaging, mice were injected with 150 mg kg<sup>-1</sup> d-luciferin i.p., then anaesthetized using 2.5% (v/v) gaseous isoflurane. They were placed in an IVIS Lumina II system (Caliper Life Science) 5-10 min after d-luciferin administration and images acquired using LivingImage 4.3. Exposure times varied from 30 s to 5 min, depending on signal intensity. After imaging, mice were revived and returned to cages. For ex vivo imaging, mice were injected with d-luciferin, and sacrificed by exsanguination under terminal anaesthesia 5 min later. They were then perfused via the heart with 10 ml 0.3 mg ml<sup>-1</sup> d-luciferin in PBS. Organs and tissues were removed and transferred to a Petri

dish in a standardized arrangement, soaked in 0.3 mg ml<sup>-1</sup> d-luciferin in PBS, and imaged using maximum detection settings (5 min exposure, large binning). The remaining animal parts and carcass were checked for residual bioluminescent foci, also using maximum detection settings (24, 25). To estimate parasite burden in live mice, regions of interest were drawn using LivingImage v.4.3 to quantify bioluminescence as total flux (photons/second), summed from dorsal and ventral images. The detection threshold for in vivo imaging was determined using uninfected mice.

#### Drug treatment and immunosuppression

Benznidazole was synthesized by Epichem Pty Ltd., Australia, and prepared at 10 mg ml<sup>-1</sup> in an aqueous suspension vehicle containing 5% (v/v) DMSO, 0.5% (w/v) hydroxypropyl methylcellulose, 0.5% (v/v) benzyl alcohol and 0.4% (v/v) Tween 80. It was administered by oral gavage. To detect any residual infection following treatment, mice were immunosuppressed with cyclophosphamide monohydrate (Sigma) in D-PBS (200 mg kg<sup>-1</sup>), administered by i.p. injection every 4 days, for 3 doses. Two weeks after the end of immunosuppression, mice that were bioluminescence negative by both in vivo and ex vivo imaging were designated as cured.

## RESULTS

### Monitoring ASP-2/TS vaccine efficacy using highly sensitive bioluminescence imaging

The *T. cruzi* amastigote surface protein 2 (ASP-2) and trypomastigote cell surface protein trans-sialidase (TS) have shown promise as vaccine candidates against *T. cruzi* infections (44–46). To further assess their efficacy, we used two replication-deficient recombinant vaccine platforms, a chimpanzee adenovirus (ChAdOx1) and a Modified Vaccinia Ankara virus (MVA), expressing ASP-2 and TS peptides from a single open reading frame (Fig 1A) (Materials and Methods)<sup>40</sup>. We used a homologous prime-boost vaccination strategy in which BALB/c mice received intramuscular injections administered one week apart (Fig 1B) and confirmed immunogenicity of the vaccine delivery system using an ex vivo IFN- $\gamma$ <sup>+</sup> ELISpot. Three weeks after receiving either a prime only, or a prime-booster vaccination, splenocytes were plated on antibody coated ELISpot plates. When these cells were then stimulated with a peptide pool representing the entire ASP-2/TS sequence, there was a pronounced increase in the number of peptide specific IFN- $\gamma$ <sup>+</sup> splenocytes, particularly in those mice that had received the booster (Fig 1C).

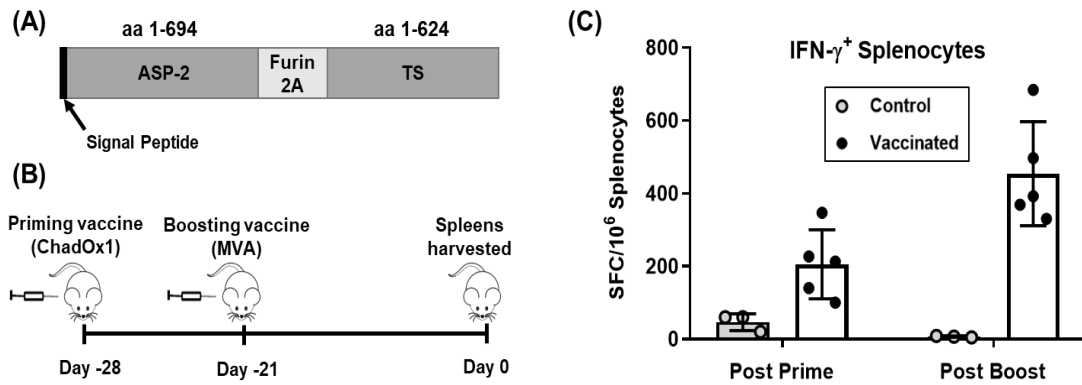


**Fig 1. Immunogenicity of the recombinant ASP-2/TS vaccine.**

(A) Open reading frame encoding ASP-2 and TS peptides, with the mouse Ig kappa chain signal peptide and furin 2A splice site linker indicated. (B) Prime-boost vaccination strategy. BALB/c mice ( $n=5$ , per vaccinated group) were inoculated one week apart with ChAdOx1 (priming) and then MVA (boosting) recombinant vaccines containing the ASP-2/TS fusion gene. Control mice received vaccinations with the same viral vectors engineered to express dengue protein NS-1 ( $n=3$ ). (C) ELISpot analysis. Splenocytes were plated onto antibody coated ELISpot plates and stimulated for 16 h with a peptide pool covering the entire ASP-2 and TS sequences (Materials and Methods). Data are presented as *ex vivo* IFN- $\gamma$  spot forming cells (SFCs) per  $10^6$  splenocytes. Data derived from single experiment

To test protective efficacy, mice were vaccinated using the homologous prime-boost strategy outlined above. Three weeks after the MVA booster, they were challenged by i.p. injection with  $10^3$  bioluminescent *T. cruzi* blood trypomastigotes (strain CL Brener) (Fig 2A). The resulting infection was monitored by *in vivo* imaging<sup>36</sup> (Materials and Methods). In BALB/c mice, parasites rapidly disseminate and proliferate, with the infection reaching a peak after approximately 2 weeks. Thereafter, a vigorous adaptive immune response reduces the parasite burden by >2 orders of magnitude, and the infection transitions to the life-long chronic stage<sup>24</sup>. No differences were observed in the bioluminescence-inferred parasite burden between vaccinated and control mice at the earliest time-point assessed (day 7, post-infection) (Figs 2B and C). However, by day 15, the peak of the acute stage, the ASP-2/TS vaccinated mice displayed a 77% reduction in the bioluminescence-inferred parasite burden. This protective effect was

maintained until day 21. By day 28, against a background of immune-mediated reduction in the parasite burden, there were no significant differences between the vaccinated and control groups. From that point onwards, the parasite burden remained similar between the groups (Figs 2B and C). Following termination of the experiment (day 95), ex vivo imaging of internal organs and tissues revealed that the profile of infection in the vaccinated cohort was typical of the chronic stage. The colon and/or stomach were the major tissues persistently parasitized, with infections in other organs being sporadic. There were no apparent differences in the tissue-specific parasite burden between vaccinated and control mice (Fig 2D). Therefore, although vaccination with the ASP-2/TS constructs can reduce parasite burden during the acute stage, it does not impact on the long term burden of chronic infections.

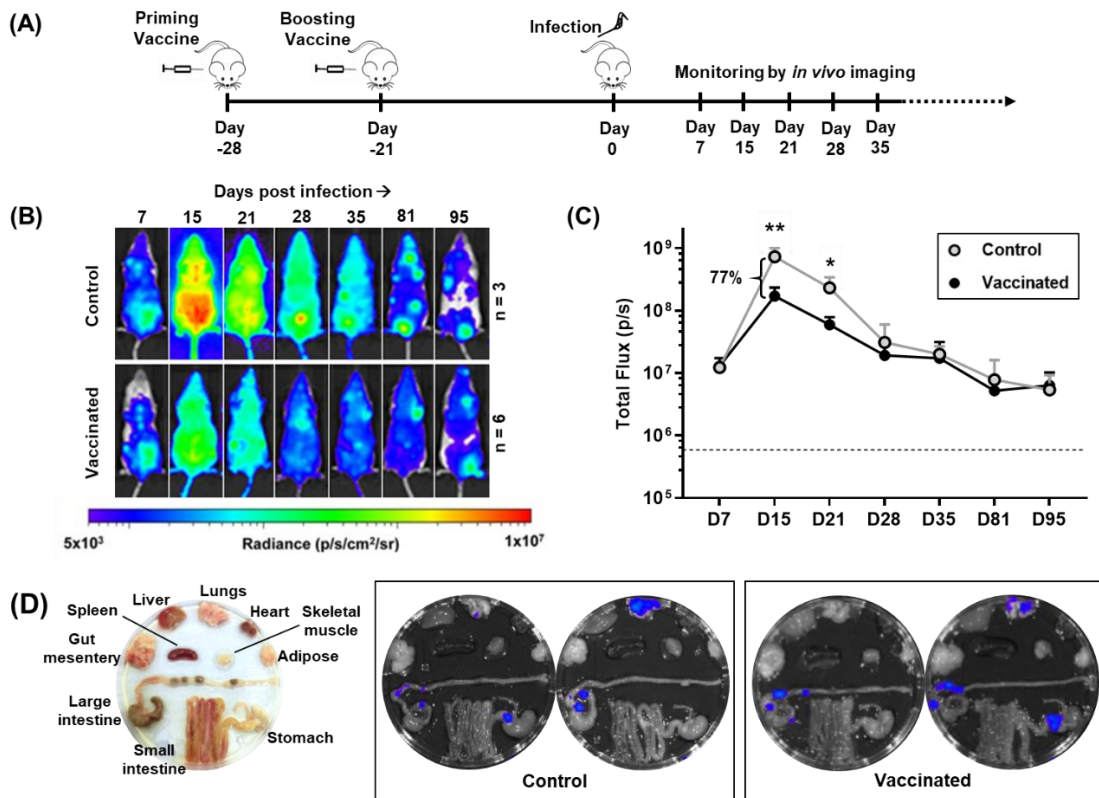


**Fig 2. Assessing the efficacy of the ASP-2/TS vaccine to protect mice against *T. cruzi* infection.**

(A) Timeline of vaccination experiment. (B) Assessment of efficacy. Vaccinated (n=5) and control BALB/c mice (n=3) were infected i.p. with  $10^3$  bioluminescent *T. cruzi* trypomastigotes and monitored by *in vivo* imaging. Representative ventral images (from a single mouse in each case) are shown at sequential time points post-infection. All images use the same log<sub>10</sub>-scale heat-map with minimum and maximum radiance values indicated. (C) Quantification of whole animal bioluminescence (ventral and dorsal) of vaccinated and control cohorts (mean + SD). Dashed line indicates background bioluminescence; (\*\*)  $p < 0.01$ , (\*)  $p < 0.05$ . (D) *Ex vivo* bioluminescence imaging. Left-hand image; arrangement of organs and tissues. Insets, representative images of organs from control and vaccinated mice, 95 days post-infection. Data derived from single experiment.

Drug-cured *T. cruzi* infection confers significant protection against challenge with a homologous strain

To place the recombinant vaccine results into context, we sought to establish the extent to which drug-cured infections could enhance the capacity of the murine immune response to protect against challenge. BALB/C mice were first inoculated i.p. with bioluminescent parasites (CL Brener strain) (n=12). At three different points post-infection (4, 14 and 36 days) (Fig 3A), we initiated treatment with benznidazole (100 mg kg<sup>-1</sup>), once daily, for 20 consecutive days. This dosing regimen was shown to be curative (Supplementary Fig 1), in line with previous results<sup>44,45</sup>. The plasma concentration of benznidazole falls below the in vitro EC50 value in approximately 12 h<sup>45</sup>. 21 days after the cessation of treatment, the cured mice were re-infected i.p. and monitored regularly by in vivo imaging (Fig 3B and C). 70 days after challenge, mice found to be bioluminescence-negative were immunosuppressed to facilitate the outgrowth and dissemination of any residual parasites, then assessed further by ex vivo imaging two weeks later (Fig 3D) (Materials and Methods).

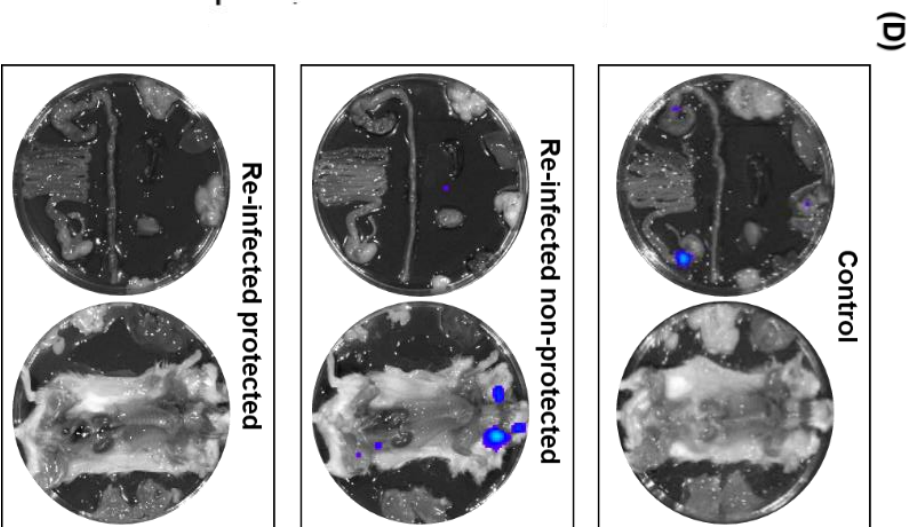
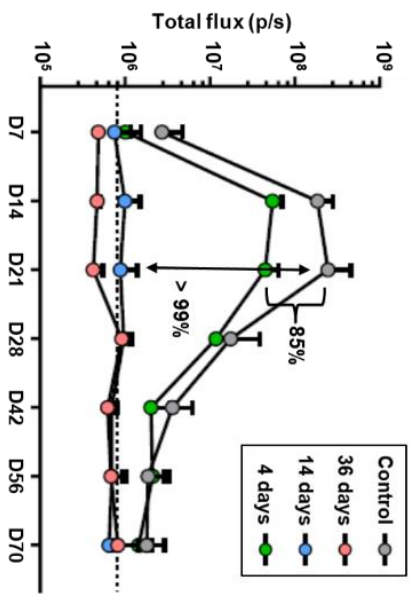
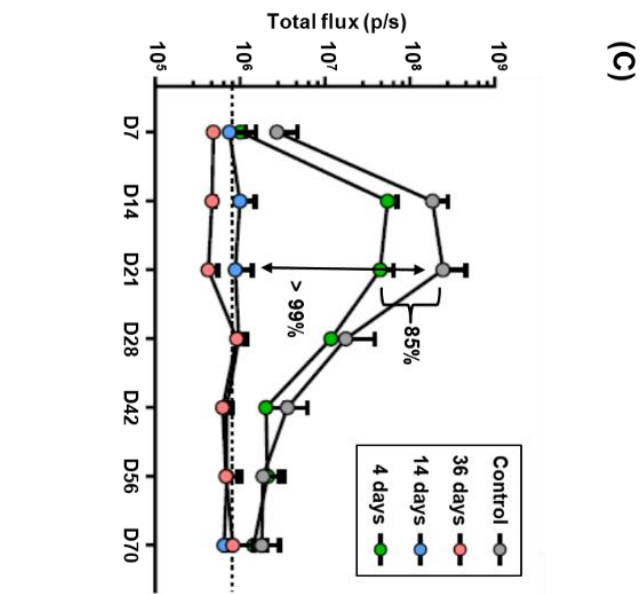
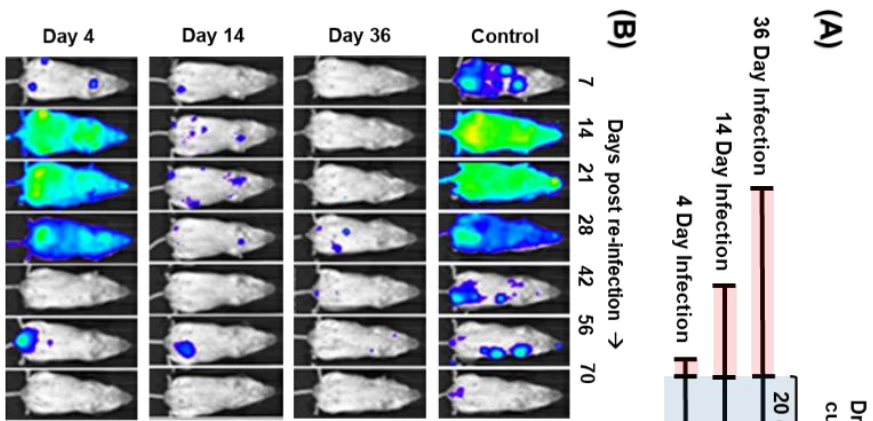


**Fig 3. Drug-cured infections confer significant protection against challenge with a homologous *T. cruzi* strain.**

(A) Outline of strategy. BALB/c mice were infected i.p. with  $10^3$  bioluminescent trypomastigotes (CL Brener strain) and subjected to curative benznidazole treatment initiated at various times post-infection. 21 days after the end of treatment, they were re-infected i.p. and monitored for a further 70 days. Bioluminescence-negative mice were then immunosuppressed using cyclophosphamide (Materials and Methods) and assessed by *ex vivo* imaging two weeks later. Results were derived from 2 independent experiments, each involving 6 mice per cohort. (B) Representative ventral images of benznidazole-cured mice following re-infection. The number of days at which drug treatment was initiated, following the primary infection, is indicated (left). All images use the same  $\log_{10}$ -scale heat-map with minimum and maximum radiance values indicated. (C) Total body bioluminescence (sum of ventral and dorsal images) of drug-cured mice following re-infection (n=12) (means  $\pm$  SD) derived by *in vivo* imaging. The length of the primary infection is indicated (inset). (D) Representative *ex vivo* bioluminescence images. Upper inset, organs from control mouse 70 days post-infection. Central inset, organs from a mouse that was re-infected following curative treatment initiated on day 36 of the primary infection. On day 70 of the challenge infection, immunosuppressive treatment was initiated and the organs then harvested. In this instance, a residual infection was identified. Lower inset, organs from a mouse treated as above, which was non-infected after challenge. Data is average of two independently run experiments

When curative treatment was initiated at 36 days post-infection, none of the mice exhibited a distinct acute stage infection peak following challenge (Figs 3B and C). There was >99% reduction in the inferred parasite burden in all cases, compared to primary infection control mice. At the experimental end-point, 6 out of 12 mice were shown to be fully protected (Table 1, Fig 3D, Supplementary Fig 2). In cases where the primary infection was allowed to proceed for 14 days prior to the initiation of curative benznidazole treatment, the infection profile following challenge was very similar to the cohort where treatment was initiated 36 days post-infection. However, a greater number of foci were detectable during the period corresponding to the acute stage of primary infections (Fig 3B), with full protection achieved in 3 out of 12 mice. In contrast to both of the above, when curative treatment began 4 days after the primary infection, there was a clear acute stage peak in the bioluminescence profile following challenge (Fig

3C). The kinetic profile mirrored that in control infected mice, although the maximum parasite burden was 85% lower, and sterile protection was restricted to a single mouse (Table 1). Therefore, although the immune response induced by a short course infection is able to impact on the burden of re-infection, the effect is significantly limited compared with what is achievable when the primary infection is allowed to progress fully into the acute stage, prior to treatment.

**Table 1**

Preliminary infection strain	Challenge strain	Route of infection	Challenge dose	Length of primary infection <sup>1</sup>	Period between cure and challenge	Mean parasite reduction <sup>2</sup>	Level of sterile protection
CL-Brener	CL-Brener	i.p.	1 x 10 <sup>3</sup>	36 days	21 days	>99%	6/12 <sup>3</sup>
CL-Brener	CL-Brener	i.p.	1 x 10 <sup>3</sup>	14 days	21 days	>99%	3/12 <sup>3</sup>
CL-Brener	CL-Brener	i.p.	1 x 10 <sup>3</sup>	4 days	21 days	85%	1/12 <sup>3</sup>
CL-Brener	CL-Brener	s.c.	1 x 10 <sup>3</sup>	36 days	21 days	>99%	4/5
CL-Brener	CL-Brener	i.p.	6 x 10 <sup>4</sup>	36 days	21 days	>99%	5/6
CL-Brener	CL-Brener	i.p.	1 x 10 <sup>3</sup>	36 days	336 days	>99%	4/6
JR	JR	i.p.	1 x 10 <sup>3</sup>	36 days	20 days	>99%	1/6
JR	CL-Brener	i.p.	1 x 10 <sup>3</sup>	36 days	20 days	>99%	0/6
CL-Brener	JR	i.p.	1 x 10 <sup>3</sup>	36 days	20 days	>99%	0/6

**Footnotes**

<sup>1</sup>Period stretching from initial infection to the commencement of drug treatment.

<sup>2</sup>Reduction of parasite burden was inferred from total body bioluminescence at the peak of the acute stage. When mice were inoculated i.p. with bioluminescent *T. cruzi* were assessed by *in vivo* imaging, there was a linear relationship between the inoculum size and the whole animal bioluminescence for 1000 parasites and above ( $R^2>0.99$ ) (24).

<sup>3</sup>Data derived from two independent experiments, each n=6

To assess whether this protective effect was dependent on the route of inoculation, we repeated the 36 day challenge experiment using the subcutaneous (s.c.) route. *T. cruzi* transmission normally occurs when parasite-infected faeces from the insect vector are rubbed into the wound produced by blood feeding; therefore, s.c. inoculation probably reflects more closely how the majority of human infections occur. The mice were inoculated s.c. with  $10^3$  bloodstream trypomastigotes for both the primary and challenge infections, but the protocols and treatment timelines were otherwise identical to those used previously (Fig 3A, 36 day infection). In control mice, the bioluminescence profile of s.c. infections, and the resulting organ-specific tropism during the chronic stage was similar to that in i.p. infections (Figs 4A, B and C), as shown previously<sup>24,25</sup>. When the challenge cohort was assessed by in vivo imaging (Fig 4A), none of the mice displayed an acute stage peak, and bioluminescence was at, or close to background levels. At the experimental end-point, all of the mice were immunosuppressed and then subjected to post-mortem ex vivo organ imaging to test for foci of infection below the limit of in vivo detection. 4 out of 5 were found to be bioluminescence negative in all analyses and were designated as protected (Table 1).

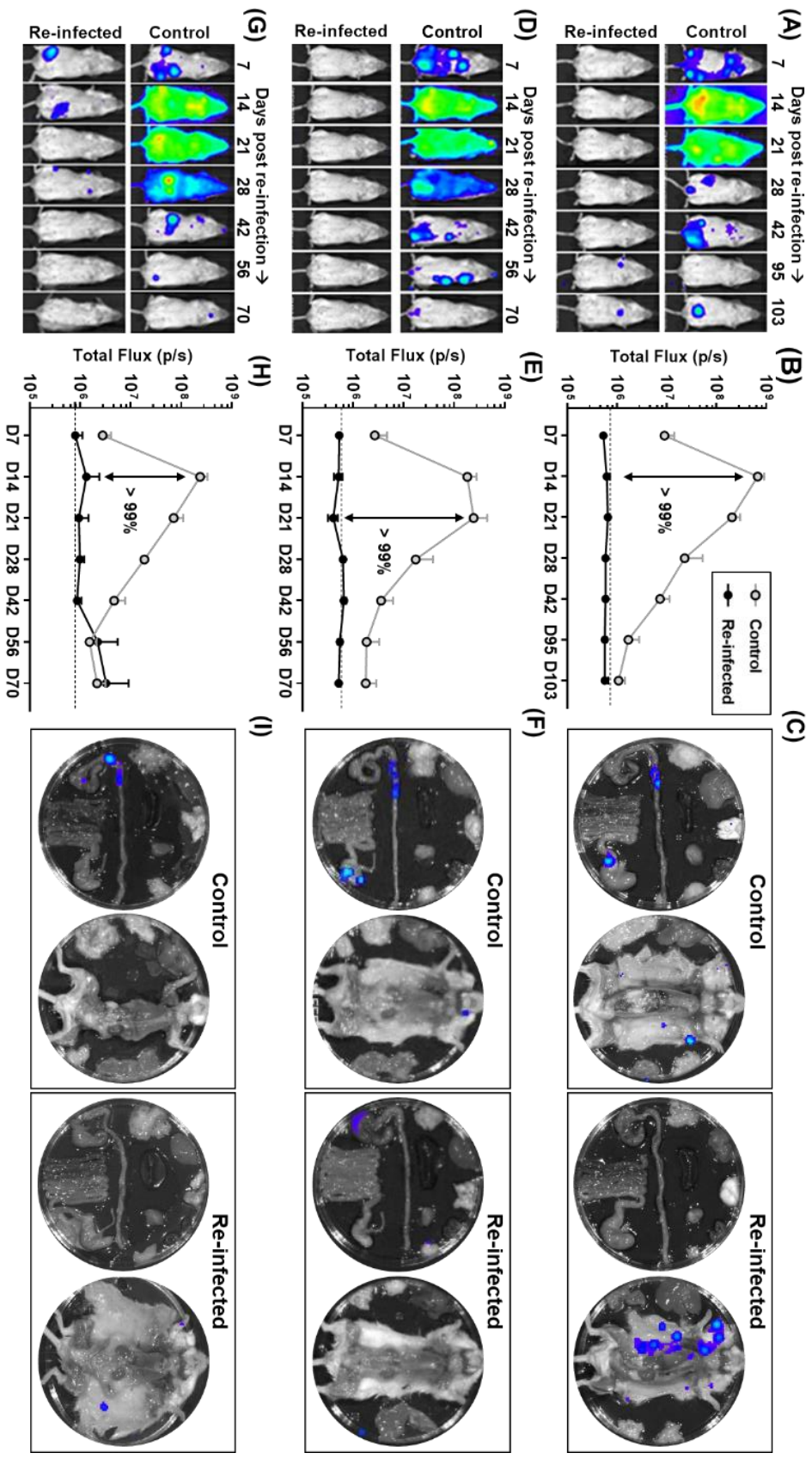


**Fig 4. Protection conferred by a benznidazole-cured infection is not dependent on the route of infection, size of the challenge inoculum or the time-period until re-infection.**

(A) BALB/c mice, infected by the subcutaneous (s.c.) route with  $10^3$  bioluminescent trypomastigotes (CL Brener strain), were subjected to curative benznidazole treatment 36 days post-infection. 21 days after the end of treatment, they were re-infected (s.c.). Control mice were also infected by the s.c. route. (B) Total body bioluminescence of drug-cured mice following s.c. re-infection (means  $\pm$  SD). (C) *Ex vivo* bioluminescence imaging of organs and carcass from a control and the re-infected mouse that was found to be non-protected after immunosuppression (Materials and Methods). (D) BALB/c mice infected i.p. with CL Brener trypomastigotes, were subjected to benznidazole treatment 36 days post-infection. 21 days after the end of treatment, they were re-infected (i.p.) with  $6 \times 10^4$  trypomastigotes. (E) Total body bioluminescence of drug-cured mice following re-infection. (F) *Ex vivo* bioluminescence imaging of organs and carcass of a control and the re-infected mouse that was found to be non-protected after immunosuppression. (G) As above, BALB/c mice were infected i.p. and subjected to curative benznidazole treatment. 338 days after the end of treatment, they were re-infected (i.p.) with  $10^3$  trypomastigotes. (H) Total body bioluminescence of drug-cured mice following re-infection. The increased mean bioluminescence of the re-infected mice towards the end of the monitoring period was due to an intense bioluminescence focus in one of the two non-protected animals. (I) *Ex vivo* bioluminescence imaging of organs and carcass of a control and a re-infected mouse that was found to be non-protected after immunosuppression. In all cases, the original cohort size was  $n=6$ . During the course of the s.c. infection experiment (A-C), one mouse failed to recover from anaesthesia, and was excluded from the analysis. Data is derived from a single experiment

It has been reported that the capacity of a cured mouse to resist re-infection is dependent on the size of the challenge inoculum (49). To investigate this using the in vivo imaging system, mice where curative treatment was initiated 36 days post-infection were challenged i.p. with  $6 \times 10^4$  CL Brener trypomastigotes, 60 times the number used previously. The outcome was similar. None of the mice displayed an acute stage parasite burden profile, and only a single mouse (out of 6) was non-protected (Fig 4D, E and F). Therefore, the level of protection conferred by a cured infection is similar when a higher challenge inoculum is used.

We next sought to determine whether protection results from the development of immunological memory, rather than retention of effector cells from the primary infection.

BALB/c mice were infected i.p. with CL Brener trypanosomes, and curative benznidazole treatment was initiated after 36 days. On this occasion, however, the mice were not re-infected until 338 days after the cessation of treatment. Following homologous challenge, the level of protection was comparable to that achieved in previous experiments when mice were reinfected 3 weeks after the last dose of benznidazole. They were able to prevent the onset of parasite proliferation during the acute stage, and 4 out of 6 mice were fully protected (Figs 4G, H, and I).

#### Assessing circulating IFN- $\gamma$ <sup>+</sup> T cells in mice after primary infection and challenge

We sought to determine if the duration of the primary infection, prior to commencement of curative drug treatment, impacted on the extent of the *T. cruzi*-specific immune response to challenge with homologous parasites. Blood was collected, 2 days prior to re-infection and at regular intervals thereafter, from mice that had been infected for 4, 14 and 36 days (Fig 5A). PBMCs were isolated, re-stimulated with an ASP-2 and TS peptide pool, and the IFN- $\gamma$ <sup>+</sup> cell frequencies measured by ELISpot (Materials and Methods). As expected for mice infected with *T. cruzi*<sup>46</sup>, the control group receiving their first parasite exposure showed a delayed peptide-specific response, with the frequency of IFN- $\gamma$ <sup>+</sup> cells on day 10 not significantly different to pre-infection levels. There were substantial increases by days 25 and 40 (Fig 5B), co-incident with the period when the parasite burden had been controlled and was undergoing major reduction (Figs 3B and C).

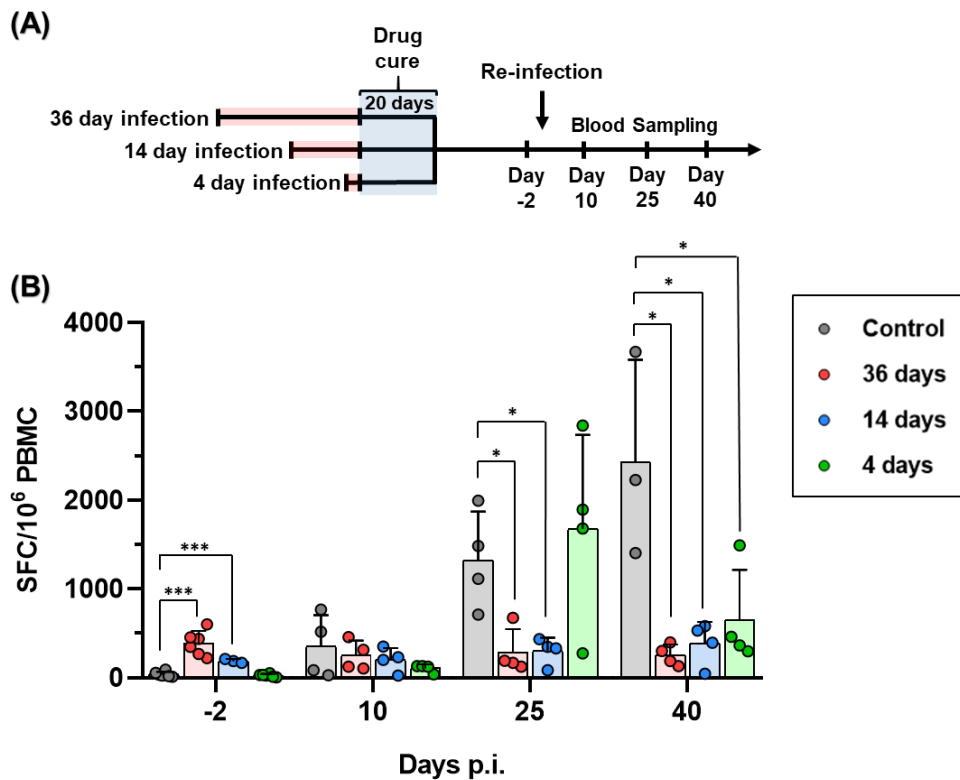


**Fig 5. The length of the primary infection affects the level of circulating murine IFN- $\gamma$ <sup>+</sup> T cells after challenge.**

(A) Timeline of experiment. Infected BALB/c mice were subjected to curative benznidazole treatment initiated 36, 14 or 4 days post-infection (as in **Figure 3**). 21 days after the end of treatment, they were re-infected (i.p.,  $10^3$  CL Brener trypomastigotes) and blood was collected by venesection on the days indicated. (B) ELISpot analysis. PBMCs were isolated from re-infected mice at pre and post re-infection, as indicated. IFN- $\gamma$ <sup>+</sup> PBMCs were quantified after overnight stimulation with a 20-mer peptide pool representing the ASP-2 and TS proteins, as in **Figure 1**. Data are presented as *ex vivo* IFN- $\gamma$  SFCs per  $10^6$  PBMCs. (\*\*\*)  $p < 0.001$ ; (\*)  $p < 0.05$ . Data is derived from a single assay, samples run in triplicate.

With benznidazole-cured mice, the pre-challenge levels of circulating *T. cruzi*-specific IFN- $\gamma$ <sup>+</sup> T cells varied, depending on the duration of the preliminary infection (Fig 5B). Initially, mice that had been infected for 36 days prior to cure displayed higher levels than the control cohort (day-2). However, these levels did not increase significantly following re-infection, although in the case of the day 14 group, there was a slight trend in this direction. In the control group, the robust adaptive response, which controlled the

infection, was associated with levels of circulating IFN- $\gamma$ <sup>+</sup> T cells that were significantly higher than in any of the benznidazole-cured mice by 40 days post-challenge (Fig 5B). Mice that had been infected for only 4 days prior to drug-cure, displayed IFN- $\gamma$ <sup>+</sup> T cell kinetics that were initially more similar to naïve mice receiving their preliminary infection, with very low levels before and 10 days post-challenge, followed by a major increase by day 25. The levels decreased thereafter, in contrast to the control group, where they continued at higher levels until day 40.

We also examined circulating parasite-specific IFN- $\gamma$ <sup>+</sup> T cells in mice that had been re-infected 338 days after drug cure (Fig 6A). Prior to re-challenge, the levels were similar to those in non-infected control mice. However, by 10 days post-challenge, there had been a 5-fold increase, in contrast to the delayed peptide-specific response typical of a *T. cruzi* infection (Fig 6B). This difference was not maintained, and on days 25 and 40 after challenge, the level of IFN- $\gamma$ <sup>+</sup> T cells was not significantly different from control mice.

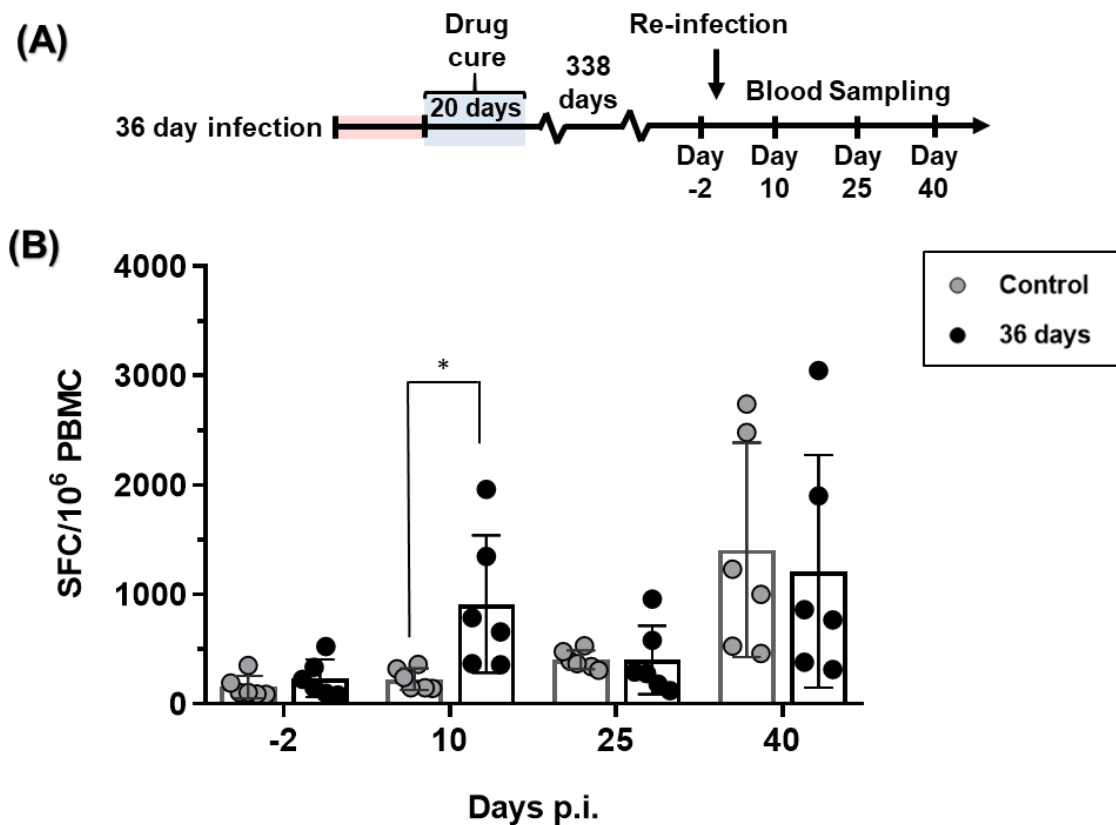


**Figure 6. Effect of delaying re-infection on the level of circulating murine IFN- $\gamma$ <sup>+</sup> T cells after challenge.**

(A) Timeline of experiment. Infected BALB/c mice were cured with benznidazole treatment, which was initiated 36 days post-infection, as in Figure 5. They were re-infected 338 days later, and blood samples collected on the days indicated. (B) PBMCs were isolated from re-infected mice at various time points pre and post re-infection. IFN- $\gamma$ <sup>+</sup> PBMCs were quantified after overnight stimulation with the 20-mer ASP-2/TS peptide pool. (\*)  $p=0.024$ . Data is derived from a single assay, samples run in triplicate.

### The capacity of drug-cured infections to confer a cross-strain protective response

*T. cruzi* displays significant genetic diversity, with the natural population subdivided into 6 lineages known as discrete typing units (DTUs), each of which has the ability to infect humans<sup>47</sup>. We therefore investigated if the capacity to confer homologous protection is a general feature of *T. cruzi* infections by performing an analogous experiment using JR strain parasites from the genetically distant TcI lineage. In BALB/c mice, infections with

this strain are slightly slower to reach the peak of the acute stage, but the bioluminescence profile is otherwise similar to that of the CL Brener strain<sup>25</sup> (DTU VI lineage). Mice were benznidazole-treated 36 days into a JR infection, and re-infected with the same strain 20 days after the end of treatment (Fig 7A). As before, we observed that the cured infection conferred significant protection. None of the mice exhibited a distinct acute stage peak, with the majority remaining close to bioluminescence background levels (Figs 7B and C). However, only a single mouse (out of 6) exhibited sterile protection when assessed by ex vivo imaging following immunosuppression (Materials and Methods) (Fig 7D).

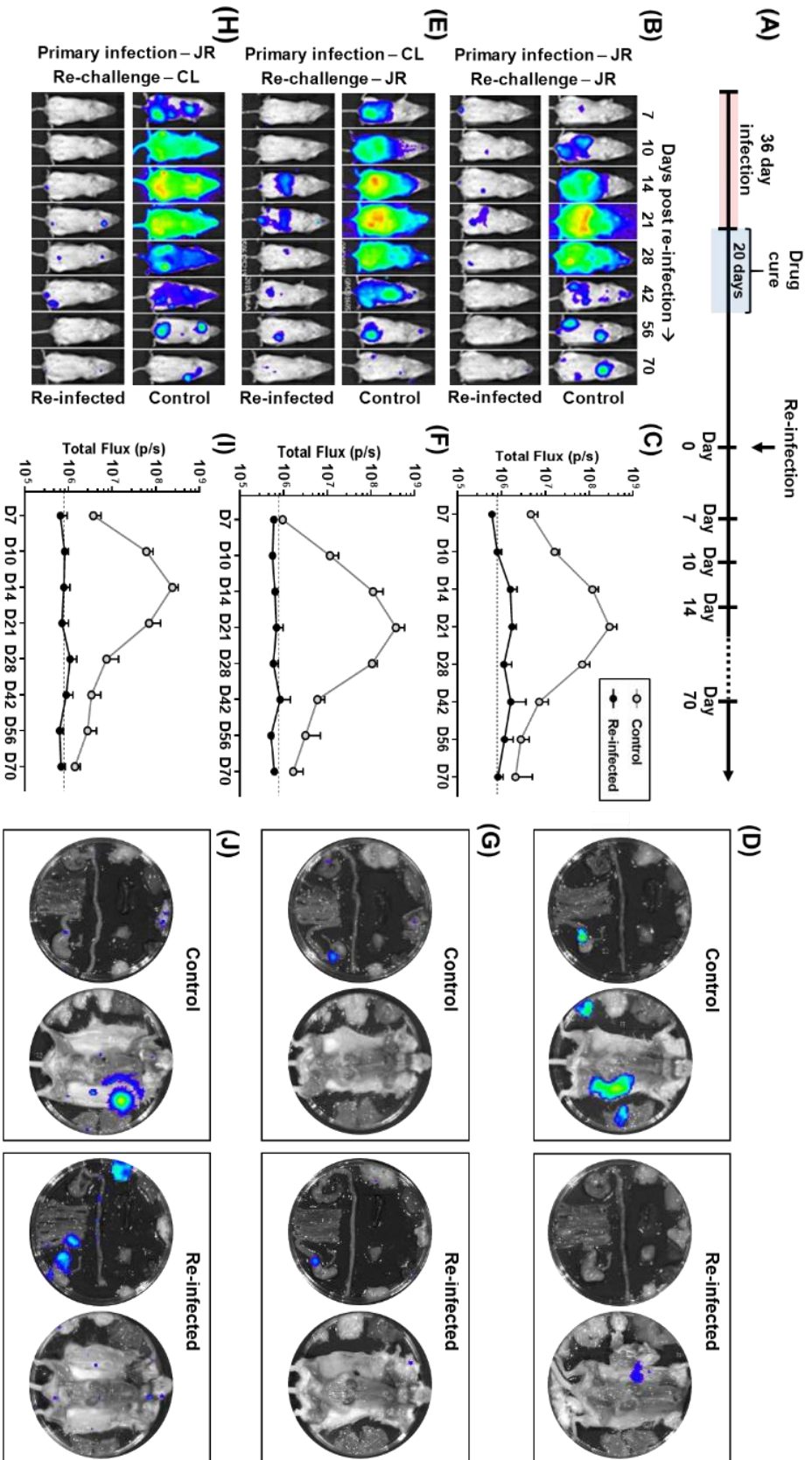


**Fig 7. Protection against challenge with a heterologous *T. cruzi* strain.**

(A) Outline strategy. BALB/c mice were infected i.p. with bioluminescent trypomastigotes (CL Brener or JR strains) and subjected to curative benznidazole treatment initiated 36 days post-infection. 20 days after the end of treatment, they were re-infected as indicated below and monitored for a further 70 days. Bioluminescence-negative mice were then immunosuppressed and assessed by ex vivo imaging. (B) Ventral images of a representative drug-cured JR infected mouse (n=6) following re-infection with the homologous JR strain. All images use the same log<sub>10</sub>-scale heat-map shown in Fig 2. (C) Total body bioluminescence (sum of ventral and dorsal images) of drug-cured JR infected mice re-infected with the JR strain (means ± SD). (D) Ex vivo bioluminescence imaging of organs and carcass of a control and re-infected mouse (non-protected). (E) Ventral images of a representative drug-cured CL Brener infected mouse (n=6) following re-infection with the JR strain. (F) Total body bioluminescence of drug-cured CL Brener infected mice re-infected with the JR strain. (G) Ex vivo bioluminescence imaging of organs and carcass of a control and re-infected mouse (non-protected). (H) Ventral images of a representative drug-cured JR infected mouse (n=6) following re-infection with the CL Brener strain. (I) Total body bioluminescence of drug-cured JR infected mice re-infected with the CL Brener strain. (J) Ex vivo bioluminescence imaging of organs and carcass of a control and re-infected mouse (non-protected). Data derived from single experiment

To assess the scope for vaccine-induced species-wide immunity, we next investigated the effectiveness of protection conferred against a heterologous challenge using the strains CL Brener (TcVI) and JR (TcI). Following the strategy outlined above, BALB/c mice were infected i.p. with 10<sup>3</sup> bloodstream CL Brener or JR trypomastigotes, benznidazole-treated, and then challenged with the heterologous strain 20 days after the end of the curative therapy. In both experiments, we observed a strong protective response (>99%) (Figs 7E-J), with no distinct acute stage peak and a reduced number of bioluminescent foci in the period corresponding to the transition to the chronic stage. However, in both cases, all mice exposed to cross-strain challenge displayed small but clear parasite foci following re-infection. None exhibited sterile protection when examined by ex vivo imaging, with each displaying the type of GI tract infections

characteristic of the chronic stage (Figs 7G and J). Therefore, although infection with a heterologous strain can have a major impact on the subsequent parasite burden, it did not confer sterile immunity in any of the mice examined.

## DISCUSSION

Although experimental *T. cruzi* vaccines have been widely shown to reduce the burden of infection in animal models<sup>27-35</sup>, there is little unambiguous evidence for sterile protection. Despite this, there have been an increasing number of reports that vaccination could have therapeutic benefits in terms of decreased cardiac pathology<sup>33,48-50</sup>. Therefore, the question as to whether the development of a Chagas disease vaccine might be a practical option for reducing the public health impact of this infection remains unanswered. Detailed assessment has been limited by difficulties in detecting the intermittent low-level parasitemia of chronic stage infections, and in identifying the tissue/organ location of persistent parasites. Here, we demonstrate that highly sensitive bioluminescent imaging can negate some of these issues, and provide novel insights into vaccine efficacy.

Initially, we tested the protective properties of two viral vectors (MVA and ChAdOx1) that had been modified to express an ASP-2/TS fusion gene (Fig 1). The reduction in peak parasite burden (77%, Fig 2C) was in a range similar to that reported for other recombinant *T. cruzi* vaccines<sup>51-53</sup>. Interestingly, vaccination had no impact on the parasite burden once the infection had transitioned to the chronic phase, suggesting that if parasites can survive until this stage of the disease, they are less susceptible to clearance by vaccine-induced immunity. This has not been reported previously. At the experimental end-point, the remaining parasites were restricted predominantly to the GI tract (Fig 2D). In BALB/c and other mice, this location serves as a permissive niche, enabling parasites to persist in an otherwise hostile immune environment<sup>24,25,37</sup>, although the mechanism(s) for this have yet to be elucidated. To determine if this might limit the utility of a Chagas disease vaccine, we therefore investigated the protective effect of benznidazole-cured infections, on the basis that these should provide optimal levels of

immunity. Curative treatment has been associated with the development of a stable anti-*T. cruzi* CD8<sup>+</sup> T cell population<sup>22</sup>.

Drug-cure was initiated after infection for 36 days (a time-point when the adaptive CD8<sup>+</sup> T cell response is controlling the infection), 14 days (the peak of the acute stage), and 4 days (just short of one complete round of the intracellular replication cycle that leads to differentiation and parasite egress) (Fig 3). Mice infected for 36 days prior to benznidazole treatment were highly protected from challenge (Fig 3B), with complete absence of a typical acute stage peak. However, sterile protection was only achieved in half of the re-infected mice (Table 1). Therefore, although drug-cured infections can generate a highly effective immune response, that prevents a second acute phase, parasites that evade this initial encounter seem to be refractory to immune-mediated elimination and are able to persist long term. This outcome was not significantly influenced by the size of the challenge inoculum or the route of infection (Fig 4). Initiating treatment after 14 days was also able to prevent a detectable acute stage peak in bioluminescence when the mice were challenged, although there was a slight reduction in the level of sterile protection (Fig 3B, Table 1). In contrast, when drug-cure was initiated after 4 days, a pronounced post-challenge acute stage peak could be observed, but even then, the parasite burden was 85% lower than in a naive infection. Therefore, 14 days exposure to an untreated infection is sufficient for the induction of a robust immune response, whereas with 4 days, the response appears to be less developed, although still sufficient to have a significant impact on the parasite burden.

A delayed onset of the CD8<sup>+</sup> T cell response is a characteristic feature of Chagas disease<sup>54</sup>, with the first round of intracellular infections passing largely undetected by the immune system. Upon invasion of mammalian cells, parasites rapidly escape from the phagolysosome, there is down-modulation of the host cell immunoproteasome<sup>55</sup>,

and minimal activation of the host-pattern recognition receptors. Induction of effective innate immunity requires a full cycle of parasite replication, host cell lysis, and the release of trypomastigotes into the extracellular milieu, a process that takes at least 4-5 days. This is followed by the production of pathogen-associated and damage-associated molecular patterns that promote innate immune responses, allowing parasitized cells to flag up their infected status by MHC class I antigen presentation. Full development of the CD8<sup>+</sup> T cell response to *T. cruzi* infections takes around 3 weeks<sup>54</sup>. In mice where curative treatment was initiated 14 or 36 days postinfection, circulating parasite peptide-specific IFN- $\gamma$ <sup>+</sup> T cells were readily detectable prior to challenge (Fig 5B), and were associated with protection against the development of a second acute phase profile. In many cases, this response was sufficient to promote complete elimination of the secondary infection. Experimental challenge did not lead to a significant increase in the level of IFN- $\gamma$ <sup>+</sup> T cells, suggesting that the pre-existing effector population was able to contain the secondary infection without further induction. Even when preliminary infection did not confer sterile protection, there was no further enhancement of the peptide-specific response. Therefore, if parasites in the challenge inoculation can avoid early elimination, and are able to establish a long term chronic infection, it appears that they survive in an environment or state that does not trigger additional T cell activation.

In mice where curative treatment was initiated 4 days into the primary infection, the level of *T. cruzi*-specific IFN- $\gamma$ <sup>+</sup> T cells prior to re-infection was negligible, and the kinetics of the response induced over the first 25 days of the challenge infection was similar to that in the controls (Fig 5). Despite this, there was an 85% reduction in the parasite burden at the peak of the re-infection. Therefore, the induced partially protective effect in these mice is conferred either by an extremely low level of circulating parasite-specific IFN- $\gamma$ <sup>+</sup> T cells, or by other factors that operate to moderate the infection. In mice challenged almost a year after curative treatment of the primary infection, the level of protection was

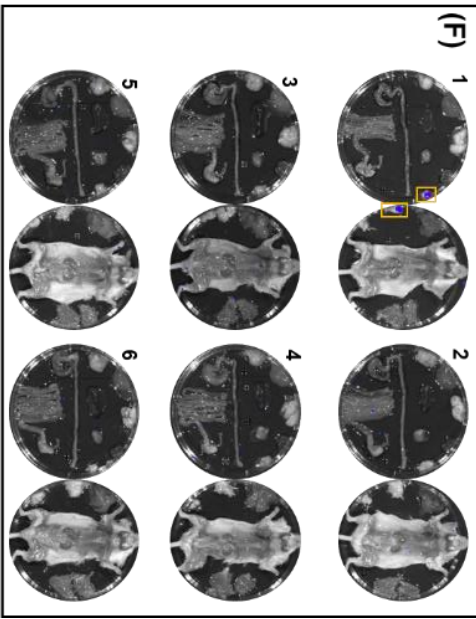
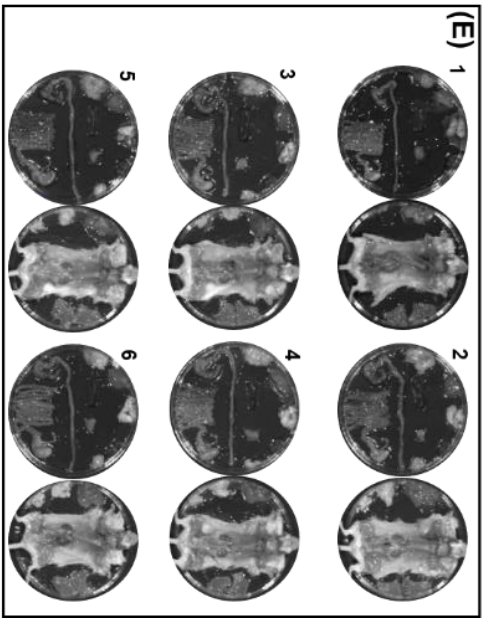
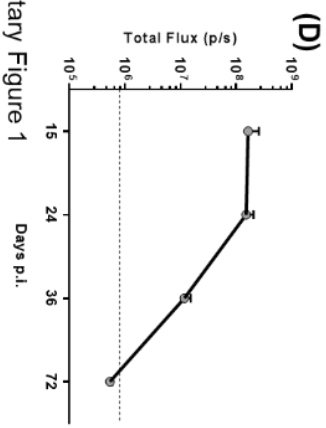
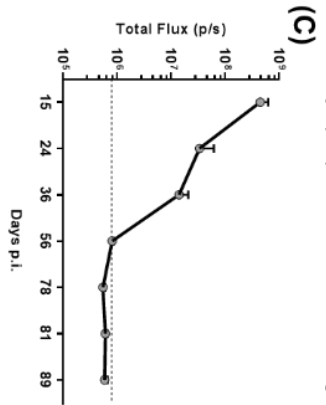
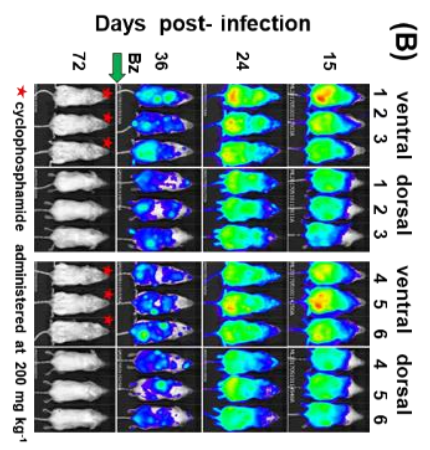
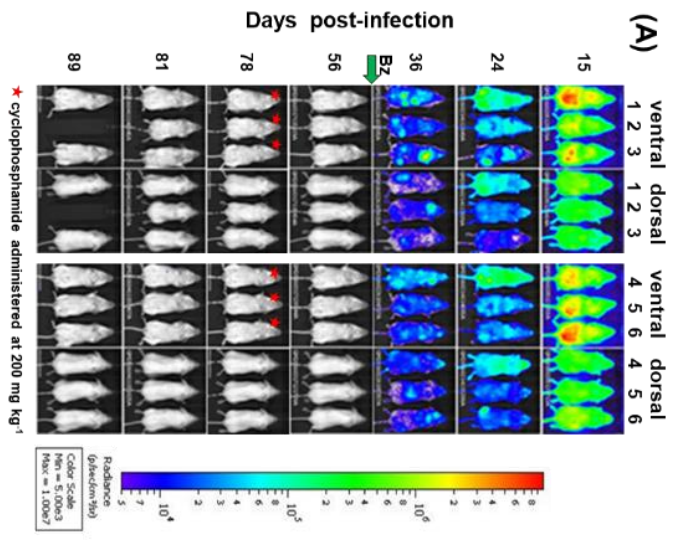
similar to mice in which the gap between the end of treatment and challenge was only ~20 days. However, unlike these mice, re-infection after almost a year was accompanied by induction of peptide-specific T cells, with kinetics that were more rapid than in the naive control cohort (Fig 6). This evidence for a memory response suggests that vaccine-mediated long term protection against fulminant *T. cruzi* infection may be a feasible goal. Furthermore, if these results can be extrapolated to humans, it would imply that patients who have undergone curative drug treatment should have the added benefit of a high level of long term protection against re-infection.

We also investigated the extent to which benznidazole-cured infections could provide cross-strain protection. *T. cruzi* is highly diverse, with six major genetic lineages that display considerable geographic overlap. Taxonomy is further complicated by the widespread existence of hybrid strains<sup>56</sup>. Mice initially infected with the *T. cruzi* CL Brener (TcVI) were challenged with the JR strain (TcI), and vice-versa. Although, suppression of the parasite burden was similar to that in a homologous challenge (>99%), sterile protection was not achieved (Fig 7), with surviving parasites persisting at very low levels. We have suggested a model for chronic Chagas disease<sup>37</sup> in which the gut (and perhaps other tissues, such as the skin or skeletal muscle) acts as an immunologically tolerant reservoir for *T. cruzi* persistence, with periodic trafficking to other sites, where the parasites are then destroyed rapidly by immune effector mechanisms. In the heart, this can lead to cumulative collateral damage that ultimately gives rise to cardiac pathology<sup>57</sup>.

We propose that when parasites establish infections in the GI tract, or other permissive sites, they become refractory to elimination by the vigorous adaptive responses induced by drug-cured infections. Thus, the effectiveness of a Chagas disease vaccine could

depend on the efficiency with which the primed immune system prevents *T. cruzi* from reaching the relative safety of these sites of persistence, and its ability to maintain this response over time against a wide range of strains. The results presented here, and elsewhere [31-34,48-53,58,59](#), highlight the possibility that current subunit/DNA vaccines may be unable to fulfil these requirements, although their ability to prevent lethal outcomes<sup>31-34,49,52,58,59</sup> and provide therapeutic benefits<sup>33,48-51,53</sup> merits further research. As we have shown here however, the long term protection conferred by live infection, followed by drug-mediated cure, suggests that the use of genetically attenuated parasite strains may be the best approach to achieving an effective vaccine.

Supplementary



Supplementary Figure 1

**Supplementary Figure 1. Assessing the curative ability of benznidazole.** (A, B) *In vivo* imaging of BALB/c mice infected with CL Brener (A) and (JR) strains of *T. cruzi*. Treatment with benznidazole, 100 mg kg<sup>-1</sup> once daily by the oral route for 20 days, was initiated 36 days post-infection. Following cessation of treatment, mice were immunosuppressed with 3 doses of 200 mg kg<sup>-1</sup> cyclophosphamide (Materials and Methods). All images use the same log<sub>10</sub>-scale heat-map with minimum and maximum radiance values indicated. (C and D) Total body bioluminescence (sum of ventral and dorsal images) of CL Brener (C) and JR (D) infected mice. Dashed lines indicate background bioluminescence. All images use the same log<sub>10</sub>-scale heat-map with minimum and maximum radiance values indicated. (E and F) *Ex vivo* bioluminescence imaging of organs and carcasses from CL Brener (E) and JR (F) infected mice at the experimental end-point. A minor bioluminescent focus was observed in the adipose tissue of mouse 1 (JR infection). Mouse 2 (CL Brener infection) was euthanised prior to day 89, due to weight loss during immunosuppressive treatment. It was negative by both *in vivo* and *ex vivo* imaging. Data representative of two independently run experiments



**Supplementary Figure 2. Benznidazole-cured infections confer significant protection against re-challenge with the *T. cruzi* CL Brener strain.** (A) Timeline. BALB/c mice infected i.p. with  $10^3$  trypomastigotes (CL Brener strain) were subjected to curative benznidazole treatment initiated 36 days post-infection. 23 days after the end of treatment, they were re-infected i.p. After a further 75 days, the mice were immunosuppressed using cyclophosphamide (red stars) and assessed by *ex vivo* imaging. (B) Ventral and dorsal bioluminescence images from a cohort of 6 mice. The days post re-infection are indicated (left). All images use the same  $\log_{10}$  scale heat-map with minimum and maximum radiance values indicated. (C) *Ex vivo* bioluminescence imaging of organs and carcasses harvested at the experimental end-point. (D) Total body bioluminescence (sum of ventral and dorsal images) of drug-cured mice following re-infection (means  $\pm$  SD) derived by *in vivo* imaging. Mice 3 and 4 were designated as non-protected on the basis of *in vivo* and/or *ex vivo* imaging. Data representative of two independently run experiments

## References

- 1 Hashimoto, K. & Yoshioka, K. Review: surveillance of Chagas disease. *Adv Parasitol* **79**, 375-428, doi:10.1016/B978-0-12-398457-9.00006-8 (2012).
- 2 Bern, C. Chagas' Disease. *N Engl J Med* **373**, 456-466, doi:10.1056/NEJMra1410150 (2015).
- 3 Lee, B. Y., Bacon, K. M., Bottazzi, M. E. & Hotez, P. J. Global economic burden of Chagas disease: a computational simulation model. *Lancet Infect Dis* **13**, 342-348, doi:10.1016/S1473-3099(13)70002-1 (2013).
- 4 Bustamante, J. & Tarleton, R. Reaching for the Holy Grail: insights from infection/cure models on the prospects for vaccines for *Trypanosoma cruzi* infection. *Mem Inst Oswaldo Cruz* **110**, 445-451, doi:10.1590/0074-02760140440 (2015).
- 5 Ribeiro, A. L., Nunes, M. P., Teixeira, M. M. & Rocha, M. O. Diagnosis and management of Chagas disease and cardiomyopathy. *Nat Rev Cardiol* **9**, 576-589, doi:10.1038/nrcardio.2012.109 (2012).
- 6 Cunha-Neto, E. & Chevillard, C. Chagas disease cardiomyopathy: immunopathology and genetics. *Mediators Inflamm* **2014**, 683230, doi:10.1155/2014/683230 (2014).
- 7 Bonney, K. M. Chagas disease in the 21st century: a public health success or an emerging threat? *Parasite* **21**, 11, doi:10.1051/parasite/2014012 (2014).
- 8 Dias, J. C. Evolution of Chagas disease screening programs and control programs: historical perspective. *Glob Heart* **10**, 193-202, doi:10.1016/j.gheart.2015.06.003 (2015).
- 9 Sosa-Estani, S. & Segura, E. L. Integrated control of Chagas disease for its elimination as public health problem--a review. *Mem Inst Oswaldo Cruz* **110**, 289-298, doi:10.1590/0074-02760140408 (2015).
- 10 Wilkinson, S. R. & Kelly, J. M. Trypanocidal drugs: mechanisms, resistance and new targets. *Expert Rev Mol Med* **11**, e31, doi:10.1017/S1462399409001252 (2009).
- 11 Gaspar, L. *et al.* Current and Future Chemotherapy for Chagas Disease. *Curr Med Chem* **22**, 4293-4312, doi:10.2174/0929867322666151015120804 (2015).
- 12 Chatelain, E. Chagas disease research and development: Is there light at the end of the tunnel? *Comput Struct Biotechnol J* **15**, 98-103, doi:10.1016/j.csbj.2016.12.002 (2017).
- 13 Iwai, L. K., Juliano, M. A., Juliano, L., Kalil, J. & Cunha-Neto, E. T-cell molecular mimicry in Chagas disease: identification and partial structural analysis of multiple cross-reactive epitopes between *Trypanosoma cruzi* B13 and cardiac myosin heavy chain. *J Autoimmun* **24**, 111-117, doi:10.1016/j.jaut.2005.01.006 (2005).

- 14 Bermejo, D. A. *et al.* Trypanosoma cruzi infection induces a massive extrafollicular and follicular splenic B-cell response which is a high source of non-parasite-specific antibodies. *Immunology* **132**, 123-133, doi:10.1111/j.1365-2567.2010.03347.x (2011).
- 15 Kierszenbaum, F. Where do we stand on the autoimmunity hypothesis of Chagas disease? *Trends Parasitol* **21**, 513-516, doi:10.1016/j.pt.2005.08.013 (2005).
- 16 Gutierrez, F. R., Guedes, P. M., Gazzinelli, R. T. & Silva, J. S. The role of parasite persistence in pathogenesis of Chagas heart disease. *Parasite Immunol* **31**, 673-685, doi:10.1111/j.1365-3024.2009.01108.x (2009).
- 17 Bonney, K. M. & Engman, D. M. Autoimmune pathogenesis of Chagas heart disease: looking back, looking ahead. *Am J Pathol* **185**, 1537-1547, doi:10.1016/j.ajpath.2014.12.023 (2015).
- 18 Tarleton, R. L. CD8+ T cells in Trypanosoma cruzi infection. *Semin Immunopathol* **37**, 233-238, doi:10.1007/s00281-015-0481-9 (2015).
- 19 Bonney, K. M., Luthringer, D. J., Kim, S. A., Garg, N. J. & Engman, D. M. Pathology and Pathogenesis of Chagas Heart Disease. *Annu Rev Pathol* **14**, 421-447, doi:10.1146/annurev-pathol-020117-043711 (2019).
- 20 Kayama, H. & Takeda, K. The innate immune response to Trypanosoma cruzi infection. *Microbes Infect* **12**, 511-517, doi:10.1016/j.micinf.2010.03.005 (2010).
- 21 Campos, M. A. & Gazzinelli, R. T. Trypanosoma cruzi and its components as exogenous mediators of inflammation recognized through Toll-like receptors. *Mediators Inflamm* **13**, 139-143, doi:10.1080/09511920410001713565 (2004).
- 22 Bustamante, J. M., Bixby, L. M. & Tarleton, R. L. Drug-induced cure drives conversion to a stable and protective CD8+ T central memory response in chronic Chagas disease. *Nat Med* **14**, 542-550, doi:10.1038/nm1744 (2008).
- 23 Martin, D. L. *et al.* CD8+ T-Cell responses to Trypanosoma cruzi are highly focused on strain-variant trans-sialidase epitopes. *PLoS Pathog* **2**, e77, doi:10.1371/journal.ppat.0020077 (2006).
- 24 Lewis, M. D. *et al.* Bioluminescence imaging of chronic Trypanosoma cruzi infections reveals tissue-specific parasite dynamics and heart disease in the absence of locally persistent infection. *Cell Microbiol* **16**, 1285-1300, doi:10.1111/cmi.12297 (2014).
- 25 Lewis, M. D., Francisco, A. F., Taylor, M. C., Jayawardhana, S. & Kelly, J. M. Host and parasite genetics shape a link between Trypanosoma cruzi infection dynamics and chronic cardiomyopathy. *Cell Microbiol* **18**, 1429-1443, doi:10.1111/cmi.12584 (2016).

- 26 Pack, A. D., Collins, M. H., Rosenberg, C. S. & Tarleton, R. L. Highly competent, non-exhausted CD8<sup>+</sup> T cells continue to tightly control pathogen load throughout chronic *Trypanosoma cruzi* infection. *PLoS Pathog* **14**, e1007410, doi:10.1371/journal.ppat.1007410 (2018).
- 27 Rodriguez-Morales, O. *et al.* Experimental Vaccines against Chagas Disease: A Journey through History. *J Immunol Res* **2015**, 489758, doi:10.1155/2015/489758 (2015).
- 28 Pizzi, T. & Prager, R. [Immunity to infection induced by culture of *Trypanosoma cruzi* of attenuated virulence; preliminary communication]. *Bol Inf Parasit Chil* **7**, 20-21 (1952).
- 29 Perez Brandan, C., Padilla, A. M., Xu, D., Tarleton, R. L. & Basombrio, M. A. Knockout of the dhfr-ts gene in *Trypanosoma cruzi* generates attenuated parasites able to confer protection against a virulent challenge. *PLoS Negl Trop Dis* **5**, e1418, doi:10.1371/journal.pntd.0001418 (2011).
- 30 Ruiz, A. M., Esteva, M., Cabeza Meckert, P., Laguens, R. P. & Segura, E. L. Protective immunity and pathology induced by inoculation of mice with different subcellular fractions of *Trypanosoma cruzi*. *Acta Trop* **42**, 299-309 (1985).
- 31 Wrightsman, R. A., Miller, M. J., Saborio, J. L. & Manning, J. E. Pure paraflagellar rod protein protects mice against *Trypanosoma cruzi* infection. *Infect Immun* **63**, 122-125 (1995).
- 32 Luhrs, K. A., Fouts, D. L. & Manning, J. E. Immunization with recombinant paraflagellar rod protein induces protective immunity against *Trypanosoma cruzi* infection. *Vaccine* **21**, 3058-3069, doi:10.1016/s0264-410x(03)00108-7 (2003).
- 33 Gupta, S. & Garg, N. J. TcVac3 induced control of *Trypanosoma cruzi* infection and chronic myocarditis in mice. *PLoS One* **8**, e59434, doi:10.1371/journal.pone.0059434 (2013).
- 34 Nogueira, R. T. *et al.* Recombinant yellow fever viruses elicit CD8<sup>+</sup> T cell responses and protective immunity against *Trypanosoma cruzi*. *PLoS One* **8**, e59347, doi:10.1371/journal.pone.0059347 (2013).
- 35 Vasconcelos, J. R. *et al.* Adenovirus vector-induced CD8(+) T effector memory cell differentiation and recirculation, but not proliferation, are important for protective immunity against experimental *Trypanosoma cruzi* Infection. *Hum Gene Ther* **25**, 350-363, doi:10.1089/hum.2013.218 (2014).

- 36 Lewis, M. D., Francisco, A. F., Taylor, M. C. & Kelly, J. M. A new experimental model for assessing drug efficacy against *Trypanosoma cruzi* infection based on highly sensitive in vivo imaging. *J Biomol Screen* **20**, 36-43, doi:10.1177/1087057114552623 (2015).
- 37 Lewis, M. D. & Kelly, J. M. Putting Infection Dynamics at the Heart of Chagas Disease. *Trends Parasitol* **32**, 899-911, doi:10.1016/j.pt.2016.08.009 (2016).
- 38 Sanchez-Valdez, F. J., Padilla, A., Wang, W., Orr, D. & Tarleton, R. L. Spontaneous dormancy protects *Trypanosoma cruzi* during extended drug exposure. *Elife* **7**, doi:10.7554/eLife.34039 (2018).
- 39 Branchini, B. R. *et al.* Red-emitting luciferases for bioluminescence reporter and imaging applications. *Anal Biochem* **396**, 290-297, doi:10.1016/j.ab.2009.09.009 (2010).
- 40 Fang, J. *et al.* Stable antibody expression at therapeutic levels using the 2A peptide. *Nat Biotechnol* **23**, 584-590, doi:10.1038/nbt1087 (2005).
- 41 Dicks, M. D. *et al.* A novel chimpanzee adenovirus vector with low human seroprevalence: improved systems for vector derivation and comparative immunogenicity. *PLoS One* **7**, e40385, doi:10.1371/journal.pone.0040385 (2012).
- 42 Gomez, C. E., Perdiguero, B., Garcia-Arriaza, J. & Esteban, M. Clinical applications of attenuated MVA poxvirus strain. *Expert Rev Vaccines* **12**, 1395-1416, doi:10.1586/14760584.2013.845531 (2013).
- 43 Gilbert, S. C. Clinical development of Modified Vaccinia virus Ankara vaccines. *Vaccine* **31**, 4241-4246, doi:10.1016/j.vaccine.2013.03.020 (2013).
- 44 Francisco, A. F. *et al.* Limited Ability of Posaconazole To Cure both Acute and Chronic *Trypanosoma cruzi* Infections Revealed by Highly Sensitive In Vivo Imaging. *Antimicrob Agents Chemother* **59**, 4653-4661, doi:10.1128/AAC.00520-15 (2015).
- 45 Francisco, A. F. *et al.* Nitroheterocyclic drugs cure experimental *Trypanosoma cruzi* infections more effectively in the chronic stage than in the acute stage. *Sci Rep* **6**, 35351, doi:10.1038/srep35351 (2016).
- 46 Tzelepis, F. *et al.* Distinct kinetics of effector CD8+ cytotoxic T cells after infection with *Trypanosoma cruzi* in naive or vaccinated mice. *Infect Immun* **74**, 2477-2481, doi:10.1128/IAI.74.4.2477-2481.2006 (2006).
- 47 Messenger, L. A., Miles, M. A. & Bern, C. Between a bug and a hard place: *Trypanosoma cruzi* genetic diversity and the clinical outcomes of Chagas disease. *Expert Rev Anti Infect Ther* **13**, 995-1029, doi:10.1586/14787210.2015.1056158 (2015).

- 48 Gupta, S. & Garg, N. J. Prophylactic efficacy of TcVac2 against *Trypanosoma cruzi* in mice. *PLoS Negl Trop Dis* **4**, e797, doi:10.1371/journal.pntd.0000797 (2010).
- 49 Arce-Fonseca, M., Rios-Castro, M., Carrillo-Sanchez Sdel, C., Martinez-Cruz, M. & Rodriguez-Morales, O. Prophylactic and therapeutic DNA vaccines against Chagas disease. *Parasit Vectors* **8**, 121, doi:10.1186/s13071-015-0738-0 (2015).
- 50 Barry, M. A. *et al.* A therapeutic vaccine prototype induces protective immunity and reduces cardiac fibrosis in a mouse model of chronic *Trypanosoma cruzi* infection. *PLoS Negl Trop Dis* **13**, e0007413, doi:10.1371/journal.pntd.0007413 (2019).
- 51 de la Cruz, J. J. *et al.* Production of recombinant TSA-1 and evaluation of its potential for the immuno-therapeutic control of *Trypanosoma cruzi* infection in mice. *Hum Vaccin Immunother* **15**, 210-219, doi:10.1080/21645515.2018.1520581 (2019).
- 52 Arce-Fonseca, M. *et al.* Recombinant Enolase of *Trypanosoma cruzi* as a Novel Vaccine Candidate against Chagas Disease in a Mouse Model of Acute Infection. *J Immunol Res* **2018**, 8964085, doi:10.1155/2018/8964085 (2018).
- 53 Martinez-Campos, V. *et al.* Expression, purification, immunogenicity, and protective efficacy of a recombinant Tc24 antigen as a vaccine against *Trypanosoma cruzi* infection in mice. *Vaccine* **33**, 4505-4512, doi:10.1016/j.vaccine.2015.07.017 (2015).
- 54 Padilla, A. M., Simpson, L. J. & Tarleton, R. L. Insufficient TLR activation contributes to the slow development of CD8+ T cell responses in *Trypanosoma cruzi* infection. *J Immunol* **183**, 1245-1252, doi:10.4049/jimmunol.0901178 (2009).
- 55 Camargo, R. *et al.* *Trypanosoma cruzi* infection down-modulates the immunoproteasome biosynthesis and the MHC class I cell surface expression in HeLa cells. *PLoS One* **9**, e95977, doi:10.1371/journal.pone.0095977 (2014).
- 56 Francisco, A. F., Jayawardhana, S., Lewis, M. D., Taylor, M. C. & Kelly, J. M. Biological factors that impinge on Chagas disease drug development. *Parasitology* **144**, 1871-1880, doi:10.1017/S0031182017001469 (2017).
- 57 Francisco, A. F., Jayawardhana, S., Taylor, M. C., Lewis, M. D. & Kelly, J. M. Assessing the Effectiveness of Curative Benznidazole Treatment in Preventing Chronic Cardiac Pathology in Experimental Models of Chagas Disease. *Antimicrob Agents Chemother* **62**, doi:10.1128/AAC.00832-18 (2018).
- 58 Costa, F. *et al.* Immunization with a plasmid DNA containing the gene of trans-sialidase reduces *Trypanosoma cruzi* infection in mice. *Vaccine* **16**, 768-774, doi:10.1016/s0264-410x(97)00277-6 (1998).

- 59 Boscardin, S. B., Kinoshita, S. S., Fujimura, A. E. & Rodrigues, M. M. Immunization with cDNA expressed by amastigotes of *Trypanosoma cruzi* elicits protective immune response against experimental infection. *Infect Immun* **71**, 2744-2757, doi:10.1128/iai.71.5.2744-2757.2003 (2003).

## Chapter 3:

# Correlates of Protection in Viral Vectored Vaccination & in a Live Vaccine

### **3.1 Introduction**

The vaccine study and the re-infection studies performed in Chapter 2 represent significant investments of time. In order to take advantage of the unique experimental conditions, and to optimise animal usage, we performed a number of other experiments on these mice with the following aims.

1. To better understand correlates of viral vaccine induced protection
2. To explore additional correlates of protection in infection experienced mice upon a re-infection

These experiments were outside of the specific remit of the main body of work in chapter 2. However, they present interesting and relevant findings which are worth discussion as they could form the basis of further experimentation by our group or the wider *T. cruzi* and vaccine community.

#### **3.1.1 Vaccine induced immunity**

CD8<sup>+</sup> T cells are instrumental in the development of natural immunity in *T. cruzi*, as was discussed in the Introduction, Chapter 1. Their importance in vaccine mediated protection is also beyond question, which is what makes viral vectors, natural inducers of CD8<sup>+</sup> T cell immunity, such an attractive platform<sup>1</sup>. The importance of CD8<sup>+</sup> T cells can be demonstrated experimentally in studies which deplete CD8<sup>+</sup> cells post-vaccination. This completely abolishes vaccine induced protection in a *T. cruzi* experimental challenge<sup>2</sup>.

We demonstrated in Chapter 2 the immunogenicity of our novel vaccine based on the viral vectors ChadOx1 and MVA. Vaccination of BALB/c mice with these viral vectors, expressing the parasite proteins ASP-2 and TS, resulted in an elevated frequency of antigen specific T cells prior to challenge (Chapter 2, Figure 1). We sought to establish

how the kinetics of the T cell response evolved post-challenge in vaccinated and non-vaccinated mice. The parasite proteins ASP-2 and TS, either alone or in combination, have been the targets of several experimental vaccines. However, none of these have been studied in a non-lethal challenge model<sup>2-6</sup>. Vaccine mediated protection in experimental challenge is commonly measured as function of host survival, however this is not reflective of the human infection<sup>7</sup>. Using the bioluminescence system, we sought to study the kinetics of the T cell response amongst vaccinated mice and how this correlated with the level of protection.

In addition to studying the frequency of vaccine induced *T. cruzi* specific T cells post-challenge, we also analysed the functional properties of these cells at the experimental end point using flow cytometry. The spleens of vaccinated and control mice were harvested and splenocytes were re-stimulated with peptide pools representing the vaccine expressed parasite proteins. This was of interest because previous studies in *T. cruzi* have reported a re-programming of the immune system after vaccination with a viral vectored vaccine<sup>8</sup>. This re-programming resulted in an altered T cell profile in the chronic stage of the infection, with vaccinated mice demonstrating a significantly reduced cytotoxic response. This modified T cell response was associated with improved heart pathology. We wanted to explore whether we could observe this phenomenon using our viral vectored approach and what implications this may have for heart pathology in our model.

Finally, as part of our first aim, we sought to establish the protective effect of our vaccine on preventing chronic chagasic cardiomyopathy (CCC). Fibrosis is a common presentation of CCC. It is observed in the hearts of chronic patients and is a predictor of adverse outcomes in Chagas disease<sup>9</sup>. Likewise, in the mouse model, reduced heart fibrosis correlates with improvements in other measurements of heart health, such as serum creatine kinase enzyme concentrations and ECG results<sup>8</sup>.

CCC is modelled well by experimental infection in mice and fibrosis can be measured by standard histology protocols<sup>10, 11</sup>. Both drug and vaccine studies have shown that by reducing the parasite burden, it is possible to impact on cardiac fibrosis, resulting in favourable outcomes<sup>12, 13</sup>. Therefore, upon seeing protection in the acute stage of our vaccine experiment (Chapter 2, Figure 2), we sought to measure cardiac fibrosis in our vaccinated mice and to determine whether it was diminished by a reduction in acute phase parasite burden.

### **3.1.2 Correlates of protection in re-infection**

In vaccine development, understanding the correlates of protection is important in optimising efficacy<sup>14</sup>. In this study, we explored how a natural infection (live vaccination) can protect against subsequent infection with *T. cruzi*.

The antibody response, although less well studied in *T. cruzi* than the T cell response, is an essential part of protective immunity. When B cell deficient mice are primed against *T. cruzi* with an avirulent strain, they fail to be protected against subsequent challenge with a virulent strain<sup>15</sup>. The potential benefits of harnessing antibodies in vaccination have been highlighted by a recently developed alpha-gal-based glycovaccine<sup>16</sup>. This has been shown to protect mice against lethal *T. cruzi* infection through the induction of a strong antibody response to parasite surface glycoproteins.

Using our infection – re-infection model, we saw a good opportunity to study how well parasite specific antibodies develop in infection experienced mice and how these might correlate with protection.

## **3.2 Methods**

### **Flow cytometry**

Mice were killed by exsanguination under terminal anaesthesia and spleens were harvested. Spleens were passed with a sterile syringe plunger through a 70 µm cell sieve into whole medium (RPMI 1640 with 10% v/v heat inactivated FCS, 100 U/ml penicillin, 100µg/ml streptomycin) to form a single cell suspension. RBCs were removed with ACK lysis buffer (Lonza).

Cells were stimulated with either a 20-mer peptide pool, consisting of the vaccine peptides ASP2 and TS at 10µg/ml (Pepscan Presto), non-stimulated with whole medium alone (negative control) or stimulated with a cell stimulation cocktail (positive control, ebiosciences). Golgi plug, containing brefeldin A and Golgi block, containing monensin were added to all conditions (BD biosciences). Anti-CD107a-FITC (1:400, BD Biosciences) was added at the start of peptide stimulation. Incubations were 5 hours at 37°C in a 5% CO<sub>2</sub> incubator.

After incubation with peptide, cells were washed in PBS and the following cell surface stains were performed in FACS buffer (1% v/v FCS in PBS). Anti-CD3-V500 (1:300, BD Biosciences), anti-CD4-efluor 450 (1:1200, ebiosciences), anti-CD8a-APC-efluor 780 (1:800, ebiosciences), anti-CD11a-PE-Cy7 (1:400, ebiosciences), anti-CD44-APC (1:400, ebiosciences) and Live/Dead (1:1500, Invitrogen). Cells were incubated for 40 minutes at 4°C before being washed in FACS buffer. Cells were permeabilised in cytofix (BD Biosciences) for 20 minutes at 4°C as per manufacturer instructions before being washed in Perm/Wash solution (BD Biosciences). Intracellular cytokine staining was performed with antibodies diluted in Perm/Wash. Anti-IFN $\gamma$ -PE (1:400, ebiosciences) and anti-TNF-PerCP-Cy5.5 (1:800, BD Biosciences) staining was performed for 20 minutes at 4°C. Cells were washed in Perm/Wash and re-suspended in 4% PFA in PBS for 20 minutes before being transferred back into FACS solution for acquisition.

Data were acquired on an LSR II flow cytometer (BD Biosciences) using FACSDiva software. Compensation was performed on individually stained OneComp eBeads (ebiosciences). Analysis was performed using FlowJo and analysis gates were set with the aid of appropriate FMO controls.

### **Histology**

Hearts were cut longitudinally and were fixed in Glyo-Fixx solution (ThermoFisher) for 24 hours. Tissues were then dehydrated in a step wise manner in ethanol, starting by submersion in a 70% solution and increasing the ethanol percentage until the tissues were submerged in 100% ethanol. Tissues were cleared with Histo-Clear clearing agent (National Diagnostics) before being embedded in paraffin. Sections of heart tissue were cut to a thickness of 3 microns and with the aid of a water bath, the tissue sections were mounted on glass slides. Paraffin was removed with xylene and tissue sections were rehydrated in decreasing concentrations of ethanol in preparation for staining. Tissues were stained with Masson's Trichrome. A cardiac fibrosis score was calculated from the collagen content in a total of 10 randomly selected fields from each tissue. Images were acquired using a Leica DFC295 camera attached to a light microscope and analysed with the Leica Application Suite V4.5.

### **ELISA**

Immulon 4HBX plates (VWR) were coated with epimastigote lysate at 0.2µg per well in carbonate coating buffer overnight at 4°C. Unbound lysate was removed with 3 washes in PBS/0.05% Tween 20 and blocked with a solution of PBS/2% milk powder at 37°C for 2 hours. Plates were washed again x3 and plasma samples were diluted at 1:50 in PBS/Milk/Tween buffer. Across the 12 wells of the plate a 1/2 serial dilution of plasma in PBS/Milk/Tween was made and the plate was incubated at 37°C for 1 hour. Plates were washed and 100ul/well of goat anti-mouse IgG-HRP (Jackson Labs) at 1:5,000 dilution in PBS/Milk/Tween buffer was applied and incubated at 37°C for 1 hour. Plates

were washed a final time and then developed with KPL ABTS Peroxidase Substrate System (SeraCare). Reactions were stopped with 2M H<sub>2</sub>SO<sub>4</sub> and plates read at an absorbance of 405nm. End point titres were calculated using the method outlined<sup>17</sup>.

### **Epimastigote lysate preparation**

Epimastigotes of the CL Brener strain were grown to late log phase cultures in Nunc cell culture flasks (ThermoFisher) at 28°C. Epimastigotes were washed in PBS with Pierce protease inhibitor (ThermoFisher) before undergoing 4 rounds of freeze-thaw in order to lyse parasites. The lysate was then sonicated 3 times, each time for one minute on ice. Lysate was centrifuged at 10,000g for 20 minutes at 4°C and the supernatant removed to obtain soluble antigen. The protein concentration was measured using the Pierce BCA Protein Assay Kit (ThermoFisher). Aliquots of soluble epimastigote proteins were frozen at -80°C until required.

### **Experimental Design and Statistical Analysis**

Animal work was performed under UK Home Office project licence (PPL 70/8207) and approved by the LSHTM Animal Welfare and Ethical Review Board. Procedures were in accordance with the UK Animals (Scientific Procedures) Act 1986 (ASPA). BALB/c mice were purchased from Charles River (UK), and CB17 SCID mice were bred in-house. Animals were maintained under specific pathogen-free conditions in individually ventilated cages. They experienced a 12 h light/dark cycle, with access to food and water ad libitum. SCID mice were infected with 1×10<sup>4</sup> bioluminescent bloodstream trypomastigotes (BTs) in 0.2 ml PBS via intraperitoneal (i.p.) injection (24, 25, 36). BALB/c female mice, aged 8-10 weeks, were infected i.p with 1×10<sup>3</sup> BTs derived from SCID mouse blood. At experimental end-points, mice were sacrificed by exsanguination under terminal anaesthesia.

A sample size of 6 mice per experimental group was used, with 3 mice being allocated to the control group, unless otherwise stated. Allocations of mice to each group was

random and not performed by the investigator. Calculations of group sizes were made based on prior imaging experience and with consideration to the feasibility of imaging multiple mice in a single day. Power calculations were not performed in determining the group size.

All statistical analyses were performed using GraphPad Prism 8 software. The correlation coefficient ( $r$ ) was calculated assuming a Gaussian distribution, for X vs every Y in the dataset. The P value was calculated in a two-tailed test with a confidence interval of 95%.

The students t-test was used to calculate statistical significance between experimental groups for the flow cytometry analysis and the analysis of tissue fibrosis. Calculations were performed without correcting for multiple comparisons.

## **3.3 Results**

### **3.3.1 Exploring mechanisms of vaccine induced protection**

#### **Kinetics of IFN- $\gamma$ <sup>+</sup> T cell response in vaccinated and non-vaccinated mice post-challenge**

We collected blood from the tail veins of vaccinated mice on day 21 post challenge, a time point during which there was clearly a vaccination induced reduction in the parasite burden (Chapter 2, Figure 2). PBMCs were isolated with histopaque 1083 and an ELISPOT assay was performed to measure the frequency of peptide specific IFN- $\gamma$ <sup>+</sup> T cells (Chapter 2 Materials and Methods). The frequency of IFN- $\gamma$ <sup>+</sup> T cells was plotted against the total body bioluminescence of the same mouse, which was also measured on day 21. The data points showed a clear linear pattern (Figure 3.1). A Pearson correlation coefficient of -0.88 ( $p < 0.05$ ) was calculated, demonstrating an inverse correlation between the frequency of peptide specific T cells and the total body bioluminescence. In effect, a higher frequency of ASP2-TS specific IFN- $\gamma$ <sup>+</sup> T cells associated with better protection.

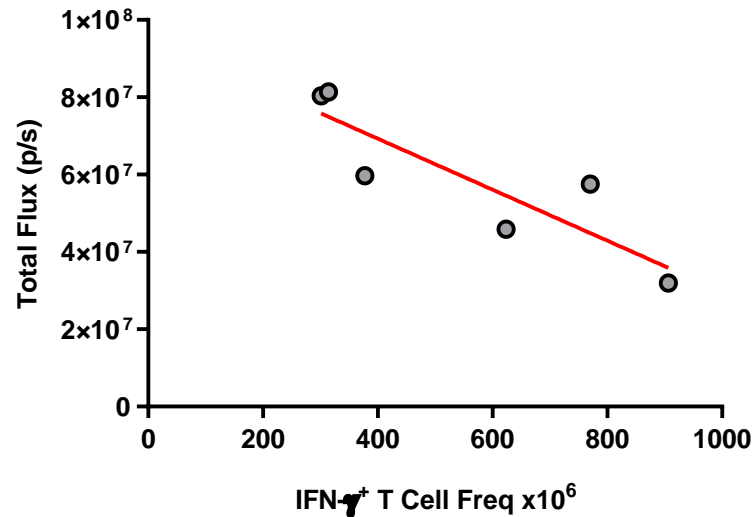


**Figure 3.1** – 21 days post-challenge, PBMCs were isolated from vaccinated mice (n=6) and the frequency of vaccine peptide specific IFN- $\gamma$ <sup>+</sup> T cells was measured by ELISPOT (x axis). The data points were plotted against the total body bioluminescence of the same mice (summation of ventral and dorsal values) (y axis). The correlation coefficient was calculated at -0.88. Red line represents best fit. Data derived from a single experiment

### **Characterising infection induced T Cells by flow cytometry**

We sought to establish whether vaccination resulted in an altered T cell profile in vaccinated mice in the chronic infection. At the experimental end point (day 95 post-challenge), after the final *in vivo* image (Chapter 2, Figure 2), the 6 vaccinated and the 3 non-vaccinated mice underwent necropsy and their spleens were harvested for peptide re-stimulation.

Cell surface and intracellular cytokine staining was performed as described in the Methods and cells were analysed by flow cytometry. Gating was performed as shown for analysis of the CD3<sup>+</sup>CD8<sup>+</sup> population (Figure 3.2). An identical gating strategy was also put in place for the analysis of the CD3<sup>+</sup>CD4<sup>+</sup> population.

The number of CD4<sup>+</sup> and CD8<sup>+</sup> T cells (expressed as a percentage of the total number of lymphocytes) was similar between the vaccinated and non-vaccinated mice (Table

3.1). T lymphocytes were gated on the CD11a<sup>+</sup>/CD44<sup>+</sup> double positive population, because the expression of these surface molecules is used as a proxy for antigen experienced cells<sup>18</sup>.

**Table 3.1**

	Cells as a % of Total Lymphocytes			
	Vaccinated		Non Vaccinated	
	Peptide Stim	Non Stim	Peptide Stim	Non Stim
CD3+CD4+	17.9±2.0	17.5±2.1	16.6±0.6	16.2±0.4
CD3+CD8+	20.0±1.7	19.8±1.9	19.4±0.5	18.6±1.1

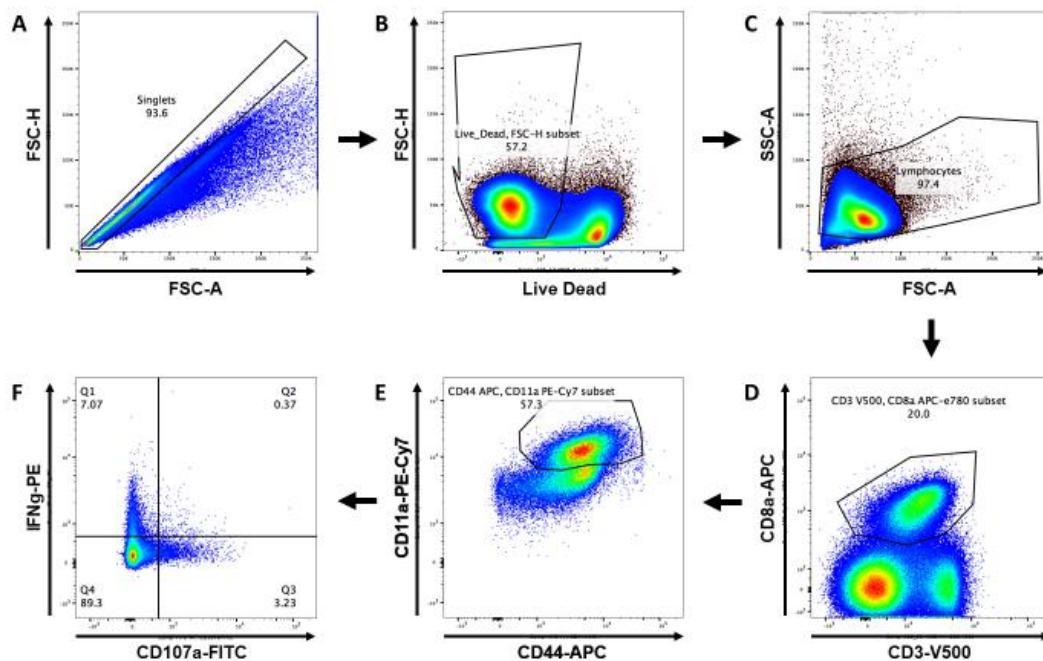


**Figure 3.2** – Gating strategy used for splenocytes. BALB/c mice were vaccinated with ChadOx1 (ASP2-TS) and 3 weeks later with MVA (ASP2-TS). On day 95 post-challenge, splenocytes were re-stimulated with the vaccine antigens and antibody stained for analysis by flow cytometry. Vaccinated n=6, non-vaccinated n=3. Gating was performed in the following sequence for each sample A) singlet cells, B) Live cells, C) Lymphocytes, D) CD3<sup>+</sup>CD8<sup>+</sup>, E) CD44<sup>+</sup>CD11a<sup>+</sup>. F) IFN-γ<sup>+</sup>/CD107a<sup>+</sup>. Gating was set using unstained cells (FMOs). Data derived from a single experiment.

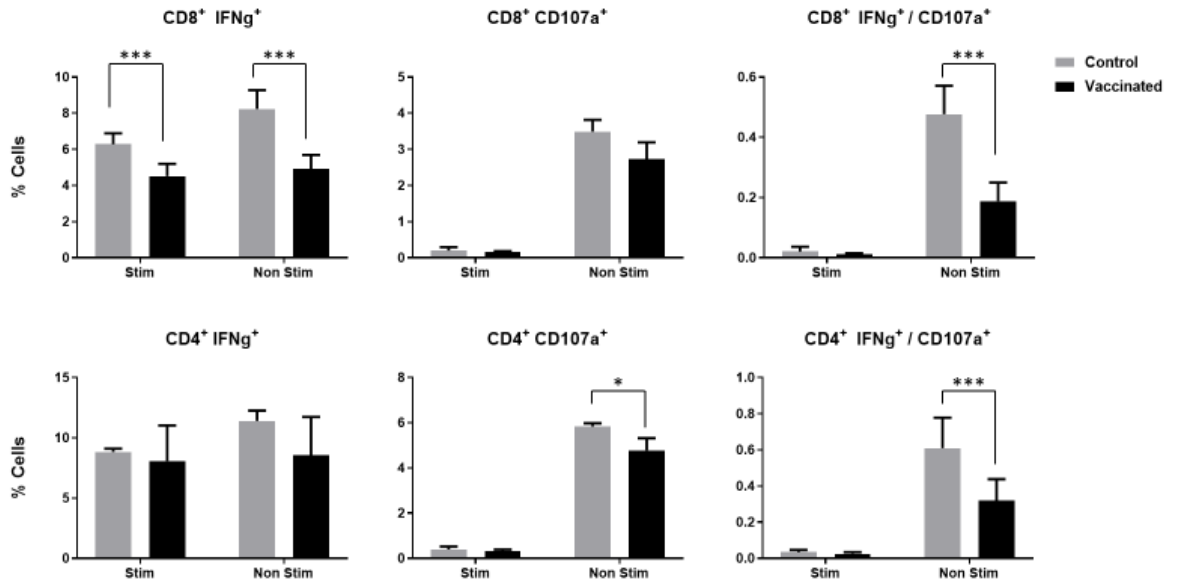


**Figure 3.3** – BALB/C mice were vaccinated with ChadOx1 (ASP2-TS) and 3 weeks later with MVA (ASP2-TS). On day 95 post-challenge, splenocytes were re-stimulated with the vaccine antigens and antibody stained for analysis by flow cytometry. Vaccinated n=6, non-vaccinated n=3. Data is expressed as % of the total CD11a<sup>+</sup>/CD44<sup>+</sup> CD3<sup>+</sup>CD8<sup>+</sup> T cells, or CD11a<sup>+</sup>/CD44<sup>+</sup> CD3<sup>+</sup>CD4<sup>+</sup> T cells. Stim = Peptide stimulated. Non Stim = non-stimulated. Data are mean±SD. Data derived from a single experiment.

CD107a is a marker for degranulation. Positive CD107a staining indicates that a cell was actively degranulating<sup>19</sup>. The low numbers of CD107a<sup>+</sup> or double positive cells amongst the CD8<sup>+</sup> and the CD4<sup>+</sup> groups following peptide stimulation was peculiar (Figure 3.3). Although the reason for the unexpectedly low numbers is not clear, amongst the positive controls, the CD107a<sup>+</sup> response was also weak (Supplementary Figure 3.1). It seems that in response to a stimulus (peptide and positive control), but not amongst non-stimulated cells, we are unable to detect T cell degranulation.

IFN-γ<sup>+</sup> secretion on the other hand was high, as expected amongst the positive control samples (Supplementary Figure 3.1). Vaccinated mice present with a lower number of IFN-γ<sup>+</sup> CD8<sup>+</sup> T cells when compared to non-vaccinated mice in both the peptide stimulated and the non-stimulated group (p<0.001), whereas in the CD4 T cell

compartment, the levels of IFN-  $\gamma^+$  remains similar between vaccinated and non-vaccinated mice.

Interestingly, amongst the non-stimulated cells, both the CD4<sup>+</sup> and CD8<sup>+</sup> T cell compartments show a reduced frequency of IFN<sup>+</sup>/CD107a<sup>+</sup> cells in vaccinated mice compared to non-vaccinated. This reduced frequency was also reflected amongst the CD4<sup>+</sup> population in CD107a<sup>+</sup> cells and despite not reaching significance, the data for the CD8<sup>+</sup> T cell compartment also showed a similar trend of fewer CD107a<sup>+</sup> cells amongst vaccinated mice.

### **Histopathology of cardiac tissue from vaccinated versus non-vaccinated mice**

We aimed to address the question of whether our viral vectored vaccine, which was effective in reducing the acute stage parasite burden, impacted on cardiac fibrosis, a hallmark of CCC. On day 95 post-challenge, the heart tissues from the 6 vaccinated and 3 non-vaccinated BALB/c mice were taken for analysis by histology. Heart tissues were processed as described in the Methods and stained with Masson's trichrome, allowing the identification of collagen deposition<sup>20</sup>.

On microscopic inspection, collagen staining could be seen in the heart tissues of all of the infected mice, whether vaccinated or non-vaccinated. No parasite nests were observed in any of the sections studied. Areas of collagen deposition were abundantly clear due to the contrast of the blue collagen stain against the backdrop of the red stained cardiomyocytes (Figure 3.4A). Collagen deposition was often present in the spaces between muscle fibres. Local areas of heavier collagen deposition were associated with larger gaps between myocytes, indicating reduced structural integrity of the tissue. In line with previous reports from our group<sup>20</sup>, there was variation between individual mice within groups, with some mice displaying very little fibrosis in any of the fields analysed and other showing abundant fibrosis across all fields.

For each mouse, 10 images were taken of random fields across two different sections of heart tissue. The level of collagen deposition was calculated using Leica Application Suite analysis software, which summed the total area of blue stain in each section and presented the data as collagen per  $\mu\text{m}^2$ . The data reveals that overall, there were no differences in the level of collagen deposition between the vaccinated and non-vaccinated mice (Figure 3.4B). Overall the collagen deposition in vaccinated vs non-vaccinated mice was  $1803 \pm 1291$  vs  $2160 \pm 547$ , ( $p=0.70$ ).

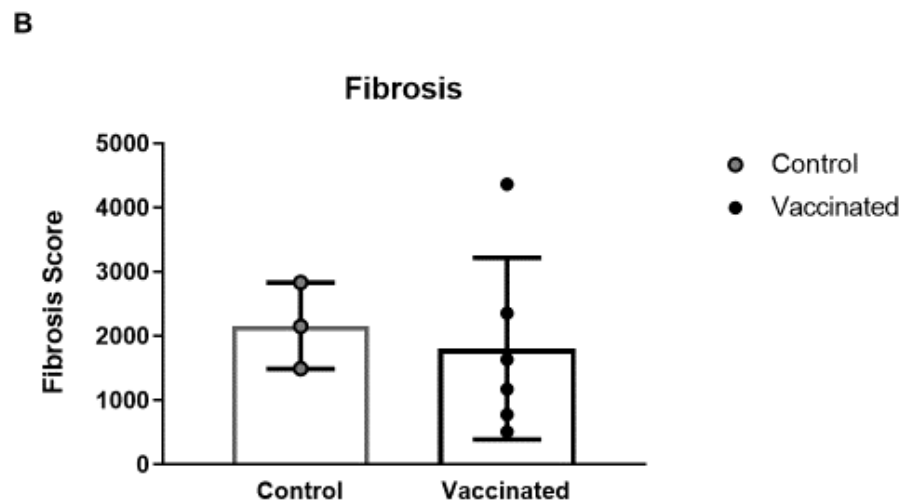
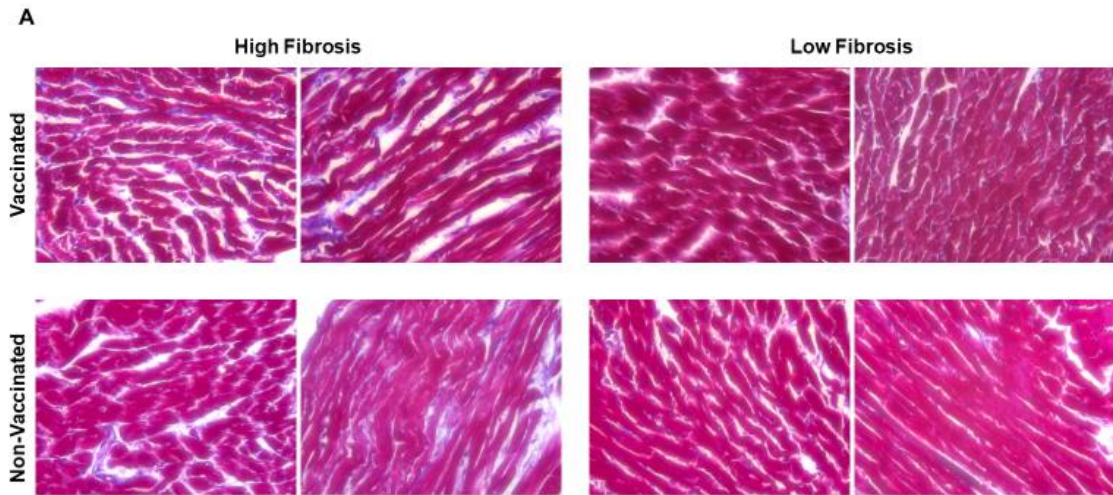


**Figure 3.4** – Histological examination of heart tissues 95 days post infection. A) Heart tissues were removed from vaccinated (n=6) and non-vaccinated (n=3) BALB/c mice. Tissues were cut into sections and stained with Masson’s Trichrome (red is myocardial tissue, blue is collagen). Presented are representative examples of vaccinated and non-vaccinated mice B) Total collagen deposition for each mouse was calculated from 10 random microscope fields from two separate tissue sections of each heart. Data are mean±SD. Data derived from a single experiment.

### 3.3.2 Studying the antibody response as a correlate of immune protection in infection experienced mice

#### The change in the IgG antibody titre in infection experienced mice

We studied the antibody response to a *T. cruzi* re-infection in order to assess whether this response correlated with protection. Briefly, BALB/c mice were infected with the CL Brener strain for either 36, 14 or 4 days prior to a 20 day curative drug treatment. Upon re-infection the different groups of mice displayed varying levels of immunity (Chapter 2, Figure 3). Prior to re-infection, and at various points during the re-infection (Figure 3.5A), mice had their blood sampled. Blood plasma was obtained by histopaque 1083 isolation and stored at -80°C until the end of the experiment, at which point we conducted a reciprocal end point antibody assay on all of the samples collectively. Plasma samples were probed against a *T. cruzi* epimastigote lysate (refer to Methods).

Prior to re-infection, parasite specific IgG was undetectable in control mice, as expected since these mice had not yet received their first infection (Figure 3.5B). Control mice first displayed detectible IgG on day 25 of the infection, the titre however (1/600 on day 25 and 1/167 on day 40), indicated a low concentration of parasite specific IgG. In contrast, mice that had been drug treated after 36 days of a first infection had detectible antibodies prior to re-infection (1/950,  $p < 0.05$ ). The endpoint antibody titre for the 36 day infected group of mice was boosted by the re-infection and rose to 1/3600 ( $p < 0.05$ ) on day 10. The end point titre of these mice remained high until day 40 after re-infection (Figure 3.5B).

Mice that been infected for 14 days prior to re-infection had a low, but detectible antibody titre prior to re-infection, however it was not at a level considered to be statistically significant relative to controls. As with the 36 day infected group, the 14 day infected mice boosted their antibody production in response to re-infection and on day 10 of the infection went from having a 1/75 endpoint titre to 1/800 ( $p < 0.01$ ). Compared to the 36

day group, the 14 day infected and cured mice did not produce as powerful an antibody response (Figure 3.5B). The end point titre of the 14 day group rose comparatively slowly compared to the 36 day group and only increased to a maximum of 1/1200 on day 40 ( $p < 0.01$ ). The 4 day infected and cured group of mice showed antibody kinetics most similar to the control mice. The antibody response was undetectable on days -2 and 10 of the infection and only became detectable on day 25 when the end point titre of the re-infected mice was similar to controls. However on day 40 there was a small but appreciable increase in the antibody response above control mice at 1/400 ( $p < 0.001$ ).

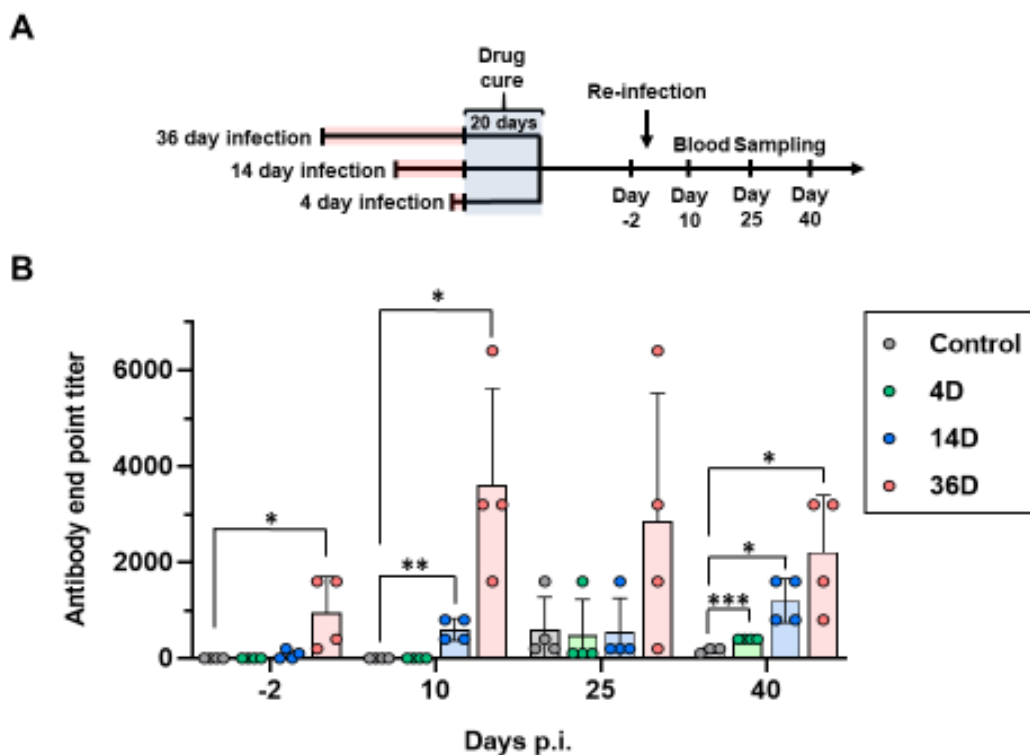


**Figure 3.5** – IgG antibody titer of re-infected BALB/c mice. A) Blood plasma was sampled from mice on the days indicated prior to and following re-infection with  $10^3$  bioluminescent CL Brener strain parasites (as described in Chapter 2). Plasma was stored as indicated in methods. B) End point antibody titers were calculated by ELISA ( $n=4$  across each group). Data are mean $\pm$ SD. 4-5 mice were used as negative controls per assay. Data is derived from a single assay, samples run in triplicate.

In addition to studying the antibody kinetics in mice that experienced a re-infection shortly after drug cure, we also studied the kinetics of the antibody response in mice that were drug cured one year prior to a re-infection (Figure 3.6 A). This was performed to better understand the role of antibodies in mediating protection in the long-term memory response. Similar to mice that were re-infected 3 weeks post drug cure (Figure 3.5), the antibody titre in mice that were cured a year previously was significantly higher than in control mice ( $p < 0.001$ ). However, after the re-infection the antibody titre remained stable at pre – re-infection levels up until day 10. The antibody response then increased by day 25, and remained at a higher level until at least day 40.

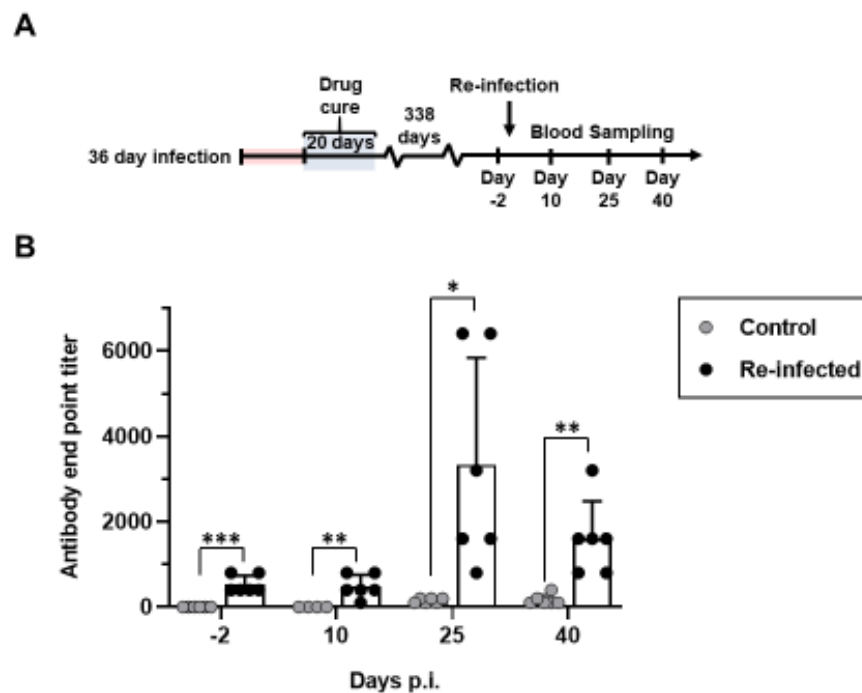


**Figure 3.6** – IgG antibody titer of re-infected BALB/c mice 338 days after drug cure. A) Blood plasma was sampled from mice on the days indicated prior to and following challenge with the bioluminescent CL Brener strain. B) End point antibody titers were calculated by ELISA (n=6 across both groups). Data are the mean±SD. 4-5 mice were used as negative controls per assay.. Data is derived from a single assay, samples run in triplicate.

### **3.4 Discussion**

Understanding the relationship between anti-*T. cruzi* immunity, and the outcomes for the host are important for rational vaccine design. In this study, we used a novel viral vectored vaccine to induce protective immunity in a *T. cruzi* infection. Using a non-lethal challenge model, we were able to correlate the strength of the immune mediated protection to the frequency of vaccine induced IFN- $\gamma$ <sup>+</sup> T cells. Furthermore, we showed that vaccination has a lasting effect on the immune response. However, using cardiac fibrosis as a barometer of CCC, we were unable to detect vaccine induced protection against heart damage, at least in the context of the infection protocol used in this experiment.

Several viral vectored vaccines have been developed and tested experimentally in the mouse model<sup>2, 8, 21</sup>. However, many of these studies use a lethal challenge model to assess vaccine efficacy. We tested a novel *T. cruzi* vaccine in a non-lethal challenge experiment using a highly sensitive bioluminescent model. We developed a vaccine based on the promising viral vectors ChadOx1 and MVA, two vaccine vectors that are undergoing clinical trials for a number of infectious diseases and as potential cancer vaccines (clinical trial identifier NCT02390063) (clinical trial identifier NCT01818362). These vaccines proved to be partially efficacious in the acute stage of an experimental *T. cruzi* infection (Chapter 2, Figure 2), although sterile protection was not achieved, and the response was relatively short-lived.

With our non-lethal challenge model, we were able to accurately measure the efficacy of the vaccine using the bioluminescence inferred parasite burden. Other vaccines targeting TS and ASP-2 have previously demonstrated that IFN- $\gamma$ <sup>+</sup> secretion by CD4 and CD8 T cells correlates with protection<sup>22</sup>. We performed a T cell ELISPOT to better understand the nature of protection with the viral vectored vaccine. We observed a correlation between protection and the frequency of vaccine induced T cells expressing

IFN- $\gamma$ , at the level of individual mice. Using the Pearson's correlation coefficient, we measured an  $r$  value of -0.87, indicating a strong relationship.

Reliable and accurate immune correlates are key to vaccine design and help us to understand why vaccines are, or are not, efficacious. Our viral vectored vaccine was effective at reducing the parasite burden during the acute stage of infection (days 14 and 21 post infection), but it was not effective on day 7, or at later stages as the infection transitioned to the chronic stage (Chapter 2, Figure 2). To understand how we could develop this vaccine further, and improve on the efficacy, the bioluminescence model allows us to measure how this correlate of protection changes in vaccinated mice during the long term course of the infection. Possible reasons for the ineffectiveness of vaccination at the early stage could be due to the lack of a sufficiently vigorous proliferative response after challenge, despite vaccination. In contrast, a lack of efficacy in spite of a strong proliferative response early on could mean that we need to reconsider the target genes included in the vaccine<sup>23</sup>. Previously it has been difficult to monitor vaccine efficacy during the chronic phase. The lack of efficacy that we observed here, suggests that during this stage of the infection, parasites must exist in a location and/or state where they are refractory to the immune response induced by the vaccine, and the subsequent (reduced) acute stage infection. This could have important implications for the potential of vaccines as a viable public health measure.

We wanted to explore the extent of any long-term functional changes that vaccination imparted on the immune system. Such a phenomenon has previously been reported, whereby a viral vectored vaccine induced reduction in the CD107a<sup>+</sup> CD8<sup>+</sup> T cell compartment correlated with protection from CCC in experimental challenge<sup>8</sup>. To this end, we measured the IFN- $\gamma$ <sup>+</sup> and CD107a<sup>+</sup> response of the T cell compartment on day 95 of the infection in our vaccinated and non-vaccinated mice (Figure 3.3).

Analysis of our data was complicated by the fact that peptide stimulation did not induce the expected boost in the IFN- $\gamma$ <sup>+</sup> population above the non-stimulated samples. Neither did it result in increased T cell degranulation. By studying our positive control samples (supplementary Figure 3.1), we observed that PMA / ionomycin induced cell stimulation resulted in a large increase in IFN- $\gamma$ <sup>+</sup>, but did not impact upon CD107a<sup>+</sup> detection. The reasons for this were not obvious, however we speculate that it may lie in the fact that peptide stimulation for 5 hours was insufficient. Far longer incubation times have been used for similar assays in other reports<sup>8</sup>.

However the data do present some interesting findings. The CD8<sup>+</sup> T cell repertoire in the vaccinated mice had fewer IFN- $\gamma$ <sup>+</sup> and IFN- $\gamma$ <sup>+</sup>/CD107a<sup>+</sup> T cells than in non-vaccinated cohort (Figure 3.3). Similarly, there were lower numbers of IFN- $\gamma$ <sup>+</sup>/CD107a<sup>+</sup> cells in the CD4<sup>+</sup> T cell population amongst the vaccinated mice (Figure 3.3). This suggests that there were vaccine induced changes in the immune response toward a less inflammatory profile. The underlying reasons behind these changes are not clear, however they do not seem to impact on the ability of vaccinated mice to suppress parasites as both vaccinated and non-vaccinated mice control the parasite burden equally well in the chronic stage.

It may seem counterintuitive that in *T. cruzi*, the pro-inflammatory properties of T cells that are associated with protection should be downregulated in vaccinated mice. However, there is precedent for these findings. A human adenoviral vectored vaccination targeting the same parasite proteins in *T. cruzi* also showed reduced CD107a<sup>+</sup> amongst CD8 T cells in the chronic infection<sup>8</sup>. Exactly what causes the response in vaccinated mice to evolve from one that is pro-inflammatory and mediates effective parasite killing in the acute stage, to one that is more moderated, but still able to suppress parasites is not clear. Presumably these changes preserve the health of the host through reducing inflammatory mediated damage to host tissues such as the heart<sup>8</sup>.

CCC is the most common disease pathology in Chagas disease. We took the heart tissues of vaccinated and non-vaccinated mice and assessed the level of fibrosis, a marker of infection induced heart damage. Heart tissues were cut, fixed onto glass slides and stained with Masson's Trichrome to allow the visualisation of collagen deposits. This study was taken forward as a preliminary investigation that would optimise and add value to the information obtained from an animal experiment designed primarily to test vaccine efficacy. We recognised that it would be insufficiently powered for an in-depth analysis of disease pathology, but proceeded on the basis that it would inform and guide future work in this area.

Cardiac fibrosis was similar between our vaccinated and non-vaccinated mice (Figure 3.4), tentatively indicated the absence of vaccine induced protection against heart damage by day 95 of the infection. In earlier studies, it has been shown that the level of fibrosis in non-infected BALB/c mice was significantly different from mice that were infected and treated in the chronic stage of the infection<sup>20</sup>. Although the viral vectored vaccine used was a novel vaccine, the parasite proteins which were targeted are well studied vaccine candidates. Vaccines against these targets have in the past shown some level of protection against, and even reversal of, infection induced heart damage<sup>8</sup>.<sup>25</sup>. Our initial analysis was limited in extent, however, as fibrosis is a single measure of heart pathology and other measures such as ECG and the levels of serum CK-MB could also provide additional information about heart function.

To state unequivocally that viral vectored vaccination with the ChadOx1 and MVA vectors is protective, or not, against disease pathology or not, will require a far more extensive study, with additional parameters of heart damage. However, our preliminary data (Figure 3.4) do suggest that a vaccine that does not confer sterile protection might have limited effectiveness in terms of therapeutic benefits.

Finally, in a separate set of experiments (the infection – re-infection study), we sought to study the development of an antibody response and its potential role in protecting against re-infection. This was of interest because the antibody response is less well studied than the T cell response in *T. cruzi* infections. A recent study showcased the importance of antibodies in immune mediated protection against this parasite by developing a novel glycovaccine that works primarily through antibody mediated immunity<sup>16</sup>. At various points of the re-infection experiments, we sampled blood and studied plasma antibody levels.

In the absence of a standard for our assay, we used the end point assay to determine the relative levels of antibody titres in the blood plasma of re-infected mice. We chose to measure IgG levels, as this represents the mature, long-lived response and does not wane over the course of an infection like IgM. The results demonstrated that mice infected for 36 days prior to drug cure showed a detectible antibody response prior to re-infection. This was also the case with mice that were drug cured 21 days prior to re-infection (Figure 3.5) and mice that were drug cured almost one year prior to re-infection. What is interesting is that both of these groups of mice displayed robust resistance against re-infection, with a dramatically reduced parasite burden at the first imaging point post re-infection at day 7 (Chapter 2, Figure 3). This pre-existing antibody titre could therefore be an explanatory factor for at least some of the protection that we observe in these groups.

Mice that have been infected for 14 days prior to drug cure showed a lower antibody titre than 36 day infected mice, with the antibody titre increasing slowly during the re-infection but not reaching the same levels as in 36 day infected mice. 4 day infected mice showed antibody kinetics most similar to control mice, with no detectible antibodies prior to re-infection, or on day 10 post-challenge, these mice only displayed a significantly higher antibody titre on day 40 of re-infection.

The antibody kinetics in the 4 day infected group do not necessarily reflect the protection that these mice display. In the 4 day infected group, the antibody titre in re-infected mice only increased above the controls by day 40. However, protection in these mice was only apparent in the first 21 days after re-infection. By day 40 the control mice and re-infected mice showed the same parasite burden (Chapter 2, Figure 3). One factor that we must consider is that the data presented here are specific to IgG. IgM also plays a role in protection in *T. cruzi*, but was not measured in this study<sup>26</sup>. IgM could therefore be contributing to the protection we observed, obscuring our ability to draw a straight correlation between antibody titre and protection from these results.

Further studies that explore the functional capacity of these antibodies would be beneficial in determining whether antibodies are playing an active role in protecting against re-infection or whether they are generated as a result of infection but do not perform a protective role.

### 3.5 Supplementary

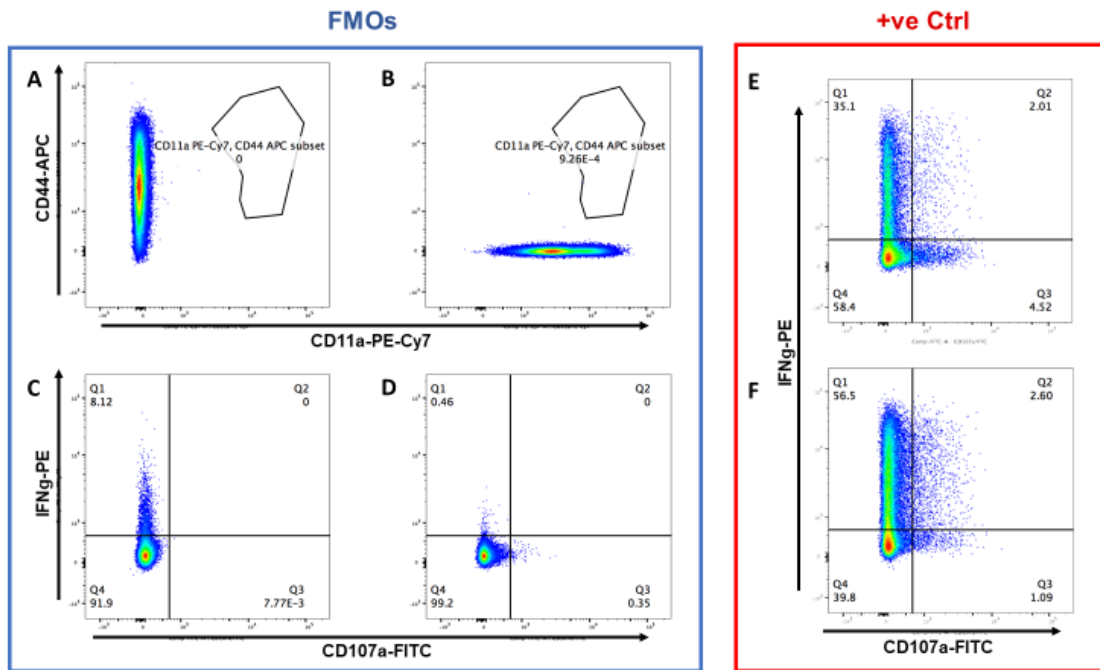


**Figure S3.1** – BALB/C mice were vaccinated with ChadOx1 – MVA carrying the parasite encoded genes ASP2-TS in a prime-boost manner. On day 95 post-challenge, splenocytes were re-stimulated with the vaccine antigens and antibody stained for analysis by flow cytometry. Analysis gates were set by using non-stained cells (FMOs). In the blue box. A) Cells not stained for CD11a B) Cells not stained for CD44 C) Cells not stained for CD107a D) Cells not stained for IFN- $\gamma$ . E) Positive control sample gated on CD8<sup>+</sup> Cells. F) Positive control sample gated on CD4<sup>+</sup> T cells. Data derived from a single experiment

### 3.6 References

1. Ura, T., K. Okuda, and M. Shimada, Developments in Viral Vector-Based Vaccines. *Vaccines (Basel)*, 2014. **2**(3): p. 624-41.
2. Duan, X., et al., Efficient protective immunity against *Trypanosoma cruzi* infection after nasal vaccination with recombinant Sendai virus vector expressing amastigote surface protein-2. *Vaccine*, 2009. **27**(44): p. 6154-9.
3. Tzelepis, F., et al., Distinct kinetics of effector CD8+ cytotoxic T cells after infection with *Trypanosoma cruzi* in naive or vaccinated mice. *Infect Immun*, 2006. **74**(4): p. 2477-81.
4. Araujo, A.F., et al., CD8+-T-cell-dependent control of *Trypanosoma cruzi* infection in a highly susceptible mouse strain after immunization with recombinant proteins based on amastigote surface protein 2. *Infect Immun*, 2005. **73**(9): p. 6017-25.
5. Fontanella, G.H., et al., Immunization with an engineered mutant trans-sialidase highly protects mice from experimental *Trypanosoma cruzi* infection: a vaccine candidate. *Vaccine*, 2008. **26**(19): p. 2322-34.
6. Bontempi, I., et al., Trans-sialidase overcomes many antigens to be used as a vaccine candidate against *Trypanosoma cruzi*. *Immunotherapy*, 2017. **9**(7): p. 555-565.
7. Martins-Melo, F.R., et al., Epidemiology of mortality related to Chagas' disease in Brazil, 1999-2007. *PLoS Negl Trop Dis*, 2012. **6**(2): p. e1508.
8. Pereira, I.R., et al., A human type 5 adenovirus-based *Trypanosoma cruzi* therapeutic vaccine re-programs immune response and reverses chronic cardiomyopathy. *PLoS Pathog*, 2015. **11**(1): p. e1004594.
9. Senra, T., et al., Long-Term Prognostic Value of Myocardial Fibrosis in Patients With Chagas Cardiomyopathy. *J Am Coll Cardiol*, 2018. **72**(21): p. 2577-2587.
10. Higuchi, M.L., et al., The role of active myocarditis in the development of heart failure in chronic Chagas' disease: a study based on endomyocardial biopsies. *Clin Cardiol*, 1987. **10**(11): p. 665-70.
11. Pereira, I.R., et al., Severity of chronic experimental Chagas' heart disease parallels tumour necrosis factor and nitric oxide levels in the serum: models of mild and severe disease. *Mem Inst Oswaldo Cruz*, 2014. **109**(3): p. 289-98.
12. Andrade, S.G., et al., Reversibility of cardiac fibrosis in mice chronically infected with *Trypanosoma cruzi*, under specific chemotherapy. *Mem Inst Oswaldo Cruz*, 1991. **86**(2): p. 187-200.

13. Barry, M.A., et al., A therapeutic vaccine prototype induces protective immunity and reduces cardiac fibrosis in a mouse model of chronic *Trypanosoma cruzi* infection. *PLoS Negl Trop Dis*, 2019. **13**(5): p. e0007413.
14. Plotkin, S.A., Correlates of protection induced by vaccination. *Clin Vaccine Immunol*, 2010. **17**(7): p. 1055-65.
15. Kumar, S. and R.L. Tarleton, The relative contribution of antibody production and CD8+ T cell function to immune control of *Trypanosoma cruzi*. *Parasite Immunol*, 1998. **20**(5): p. 207-16.
16. Portillo, S., et al., A prophylactic alpha-Gal-based glycovaccine effectively protects against murine acute Chagas disease. *NPJ Vaccines*, 2019. **4**: p. 13.
17. Frey, A., J. Di Canzio, and D. Zurakowski, A statistically defined endpoint titer determination method for immunoassays. *J Immunol Methods*, 1998. **221**(1-2): p. 35-41.
18. Rai, D., et al., Tracking the total CD8 T cell response to infection reveals substantial discordance in magnitude and kinetics between inbred and outbred hosts. *J Immunol*, 2009. **183**(12): p. 7672-81.
19. Aktas, E., et al., Relationship between CD107a expression and cytotoxic activity. *Cell Immunol*, 2009. **254**(2): p. 149-54.
20. Francisco, A.F., et al., Assessing the Effectiveness of Curative Benznidazole Treatment in Preventing Chronic Cardiac Pathology in Experimental Models of Chagas Disease. *Antimicrob Agents Chemother*, 2018. **62**(10).
21. Nogueira, R.T., et al., Recombinant yellow fever viruses elicit CD8+ T cell responses and protective immunity against *Trypanosoma cruzi*. *PLoS One*, 2013. **8**(3): p. e59347.
22. Vasconcelos, J.R., et al., Protective immunity against *trypanosoma cruzi* infection in a highly susceptible mouse strain after vaccination with genes encoding the amastigote surface protein-2 and trans-sialidase. *Hum Gene Ther*, 2004. **15**(9): p. 878-86.
23. Kurup, S.P. and R.L. Tarleton, The *Trypanosoma cruzi* flagellum is discarded via asymmetric cell division following invasion and provides early targets for protective CD8(+) T cells. *Cell Host Microbe*, 2014. **16**(4): p. 439-49.
24. Silverio, J.C., et al., CD8+ T-cells expressing interferon gamma or perforin play antagonistic roles in heart injury in experimental *Trypanosoma cruzi*-elicited cardiomyopathy. *PLoS Pathog*, 2012. **8**(4): p. e1002645.
25. Araujo, A.F., et al., Genetic vaccination against experimental infection with myotropic parasite strains of *Trypanosoma cruzi*. *Mediators Inflamm*, 2014. **2014**: p. 605023.

26. Bryan, M.A., S.E. Guyach, and K.A. Norris, Specific humoral immunity versus polyclonal B cell activation in *Trypanosoma cruzi* infection of susceptible and resistant mice. *PLoS Negl Trop Dis*, 2010. 4(7): p. e733.

## Chapter 4 :

# The Effects of Chemical Induced Colonic Inflammation on Chronic *T. cruzi* Infection

## **4.1 Introduction**

For several decades now, the only therapeutic interventions available to treat a *T. cruzi* infection and prevent the development of Chagas disease has been the toxic nitroheterocyclic drugs benznidazole and nifurtimox<sup>1,2</sup>. In addition to having several off target effects, which impact greatly on drug tolerability, the recommended treatment periods are up to 60 days and the drugs are not 100% efficacious<sup>3</sup>. There is a need for new therapeutics and a joint effort amongst public and private stakeholders, bought together by organisations such as DNDi, are developing and testing new compounds in the fight against Chagas disease<sup>4</sup>.

As a proof of concept study, we decided to utilise our bioluminescent model of *T. cruzi* infection to try and take a different approach towards a potential therapy. We attempted to induce inflammation in a parasitological niche that was identified in the chronic infection in the mouse. We wanted to test the concept that the induction of local inflammation in a tissue of parasite persistence could be used as a novel therapeutic option to combat the infection.

### **4.1.1 Parasitological niche of *T. cruzi* in the mammal**

One of the longstanding questions in *T. cruzi* research has been in understanding how despite a vigorous adaptive immune response, capable of killing parasitized cells, that people can remain infected and harbour parasites over their entire lifetime<sup>5</sup>. In the search for answers, researchers took identifying specific tissues that would act as sites of parasite persistence. One of these proposed sites has been the adipose tissue, which has been identified to be infected in both mouse and human chronic infections<sup>6-8</sup>. It was hypothesised that the adipose tissue, with its long half-life and abundance of triglycerides, would provide the parasite with a niche that would meet its metabolic

needs, allowing it to remain dormant in the adipose tissue for many decades<sup>9-11</sup>. The topic of parasite dormancy and whether this is a contributing factor to parasite persistence is still the subject of investigation<sup>12</sup>.

Advances in imaging technology have improved our ability to localise parasites during a *T. cruzi* infection. In experiments designed to characterise the dynamics of infection in the BALB/c – CL LUC model, it was found that the gastrointestinal tract (GIT) is a persistently infected tissue in the chronic stage. Specifically, the lower portion of the stomach and portions of the were consistently observed as being bioluminescent positive upon end point *ex vivo* imaging<sup>13</sup>.

Further investigation of this phenomenon across several parasite and host strain combinations revealed the gut to be the principal site of chronic infection, these combination included C57BL/6, C3H/He and BALB/c mice and the diverse parasite strains CL Brener (DTU VI), Sylvio X10/6 (DTU I) and JR (DTU I)<sup>14</sup>. The findings of this study suggested a model for infection whereby the gut was a site of parasite persistence from which infections in other tissues such as the heart were continuously seeded. The model supports an infection dynamic whereby the peripheral infections (infected tissues outside the GI tract) are more susceptible to the immune response and are cleared more efficiently by the host. However, the gut, for an unknown reason, remained privileged from the same mechanisms of parasite clearance.

This finding was interesting in the context of a therapeutic intervention. If the gut is a site of parasite persistence, then use of a therapeutic approach that specifically targets the gut could represent a strategy by which we could eliminate parasites from the host. We decided to explore methods of inducing colonic inflammation in order to see whether we could target gut parasites for elimination by host immunity.

#### 4.1.2 Murine models of colitis

Murine models of colitis are commonly used to study aspects of human inflammatory bowel diseases. Several different models are in existence and differ in their ease of implementation, susceptibility of different mouse strains, and most importantly, the type of inflammation that the investigator wishes to induce<sup>15</sup>. These models of colonic inflammation presented a rational option for the induction of inflammation in our model of infection. They are commonly used, they are well characterised, and we would be able to implement them without the requirement for specialist equipment. We considered two methods of chemically induced inflammation. One had been used previously in a short pilot experiment conducted in our lab, the results of which were taken into consideration when deciding on which mode of inflammation was most appropriate.

Dextran sodium sulphate (DSS) colitis is induced through the administration of the chemical in the drinking water. Both the C57BL/6 and BALB/c strains show susceptibility to DSS induced inflammation<sup>16</sup>. This type of inflammation resembles the human inflammatory disease Ulcerative Colitis (UC) and can be induced in an acute (short term) or a chronic (long term) inflammatory format. 2,4,6-trinitro-benzene sulfonic acid (TNBS) is a different chemically induced colitis and is used to mimic the human condition Crohn's Disease (CD), with BALB/c mice showing susceptibility to this form of chemically induced colitis and C57BL/6 showing relative resistance to colitis by this method<sup>17</sup>. TNBS is administered in a solution of ~ 40% ethanol, intrarectally by an enema, directly to the colon. Like DSS, it can be administered to induce an acute colitis, or it can also be administered in a different dosing schedule that induces a chronic inflammation, lasting several weeks.

The main reasons for choosing between the two models centre on the fact that they induce different types of inflammation. Clinically, both inflammatory models result in weight loss, loose and bloody stools as well as shortening of the length of the colon.

However, when we look at the histopathological changes that occur in a DSS or a TNBS driven inflammatory response in the colon, there are differences in the severity of the pathology and in the types of inflammation induced<sup>17</sup>.

Histologically, DSS induced colitis presents as goblet cell loss, erosion of the epithelium and a diffuse lymphocytic infiltration. In contrast, TNBS induces a more exaggerated loss of mucosal architecture, with the presence of oedema and sometimes a transmural inflammation that crosses the mucosal and muscle layers, as opposed to the relatively superficial inflammatory infiltration of DSS induced colitis<sup>18</sup>.

The DSS model of inflammation is initially characterised by high levels of macrophage produced TNF- $\alpha$  and Th17 produced IL-17. However, after several cycles of DSS administration and epithelial cell wall regeneration, a Th2 type response takes over, characterised by high levels of IL-4 and IL-10. DSS induced colitis is therefore widely considered to be a Th2-like inflammatory colitis<sup>19</sup>. TNBS on the other hand is considered to induce a Th1/Th17 inflammatory profile. Administration of TNBS induces a systemic increase in IL-12, IFN- $\gamma$ , IL-17 and MIP-1 $\alpha$ . However, IL-12 and IL-17 are also produced in increased quantities at the mucosal surface. As the inflammatory response develops from an acute to a chronic inflammation, TNBS induced inflammation does not transition to a Th2 type profile as with DSS, instead it remains a Th1/Th17 mediated inflammatory response<sup>19</sup>.

Previously in our lab, a small and unpublished pilot study was conducted in chronically infected BALB/c mice (>100 days p.i.) with DSS (Lewis et al.). The aim was to monitor how DSS administration and chemically induced colitis was tolerated in infected mice as compared to non-infected control mice. DSS was administered over the course of several days in order to induce inflammation. Weight change was monitored and revealed a trend toward protection against weight loss in chronically infected mice

relative to non-infected mice. This data were suggestive that chronically infected mice may have developed a resistance to chemically induced inflammation.

Despite this interesting observation, the aim of our study was to induce an inflammatory response that would overcome the mechanisms of parasite persistence. We took the view that the induction of a reliable Th1/Th17 mediated inflammation may be more advantageous than a Th2 response in terms of observing an effect on the parasite load. This is because an IFN- $\gamma$  mediated Th1 immune response, and to some extent, the IL-17 mediated Th17 response are well characterised features of successful immunity against *T. cruzi*<sup>20,21</sup>. Therefore, we decided that we would use TNBS to induce colitis in our infection model. The challenge in using TNBS induced colitis was that there was no standard practice for the model. Since the first report of TNBS as a chemical inducer of colitis, there have been many variations on the method, all using different concentrations of the drug, different concentrations of ethanol, different numbers of treatment doses and in different mouse strains<sup>22,23</sup>.

We set out with the following aims.

1. To optimise a dosing strategy for the induction of chronic TNBS induced colitis in the BALB/C mouse. Using histopathology to assess gut inflammation in response to different doses of TNBS.
2. To administer TNBS in a dosing regimen that would induce inflammation in the gut in *T. cruzi* chronically infected mice.

The objective of this study was to evaluate whether chemically induced inflammation in the colon has the potential to impact on the parasite burden in a specific niche during chronic infections in the BALB/c model.

## 4.2 Methods

### Murine infections and bioluminescent imaging

All animal work was performed under UK Home Office project licence (PPL 70/8207) and approved by the LSHTM Animal Welfare and Ethical Review Board. Procedures were in accordance with the UK Animals (Scientific Procedures) Act 1986 (ASPA). Female BALB/C mice were purchased from Charles River (UK), and CB17 SCID mice were bred in-house. Animals were maintained under specific pathogen-free conditions in individually ventilated cages. Animals experienced a 12-hour light/dark cycle, with access to food and water *ad libitum*. At regular intervals prior to the start of the TNBS dosing regimen, the cage bedding of the BALB/C mice was gathered and redistributed evenly between all of the cages of the mice involved in the experiment. This redistribution of bedding was done in order to equalise the microbiome between all of the mice in the study and reduce any possible cage effects brought about by separate housing<sup>17</sup>.

SCID mice were infected with  $1 \times 10^4$  bioluminescent bloodstream trypomastigotes (BTs) of CL Brener (CL LUC) in 0.2 ml PBS via intraperitoneal (i.p.) injection. BALB/C mice, aged 8-10 weeks, were infected i.p. with  $1 \times 10^3$  BTs derived from SCID mouse blood. At experimental endpoints, mice were sacrificed by exsanguination under terminal anaesthesia.

For *in vivo* imaging, mice were injected with  $150 \text{ mg kg}^{-1}$  d-luciferin i.p. then anaesthetized using 2.5% (v/v) gaseous isoflurane. They were placed in an IVIS Lumina II system (Caliper Life Science) 5-10 min after d-luciferin administration and images were acquired using Living Image 4.3. Exposure times were set at 5 mins. After imaging, mice were revived and returned to cages. For *ex vivo* imaging, mice were injected with d-luciferin, and sacrificed by exsanguination under terminal anaesthesia 5 min later. They were then perfused via the heart with 10 ml  $0.3 \text{ mg ml}^{-1}$  d-luciferin in PBS. Organs

and tissues were removed and transferred to a Petri dish in a standardized arrangement, soaked in 0.3 mg ml<sup>-1</sup> d-luciferin in PBS, and imaged using maximum detection settings (5 min exposure, large binning). The remaining animal parts and carcass were checked for residual bioluminescent foci, also using maximum detection settings. To estimate parasite burden in live mice, regions of interest (ROI) were drawn using LivingImage v.4.3 to quantify bioluminescence as total flux (photons/second), summed from dorsal and ventral images. The detection threshold for *in vivo* imaging was determined using uninfected mice.

According to our project license, this procedure was classified as having a severity limit of 'severe'. Please refer to the 'Advisory notes on recording and reporting the actual severity of regulated procedures' in the Appendix.

#### **Induction of inflammation by TNBS administration**

Chronic inflammation was induced by the administration of TNBS (Sigma-Aldrich) into the colon via the rectum. TNBS (varying concentrations, refer to results) was dissolved in cold ethanol (45% v/v) and made up to the final volume in Milli-Q water. The solution was brought up to room temperature prior to administration. Control dose was PBS mixed with the same percentage ethanol.

100µl dose was administered per mouse via the rectum using a 3.5-F-catheter attached to a 1ml syringe. Mice were anaesthetised using 2.5% (v/v) gaseous isoflurane and the anal verge was lubricated. The catheter was inserted approximately 3.5 cm into the rectum and the contents of the syringe slowly released into the mouse. The mouse was held in the vertical position, head facing down, for 1 minute after administration in order to ensure absorbance of the TNBS across the colon.

## **Parameters used to assess the extent of colonic inflammation**

### Colon length

Upon necropsy, the colon was separated from the mesentery and the mesenteric fat. The length of the colon was measured from where the colon attaches to the caecum up until where the colon terminates at the anal sphincter.

### Histopathology

The colon was cut into equal sections, with half of the sections embedded longitudinally and the other sections embedded transversely to give two different views for histopathological analysis.

Colon sections were cleaned in PBS and fixed in Glyo-Fixx solution (ThermoFisher) for 24 hours. Tissues were then dehydrated in a step wise manner in ethanol, starting by submersion in a 70% solution and increasing the ethanol percentage until the tissues were submerged in 100% ethanol. Tissues were cleared with Histo-Clear clearing agent (National Diagnostics) before being embedded in paraffin as described above. Sections of colon were cut to a thickness of 3 microns on a microtome and with the aid of a water bath, the tissue sections were mounted on glass slides. Paraffin was removed with xylene and tissue sections were rehydrated in decreasing concentrations of ethanol in preparation for staining. Tissues were stained with H&E.

### Faecal occult blood examination

Fresh stool samples were taken from each mouse the day following TNBS or PBS administration and tested for blood using the hema-screen faecal occult blood test (Immunostics inc).

## **Experimental Design and Statistical Analysis**

Allocations of mice to each group was random and was not performed by the investigator. Calculations of group sizes were made based on the expected mortality rate, based on other published studies<sup>18,24,25</sup>. Power calculations were not performed in determining the group size.

Histological examinations were blinded, the investigator was unaware of which tissue sections belonged to which experimental groups when assigning histological scores by microscopy.

All statistical analyses were performed using GraphPad Prism 8 software. The students t-test was used to calculate statistical significance between experimental groups for weight change analysis and the analysis of differences in colon length. Calculations were performed without correcting for multiple comparisons.

## 4.3 Results

### 4.3.1 TNBS tolerability in a chronic dosing schedule

Our first step was to optimise a protocol for TNBS administration in BALB/c mice that was tolerable across multiple doses, a requirement for induction of chronic inflammation. Based on published TNBS dosing schedules, we decided to assess the tolerability of two different concentrations across a maximum of four doses<sup>26-28</sup>. In doing so, we aimed to induce inflammation that was maintained over time, whilst remaining tolerable and within the severity limits of our study. BALB/c mice were administered two different doses of TNBS, the first (referred to as the 'low dose'), was 1 mg TNBS weekly, rising to 1.5 mg after 2 weeks. The other, (referred to as 'high dose'), was a 1.5 mg weekly dose, rising to 2 mg after 2 weeks (Figure 4.1)

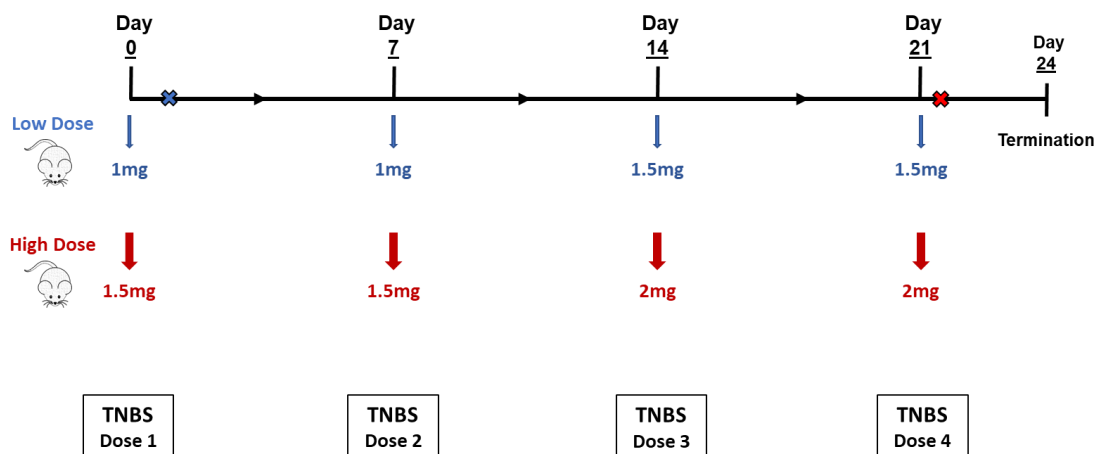


**Figure 4.1** – TNBS Dosing Schedule. 20 week old BALB/C mice were separated into 3 groups; 'low dose' (blue arrows), 'high dose' (red arrows) and control (not shown on timeline) (n=3). All mice were non-infected. TNBS was administered on a weekly basis, starting on day 0. Black line represents time, blue arrows indicate TNBS dose for low dose group, red arrows indicate TNBS dose for high dose group. Blue cross on timeline indicates end point for one mouse in the low dose group, culled on day 1. Red cross indicates end point for one mouse in the high dose group, culled on day 22.

### Assessment of tolerability of dosing schedules

In order to assess whether TNBS was tolerated at these concentrations, we monitored the weight change of mice after each administration (Figure 4.2A). Control mice gained a small amount of weight at the beginning of the study and then maintained their weight throughout the 24 days. Mice receiving the low dose of TNBS on the other hand went through an initial period of weight loss within the first 8 days. This weight was recovered by day 15 and the weights of these mice remained stable throughout the remainder of the study. Mice on the higher dose showed the greatest weight loss of around 8% on day 15. The high dose group, like the low dose group, recovered some of their weight but remained below their starting weight for the remainder of the study.

During the course of the study, one mouse from each group demonstrated a major departure from their usual state, as outlined in the advisory notes (Appendix). As such, they met the requirement for a humane end point (Figure 4.2B).

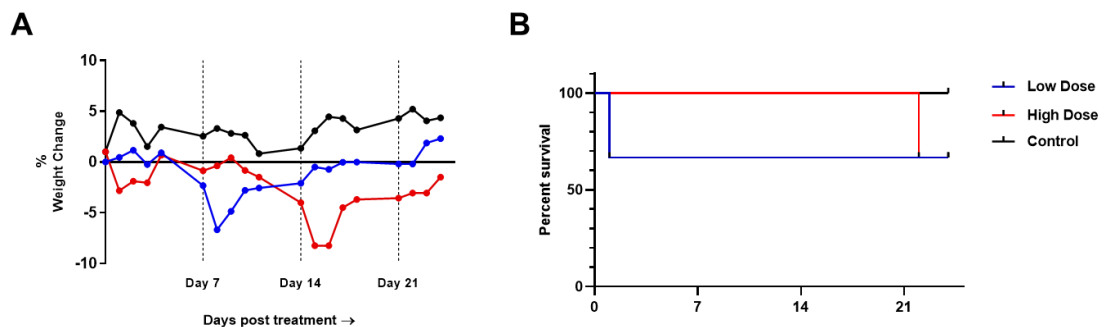


**Figure 4.2** – A) Average Weights. Mice had their weights taken for 5 consecutive days following each administration of TNBS until the end of the experiment. The black vertical lines on days 7, 14 and 21 represent each dose of TNBS. Weights are expressed as a percentage of the starting weight prior to the first dose (day 0) (n=3).

B) Survival Curve. TNBS treated mice (n=3) were monitored throughout the day following each treatment. Mice were euthanised at humane end points if required. Data is derived from a single experiment

### Histopathological analysis of colons in TNBS treated mice

To examine whether inflammation was induced in the colons of TNBS treated mice and to determine the extent of the inflammation, mice were culled on day 24 and the colons removed for histopathological analysis (Figure 4.3). A side by side comparison of transverse and longitudinal sections revealed differences in the colon architecture. Control mice, receiving PBS in ethanol presented with colons that were in line with what we would expect from a healthy mouse. The mucosal layer had defined folds with a clear branching pattern of the lumen (Figure 4.3A). There was little to no epithelial cell hyperplasia and the mucosal, submucosal and muscle layers were clearly all attached, well defined and had little to no cell infiltration. (Figure 4.3 A, B, C).

In contrast, mice treated with TNBS displayed varying degrees of inflammation, depending on the dose. Mice treated with a low dose presented with damage to the colon. They had some blunting of the mucosal layer, with the mucosal folds less defined, resulting in a more diffuse branching pattern of the lumen on transverse sections (Figure 4.3D). Additionally, there was some minor oedema, as can be seen by the gaps between the muscle layer and the submucosa (Figure 4.3E). There was also some epithelial cell hyperplasia, which resulted in elongated mucosal crypts relative to the controls (Figure 4.3F). In terms of the number of lymphoid follicles, both the low dose and high dose groups presented with similar numbers of follicles (Figure 4.3 and supplementary Figure 4.1). These were of varying sizes, however both large and small follicles could be seen in both groups. Importantly, these follicles were rarely present in the controls. On closer inspection (Figure 4.3F and I), infiltration of cells from the submucosal layer into the mucosa can be seen. This inflammatory infiltrate was more extensive in the higher dose group and often resulted in a distortion of the mucosal crypts (Figure 4.3I). This was the only real discernable difference in the inflammatory response between the low dose and the high dose group.

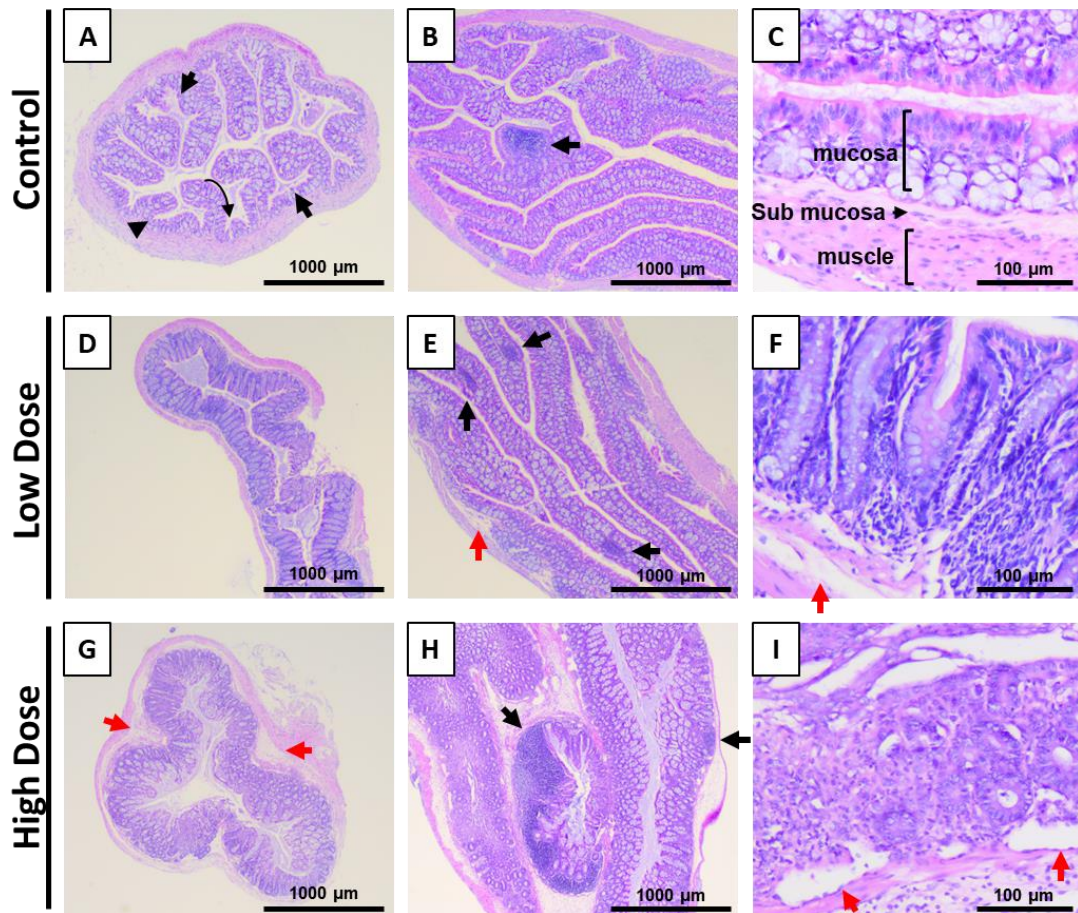


**Figure 4.3** – BALB/c mice were given 4 doses, once weekly, of either PBS in ethanol, a low dose of TNBS in ethanol, or a high dose of TNBS in ethanol (as outlined in Figure 4.1). Mice were culled on day 24 and colons removed for H&E staining.

A-C) Control mice were treated with PBS in ethanol. A, transverse section, curved arrow demonstrates fold in mucosal layer, solid arrows indicates luminal branches. B, longitudinal section, arrowhead shows a lymphoid follicle. C, magnified view of the mucosal, submucosal and muscle layers (n=3).

D-F) Low dose mice were treated with 1 mg TNBS in ethanol, rising to 1.5 mg. D, transverse section (missing part of colon is a feature of the cut, not a feature of TNBS induced changes). E, longitudinal section, black arrows indicate lymphoid follicles, red arrows highlight oedema. F, Close up view of submucosal and mucosal layers, arrow demonstrating mucosal crypts are elongated compared to image C. Also present is an oedema (red arrow) (n=2 at end point).

G-I) High dose mice were treated with 1.5 mg TNBS in ethanol, rising to 2 mg. G, transverse section of the colon, red arrows indicate oedema. H, longitudinal cut, showing large lymphoid follicle (centre) and smaller lymphoid follicle indicated by black arrow. I, close up view showing submucosal and mucosal layers, with large infiltration of cells into mucosal layer and distorted architecture of mucosa (n=2 at end point). Data are derived from single experiment.

### 4.3.2 Impact of TNBS treatment on a chronic Chagas infection

After the assessment of TNBS tolerability, we decided to use the higher concentration dosing schedule and to increase the the size of the TNBS treated group. The group size of mice receiving TNBS was increased to 9. This left 3 mice in the control (PBS) group. Chronically infected mice were administered 1.5 mg TNBS, or PBS, the same as previously (Figure 4.4). Weight change was monitored and a guiac test for fecal blood was performed the day following each administration of TNBS or PBS. After taking into consideration the change in weight of the mice (Figure 4.5) and the presence of fecal blood in several of the animals, after 3 doses of TNBS the treatment was concluded.

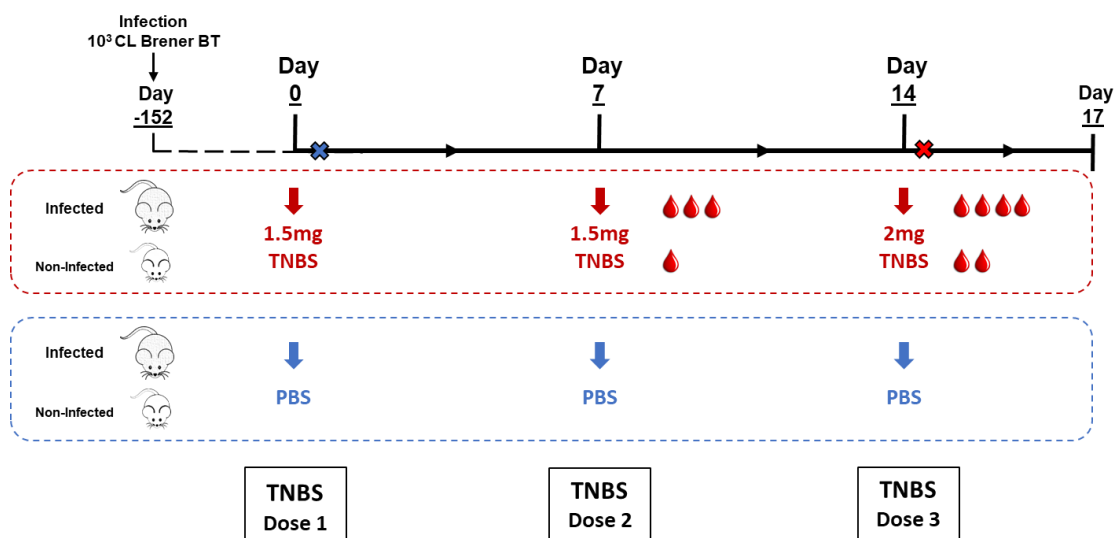


**Figure 4.4** – TNBS Dosing Schedule. Chronically infected BALB/c mice (day 152 of infection) and age matched control mice were administered weekly doses of TNBS, or PBS intrarectally. Mice received a total of 3 doses. 3 days following the final administration, the experiment was terminated.

Black line represents time. Blue cross on timeline indicates end point for one mouse in the PBS group, culled day 1. Red cross indicates end point for one mouse in the TNBS group, culled day 15. Red blood drops represent number of mice that were positive for faecal blood (4 mice in infected and 2 mice in non-infected). (TNBS n=9. PBS n=3)

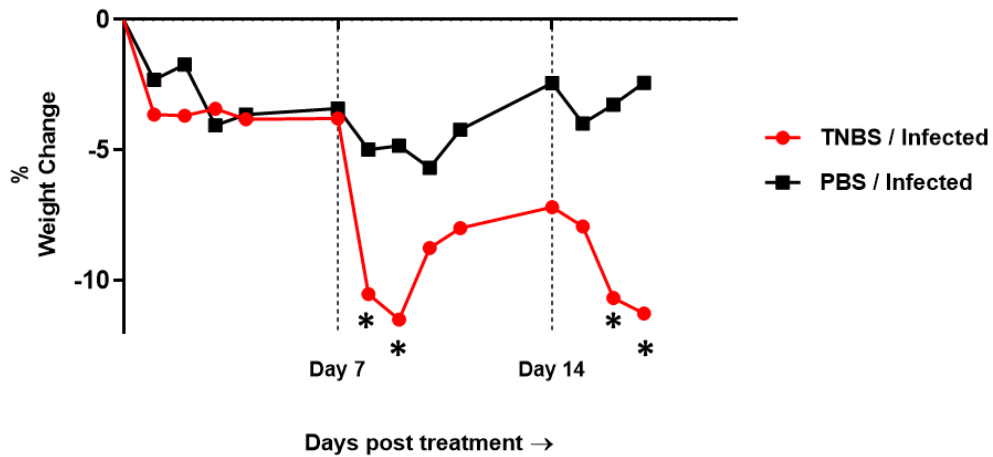


**Figure 4.5** –Average Weights. Mice had their weights taken for 5 consecutive days following each administration of TNBS or PBS. The black vertical lines on days 7 and 14 represent the timings of each dose. Weights are expressed as a percentage of the starting weight prior to the first dose (day 0) (n=9, infected; n=3, non-infected). Data are derived from a single experiment.

#### Bioluminescent imaging of TNBS treated mice

Chronically infected mice were monitored by bioluminescent imaging throughout the study in order to monitor changes in the infection burden (Figure 4.6A). Mice were imaged during the acute stage in order to confirm that they were successfully infected and were imaged again on day 74 to confirm that the parasite burden was consistent with a chronic stage infection prior to the commencement of the TNBS treatment (Supplementary Figures 4.3 and 4.4).

Bioluminescent imaging was performed immediately prior to each administration of PBS or TNBS. Despite repeated administrations of TNBS, the parasite burden remained similar between PBS treated and TNBS treated mice throughout the study and no significant differences between the two groups was detected, as judged by *in vivo* imaging (Figure 4.6B). The infection dynamics were consistent with a normal chronic stage infection<sup>13</sup>. Foci were spatiotemporally dynamic, changing both position and intensity from one week to the next. After the third TNBS treatment, mice were imaged

a final time on day 169 post infection, before necropsy and *ex vivo* imaging of the organs and mouse carcasses was performed.

One of the TNBS treated mice was euthanised point prior to the end of the experiment (Figure 4.4), therefore a total of 8 TNBS treated mice underwent necropsy. Of the 8 mice, 5 displayed no bioluminescence in the GI tract. Amongst the PBS treated mice, all displayed bioluminescence in either the organs or the carcass, however one of these mice displayed no bioluminescence in the GI tract (Figure 4.6C).

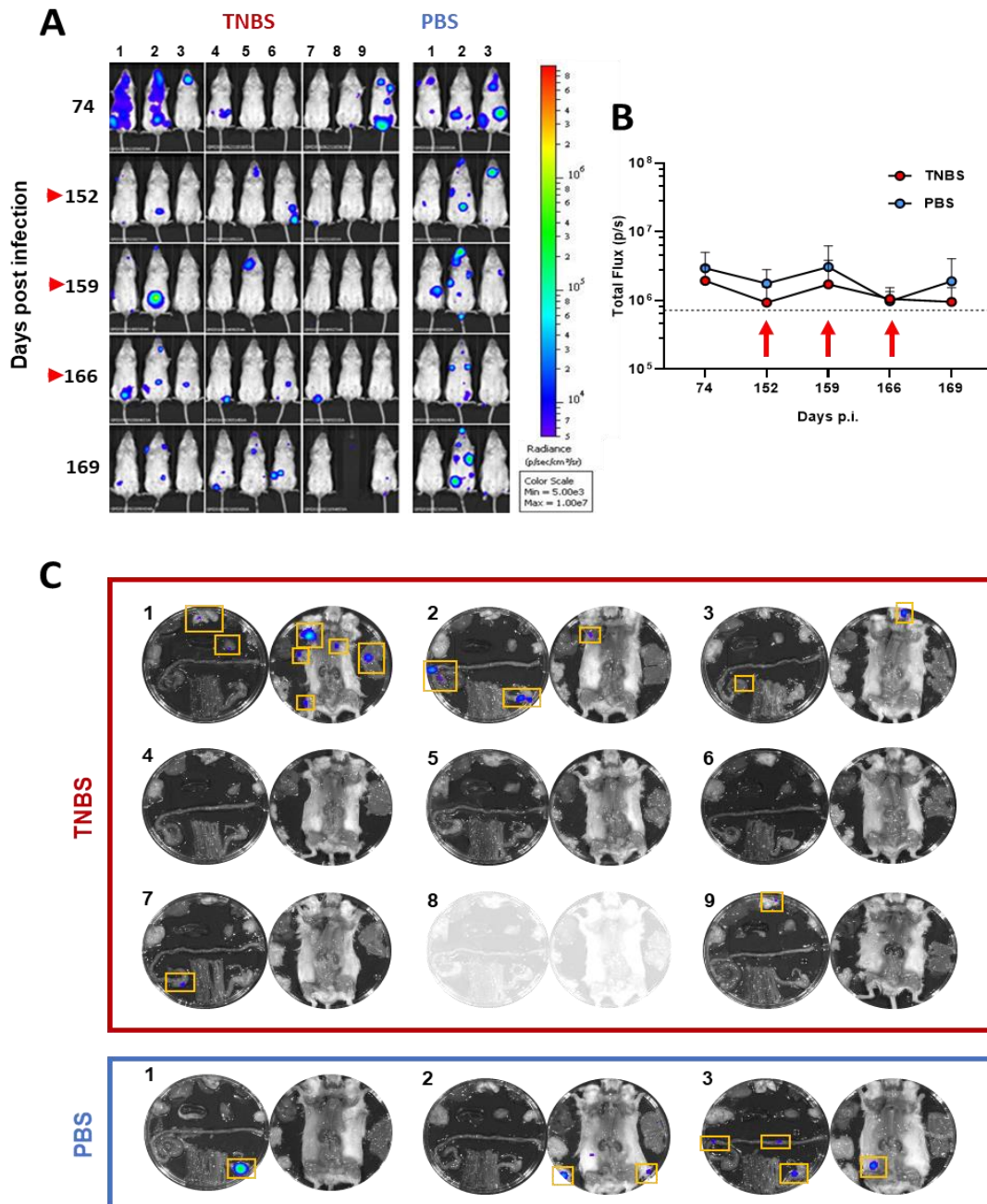


**Figure 4.6** – Bioluminescent imaging of infected, TNBS treated mice. A) *In vivo* imaging was performed on infected mice immediately prior to administration of TNBS or PBS. The ventral images of 9 TNBS treated mice and of 3 PBS treated mice are shown, with heat maps overlaid, representing the bioluminescence inferred parasite burden. The red arrows indicate the days on which TNBS or PBS were administered.

B) The sum of the ventral and dorsal images of each mouse were averaged across the group and are displayed on a logarithmic scale.

C) *Ex vivo* bioluminescent images of the organs and carcasses of necropsied mice. Heat maps use the same scale bar as in (A). Yellow boxes highlight areas of bioluminescence. Data are derived from a single experiment

### Histopathological analysis of colons in TNBS treated mice

We wanted to understand whether the absence of bioluminescence in the colon tissue of infected mice on necropsy was attributable to TNBS induced colitis. We studied the severity of the TNBS induced pathology and inflammation in the colons of mice to determine whether either of these parameters correlated with what we observed by *ex vivo* imaging.

Firstly, we measured the lengths of the colons as they were removed for *ex vivo* imaging (Figure 4.7). Colon length is a common measure of disease severity in experimental models of colitis<sup>18</sup>. Amongst the infected mice, there was a significant difference in the colon length between the TNBS treated and PBS treated groups ( $p < 0.05$ ). Furthermore, those mice that had a bioluminescent negative colon on *ex vivo* assessment (red dots on Figure 4.7) displayed the shortest colons in the TNBS treated group.

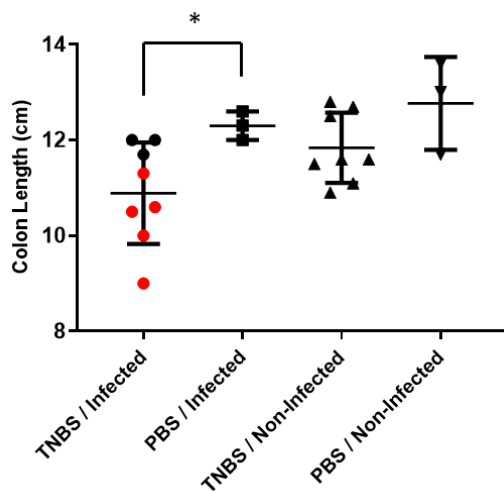


**Figure 4.7** – Colon length on necropsy. The length of the colon was measured immediately after being removed from the mouse for necropsy. The red dots represent the mice whose colons were negative for bioluminescence on *ex vivo*. \* $p < 0.05$ . Data are derived from a single experiment

After *ex vivo* imaging, the colon tissues were fixed, embedded and sectioned, as previously. In order to measure the severity of tissue pathology and the level of inflammation induced, tissue sections were attributed a score for two different parameters, damage and inflammation (Table 4.1 and 4.2). We based this damage

index and the inflammation index on a previously published guide<sup>29</sup>. The inflammation index (Table 4.1) is based on the extent of inflammation through all of the different tissue layers that make up the colon, with 0 being the least extensive inflammation and 3 being the most extensive. The damage index (Table 4.2) is based on common pathological features of TNBS colitis that we observed in the tissue sections. The presence of any of these features in at least 2 tissue sections from the same animal adds 1 to the overall damage index score for each mouse. The scores are presented in Figure 4.8.

On assessment of the tissue sections, based on the aforementioned criteria, a pattern emerged whereby the mice that did not display bioluminescence in the GI tract on necropsy were the mice that presented with the most tissue damage on histology (Figure 4.8A). Mice that were positive for bioluminescence presented with less severe pathology. Between PBS and TNBS treated mice, there were no significant differences in the overall damage index, regardless of whether the mice were infected or non-infected.

On assessing the tissue sections for the extent of inflammation (scoring based on Table 4.1), the same pattern emerged, whereby those mice that were bioluminescent negative in the GI tract were the mice that presented with the highest levels of inflammation (Figure 4.7B). Despite this trend, there were no significant differences in the inflammation index amongst TNBS and PBS treated mice.

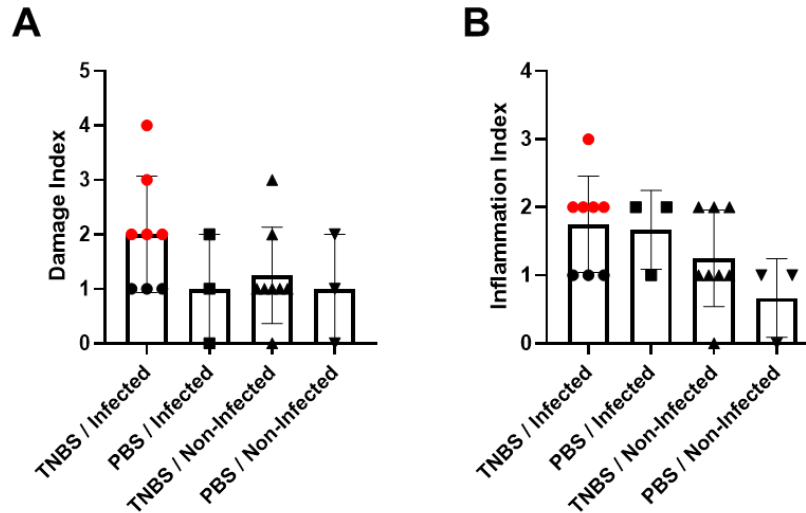


**Figure 4.8** – Chronically infected and non-infected BALB/c mice were treated with TNBS or PBS. The colons were removed following the end of the treatment and sections were scored based on the histopathological features. A) Each dot represents a mouse that was given a score based on the number of histopathological features associated with colon damage as outlined in Table 4.2. B) Each dot represents a mouse that was given a score based on the extent of inflammation as outlined in Table 4.1. Data are derived from a single experiment

The red dots identify those mice whose colons were negative for bioluminescence on *ex vivo*.

**Table 4.1**

Inflammation Index			
Inflammation	SEVERITY	DESCRIPTION	SCORE
	None	-	0
	Mild	Mucosal infiltration	1
	Moderate	Submucosal infiltration	2
	Severe	Transmural infiltration	3

**Table 4.2**

Damage Index		
Architectural Changes	Erosion of the mucosal surface	1
	Crypt elongation	1
	Oedema	1
	Distortion of mucosal crypt architecture	1
	Mucosal abscesses	1

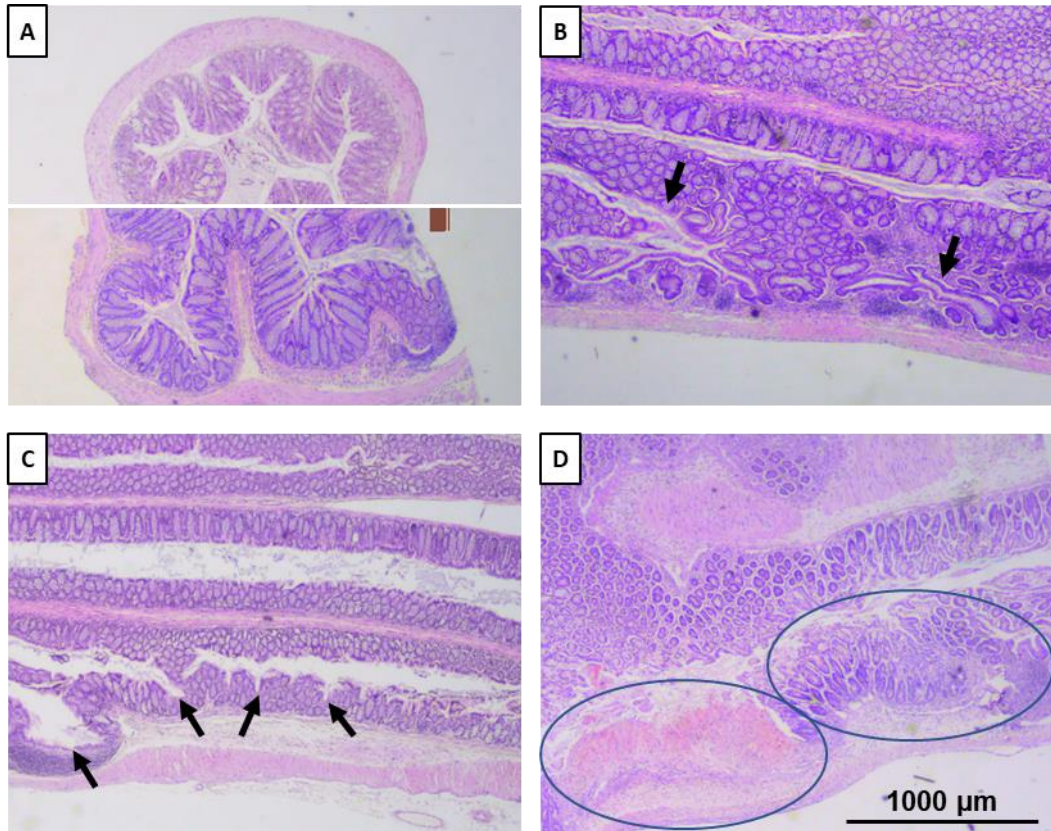


**Figure 4.9** – Representative examples of colons taken from infected and TNBS treated mice. Tissue sections were stained with H&E. Pictures are representative of different features of colon damage by which tissues were scored.

A) Transverse sections of colon, demonstrating epithelial cell hyperplasia, resulting in crypt elongation. Top half of 'A' is a PBS treated mouse, crypts are shorter in length compared to bottom half of 'A', which is a TNBS treated mouse.

B) Abscesses, indicated by black arrows present within the mucosal layer.

C) Erosion of surface epithelium, as indicated by arrows.

D) Distortion of normal architecture. Left hand circle demonstrates area devoid of mucosa. Right hand circle demonstrates an area of the mucosa which has lost uniformity due to inflammation.

Data are derived from a single experiment

## 4.4 Discussion

### **Establishment of a TNBS dosing schedule**

Treatment options for Chagas disease are limited. We sought to explore the possibility of using immunotherapy to target a site of known parasite persistence. To this end, we optimised a treatment regimen with TNBS to induce chronic inflammation in the colon of BALB/c mice. We administered this treatment to mice infected long-term with *T. cruzi* and demonstrated that there is a possible link between the development of colitis and the bioluminescence inferred parasite burden in the colon.

The first objective of this work was to optimise a TNBS dosing regimen that could induce chronic colitis. The chronic form of inflammation has been less well studied than the acute form, however we postulated that a longer inflammatory response would have a higher chance of impacting on the parasite burden than a single inflammatory event. One of the hurdles of TNBS induced colitis is toxicity, which can have a fatal outcome<sup>24</sup>. Therefore mice were subjected to regular observation and weight checks. A single mouse in each of the dosing groups was euthanised because it reached a humane end point during the study.

Weight change is a strong indicator of mouse health and occurs rapidly after TNBS administration, with mice often losing a significant portion of weight within 24 hours (Comparison of experimental mouse models of inflammatory bowel disease). We found a difference between the low dose and high dose groups (Figure 4.2). Mice on the low dose treatment exhibited little weight change after the first administration, with their weight reaching a minimum on day 8, following the second administration. The mice on the higher dose lost more weight, however the pattern of weight loss was different. Their weight reached a minimum on day 14, after the third TNBS dose. Overall, this weight loss, even in the higher dose mice, fell within acceptable limits of severity.

TNBS colitis is associated with lymphoid follicle hypertrophy in response to luminal antigens. Lymphoid follicles are aggregates of immune cells, and have a cellular organisation which is comparable to that of the Peyer's patches in the small intestine, containing T cell and B cell zones with germinal centres<sup>30</sup>. We observed these patches in tissue sections from TNBS treated mice, although there were no significant differences between the low dose and the high dose groups. Generally, both developed enlarged lymphoid follicles, as expected with a TNBS enema<sup>31</sup>. Close inspection of the mucosal layer did however reveal a difference in the level of inflammation. Mice receiving a higher dose of TNBS developed more extensive inflammatory cell infiltrate. As a result, the mucosa in the higher dose group was often less well defined and had more areas lacking architectural integrity. This was a possible contributing factor to the increased weight loss in these mice, and suggests a more intense inflammatory response than in the low dose group.

Based on this, the higher dose treatment was judged to induce a higher inflammatory response, whilst staying within acceptable limits of severity. We therefore chose these conditions for assessing the effect of chronic *T. cruzi* infection.

### **Effect of high dose TNBS treatment on chronic *T. cruzi* infection**

TNBS administration at the higher dose did not affect the parasite inferred bioluminescence as judged by whole body *in vivo* imaging. The bioluminescence profile initially showed a small dip on day 152 (Figure 4.6), however this rebounded by day 159, and it became apparent that this change was unlikely to be due to TNBS, but instead, was a feature of the natural infection dynamics that are inherent in the chronic stage of the infection. After 3 doses, we saw no significant differences in the parasite burden between the two groups, or any obvious departure from the normal pattern of infection.

Three days after the third dose, we performed a necropsy followed by imaging of the tissues *ex vivo*. This revealed a surprising result. Despite the fact that the *in vivo* imaging

did not show any departure from what we would expect in a chronic infection, there was an unusual pattern of parasite distribution. In five out of the eight TNBS treated mice, there were no infection foci in the colon; in three of these mice there was no detectable organ associated bioluminescence. This was surprising for two reasons, firstly, because *in vivo* imaging demonstrated no major differences in the whole body parasite burden, secondly, the GI tract is a site that is persistently found to be infected during the chronic stage<sup>13</sup>. Therefore, taken together, *in vivo* and *ex vivo* data suggest that TNBS administration impacts on parasite persistence in both the colon, and other organ/tissue sites, perhaps by perturbing the global immune response.

When studying the control group, one of the three mice was also observed to lack detectable foci of infection in the colon/stomach. In BALB/c mice, less than 5% of chronic infections display this characteristic. One explanation could be that the phenomenon is linked to the role of ethanol in the enema, which is to break down the epithelial barrier and expose the mucosa to luminal antigens. Larger numbers of mice in the control cohorts would be needed to explore this further. However, to observe five out of eight mice that are negative for bioluminescence in the GI tract and to have three mice that are bioluminescent negative at a whole body level was unusual, and not an observation that has been made before in a regular necropsy of chronically infected mice<sup>13,14</sup>.

TNBS treated mice had significantly shorter colons than mice treated with PBS (Figure 4.7). Additionally, there was a clear correlation between the colon length in TNBS treated mice and the presence of parasites in the colon, as revealed by *ex vivo* imaging. Mice that were bioluminescent negative had the shortest colons in the TNBS treated group. Furthermore, 4 out of 5 mice provided positive blood samples in their faeces by guaiac test. Colon length and bloody faeces are both critical indicators of the severity of colitis. As judged by both of these parameters, mice that were bioluminescence negative in the colon fared worse than mice that were bioluminescence positive, tentatively linking the absence of parasites to the severity of colitis. Histopathological analysis of the colon

tissues further supported this assessment. There was a clear pattern, whereby mice that suffered the most severe tissue pathology and had the greatest inflammation were more likely to be bioluminescence negative in the colon.

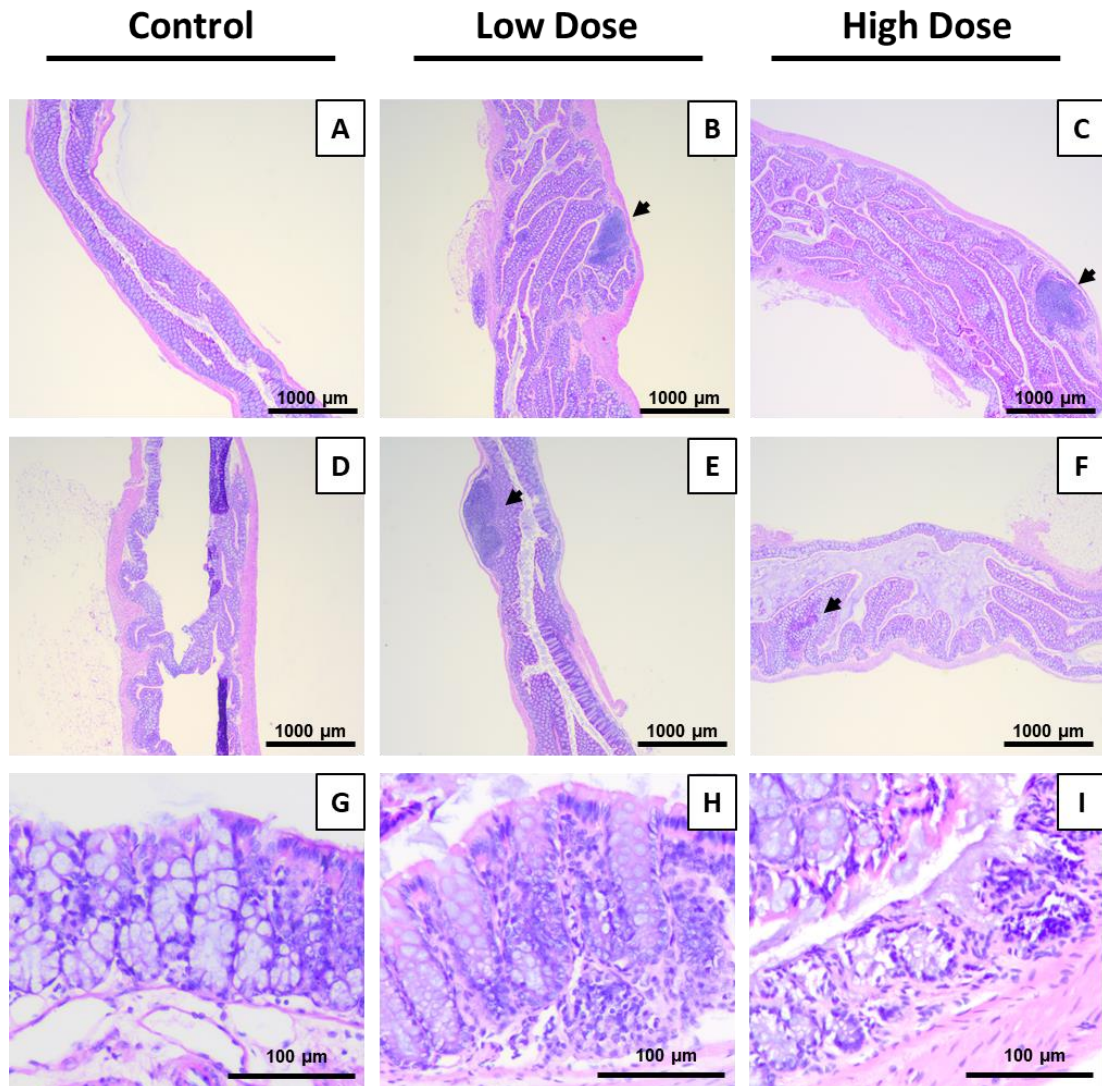
Some of the observations in this study also raised another question - does infection with *T. cruzi* impact on the severity of induced colitis? Non-infected TNBS treated mice tended to lose less weight than the infected treated mice (Supplementary Figure 2). In addition, they presented with less severe inflammation or tissue damage, as well as having longer colons and a reduced instance of bloody stools (Figure 4.7). Although not statistically significant at the level of individual parameters, collectively these data hint at the possibility that a *T. cruzi* infection may be responsible for inducing differences in the local immune environment, essentially protecting mice from chemically induced inflammation. As *T. cruzi* is very well documented to be successful in immune evasion and in immune modulation, this is a plausible theory that should merit further investigation<sup>32</sup>.

## **Conclusion**

Although TNBS-induced colitis was a rather blunt approach for assessing the impact of inflammation on parasite persistence in the GI tract, we reasoned that the wide-ranging effects that it produces would be a useful preliminary method for exploring the question. Clearly the benefits of a targeted strategy of inflammation as a therapeutic option need to be weighed against the risk of the undesired effects of colitis, since disruption of immune homeostasis in this tissue can lead to local debilitating disease, with perhaps more widespread consequences. Our work intended to explore the principle that targeted elimination of the parasite in its niche in the host would lead to total eradication. We did provide evidence that induced colitis could lead to parasite elimination, however, this outcome was not universal, and less effective than could be provided by conventional chemotherapy<sup>33</sup>. Although this preliminary study did demonstrate that

inflammation in the colon can be beneficial in some cases from the perspective of parasite elimination, the costs to the host do not merit the outcome. In future, it may be worth exploring a more targeted approach to immunotherapy, using approaches that might enhance parasite elimination, in the absence of major side effects.

## 4.5 Supplementary



**Supplementary 4.1** – BALB/C mice were given 4 treatments, once weekly, of either PBS in ethanol, a low dose of TNBS in ethanol, or a high dose of TNBS in ethanol (as outlined in figure 4.1). Mice were culled on day 24 and colons were removed for H&E staining.

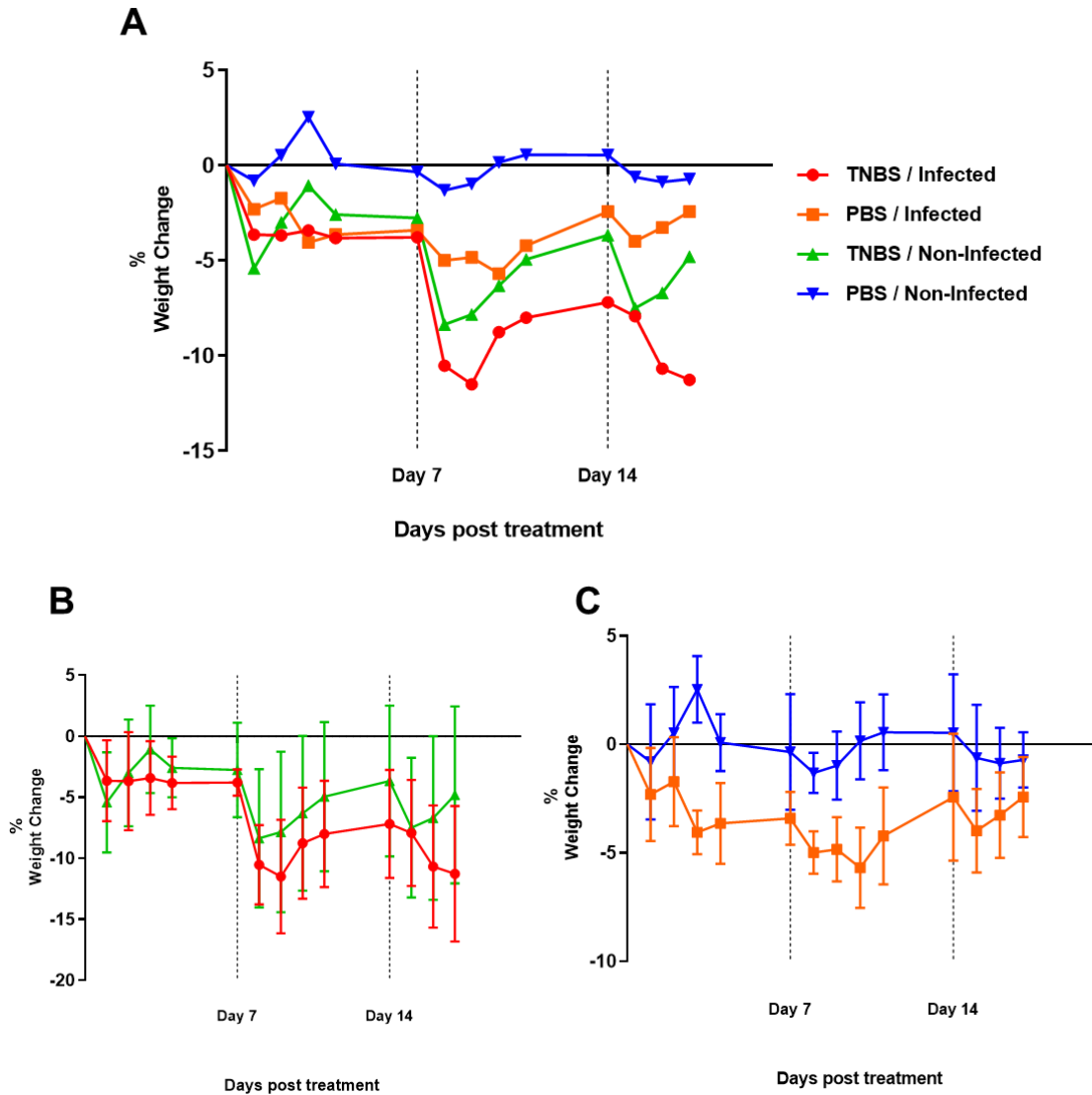
A and D) PBS treated mice showed little or no lymphoid aggregates. Image D has part of mucosa folded over on itself.

B and E) Low dose TNBS group. Black arrows indicate lymphoid follicles.

C and F) High dose TNBS group. Black arrows indicate lymphoid follicles.

G, H and I) Close up images demonstrating cell infiltration into mucosa.

Data are derived from a single experiment



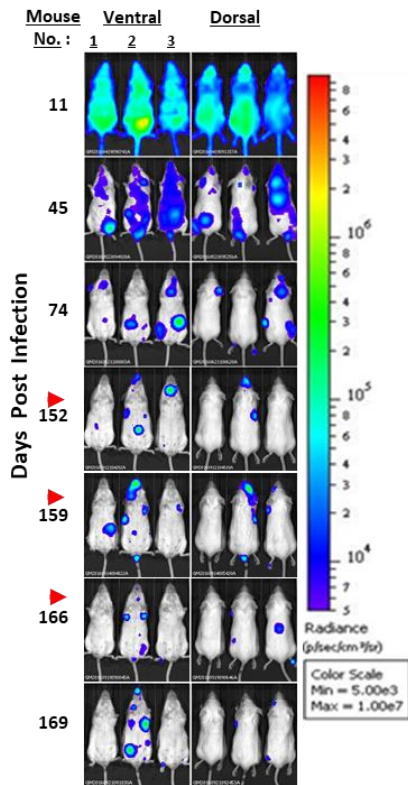
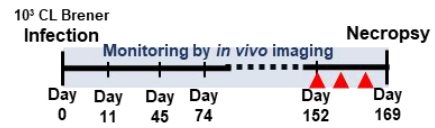
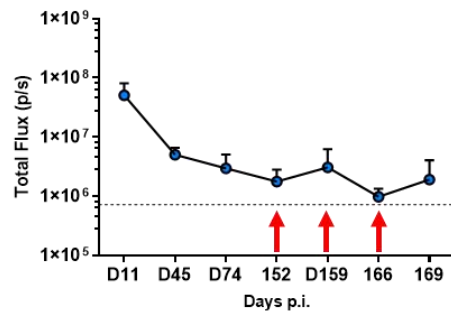
**Supplementary Figure 4.2 –Average Weights.** Infected and non-infected mice treated with either TNBS or PBS had their weights taken for 5 consecutive days following each administration of TNBS or PBS. The black vertical lines on days 7 and 14 represent the timings of each dose. Weights are expressed as a percentage of the starting weight prior to the first dose (day 0). Data are derived from a single experiment.

A) Mean weights of each group

B) Mean weights  $\pm$ SD of infected mice

C) Mean weights  $\pm$ SD of non-infected mice

(n=9, TNBS treated; n=3, PBS treated).

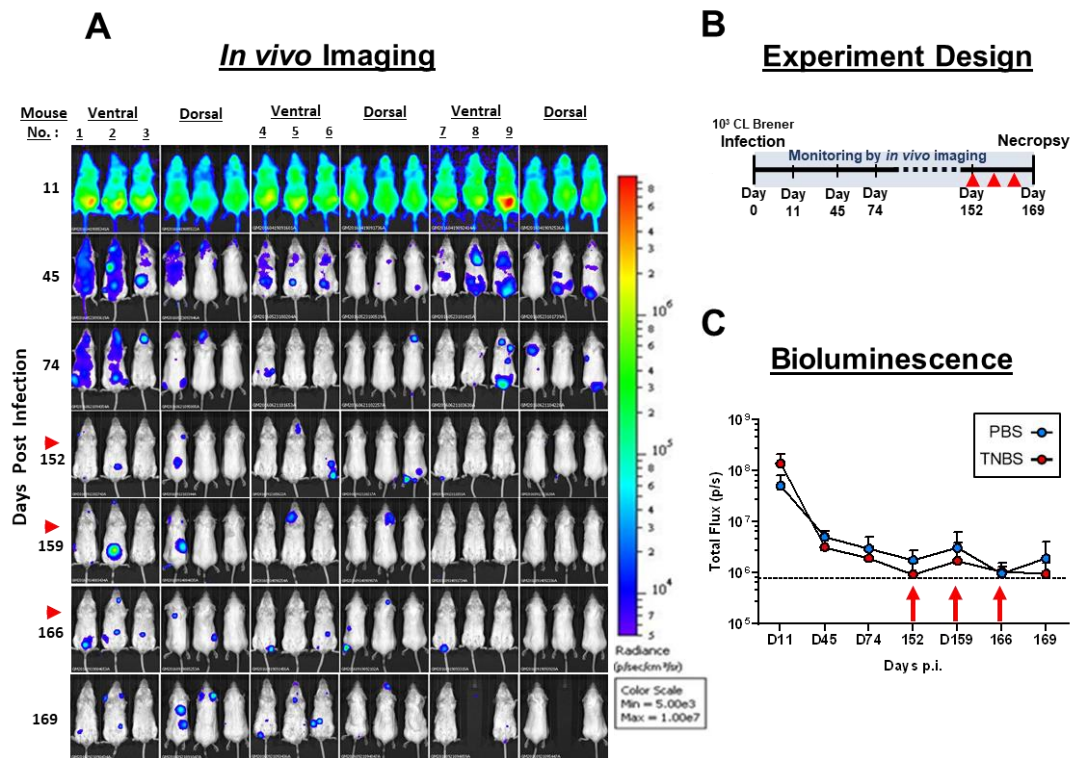
**A****In vivo Imaging****B****Experiment Design****C****Bioluminescence****Supplementary Figure 4.3 – *In vivo* images of infected and PBS treated mice.**

A) *In vivo* imaging was performed on infected mice immediately prior to administration of TNBS or PBS. The ventral and dorsal images of 3 PBS treated mice are shown, with heat maps overlaid, representing the bioluminescence inferred parasite burden. The red arrows indicate the days on which PBS was administered

B) Experimental outline. Mice were infected on day 0 and imaged on the days outlined. PBS treatment was performed on the days indicated

C) The sum of the ventral and dorsal images of each mouse were averaged across the group and are displayed on a logarithmic scale.

(n=3), data are derived from a single experiment.



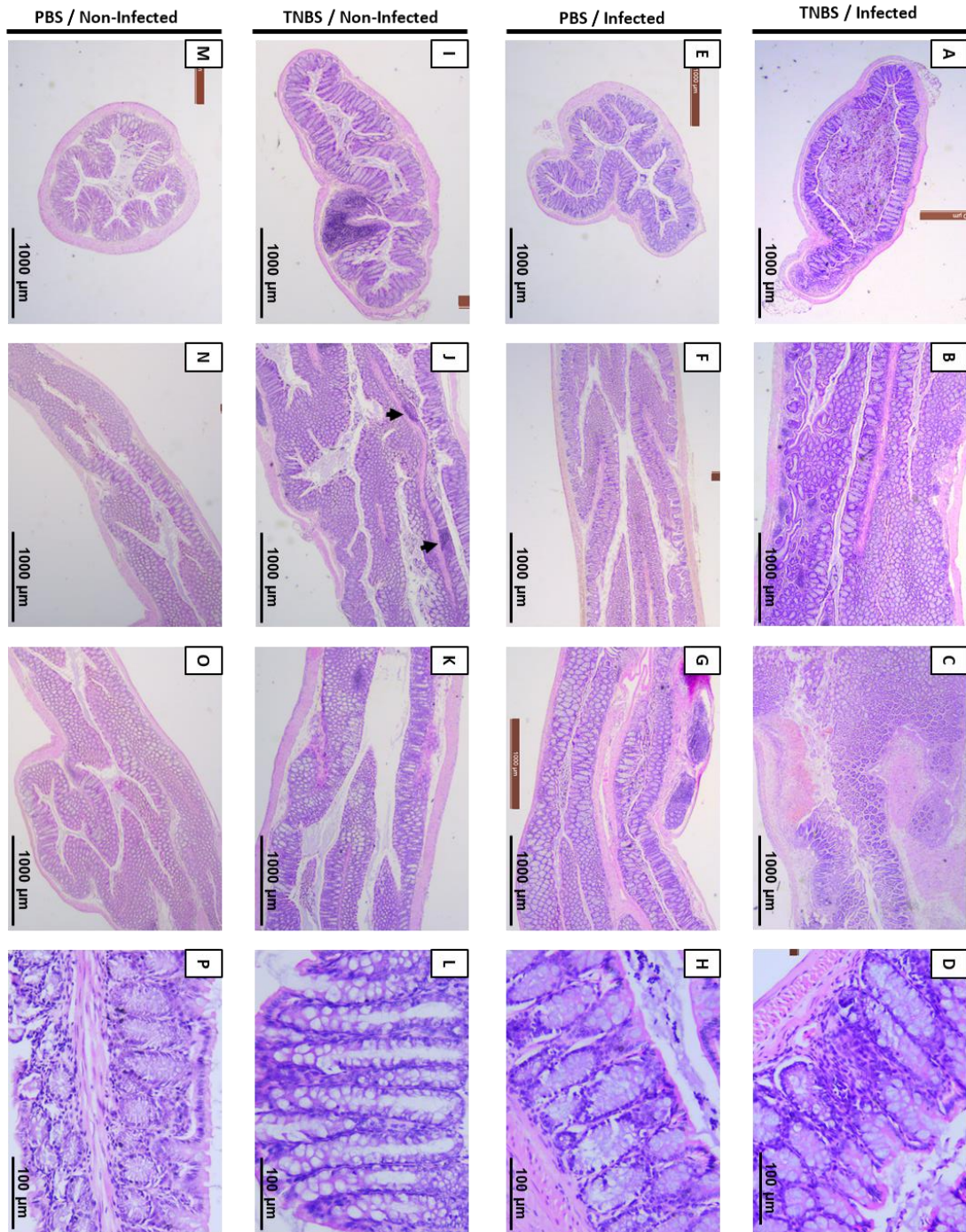
**Supplementary Figure 4.4 – *In vivo* images of infected and TNBS treated mice.**

A) *In vivo* imaging was performed on infected mice immediately prior to administration of TNBS or PBS. The ventral and dorsal images of 9 TNBS treated mice are shown, with heat maps overlaid, representing the bioluminescence inferred parasite burden. The red arrows indicate the days on which TNBS was administered

B) Experimental outline. Mice were infected on day 0 and imaged on the days outlined. TNBS treatment was performed on the days indicated

C) The sum of the ventral and dorsal images of each mouse were averaged across the group and are displayed on a logarithmic scale.

(n=9), data are derived from a single experiment.



**Supplementary Figure 4.5** – Representative examples of colons taken from infected and non-infected TNBS treated and PBS treated mice. Tissue sections were stained with H&E.

A-D) Infected TNBS treated mice. n=9. E-H) Infected PBS treated mice. n=9. I-L) Non-infected TNBS treated mice. n=3. M-P) Non-infected PBS treated. n=3

Data are derived from single experiment

## 4.6 References

- 1 Aldasoro, E. *et al.* What to expect and when: benznidazole toxicity in chronic Chagas' disease treatment. *J Antimicrob Chemother* **73**, 1060-1067, doi:10.1093/jac/dkx516 (2018).
- 2 Crespillo-Andujar, C. *et al.* Toxicity of nifurtimox as second-line treatment after benznidazole intolerance in patients with chronic Chagas disease: when available options fail. *Clin Microbiol Infect* **24**, 1344 e1341-1344 e1344, doi:10.1016/j.cmi.2018.06.006 (2018).
- 3 Castro, J. A., de Mecca, M. M. & Bartel, L. C. Toxic side effects of drugs used to treat Chagas' disease (American trypanosomiasis). *Hum Exp Toxicol* **25**, 471-479, doi:10.1191/0960327106het653oa (2006).
- 4 Sales Junior, P. A. *et al.* Experimental and Clinical Treatment of Chagas Disease: A Review. *Am J Trop Med Hyg* **97**, 1289-1303, doi:10.4269/ajtmh.16-0761 (2017).
- 5 Marcon, G. E. *et al.* Trypanosoma cruzi: parasite persistence in tissues in chronic chagasic Brazilian patients. *Mem Inst Oswaldo Cruz* **106**, 85-91, doi:10.1590/s0074-02762011000100014 (2011).
- 6 Shoemaker, J. P., Hoffman, R. V., Jr. & Huffman, D. G. Trypanosoma cruzi: preference for brown adipose tissue in mice by the Tulahuen strain. *Exp Parasitol* **27**, 403-407 (1970).
- 7 Andrade, Z. A. & Silva, H. R. Parasitism of adipocytes by Trypanosoma cruzi. *Mem Inst Oswaldo Cruz* **90**, 521-522, doi:10.1590/s0074-02761995000400018 (1995).
- 8 Ferreira, A. V. *et al.* Evidence for Trypanosoma cruzi in adipose tissue in human chronic Chagas disease. *Microbes Infect* **13**, 1002-1005, doi:10.1016/j.micinf.2011.06.002 (2011).
- 9 Tanowitz, H. B., Scherer, P. E., Mota, M. M. & Figueiredo, L. M. Adipose Tissue: A Safe Haven for Parasites? *Trends Parasitol* **33**, 276-284, doi:10.1016/j.pt.2016.11.008 (2017).
- 10 Combs, T. P. *et al.* The adipocyte as an important target cell for Trypanosoma cruzi infection. *J Biol Chem* **280**, 24085-24094, doi:10.1074/jbc.M412802200 (2005).
- 11 Spalding, K. L. *et al.* Dynamics of fat cell turnover in humans. *Nature* **453**, 783-787, doi:10.1038/nature06902 (2008).

- 12 Sanchez-Valdez, F. J., Padilla, A., Wang, W., Orr, D. & Tarleton, R. L. Spontaneous dormancy protects *Trypanosoma cruzi* during extended drug exposure. *Elife* **7**, doi:10.7554/eLife.34039 (2018).
- 13 Lewis, M. D. *et al.* Bioluminescence imaging of chronic *Trypanosoma cruzi* infections reveals tissue-specific parasite dynamics and heart disease in the absence of locally persistent infection. *Cell Microbiol* **16**, 1285-1300, doi:10.1111/cmi.12297 (2014).
- 14 Lewis, M. D., Francisco, A. F., Taylor, M. C., Jayawardhana, S. & Kelly, J. M. Host and parasite genetics shape a link between *Trypanosoma cruzi* infection dynamics and chronic cardiomyopathy. *Cell Microbiol* **18**, 1429-1443, doi:10.1111/cmi.12584 (2016).
- 15 Bamias, G., Arseneau, K. O. & Cominelli, F. Mouse models of inflammatory bowel disease for investigating mucosal immunity in the intestine. *Curr Opin Gastroenterol* **33**, 411-416, doi:10.1097/MOG.0000000000000402 (2017).
- 16 Perse, M. & Cerar, A. Dextran sodium sulphate colitis mouse model: traps and tricks. *J Biomed Biotechnol* **2012**, 718617, doi:10.1155/2012/718617 (2012).
- 17 Wirtz, S. *et al.* Chemically induced mouse models of acute and chronic intestinal inflammation. *Nat Protoc* **12**, 1295-1309, doi:10.1038/nprot.2017.044 (2017).
- 18 Oh, S. Y., Cho, K. A., Kang, J. L., Kim, K. H. & Woo, S. Y. Comparison of experimental mouse models of inflammatory bowel disease. *Int J Mol Med* **33**, 333-340, doi:10.3892/ijmm.2013.1569 (2014).
- 19 Alex, P. *et al.* Distinct cytokine patterns identified from multiplex profiles of murine DSS and TNBS-induced colitis. *Inflamm Bowel Dis* **15**, 341-352, doi:10.1002/ibd.20753 (2009).
- 20 Cai, C. W., Blase, J. R., Zhang, X., Eickhoff, C. S. & Hoft, D. F. Th17 Cells Are More Protective Than Th1 Cells Against the Intracellular Parasite *Trypanosoma cruzi*. *PLoS Pathog* **12**, e1005902, doi:10.1371/journal.ppat.1005902 (2016).
- 21 Kumar, S. & Tarleton, R. L. Antigen-specific Th1 but not Th2 cells provide protection from lethal *Trypanosoma cruzi* infection in mice. *J Immunol* **166**, 4596-4603, doi:10.4049/jimmunol.166.7.4596 (2001).
- 22 Scheiffele, F. & Fuss, I. J. Induction of TNBS colitis in mice. *Curr Protoc Immunol* **Chapter 15**, Unit 15 19, doi:10.1002/0471142735.im1519s49 (2002).
- 23 te Velde, A. A., Verstege, M. I. & Hommes, D. W. Critical appraisal of the current practice in murine TNBS-induced colitis. *Inflamm Bowel Dis* **12**, 995-999, doi:10.1097/01.mib.0000227817.54969.5e (2006).

- 24 Antoniou, E. *et al.* The TNBS-induced colitis animal model: An overview. *Ann Med Surg (Lond)* **11**, 9-15, doi:10.1016/j.amsu.2016.07.019 (2016).
- 25 Boirivant, M., Fuss, I. J., Ferroni, L., De Pascale, M. & Strober, W. Oral administration of recombinant cholera toxin subunit B inhibits IL-12-mediated murine experimental (trinitrobenzene sulfonic acid) colitis. *J Immunol* **166**, 3522-3532, doi:10.4049/jimmunol.166.5.3522 (2001).
- 26 Fichtner-Feigl, S. *et al.* Induction of IL-13 triggers TGF-beta1-dependent tissue fibrosis in chronic 2,4,6-trinitrobenzene sulfonic acid colitis. *J Immunol* **178**, 5859-5870, doi:10.4049/jimmunol.178.9.5859 (2007).
- 27 Fitzpatrick, L. R. *et al.* A new model of chronic hapten-induced colitis in young rats. *J Pediatr Gastroenterol Nutr* **50**, 240-250, doi:10.1097/MPG.0b013e3181cb8f4a (2010).
- 28 Fichtner-Feigl, S., Fuss, I. J., Preiss, J. C., Strober, W. & Kitani, A. Treatment of murine Th1- and Th2-mediated inflammatory bowel disease with NF-kappa B decoy oligonucleotides. *J Clin Invest* **115**, 3057-3071, doi:10.1172/JCI24792 (2005).
- 29 Erben, U. *et al.* A guide to histomorphological evaluation of intestinal inflammation in mouse models. *Int J Clin Exp Pathol* **7**, 4557-4576 (2014).
- 30 Dohi, T. *et al.* Hapten-induced colitis is associated with colonic patch hypertrophy and T helper cell 2-type responses. *J Exp Med* **189**, 1169-1180, doi:10.1084/jem.189.8.1169 (1999).
- 31 Cromer, W. E. *et al.* VEGF-A isoform modulation in an preclinical TNBS model of ulcerative colitis: protective effects of a VEGF164b therapy. *J Transl Med* **11**, 207, doi:10.1186/1479-5876-11-207 (2013).
- 32 Cardillo, F., de Pinho, R. T., Antas, P. R. & Mengel, J. Immunity and immune modulation in Trypanosoma cruzi infection. *Pathog Dis* **73**, ftv082, doi:10.1093/femspd/ftv082 (2015).
- 33 Francisco, A. F., Jayawardhana, S., Taylor, M. C., Lewis, M. D. & Kelly, J. M. Assessing the Effectiveness of Curative Benznidazole Treatment in Preventing Chronic Cardiac Pathology in Experimental Models of Chagas Disease. *Antimicrob Agents Chemother* **62**, doi:10.1128/AAC.00832-18 (2018).

## Chapter 5 :

# Generating Attenuated *T. cruzi* Parasites Using Cas9 Genome Engineering

## **5.1 Introduction**

The theme of re-infection which we explored in chapter 2 provided us with new insights into the potential of host immunity to combat *T. cruzi*. We saw that host immunity is capable of mediating robust protection that is long-lived as well as being cross-strain protective, in most cases providing over a 99% reduction in the parasite burden. A noteworthy observation from our work in chapter 2 was the significant benefit of live vaccination over viral vectored vaccination in suppressing the parasite burden. The gulf in efficacy was impressive, especially considering that the vaccine targets are well studied and are amongst leading candidates for the development of a *T. cruzi* vaccine<sup>1-3</sup>.

Revolutionary developments in genome engineering technology over the course of this PhD were optimised for use in kinetoplastids and were successfully applied to *T. cruzi* in our laboratory<sup>4, 5</sup>. This opened the door for the development of genetically attenuated parasites with a precision, and more importantly, a speed that was previously not possible. Upon realising the potential of live vaccination, we sought to take advantage of these developments in genome engineering in order to explore whether we could develop genetically attenuated parasites for testing as a live vaccine.

### **5.1.1 Live vaccines**

The first widespread use of live vaccination followed the observations of Edward Jenner<sup>6</sup>. The advent of biotechnology and our understanding of immunology have since led to the development of many more diverse types of vaccine. However, live vaccines remain a mainstay in public health efforts to combat infectious diseases<sup>7, 8</sup>. This is because many live vaccines are inexpensive to manufacture and produce less waste than other forms of vaccination<sup>9</sup>. More importantly, live attenuated vaccines can be

administered by the same route as a pathogenic infection, inducing a local immune response at the site of pathogen entry. Because live vaccines mimic an infection, they generally also generate a broader immune response, recognising a wider array of epitopes and involving both B and T cells. As a result, they often demonstrate superior protective immunity over other forms of vaccination<sup>10, 11</sup>.

Two different strategies for live vaccination have been experimented with for *T. cruzi*. These are the use of *T. cruzi* related organisms and the use of live attenuated *T. cruzi*. The use of *T. cruzi* related organisms is attractive due to the fact that these are not pathogenic in humans. Their relatedness to *T. cruzi* means that immunity against them is cross-protective<sup>12, 13</sup>. The tomato plant protazoan parasite, *Phytomonas serpens* and the mammalian infectious (but non-pathogenic) *Trypanosoma rangeli* have both been tested as live vaccines in experimental settings, providing moderate protection. Experiments report fewer mice succumbing to lethal challenge and a reduced, but detectable blood parasitaemia<sup>14, 15</sup>.

Using a live attenuated *T. cruzi* parasite shows superior protection than using a *T. cruzi* related parasite. Vaccination with the attenuated strain CL-14, a clone derived from the CL Brener strain of *T. cruzi*, completely prevented the development of blood parasitaemia in challenged mice<sup>16</sup>.

As with any live-attenuated vaccine, one of the biggest risks is the possibility of reversion. This is especially risky for a live attenuated vaccine for *T. cruzi*, considering that immunity to wild type *T. cruzi* is non-sterilising and the infection is potentially lethal. The attenuation of the CL-14 clone of CL Brener is reported to have been obtained through empiric methods, passaging the parasite *in vitro*<sup>16</sup>. This method of attenuation relies on the success of random mutations that render the parasite less virulent. There are safety concerns with this approach to attenuation. Random mutations in response to environmental pressures do not ensure that parasites will not revert to a virulent

phenotype in their natural host<sup>17</sup>. However, this is a risk that can be mitigated by intelligent vaccine design. Through the targeted deletion of a gene that is important in parasite development, replication or virulence, we can develop attenuated parasite lines. If entire open reading frames are deleted, and no alleles remain, there is little to no possibility for reversion back to wild-type.

We sought to take a rational approach to developing attenuated parasites, employing a new genome engineering technology.

### **5.1.2 Cas9 technology for the development of genetically modified parasites**

Clustered regularly interspaced short palindromic repeats - CRISPR associated gene 9 (CRISPR-Cas9) genome editing is a revolutionary method of genome engineering which is precise and quick. Discovered in prokaryotes as a mechanism of immunity, the system has been adapted for genome engineering in many other organisms, including kinetoplastids<sup>4</sup>. The main component of the system is the Cas9 endonuclease, which is able to form double stranded breaks in DNA. The endonuclease activity is specific and is guided to the cleavage site by an associated, single stranded, RNA sequence called single guide RNA (sgRNA). Modifications to the sgRNA mean that the Cas9 endonuclease can be hijacked and an investigator can target the Cas9 protein toward any desired part of the genome.

The double stranded break introduced by the Cas9 endonuclease provides the opportunity to modify the DNA sequence. The addition of a donor DNA which repairs the break through a shared homology sequence either side of the break can result in modifications of the native sequence. This technology has been modified for use in kinetoplastids and was integrated and optimised for use in *T. cruzi* in our lab by Costa et al<sup>5</sup>.

Our system benefits from minimising the number of steps required by the investigator. No cloning is required and the DNA templates encoding the sgRNA and the donor repair DNA are produced by PCR reactions before being transfected into the parasites in a single electroporation step<sup>5</sup>.

*T. cruzi* parasites of the previously described strain CL-LUC were modified to constitutively express the Cas9 gene and a T7 RNA polymerase. The integration of a T7 polymerase allows *in vivo* transcription of the guide RNA from the DNA template. Once transcribed, the guide RNA would form a complex with the constitutively expressed Cas9 endonuclease and target the protein to the desired site. The degradation of the donor DNA prevented the ongoing transcription of sgRNA and any subsequent Cas9 endonuclease activity. *T. cruzi* null mutants of the gene *GP72* were generated using this technique in under 4 weeks<sup>5</sup>. A further modification that was made to the Cas9 expressing parasite was the fusion of the *mNeonGreen* gene to the *PpyRe9h* gene encoding luciferase, resulting in a bioluminescent-fluorescent dual reporter parasite (CL-Luc::Neon/Cas9). Whereas bioluminescence is an ATP dependent process, fluorescence is an intrinsic property of the protein and widens the spectrum of *post mortem* and *in vitro* analyses that can be performed with the parasites.

We sought to use Cas9 technology to generate null mutants of CL-Luc::Neon/Cas9 and CL-Luc::Neon parasites. We hoped that in developing attenuated parasites, we would be able to use these as tools to develop and to further study live attenuated vaccines for *T. cruzi*.

### **5.1.3 The *T. cruzi* genes *AP-1* and *TcPOT***

We identified two genes in the literature that were reported to abrogate the infectivity of *T. cruzi* parasites<sup>18, 19</sup>. *T. cruzi* null mutants had been reported for both of the genes, however, neither of the null parasites were used to infect *in vitro*.

One of these genes encoded a high-affinity transporter (TcPOT) of the diamines putrescine and cadaverine. Scavenging of these diamines is an obligatory requirement of the *T. cruzi* parasite. They are required for important cellular processes such as growth and differentiation. However, because *T. cruzi* cannot synthesise these compounds *de novo*, it relies on the scavenging of them from the host. The null mutant displayed a defective ability to maintain an infection in Vero cells. Metacyclic trypomastigotes did not show an altered ability to infect cells, however the number of individual parasites per cell was significantly reduced<sup>18</sup>.

The other gene that we wanted to target was the gamma subunit of the AP1 adaptor complex (TcAP1- $\gamma$ ), a protein which forms part of a complex involved in vesicle trafficking in *T. cruzi*. Null mutants are less infective than WT parasites, with the infectivity of metacyclic trypomastigotes and amastigote replication being affected<sup>19</sup>.

Both candidate genes showed promise as potential vaccines due to the loss of infectivity in null mutants. Our aim was to develop null mutants of each of these two genes in the Cas9LNG CL Brener parasite strain for testing *in vivo*.

The objective of this work was to develop an attenuated parasite strain that would generate a self-limiting infection and that could be used to study the potential for live-attenuated vaccination.

## **5.2 Methods**

### Parasite culture

CL-Luc::Neon/Cas9 and CL-Luc::Neon epimastigotes as described previously<sup>5</sup>, were cultured at 27°C in RPMI-1640 with HEPES modification and supplemented with 10% FCS, 14 ml trypticase (17.5g/100ml) and 4ml hemin (2.5mg/ml). Genetically modified parasites were cultured under the appropriate drug selectable marker. Cas9 expression was maintained under selection of G418 and Luc::Neon expression was maintained under selection of hygromycin. Blastidicin and puromycin were used as selectable markers for targeted gene replacement as outlined in the results. Drugs were used at the following concentrations. Hygromycin, 150 µg ml<sup>-1</sup>; puromycin, 5 µg ml<sup>-1</sup>; blastidicin, 10 µg ml<sup>-1</sup>; G418, 100 µg ml<sup>-1</sup>.

### Design of sgRNA and repair templates

Primer design for sgRNA transcription was performed using the Eukaryotic Pathogen CRISPR guide Design Tool (<http://grna.ctegd.uga.edu/>). The parameters given were SpCas9: sgRNA 20nt; PAM sequence: NGG, all other parameters were default. The sgRNA sequence was selected based on total score. Two additional sequences were inserted into the primers; upstream of the guide sequence was the T7 promoter site (gaaattaatacgaactcactatagg) and downstream of the guide sequence was the leading 20 nt of the sgRNA scaffold, required for Cas9 binding (gttttagagctagaaatagc). Amplification of the guide template was performed with the gene specific forward primer and a reverse primer that was specific for the downstream scaffold sequence. Each PCR reaction consisted of 4 µl each of the forward and reverse primers at 10µM; 10µl Master Mix (ThermoScientific); 2 µl H<sub>2</sub>O. PCR steps for guides: initial step of 98°C 30 seconds, followed by 35 cycles of 10 seconds at 98°C; 30 seconds at 60°C, 15 seconds at 72°C.

Each primer for the repair templates consisted of a 30 nt sequence homologous to the targeted gene in *T. cruzi*, directly adjacent to the Cas9 cut site. This 30 nt sequence flanked a neighbouring 20 nt sequence homologous to the pPOT and pTbBlast plasmids, encoding the puromycin or the blasticidin resistance genes<sup>5</sup>. The PCR reaction consisted of 4 µl each of the forward and reverse PCR primers at 10 µM; 20 µl Master Mix (ThermoScientific); 1.2 µl DMSO; 9.8 µl H<sub>2</sub>O; 1µl pPOT or pTbBlast template. The resulting PCR product incorporated the drug resistance gene encoded by the pPOT or pTbBlast plasmid and incorporated a homology flank on either end. PCR steps for repair template: initial step of 98°C 5 minutes, followed by 40 cycles of 30 seconds at 98°C; 30 seconds at 65°C, 2 minutes 15 seconds at 72°C and a final elongation at 72°C for 7 minutes. All DNA Oligos were ordered from Integrated DNA Technologies.

#### Parasite transfection

The entire volume of the PCR reactions from the sgRNA and the repair templates (as above) were mixed and cleaned using the clean-up kit by Qiagen. The mixture was eluted in 50µl H<sub>2</sub>O and mixed with 10<sup>8</sup> epimastigotes, re-suspended in 200µl Tb-BSF buffer<sup>20</sup>. This 250µl solution was electroporated using the Lonza nucleofector system, using the program X-014. Transfected epimastigotes were incubated at 27°C overnight before the drug selectable marker (blasticidin or puromycin) was applied. In experiments where CL-Luc::Neon parasites were used in transfections, 5 µl of pLEW-Cas9 plasmid was provided at 400 ng/µl prior to transfection.

#### Gene IDs

The gene sequences were downloaded from the TriTryp database. TcPOT1.1 (TcCLB.504213.110), TcPOT1.2 (TcCLB.506985.40). TcAP1-γ CL Brener (TcCLB.508257.260), TcAP1-γ Dm28c (TCDM\_02471), Adaptin N-terminal region Sylvio X10 (TcSYL\_0046920).

## 5.3 Results

### 5.3.1 Targeted deletion of the diamine transporter TcPOT and of the AP-1 gamma subunit TcAP1-γ

The TcPOT gene is biallelic, with one allele each inherited from one of the two *T. cruzi* haplotypes that make up the hybrid strain CL Brener. A nucleotide blast showed the TcPOT 1.1 and 1.2 alleles to be 98% similar, therefore it was possible to design a single 5' sgRNA and a single 3' sgRNA that was complementary to both alleles, allowing us to target them with an identical sgRNA.

sgRNA templates were designed that would target the 5' and the 3' ends of the open reading frames (ORF) of both alleles. In addition, repair templates were also designed, one encoding a blasticidin resistance gene, specific to the 1.1 allele and another encoding a puromycin resistance gene, specific to the 1.2 allele. Each sharing 30 nucleotide homology flanks directly adjacent to the cut sites (Table 5.1).

Unlike with the TcPOT gene, there is only a single published sequence of the TcAP1-γ gene in the CL Brener genome. sgRNA and homology arms were designed according to the published sequence. sgRNA templates were designed that would cut within the open reading frame of the gene at the 5' and 3' ends, with repair templates designed to incorporate homology flanks of 30 nucleotides adjacent to the cut sites (Table 5.2).

**Table 5.1** sgRNA and repair templates. **Bold** highlights sequence homology with TcPOT.

	Guides	5' sgRNA	<code>gaaattaatacgactcactatagg<b>GTACGGAGCGTAATCATGT</b>gttttagagctagaaatagc</code>
		3' sgRNA	<code>gaaattaatacgactcactatagg<b>AAGCCCCGGCCTTCTCCATT</b>gttttagagctagaaatagc</code>
Repair Templates	TcPOT1.1	5' to 3'	<code>aagtttaggtgacaggaaggaagttgttataatgcagacctgtgc</code>
		3' to 5'	<code>gtcaggaggtg<b>ccggcgttttagttt</b>gtccaattgagagacctgtgc</code>
	TcPOT1.2	5' to 3'	<code>agtttaggtgacaggaaggaaggtgttataatgcagacctgtgc</code>
		3' to 5'	<code>gtcaggaggtg<b>ccggcgtttt</b>gtccaattgagagacctgtgc</code>

**Table 5.2** sgRNA and repair templates. **Bold** highlights sequence homology with TcAP1-γ.

	Guides	5' sgRNA	<code>gaaattaatacgactcactatagg<b>GATGAGCGCTCTCTCCTCGG</b>gttttagagctagaaatagc</code>
		3' sgRNA	<code>gaaattaatacgactcactatagg<b>GAACAATGCGCCCAT</b>AAGGGgttttagagctagaaatagc</code>
Repair Templates	TcAP1-γ	5' to 3'	<code>ATCGTTG<b>CCGTGCGACGGTGCCGCACCTCC</b>gtataatgcagacctgtgc</code>
		3' to 5'	<code>TTGCTATTGGAGTGTG<b>CGACAATAAGCTGC</b>ccaattgagagacctgtgc</code>

CL-Luc::Neon/Cas9 parasites were transfected with the guides and the repair templates in a single electroporation (figure 5.1 and 5.2). The parasites were then transferred to a flask in 10 ml medium where hygromycin and G418 drug selection pressure was maintained for the selection of the Luc::Neon fusion gene and the Cas9 gene respectively. After 24 hours, the parasite culture was split into 3 new flasks with the following conditions. One flask was supplemented with puromycin and another was supplemented with blasticidin for the selection of single knockout parasites. The third flask was supplemented with both drugs for the selection of double knockout parasites.

We were unable to grow cultures of parasites under double drug selection. Only parasites under single drug selection grew out. This indicated that parasites may have been single knockouts, integrating one resistance gene and retaining a single copy of the TcPOT or the TcAP1- $\gamma$  gene. Clones of the transfectants were obtained through a limiting dilution in a 96 well plate. Log phase cultures of the parasite clones were processed for DNA extraction. In order to confirm the genotype of the parasites, primers were designed to span the untranslated region (UTR) and the adjacent drug resistance gene or the gene targeted for knockout. We performed a PCR on the DNA samples and ran the PCR product on an agarose gel (figure 5.1C and 5.2C) (full gel in supplementary). The PCR confirmed that we had successfully generated TcPOT<sup>+/-</sup> and TcAP1- $\gamma$ <sup>+/-</sup> single knockouts, but did not generate any double knockout parasites.

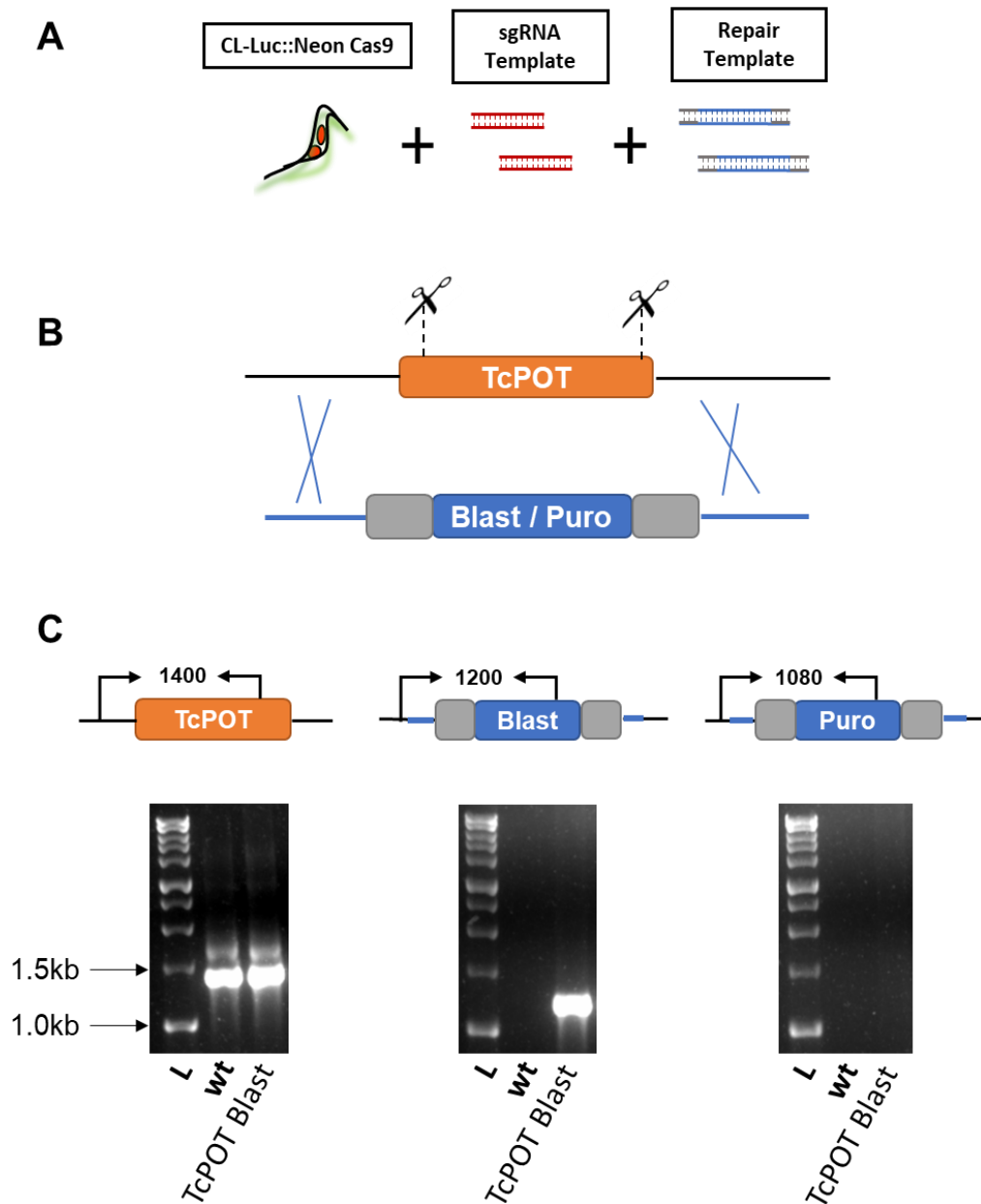


**Figure 5.1** – TcPOT KO. A) CL-Luc::Neon/Cas9 parasites were transfected by electroporation. B) sgRNA directed Cas9 endonuclease cut at the 5' and 3' ends of the ORF of the TcPOT gene, indicated by scissors. Repair templates (blue box) encoding either a blasticidin resistance gene or a puromycin resistance gene were integrated by homology targeting of the site adjacent to the cut. Grey boxes indicate RNA processing signals. C) PCR reactions were performed with primers spanning the UTR and ORF of the native TcPOT gene, or the blasticidin / puromycin gene. Lane 1: Ladder, 2: WT parasite, 3: TcPOT<sup>+/-</sup> with blasticidin integrated.

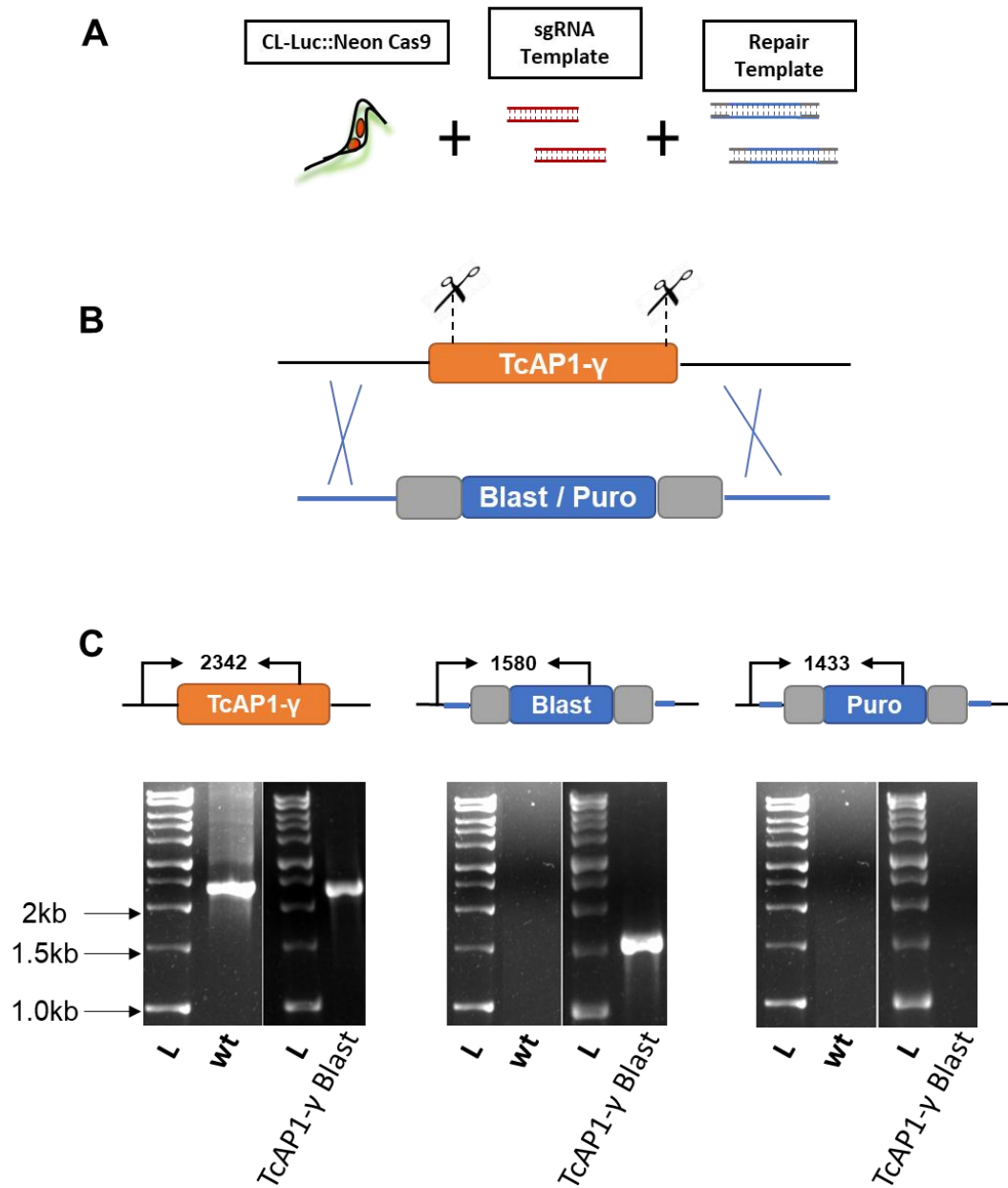


**Figure 5.2** – TcAP1- $\gamma$  KO. A) CL-Luc::Neon/Cas9 parasites were transfected by electroporation. B) sgRNA directed Cas9 endonuclease cut at the 5' and 3' ends of the ORF of the TcAP1- $\gamma$  gene, indicated by scissors. Repair templates (blue box) encoding either a blasticidin resistance gene or a puromycin resistance gene were integrated by homology targeting of the site adjacent to the cut. Grey boxes indicate RNA processing signals. C) PCR reactions were performed with primers spanning the UTR and ORF of the native TcAP1- $\gamma$  gene, or the blasticidin / puromycin gene. Lane 1: Ladder, 2: WT parasite, 3: Ladder, 4: TcAP1- $\gamma$ <sup>+/−</sup> with blasticidin integrated.

### **5.3.2 Targeted gene deletion in parasites not constitutively expressing the Cas9 endonuclease**

In parallel to the transfections we performed in CL-Luc::Neon/Cas9 parasites, we also performed transfections on CL-Luc::Neon parasites which did not constitutively express the T7 RNA Polymerase or Cas9. The inclusion of Cas9 is undesirable in an attenuated organism intended for use as a vaccine. Using identical guides and repair templates as in tables 5.1 and 5.2, we wanted to test the possibility of generating knockout parasites by providing a plasmid (pLEW-Cas9) expressing the T7 RNA polymerase and Cas9<sup>5</sup>. The transfection was performed in a single step, with a single electroporation by providing the sgRNA, repair templates and the pLEW-Cas9 plasmid at the same time (figure 5.3A).

Following electroporation epimastigotes were maintained at 27°C overnight and maintained under hygromycin. The following day, blasticidin and/or puromycin drug selection was applied and parasites that grew out were cloned by limiting dilution. Clones were grown to a log phase culture and DNA was extracted for genotyping by PCR (figure 5.3 B and C). Similarly as with the Cas9 expressing parasites, we found that we obtained only single knockout parasites. Tables 5.3 and 5.4 outline the knockouts that we were able to achieve.

**Table 5.3 – TcPOT Parasite Clones**

	Cas9 LNG	LNG
TcPOT +/- Blast Resistant	✓	✓
TcPOT +/- Puro Resistant	✓	<b>X</b>

**Table 5.4 – TcAP1-γ Parasite Clones**

	Cas9 LNG	LNG
TcAP1-γ +/- Blast Resistant	✓	✓
TcAP1-γ +/- Puro Resistant	✓	✓

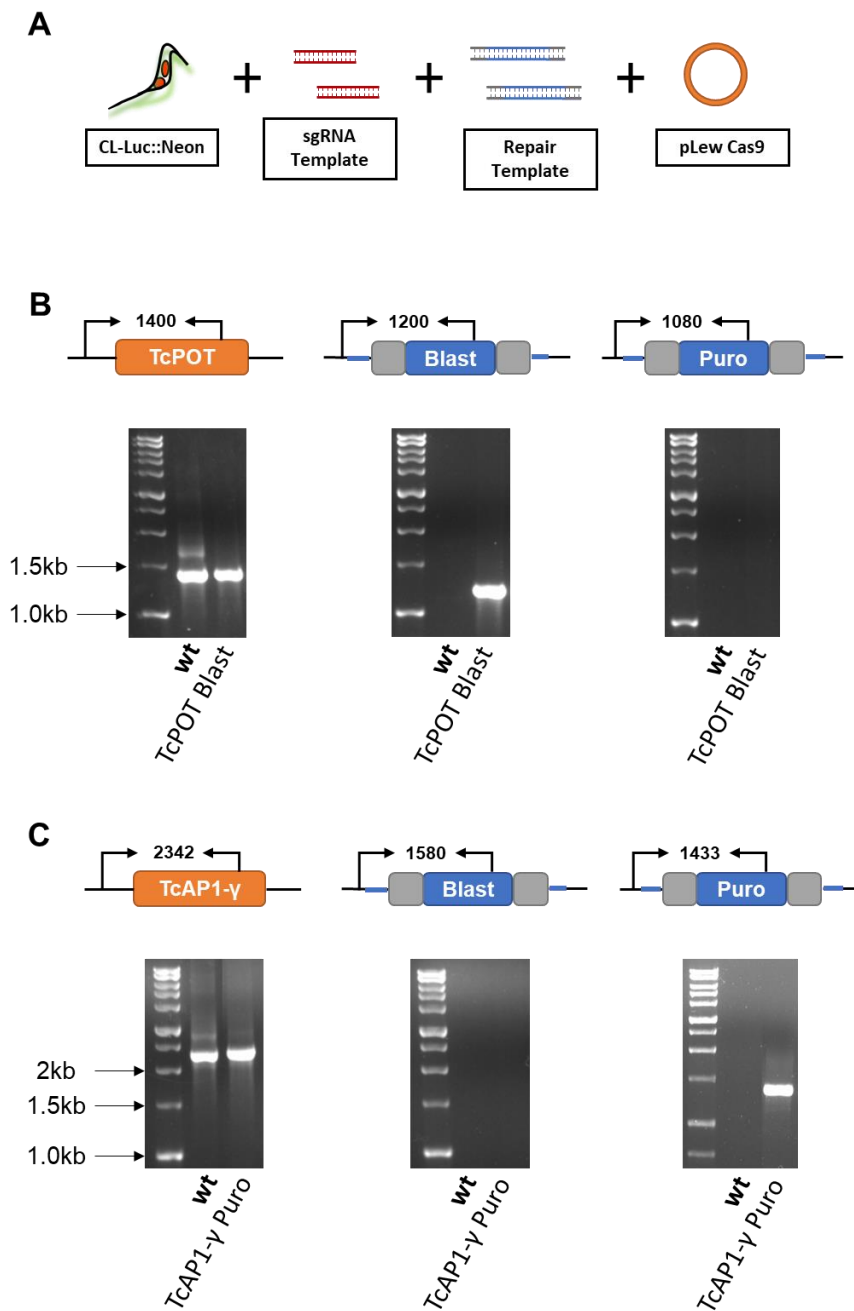


**Figure 5.3** – TcAP1- $\gamma$  KO. A) CL-Luc::Neon parasites were transfected by electroporation. B) PCR reactions were performed with primers spanning the UTR and ORF of the native TcPOT gene, or the blasticidin / puromycin gene. Lane 1: Ladder, 2: WT parasite, 3: TcPOT<sup>+/-</sup> with blasticidin integrated. C) PCR reactions were performed with primers spanning the UTR and ORF of the native TcAP1- $\gamma$  gene, or the blasticidin / puromycin gene. Lane 1: Ladder, 2: WT parasite, 3: TcAP1- $\gamma$ <sup>+/-</sup> with puromycin integrated.

## 5.4 Discussion

Our aim was to develop attenuated strains of *T. cruzi*, to test their infectivity *in vivo*, and ultimately their potential use as a tool for studying live attenuated vaccination.

We were able to generate single knockout parasites for the genes TcPOT and TcAP1- $\gamma$ . We chose these two genes as candidates as they have not previously been studied *in vivo* and as a result have not been assessed as candidates for a attenuated vaccines. Other genes have been investigated for the development of *T. cruzi* attenuated strains and studied for their suitability as live vaccines<sup>21-23</sup>, although without the high degree of sensitivity provided by the bioluminescence *in vivo* imaging system.

Using a Cas9 system that was engineered for use in *T. cruzi*, we designed sgRNA and repair templates for targeting the selected genes at the 5' and 3' ends of the ORF. We attempted to generate null mutants through the targeted deletion of both gene copies using different drug selection markers. Parasites did not grow under double drug selection, but they did grow out under single drug selection in the presence of blasticidin or puromycin. PCR reactions using primers that spanned the UTR and ORF confirmed that whilst the drug resistance gene was successfully integrated, the transfectants retained a copy of the gene that was targeted for deletion. The most obvious explanation for these outcomes is that both copies of these genes are essential for growth under the culture conditions used for selection.

Previously, this methodology was used to generate Gp72 null mutants in the same parasite strain<sup>5</sup>. In the case of the TcAP1- $\gamma^{+/-}$ , only a single copy of the gene has been published in the CL Brener strain. Therefore, another explanation as to why we were unable to generate null mutants might be due to variation between the alleles. Because CL Brener is a hybrid parasite, its genome is a mixture of two distinct haplotypes, which are representative of their ancestral lineages (DTUs). The Esmeraldo like haplotype comes from DTU II whereas the non-Esmeraldo haplotype comes from DTU III<sup>24</sup>. We

compared two other available gene sequences from the *T. cruzi* strains Dm28c and Sylvio X10. Based on the high sequence similarity between these genes, we have designed new sgRNA templates that target these regions.

In the case of the TcPOT gene, both alleles were published. Null mutants have successfully been developed for both of these genes previously, suggesting that subtle differences in the culture conditions may impact on viability.

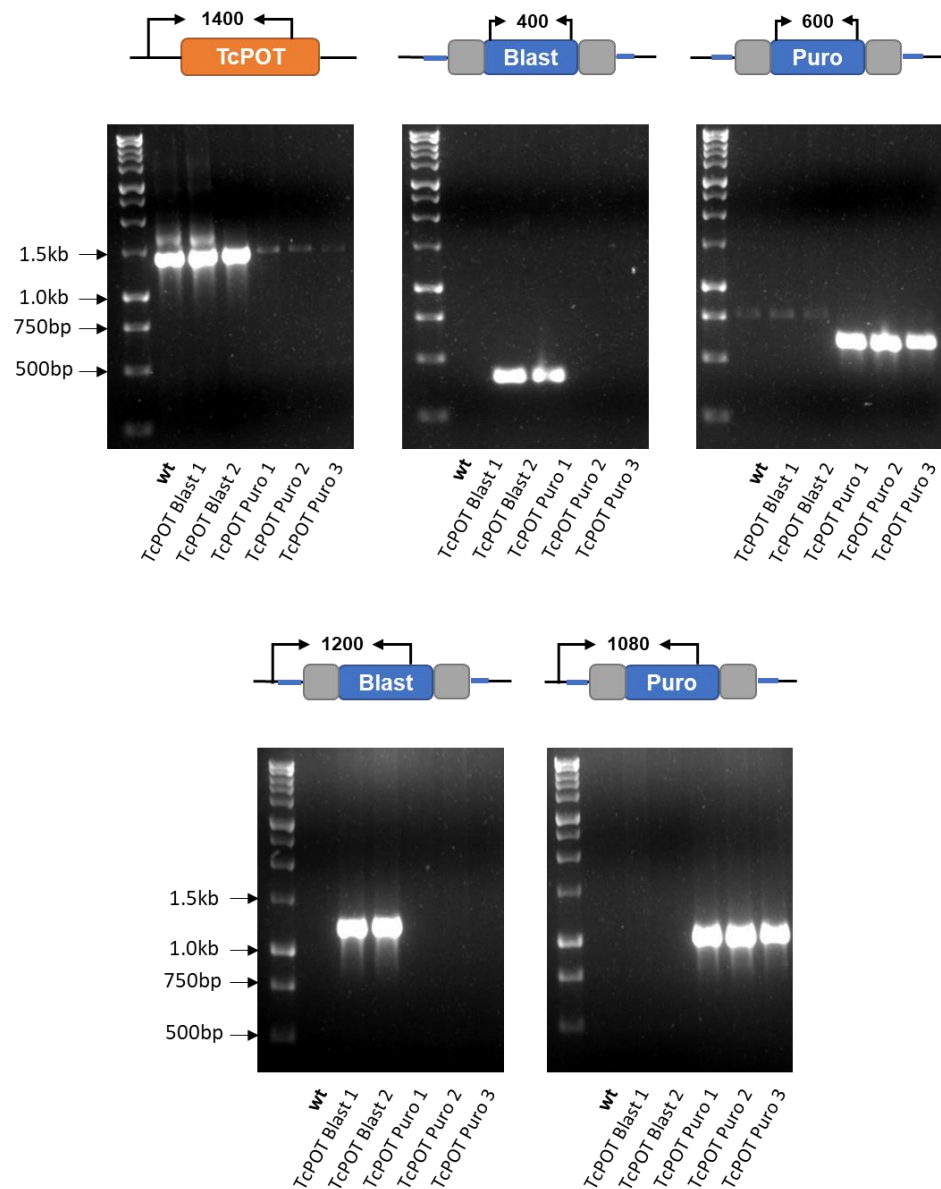
Despite the fact that single knockout mutants can display an attenuated phenotype<sup>23</sup>, developing null mutants was an important goal of this work due to the desired application of these attenuated strains as vaccines. Gene copy number variation, large gene families and the existence of aneuploidy all point to the potential of gene duplication in *T. cruzi* parasites<sup>25</sup>. Therefore, it was imperative to obtain null mutants to negate any potential for gene duplication that would allow parasite reversion back to wild type fitness.

Because the ultimate goal for these attenuated strains is to be trialled as vaccines, we wanted to test the possibility of transfecting parasites that do not constitutively express Cas9. This is important because the presence of foreign DNA in a vaccine strain is undesirable. When assessing the virulence or growth of attenuated parasites as a measure of their suitability as vaccine candidates, the presence of foreign proteins may interfere with the outcome and the results may reflect the presence of this foreign DNA. Growth defects in Cas9 expressing parasites have been reported in other groups<sup>26</sup>. To overcome this problem, we successfully transfected CL-Luc::Neon parasites that did not constitutively express the Cas9 protein. We did this by introducing the pLEW-Cas9 plasmid, which expresses the Cas9 protein as well as the T7 RNA polymerase into the transfection mixture alongside the sgRNA and repair templates<sup>5</sup>. We used all of the same conditions as for the Cas9 expressing line, aside from the fact that we did not apply drug selection for the retention of the pLEW-Cas9 plasmid. The transfections that

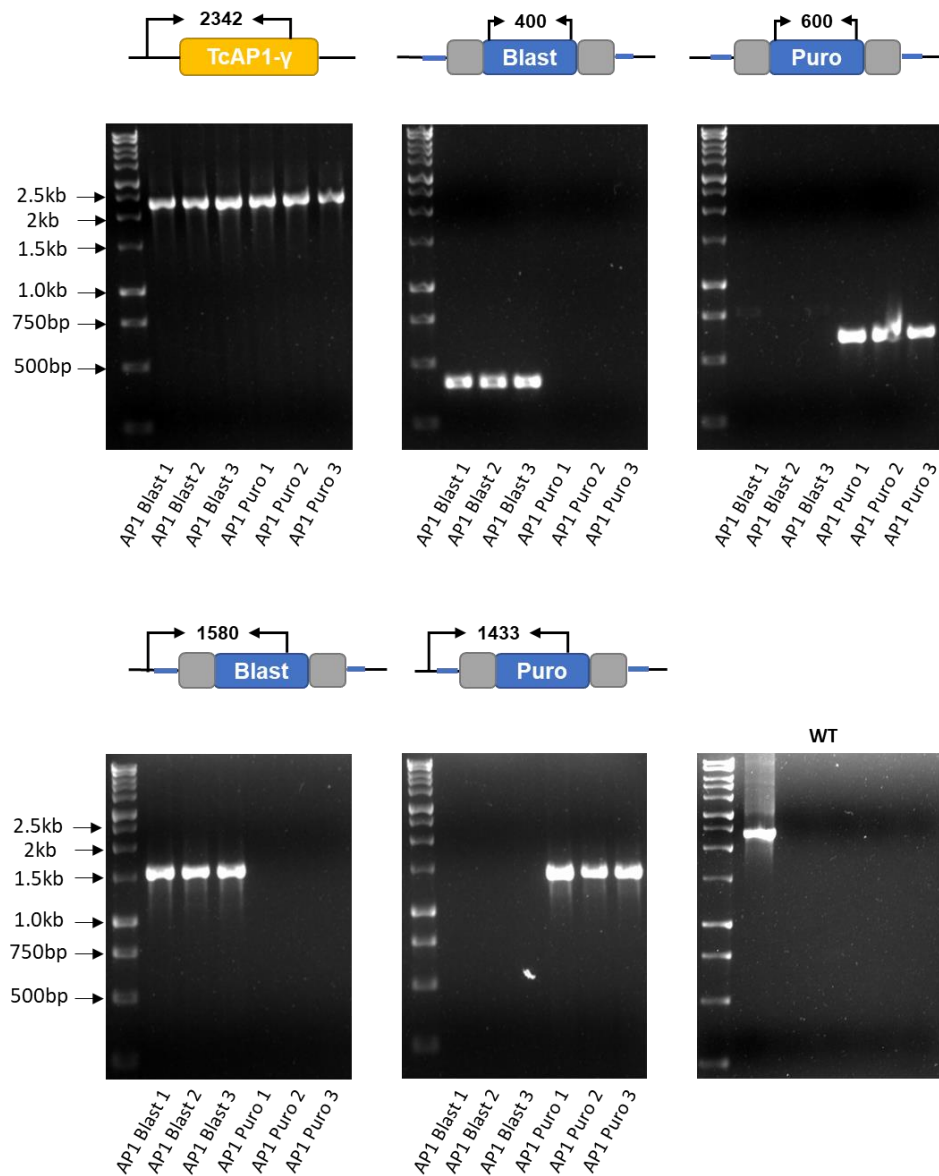
we performed on this cell line were as equally successful as those that we performed on the Cas9 expressing parasites. Importantly, this indicates that future attempts at developing attenuated vaccines could be performed using this method.

The study of *T. cruzi* has long been disadvantaged by the absence of available tools for genetic manipulation, like those that are available in other trypanosomes<sup>27</sup>. However, with the development of Cas9 technology, we are on the verge of a new era in *T. cruzi* genomics and applications of this technology in genome wide screens, something previously not possible<sup>28</sup>, will drive the identification of new drug targets, targets for vaccine development and our understanding of *T. cruzi* biology to new and exciting heights.

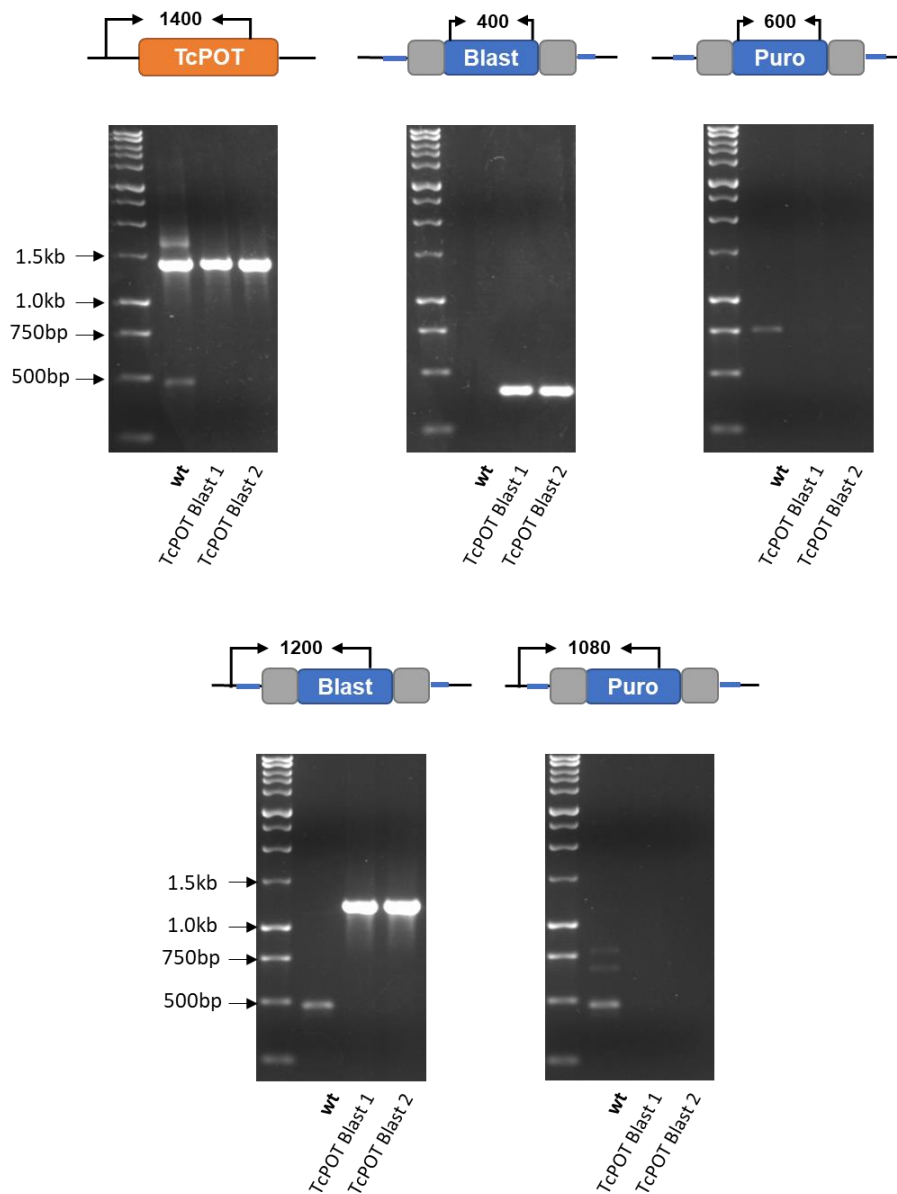
## 5.5 Supplementary



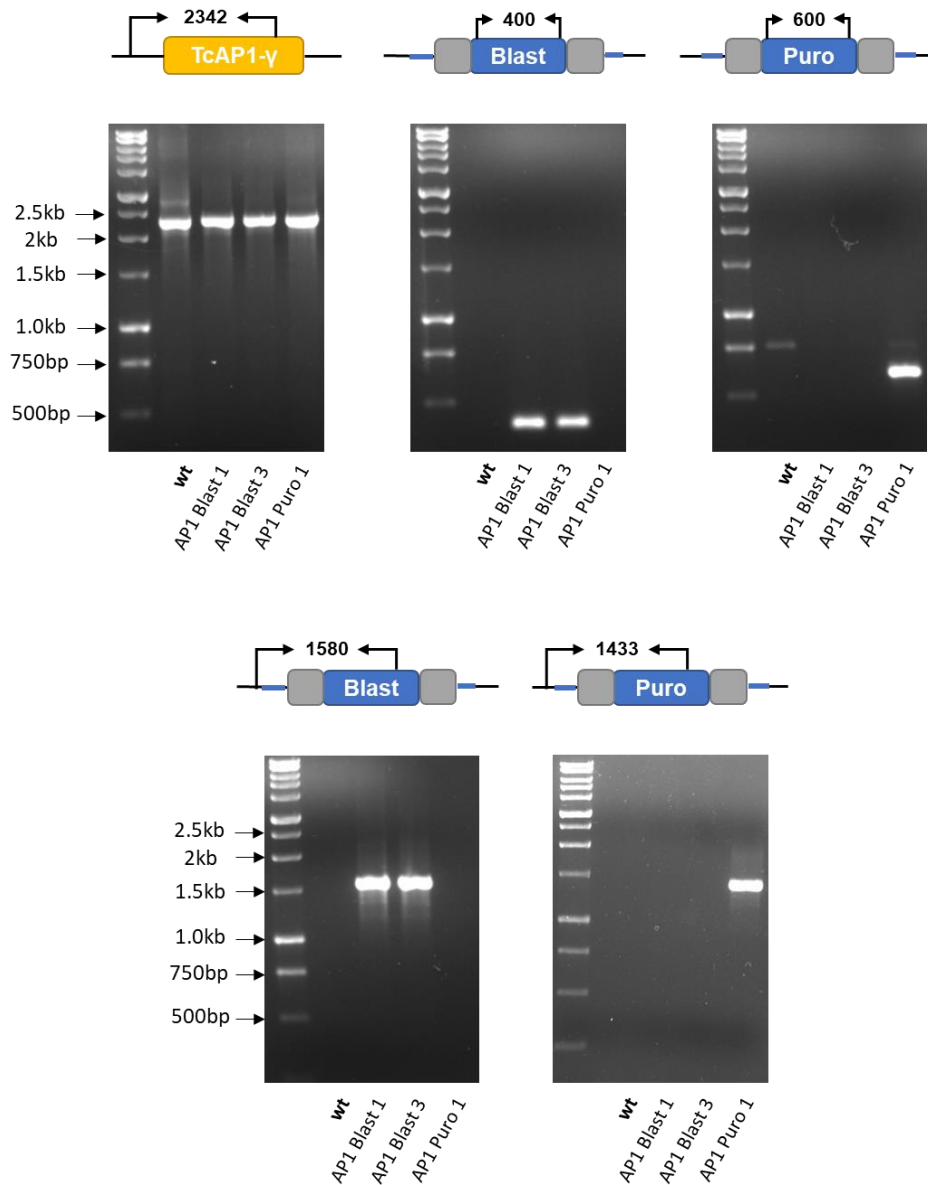
**Supplementary Figure 5.1** – CL-Luc::Neon/Cas9 TcPOT KO. Parasites were transfected with drug resistance cassettes targeting the TcPOT ORF for replacement. Clones of transfected parasites were obtained by limiting dilution and PCR reactions were performed with primers spanning the UTR and ORF of the native TcPOT gene, or the blasticidin / puromycin gene. Parasite clone is indicated in lane below gel. Image above gel indicates primer binding sites and size of expected band.



**Supplementary Figure 5.2** – CL-Luc::Neon/Cas9 TcAP1- $\gamma$  KO. Parasites were transfected with drug resistance cassettes targeting the TcAP1- $\gamma$  ORF for replacement. Clones of transfected parasites were obtained by limiting dilution and PCR reactions were performed with primers spanning the UTR and ORF of the native TcAP1- $\gamma$  gene, or the blasticidin / puromycin gene. Parasite clone is indicated in lane below gel. Image above gel indicates primer binding sites and size of expected band. DNA from WT parasites were not included in the gel alongside the clones and were run on a separate gel (bottom right). Identical PCR primers were used on WT DNA as for the other reactions. Only a single band of DNA between the sizes of 2kb and 2.5kb was produced, indicating the presence of the TcAP1- $\gamma$  gene.



**Supplementary Figure 5.3** – CL-Luc::Neon TcPOT KO. Parasites were transfected with pLEW-Cas9 plasmid and drug resistance cassettes targeting the TcPOT ORF for replacement. Clones of transfected parasites were obtained by limiting dilution and PCR reactions were performed with primers spanning the UTR and ORF of the native TcPOT gene, or the blasticidin / puromycin gene. Parasite clone is indicated in lane below gel. Image above gel indicates primer binding sites and size of expected band.



**Supplementary Figure 5.4** – CL-Luc::Neon TcAP1- $\gamma$  KO. Parasites were transfected with pLEW-Cas9 plasmid and drug resistance cassettes targeting the TcAP1- $\gamma$  ORF for replacement. Clones of transfected parasites were obtained by limiting dilution and PCR reactions were performed with primers spanning the UTR and ORF of the native TcAP1- $\gamma$  gene, or the blasticidin / puromycin gene. Parasite clone is indicated in lane below gel. Image above gel indicates primer binding sites and size of expected band.

## 5.6 References

1. Pereira, I.R., et al., A human type 5 adenovirus-based *Trypanosoma cruzi* therapeutic vaccine re-programs immune response and reverses chronic cardiomyopathy. *PLoS Pathog*, 2015. **11**(1): p. e1004594.
2. Araujo, A.F., et al., Genetic vaccination against experimental infection with myotropic parasite strains of *Trypanosoma cruzi*. *Mediators Inflamm*, 2014. **2014**: p. 605023.
3. Gomes-Neto, J.F., et al., Vaccination With Recombinant Filamentous fd Phages Against Parasite Infection Requires TLR9 Expression. *Front Immunol*, 2018. **9**: p. 1173.
4. Beneke, T., et al., A CRISPR Cas9 high-throughput genome editing toolkit for kinetoplastids. *R Soc Open Sci*, 2017. **4**(5): p. 170095.
5. Costa, F.C., et al., Expanding the toolbox for *Trypanosoma cruzi*: A parasite line incorporating a bioluminescence-fluorescence dual reporter and streamlined CRISPR/Cas9 functionality for rapid in vivo localisation and phenotyping. *PLoS Negl Trop Dis*, 2018. **12**(4): p. e0006388.
6. Jenner, E., Letter Addressed to the Medical Profession Generally, Relative to Vaccination. *Lond Med Phys J*, 1821. **45**(266): p. 277-280.
7. Bernstein, D.I., Live attenuated human rotavirus vaccine, Rotarix. *Semin Pediatr Infect Dis*, 2006. **17**(4): p. 188-94.
8. Okafor, C.N. and Momodu, II, Bacillus Calmette Guerin (BCG), in *StatPearls*. 2019: Treasure Island (FL).
9. Orme, I.M., Beyond BCG: the potential for a more effective TB vaccine. *Mol Med Today*, 1999. **5**(11): p. 487-92.
10. Tennant, S.M. and M.M. Levine, Live attenuated vaccines for invasive Salmonella infections. *Vaccine*, 2015. **33 Suppl 3**: p. C36-41.
11. Saljoughian, N., T. Taheri, and S. Rafati, Live vaccination tactics: possible approaches for controlling visceral leishmaniasis. *Front Immunol*, 2014. **5**: p. 134.
12. Bregano, J.W., et al., *Phytomonas serpens*, a tomato parasite, shares antigens with *Trypanosoma cruzi* that are recognized by human sera and induce protective immunity in mice. *FEMS Immunol Med Microbiol*, 2003. **39**(3): p. 257-64.
13. Basso, B., E.R. Moretti, and E. Vottero-Cima, Immune response and *Trypanosoma cruzi* infection in *Trypanosoma rangeli*-immunized mice. *Am J Trop Med Hyg*, 1991. **44**(4): p. 413-9.

14. Pinge-Filho, P., et al., Protective immunity against *Trypanosoma cruzi* provided by oral immunization with *Phytomonas serpens*: role of nitric oxide. *Immunol Lett*, 2005. **96**(2): p. 283-90.
15. Basso, B., E. Moretti, and R. Fretes, Vaccination with epimastigotes of different strains of *Trypanosoma rangeli* protects mice against *Trypanosoma cruzi* infection. *Mem Inst Oswaldo Cruz*, 2008. **103**(4): p. 370-4.
16. Lima, M.T., et al., *Trypanosoma cruzi*: properties of a clone isolated from CL strain. *Parasitol Res*, 1991. **77**(1): p. 77-81.
17. Bull, J.J., Evolutionary reversion of live viral vaccines: Can genetic engineering subdue it? *Virus Evol*, 2015. **1**(1).
18. Hasne, M.P., R. Soysa, and B. Ullman, The *Trypanosoma cruzi* Diamine Transporter Is Essential for Robust Infection of Mammalian Cells. *PLoS One*, 2016. **11**(4): p. e0152715.
19. Moreira, C., et al., Knockout of the gamma subunit of the AP-1 adaptor complex in the human parasite *Trypanosoma cruzi* impairs infectivity and differentiation and prevents the maturation and targeting of the major protease cruzipain. *PLoS One*, 2017. **12**(7): p. e0179615.
20. Schumann Burkard, G., P. Jutzi, and I. Roditi, Genome-wide RNAi screens in bloodstream form trypanosomes identify drug transporters. *Mol Biochem Parasitol*, 2011. **175**(1): p. 91-4.
21. Basombrio, M.A., et al., Targeted deletion of the gp72 gene decreases the infectivity of *Trypanosoma cruzi* for mice and insect vectors. *J Parasitol*, 2002. **88**(3): p. 489-93.
22. Manning-Cela, R., et al., LYT1 protein is required for efficient in vitro infection by *Trypanosoma cruzi*. *Infect Immun*, 2001. **69**(6): p. 3916-23.
23. Perez Brandan, C., et al., Knockout of the dhfr-ts gene in *Trypanosoma cruzi* generates attenuated parasites able to confer protection against a virulent challenge. *PLoS Negl Trop Dis*, 2011. **5**(12): p. e1418.
24. Porcile, P.E., et al., A refined molecular karyotype for the reference strain of the *Trypanosoma cruzi* genome project (clone CL Brener) by assignment of chromosome markers. *Gene*, 2003. **308**: p. 53-65.
25. Reis-Cunha, J.L., et al., Whole genome sequencing of *Trypanosoma cruzi* field isolates reveals extensive genomic variability and complex aneuploidy patterns within TcII DTU. *BMC Genomics*, 2018. **19**(1): p. 816.
26. Peng, D., et al., CRISPR-Cas9-mediated single-gene and gene family disruption in *Trypanosoma cruzi*. *MBio*, 2014. **6**(1): p. e02097-14.

27. Alsford, S., et al., High-throughput phenotyping using parallel sequencing of RNA interference targets in the African trypanosome. *Genome Res*, 2011. **21**(6): p. 915-24.
28. Sidik, S.M., D. Huet, and S. Lourido, CRISPR-Cas9-based genome-wide screening of *Toxoplasma gondii*. *Nat Protoc*, 2018. **13**(1): p. 307-323.

Chapter 6 :

Discussion

## **6.1 General discussion**

*T. cruzi* infection can lead to a debilitating illness known as Chagas disease. Despite over a hundred years of research, this remains the leading infectious disease burden of any parasite in the western hemisphere<sup>1,2</sup>. The only available treatments demonstrate significant off-target effects and there are no available vaccines<sup>3,4</sup>. One of the main factors impeding the development of vaccines and new therapeutics has been the lack of sufficiently sensitive tools that allow the monitoring of parasites in the chronic stage of the infection<sup>5</sup>. The development of highly sensitive bioluminescent imaging solves this problem. The sensitivity of the system allows for the detection of as few as 100 parasites injected i.p.<sup>6</sup>. Furthermore, the system is non-invasive and can therefore be used to obtain serial measurements over the lifetime of a mouse.

In this thesis, we used bioluminescent imaging in the BALB/c model of *T. cruzi* infection to test a novel vaccine candidate, measure the ability of a fully-fledged immune response to combat *T. cruzi*, study immune correlates of protection and also tested the feasibility of a novel therapeutic strategy to combat chronic infection.

Vaccination has been proposed to be an effective and economically viable solution to reducing the disease burden<sup>7</sup>. Despite this, there are no licenced vaccines for *T. cruzi*. We applied bioluminescent imaging to study the protective efficacy of a novel vaccine candidate, based on two well studied antigenic targets, ASP2 and TS<sup>8-10</sup>. This gave us the opportunity, for the first time, to assess vaccine efficacy beyond the acute stage of an infection. We found that vaccinated mice were partially protected during a short time frame within the acute stage of the infection, on days 14 and 21. However, after day 21, there were no differences observed. The implications of this are that transient and partial protection during the acute stage has little obvious impact on the subsequent development of the chronic infection. The reasons for this are unclear and will require further research, particularly to establish if there is a reduction in disease pathology.

The benefits of applying bioluminescence imaging to vaccine testing are clear. The system is sensitive and allows for serial measurements to be taken across the acute and chronic infection. However, we needed to be able to place these findings into the wider context of immune mediated protection, in order to establish a barometer against which to measure vaccine success. Using the drug cure strategy, we saw >99% knockdown in the parasite burden following re-challenge. Furthermore, some mice were able to completely prevent the establishment of a second infection. This protection did not wane, even after almost one year. These findings highlighted the full potential of the immune response in protecting against an infection. The fact that this level of protection was induced by a live vaccination begs the question of whether this form of vaccination should receive more attention in the development of a *T. cruzi* vaccine.

To understand the development of protective immunity, and explore the immunological correlates of this protection, we set up an experiment in which we infected mice for varying lengths of time prior to drug cure. We observed differences in the ability to protect against a re-infection. These differences strongly correlated with the T cell response. In the short-term re-infection experiments (14 and 36 days), protection correlated with high levels of pre-existing circulating T cells, but in the long term re-infection experiment (~1 year), protection correlated with a T cell memory response.

Integrating this model with other sophisticated tools which measure heart function can provide important information regarding the relationship between immunity, the parasite burden and heart function. A greater understanding of the relationship between these parameters can help toward the establishment of defined correlates of protection which are associated with the prevention of Chagas disease pathology and in turn, will inform the development of vaccines.

In addition to the development of a vaccine, drug development for *T. cruzi* is also very actively researched<sup>11</sup>. This is because the two front line drugs are associated with a

multitude of off-target effects, which severely hinder patient compliance<sup>3</sup>. In addition, drug efficacy is not clear, with treatment failures often reported<sup>12</sup>. Bioluminescent imaging has revealed the GIT to be a site of parasite persistence in the chronic stage of the infection in murine models<sup>13</sup>. This finding led us to investigate whether a therapeutic strategy which specifically targeted this parasitological niche could impact on the chronic stage parasite burden. We tested this using TNBS, an inducer of colonic inflammation<sup>14</sup>. On necropsy, we observed that some of the TNBS treated mice did not present any foci of infection in the colon, and that a proportion of these mice did not express any detectable bioluminescence. Despite this promising preliminary outcome, the physiological effects associated with colonic inflammation meant that such an approach would necessarily have limited applicability, and would probably be undesirable for the treatment of Chagas disease. Nevertheless, our study provides tentative support for the concept that a therapy that specifically targets the pathogen in the gut could have potential as a successful strategy for eliminating *T. cruzi* in a chronic infection. Specific targeting of the colon with immunotherapies, or the modification of more conventional drugs that would allow them to be administered intrarectally may prove to be beneficial. Bioluminescent imaging will allow such experiments to be performed using predictive animal models.

Finally, following our observation that a drug cured infection conferred strong protection against a re-infection, we sought to develop attenuate parasite strains that could be used to study the potential of live vaccination. Live vaccination has previously been explored in *T. cruzi*, however prior to the introduction of CRISPR/Cas9 genome engineering, the development of genetically modified parasite strains was an inefficient and time-consuming task. These studies are therefore few<sup>15</sup>. We used molecular tools that were recently adapted and optimised for use in *T. cruzi* to develop attenuated parasite strains<sup>16</sup>. Importantly, we were able to successfully generate genetically modified parasite clones using a parasite line that did not constitutively express Cas9. This is a

crucial step in the future application of CRISPR/Cas9 to studying *T. cruzi*. Some groups have reported that the expression of Cas9 in *T. cruzi* modifies parasite biology<sup>17</sup>. Parasite strains that do not express the Cas9 gene would therefore be far more desirable. *T. cruzi* research is no longer held back by the absence of easily tractable genetic tools and genome wide tagging projects or gene knockout libraries, akin to those that have taken place in other organisms, are now real possibilities<sup>18</sup>. The ability to genetically modify parasites, without the added complexity of constitutive expressed Cas9 would be advantageous.

The many merits of bioluminescent technology have been discussed, however, bioluminescent imaging has some caveats which must be considered when designing an experiment. Because bioluminescence relies on ATP production, a signal can only be generated in a metabolically active cell<sup>19</sup>. This is important to consider given the increasing recognition of dormant infections amongst trypanosomes<sup>20</sup>. Metabolic quiescence has been shown to exist in *Leishmania* and more recently has also been demonstrated in *T. cruzi*, being proposed as a mechanism by which the parasite may avoid immune detection in the vertebrate host<sup>21</sup>. If true, a dormant *T. cruzi* parasite would not have the same turnover of ATP as an active parasite, meaning that a dormant organism could simply not be detected with bioluminescence. With this in mind, the study of chronic infections should utilise additional technologies whose reliability does not depend on the metabolic status of the parasite, one example is fluorescence. Recognition of this potential caveat is one of the reasons for the development of the dual-reporter bioluminescent and fluorescent *T. cruzi* parasite<sup>16</sup>.

## **6.2 Conclusions and further work**

In conclusion, the work in this thesis has clearly demonstrated the benefits of applying bioluminescence imaging to the study of *T. cruzi*. We have shown that live vaccination induces robust protection that is long lived and cross strain protective. This protection correlated with the frequency of a parasite specific T cells. We have shown that the induction of inflammation in the colon of chronically infected mice can impact on the parasite burden. Finally, we demonstrate the ability to genetically modify parasites using genetic constructs designed for Cas9 mediated genome engineering, in parasites that do not constitutively express Cas9.

There is a wide scope for further research. There are three lines of work which I feel are the most important for bringing us closer towards the goal of establishing the first *T. cruzi* vaccine.

First, bioluminescence imaging should be applied on a much grander scale, to catalogue the efficacy of the many other *T. cruzi* vaccine candidates that have been developed. Many vaccine candidates have been developed and tested in pre-clinical studies. However, these use a wide range of parasite and mouse strain combinations. In addition, different laboratories use different techniques and tools to report on vaccine efficacy<sup>22-24</sup>. Because of this, it is difficult to compare vaccine experimental outcomes between different research groups. Bioluminescence imaging is highly sensitive, flexible, and quick and easy to use. It could easily be developed as a standardised technique across laboratories. The data generated by its use would help to guide vaccine development globally, and help us to further determine which characteristics of a vaccine make it more or less efficacious.

Furthermore, on the use of different tools for assessing vaccine efficacy, a concerted effort needs to be made in order to combine the different tools and technologies being used to test pre-clinical vaccines by different research groups. The implementation of

ECG technology to the monitoring of disease progression in *T. cruzi* infection has been revolutionary, allowing for the monitoring of CCC in real-time<sup>25</sup>. CCC is the major hallmark of the disease and this is well reflected in the mouse model, our ability to study the changes in CCC are vital in assessing the suitability of a vaccine. This technology has been successfully used by a number of groups and has provided useful information on the efficacy of vaccines in preventing or reversing CCC<sup>22</sup>. By combining the real-time infection monitoring technology of bioluminescence with the real-time disease monitoring offered by ECG machines, vaccine test that utilise both of these technologies would generate more useful information and therefore hold far more value. For a disease such as *T. cruzi* where no vaccine has made it to clinical testing, this kind of information would help us to identify candidates worth considering for clinical testing.

Secondly, there needs to be a consensus on specifically defined correlates of immunity in *T. cruzi*. To date, we do not know which immune responses lead to the development of Chagas disease pathology and which immune responses prevent other individuals from developing symptoms. A clear relationship needs to be defined between the parasite burden, the immune response and the development of chronic chagasic cardiomyopathy, the most common clinical manifestation of the disease. Experimental models will be crucial to dissect the relationship between these three elements. Immunological tools in murine models are already well established. In addition, a number of mechanisms, including ECG monitoring are available to measure many different aspects of heart health<sup>26</sup>. The last hurdle has been the difficulty in measuring the parasite burden. Bioluminescence imaging reduces this hurdle. Once we are able to establish a correlate of immunity, which we know is associated with the prevention of chronic chagasic cardiomyopathy, we can use this information to guide the development of vaccines that induce the exact type of immune response that we desire.

Finally, work on understanding the roles of individual genes in *T. cruzi* should follow the examples of other organisms. Genome wide screens, such as those that have been

performed in *T. gondii* are now technologically possible<sup>18</sup>. This work will be important in the identification of candidates which are functionally important for *T. cruzi* infectivity. The current indications from this thesis are that live attenuated parasites could make efficacious vaccines. Therefore, these kinds of studies will identify targets for effective parasite attenuation.

## 6.3 References

- 1 Steverding, D. The history of Chagas disease. *Parasit Vectors* **7**, 317, doi:10.1186/1756-3305-7-317 (2014).
- 2 Chagas disease in Latin America: an epidemiological update based on 2010 estimates. *Wkly Epidemiol Rec* **90**, 33-43 (2015).
- 3 Aldasoro, E. *et al.* What to expect and when: benznidazole toxicity in chronic Chagas' disease treatment. *J Antimicrob Chemother* **73**, 1060-1067, doi:10.1093/jac/dkx516 (2018).
- 4 Crespillo-Andujar, C. *et al.* Toxicity of nifurtimox as second-line treatment after benznidazole intolerance in patients with chronic Chagas disease: when available options fail. *Clin Microbiol Infect* **24**, 1344 e1341-1344 e1344, doi:10.1016/j.cmi.2018.06.006 (2018).
- 5 D'Avila, D. A. *et al.* Monitoring the parasite load in chronic Chagas disease patients: comparison between blood culture and quantitative real time PCR. *PLoS One* **13**, e0208133, doi:10.1371/journal.pone.0208133 (2018).
- 6 Lewis, M. D., Francisco, A. F., Taylor, M. C. & Kelly, J. M. A new experimental model for assessing drug efficacy against *Trypanosoma cruzi* infection based on highly sensitive in vivo imaging. *J Biomol Screen* **20**, 36-43, doi:10.1177/1087057114552623 (2015).
- 7 Lee, B. Y. *et al.* Modeling the economic value of a Chagas' disease therapeutic vaccine. *Hum Vaccin Immunother* **8**, 1293-1301, doi:10.4161/hv.20966 (2012).
- 8 Costa, F. *et al.* Immunization with a plasmid DNA containing the gene of trans-sialidase reduces *Trypanosoma cruzi* infection in mice. *Vaccine* **16**, 768-774, doi:10.1016/s0264-410x(97)00277-6 (1998).
- 9 Boscardin, S. B., Kinoshita, S. S., Fujimura, A. E. & Rodrigues, M. M. Immunization with cDNA expressed by amastigotes of *Trypanosoma cruzi* elicits protective immune response against experimental infection. *Infect Immun* **71**, 2744-2757, doi:10.1128/iai.71.5.2744-2757.2003 (2003).
- 10 Machado, A. V. *et al.* Long-term protective immunity induced against *Trypanosoma cruzi* infection after vaccination with recombinant adenoviruses encoding amastigote surface protein-2 and trans-sialidase. *Hum Gene Ther* **17**, 898-908, doi:10.1089/hum.2006.17.898 (2006).
- 11 Scarim, C. B. *et al.* Current advances in drug discovery for Chagas disease. *Eur J Med Chem* **155**, 824-838, doi:10.1016/j.ejmech.2018.06.040 (2018).

- 12 Morillo, C. A. *et al.* Randomized Trial of Benznidazole for Chronic Chagas' Cardiomyopathy. *N Engl J Med* **373**, 1295-1306, doi:10.1056/NEJMoa1507574 (2015).
- 13 Lewis, M. D. *et al.* Bioluminescence imaging of chronic *Trypanosoma cruzi* infections reveals tissue-specific parasite dynamics and heart disease in the absence of locally persistent infection. *Cell Microbiol* **16**, 1285-1300, doi:10.1111/cmi.12297 (2014).
- 14 Kim, H. S. & Berstad, A. Experimental colitis in animal models. *Scand J Gastroenterol* **27**, 529-537, doi:10.3109/00365529209000116 (1992).
- 15 Sanchez-Valdez, F. J., Perez Brandan, C., Ferreira, A. & Basombrio, M. A. Gene-deleted live-attenuated *Trypanosoma cruzi* parasites as vaccines to protect against Chagas disease. *Expert Rev Vaccines* **14**, 681-697, doi:10.1586/14760584.2015.989989 (2015).
- 16 Costa, F. C. *et al.* Expanding the toolbox for *Trypanosoma cruzi*: A parasite line incorporating a bioluminescence-fluorescence dual reporter and streamlined CRISPR/Cas9 functionality for rapid in vivo localisation and phenotyping. *PLoS Negl Trop Dis* **12**, e0006388, doi:10.1371/journal.pntd.0006388 (2018).
- 17 Peng, D., Kurup, S. P., Yao, P. Y., Minning, T. A. & Tarleton, R. L. CRISPR-Cas9-mediated single-gene and gene family disruption in *Trypanosoma cruzi*. *MBio* **6**, e02097-02014, doi:10.1128/mBio.02097-14 (2014).
- 18 Sidik, S. M., Huet, D. & Lourido, S. CRISPR-Cas9-based genome-wide screening of *Toxoplasma gondii*. *Nat Protoc* **13**, 307-323, doi:10.1038/nprot.2017.131 (2018).
- 19 Ford, S. R. *et al.* Use of firefly luciferase for ATP measurement: other nucleotides enhance turnover. *J Biolumin Chemilumin* **11**, 149-167, doi:10.1002/(SICI)1099-1271(199605)11:3<149::AID-BIO411>3.0.CO;2-Q (1996).
- 20 Kloehn, J., Saunders, E. C., O'Callaghan, S., Dagley, M. J. & McConville, M. J. Characterization of metabolically quiescent *Leishmania* parasites in murine lesions using heavy water labeling. *PLoS Pathog* **11**, e1004683, doi:10.1371/journal.ppat.1004683 (2015).
- 21 Sanchez-Valdez, F. J., Padilla, A., Wang, W., Orr, D. & Tarleton, R. L. Spontaneous dormancy protects *Trypanosoma cruzi* during extended drug exposure. *Elife* **7**, doi:10.7554/eLife.34039 (2018).
- 22 Pereira, I. R. *et al.* A human type 5 adenovirus-based *Trypanosoma cruzi* therapeutic vaccine re-programs immune response and reverses chronic cardiomyopathy. *PLoS Pathog* **11**, e1004594, doi:10.1371/journal.ppat.1004594 (2015).
- 23 Gupta, S., Salgado-Jimenez, B., Lokugamage, N., Vazquez-Chagoyan, J. C. & Garg, N. J. TcG2/TcG4 DNA Vaccine Induces Th1 Immunity Against Acute *Trypanosoma cruzi*

- Infection: Adjuvant and Antigenic Effects of Heterologous *T. rangeli* Booster Immunization. *Front Immunol* **10**, 1456, doi:10.3389/fimmu.2019.01456 (2019).
- 24 Portillo, S. *et al.* A prophylactic alpha-Gal-based glycovaccine effectively protects against murine acute Chagas disease. *NPJ Vaccines* **4**, 13, doi:10.1038/s41541-019-0107-7 (2019).
- 25 Eickhoff, C. S. *et al.* ECG detection of murine chagasic cardiomyopathy. *J Parasitol* **96**, 758-764, doi:10.1645/GE-2396.1 (2010).
- 26 Ho, D. *et al.* Heart Rate and Electrocardiography Monitoring in Mice. *Curr Protoc Mouse Biol* **1**, 123-139, doi:10.1002/9780470942390.mo100159 (2011).

# Appendix

Version 1 Jan 2014

## Advisory notes on recording and reporting the actual severity of regulated procedures

### Contents

1. Introduction	2
2. General principles	3
a. Prospective versus actual severity assessments	3
b. Requirements for all actual severity assessments	3
c. Monitoring and competence of those carrying out severity assessments	4
d. Non-regulated procedures, non-procedural and procedural harms	5
e. Informed decisions	7
f. Animals found dead	7
g. Assessing overall severity of a procedure	8
h. Re-use	9
3. Definitions of severity categories	9
a. Sub-threshold severity	9
b. Mild procedures	9
c. Moderate procedures	11
d. Severe procedures	12
e. Non-recovery	13
4. Severity for some commonly encountered procedures and effects	13
a. Weight loss	13
b. Restraint	14
c. Surgery	14

Version 1 Jan 2014

When there is no increasing impact with multiple steps or if the pain or suffering resolves completely between each step in a procedure, serial techniques may not be considered cumulative, and therefore do not increase the severity assessment. Serial steps may lead to cumulative suffering; this is certainly the case when the pain or suffering caused by individual steps in a series overlaps (i.e. no opportunity to recover between steps). In these cases a moderate or higher classification will often be appropriate even if each individual step in isolation would have been classified as mild.

There may be complete recovery between procedures and yet an additive effect of each individual impact may be appropriate because sensitisation to procedures has occurred. Similarly, there may be habituation to repeated procedures. The extent to which sensitisation or habituation occurs varies between individual animals. These factors should be considered in evaluating overall impact and determining the classification of actual severity.

#### **2.h Re-use**

In cases of re-use each individual use (procedure) should have actual severity assigned independently of previous uses or re-uses. Therefore one animal could have more than one severity category assigned during the course of its lifetime.

### **3. Definitions of severity categories**

Procedures carried out on animals are considered 'regulated procedures' only if carried out for a scientific purpose and only if the severity is above the threshold defined as equivalent to the pain, suffering or distress caused by the insertion of a hypodermic needle in line with good veterinary practice.

#### **3.a Sub-threshold severity**

It is possible that procedures authorised under a project licence could result in below threshold severity. These will be few, but will occur when it was considered that a procedure might have caused above-threshold pain or suffering, but in retrospect this did not occur for some or all of the animals involved. Examples will be the breeding of genetically altered animals under project licence authority but without a harmful phenotype or dosing with a compound in feed where the animals ate normally and suffered no consequences of being dosed.

Version 1 Jan 2014

Any such procedures should be returned under the appropriate project licence as sub-threshold.

### 3.b Mild procedures

*"Procedures on animals as a result of which the animals are likely to experience short-term mild pain, suffering or distress, as well as procedures with no significant impairment of the well-being or general condition of the animals shall be classified as mild."*

Annex VIII Animals Directive 2010/63 EU

**The key characteristic of mild procedures is that any pain or suffering experienced by an animal is, at worst, only slight or transitory and minor so that the animal returns to its normal state within a short period of time.** There is generally no lasting effect and no cumulative effect of serial steps within a protocol. An exception to this expectation that the animal will return to normal is genetically altered animals (GAAs) with a phenotype that falls into a mild categorisation (see separate advice note on GAAs – *Severity classification of genetically altered animals under the Animals (Scientific Procedures) Act 1986*).

Animals described as having experienced mild suffering in the actual severity assessment will have experienced essentially normal lives with only minor and transitory deviation from the 'five freedoms':

- freedom from hunger and thirst;
- freedom from discomfort;
- freedom from pain, injury or disease;
- freedom to express normal behaviour; and
- freedom from fear and distress.

Animals will have shown normal feeding and drinking behaviour throughout. Although there may have been a minor, transient disturbance, there will have been no significant weight loss associated with disease and no evidence of lasting systemic illness.

An example of mild pain could be the equivalent of the pain caused by injection by conventional routes, i.e. subcutaneous, intravenous, intraperitoneal or intramuscular (assuming competence of the person performing the procedure and that best practice guidelines for volume, pH, needle size, etc. are followed). Multiple injections by these routes may remain in the mild category if there are no cumulative effects.

Version 1 Jan 2014

Administration of anaesthesia is in itself a mild procedure under normal circumstances, provided the induction is rapid and the duration is such that the animal makes a rapid and uneventful recovery without the need for supportive treatment. The actual harm related to anaesthesia may increase or accumulate where anaesthesia is repeated. A regulated procedure carried out under general anaesthesia, regardless of how severe individual steps might be in a conscious animal, but having no adverse effects immediately after the animal recovers, could also be classed as an overall mild procedure. This excludes most surgical procedures where some level of discomfort if not pain will be present on recovery.

Mild distress is caused by low grade, non-painful or non-invasive stressors, such as those used in chronic mild stress protocols (repeated handling, cage changing and flooding, cage movement, introduction of unfamiliar cage mates but without fighting, etc.). It excludes aversive techniques, such as the use of electric shocks as a negative stimulus on treadmills and for fear conditioning, and stress caused by forced swimming. For the actual severity to have been mild, recovery should be immediate/rapid and there should be no lasting impact that is evident simply by examining the animal (although there may of course be, for example, biochemical or behavioural changes requiring particular tests in order to characterise effects), or as evidenced by sensitisation to later procedures.

Mild procedures generally have no lasting impact on animals; once each step within a procedure has been completed the animal should return to normality, or close to it, almost immediately. When pain or suffering does not resolve rapidly on completion of a step within a procedure, but continues, it may be considered long lasting.

### 3.c Moderate procedures

*"Procedures on animals as a result of which the animals are likely to experience short-term moderate pain, suffering or distress or long-lasting mild pain, suffering or distress as well as procedures that are likely to cause moderate impairment of the well-being or general condition of the animals shall be classified as moderate."*

Annex VIII Animals Directive 2010/63 EU

The characteristic of moderate procedures is that they do cause **a significant and easily detectable disturbance of an animal's normal state**, assuming that appropriate monitoring systems are in place and that they are used by trained and competent staff. The disturbance is **enough for an animal to show discomfort, abnormal behaviours, significant weight loss or other indicators of poor welfare, but does not prevent normal feeding and drinking** or other normal activities other than for short periods or to a limited extent for longer periods.

Version 1 Jan 2014

Pain of any significant intensity is of no more than a few hours duration and is not considered of a severe nature, as judged by species-specific criteria (for example, repeated vocalisation/persistent self trauma in rodents).

Animals that undergo procedures that produce chronic low-level pain or discomfort or dysfunction such as altered gait will usually be classified as moderate. A higher level of pain that persists, such as non-weight bearing lameness without improvement, even in the absence of other signs of severe pain, would be considered severe unless a diagnosis can be made that indicates the condition is associated with pain of a lower intensity.

Many chronic pain models, including those involving minor surgical procedures such as nerve ligation and including when this is carried out without post-operative analgesia, tend to cause allodynia rather than permanent pain. When pain detection methods are necessary to distinguish these animals from normal they are not considered to be suffering long-term pain and are classed as of moderate severity. If the animals show overt signs of pain for a prolonged period without improvement, for example, by persistently licking the affected part for more than three hours in a model such as formalin injection into the footpad, they should be classed as severe.

Self trauma is generally indicative of severe suffering. However, if it is minor and self-limiting and animals do not show evidence of pain on examination by competent staff, this can be classed as moderate. An example might be autotomy where the trauma is superficial (is restricted to nails and has not progressed to the soft tissue) and has stopped. If the autotomy is persistent or progressing, the classification would be severe.

Acute pain models, such as the writhing test or assessment of visceral pain using balloon inflation, may involve more severe pain. Where the pain is not sufficient to lead to distress and where the entire painful technique lasts no more than three hours these procedures will be classed as moderate.

If animals show signs of obvious illness, for example, piloerection, huddled posture, reluctance to move, isolation from the group in rodents, and if this is promptly detected and animals are killed immediately, procedures could be classed as moderate. If animals remain in this condition for more than 24 hours then a classification of severe will be appropriate.

### **3.d Severe procedures**

Version 1 Jan 2014

*“Procedures on animals as a result of which the animals are likely to experience severe pain, suffering or distress or long-lasting moderate pain, suffering or distress, as well as procedures that are likely to cause severe impairment of the well-being or general condition of the animals shall be classified as severe.”*

Annex VIII Animals Directive 2010/63 EU

The characteristics of severe procedures are that they **cause a major departure from the animal’s usual state of health and well-being**. It would usually include long-term disease processes where **assistance with normal activities such as feeding and drinking are required** or where **significant deficits in behaviours/activities persist**. This would include any state that a person would find difficult to tolerate or disease where clinical signs have progressed to such an extent that it threatens the life of an animal.

A severe classification should be given in any situation where animals are *in extremis*. Any animal that is found moribund should also be classified as severe unless there is evidence that a lower classification can be given, i.e. that the animal did not pass through severe suffering to reach the moribund state.

### **3.e Non-recovery**

A classification of non-recovery is used if an entire procedure is carried out under general anaesthesia and the animal does not recover. It includes unintended death of animals on recovery protocols while under anaesthesia, provided that no regulated procedures had been carried out prior to the induction of anaesthesia.

Procedures involving GAAs with a harmful phenotype should **not** be classed as non-recovery, as the birth and maintenance of such an animal constitutes a procedure; in these cases the actual severity will be the severity of the phenotype in that animal up to the time of anaesthesia. In the case of GAAs that do not show any harmful phenotype *prior to the time of anaesthesia*, ‘non-recovery’ would be appropriate.

## **4. Severity for some commonly encountered procedures and effects**

### **4.a Weight loss**

Weight loss can be a very useful objective indicator of an animal’s state of well-being. It is often used as a surrogate marker for suffering or severity associated with many disease states. **However, the use of weight loss in isolation from other considerations is likely to be inappropriate for setting the level of severity.**

Version 1 Jan 2014

The cause of any weight loss and of other indicators of welfare must be used in context. Some species show seasonal or physiological variations in weight, which should be considered within context when performing the welfare assessment. Similarly, the physiological state of the animal (for example, if it is lactating) may influence whether weight change is relevant to the well-being of the animal.

Correlation of weight loss with the general appearance and demeanour of an animal may modify the classification of any particular level of weight loss. It is also quite possible for animals to suffer significantly without losing weight, therefore absence of a significant level of weight loss does not necessarily mean that suffering was not moderate or even severe. Weight loss is a less useful indicator where other weight changes are occurring, such as tumour burden increasing or ascites is developing.

Gradual weight loss or divergence between adult experimental and normal animals of between 15 and 20 per cent (over a period of days) as a result of procedure(s), or a weight difference of this range against age/sex matched controls in growing animals, would usually be classified as moderate severity. However, very rapid weight loss (within 24 to 48 hours) within this range may indicate a significant element of dehydration and is likely to be an indication of severe suffering. Severe calorie restriction can be a cause of moderate or even severe suffering. In contrast, slow weight loss of even greater than 20 per cent due to mild calorie restriction, especially in obese individuals, may not in itself be an indication of even moderate suffering.

Where an established body condition scoring system is in place, a combination of weight measurement with body condition of the animal provides a more robust measure of likely suffering than weight alone. For example, a sheep that has dropped 15 per cent of its body weight and has reduced its condition score from 3 in 5 to 1.5 in 5 over a period of days, using the standard agricultural scoring system, is likely to be associated with at least moderate suffering, whilst a similar weight loss with a drop in body condition from 5 to 4 is not.

#### **4.b Restraint**

Restraint, including holding animals in spaces less than the Code of Practice minima, usually requires project licence authorisation. This may be found to cause sub-threshold, mild, moderate or even severe distress depending on such factors as the nature of restraint, the individual animal, the success of training and habituation. In determining actual severity the impact on the animal, not solely the duration of the restraint, should be considered.